

**Axes of diversity and their implications in the unisexual *Ambystoma* complex**

A Dissertation Submitted to the Committee on Graduate Studies  
in partial fulfillment of the Requirements for the Degree of Doctor of Philosophy  
in the Faculty of Arts and Science

TRENT UNIVERSITY

Peterborough, Ontario, Canada

© Copyright by Evan Bare 2025

Environmental and Life Sciences Ph.D. Graduate Program

September 2025

## **Abstract**

### **Axes of diversity and their implications in the unisexual *Ambystoma* complex**

Evan Bare

Measuring biodiversity has become increasingly complex as biologists and ecologists have gradually learned more about how biotic systems are structured and interact. Given the wide range of tools, techniques and approaches now in use to quantify biological diversity, it is useful to consider different “dimensions of diversity” to classify these measurements and provide context for their interpretation. Even within the genetic dimension of diversity alone, recent improvements in theory, technology, and statistics has generated several approaches which can provide distinct insights into natural systems. In this thesis, I use multiple “axes of diversity” to subdivide the dimension of genetic diversity to better understand a complex ecological system - the unisexual *Ambystoma* complex on Pelee Island, Ontario. By focusing on the genomotype axis, I found that the composition of local unisexual *Ambystoma* assemblages generally reflects the current relative abundance of the local sexual host populations. This suggests that sexual hosts can be thought of as a keystone species for the complex not only because they are required for unisexual *Ambystoma* to reproduce, but also because their relative abundance governs the composition of entire unisexual *Ambystoma* assemblages. Comparatively, when assessing the lineage axis of genetic diversity, unisexual *Ambystoma* assemblage diversity patterns primarily reflected historic landscape structure, and spatial patterns of increased lineage richness were linked to areas where both potential hosts were locally available (currently or historically). Thus, while both of the investigated axes of diversity are forms of genetic diversity, each revealed distinct factors that have shaped

contemporary diversity patterns across the landscape operating at different spatial and temporal scales. Critically, our understanding of complex ecological systems is likely to be broadened by including additional axes of diversity (e.g., allelic, loci, or chromosomal structure axes), and such investigations are not limited to clonal hybrid systems. Overall, this work illustrates the importance of combining insights from distinct conceptual and analytical toolkits to generate a comprehensive understanding of the factors which have shaped the patterns of diversity we observe today.

**Keywords:** Unisexual *Ambystoma*, Metacommunity, Genetic Diversity, Kleptogenesis, Genomotype, Clonal Lineage, Landscape Genetics, Dimensions of Diversity, Axes of Diversity

## **Acknowledgements**

This thesis could not have been completed without the time and dedication provided by Dr. Dennis Murray, Dr. Thomas Hossie, and Dr. Chris Wilson. Dr. James Bogart was gracious in providing preliminary genetic data, historic samples, and extensive insight into the dynamics of the study system. The additional field assistance from Graeme Smith, Jordan MacDonald, and the team at Scales Nature Park was crucial for sample collection. Financial assistance for this work was provided by the Province of Ontario through the SARSE, SARRFO and SARSP programs. Lastly, the added support from the crew in the OMNR Fish lab at Trent University ensured the lab processing went smoothly. Thank you all for your time and effort.

# Table of Contents

Abstract .....	ii
Acknowledgements .....	iv
List of Tables .....	viii
List of Figures .....	xi
Chapter 1: Introduction .....	1
General Introduction .....	1
Community Diversity .....	2
Sexual Parasite Ecology .....	5
Genetic Diversity .....	6
Dynamics of Clonality .....	8
Unisexual <i>Ambystoma</i> .....	9
Pelee Island .....	12
Chapter 2: Diversity and composition of mixed-ploidy unisexual salamander assemblages reflect the key influence of host species .....	15
Abstract .....	15
Introduction .....	17
Methods .....	20
Study System .....	20
Salamander Sampling .....	21
Genotyping for Taxonomic Assessment .....	23
Statistical Analysis .....	24
Results .....	26
Overview .....	26
Site Diversity .....	28
Genome Bias .....	29
Discussion .....	30
Tables and Figures .....	35
Supplemental .....	41
Procedures .....	41
Supplemental Tables and Figures .....	44
Chapter 3: Lineage diversity in unisexual salamander assemblages reveals the influence of historic landscape and biotic interactions .....	55

Abstract .....	55
Introduction .....	57
Methods .....	61
Salamander Sampling .....	61
Lineage Assignment .....	61
Statistical Analysis .....	62
Results .....	64
Overview .....	64
Lineage Diversity .....	65
Lineage Composition Dissimilarity.....	66
Connectivity.....	67
Discussion .....	67
Legacy Effect of the Historic Landscape .....	68
Genetic Legacy Effects.....	70
Conclusion.....	71
Tables and Figures .....	73
Supplemental.....	78
Details on Atex74 .....	78
Supplemental Tables and Figures.....	79
Chapter 4: Discussion .....	123
Axes of Diversity .....	123
Genomotype Diversity.....	124
Lineage Diversity .....	128
Conclusion.....	133
Appendix A: Mapping of microsatellite loci to the axolotl ( <i>A. mexicanum</i> ) genome ....	135
Introduction .....	135
Methods.....	137
Data Collection .....	137
Genome Mapping .....	137
Primer Alignment Potential.....	138
Results .....	138
Discussion .....	139

Tables and Figures .....	143
References .....	157
Appendix B: Field observations.....	185
Appendix C: Historic maps of Pelee Island, Ontario.....	187

## List of Tables

**Table 2.S1.** Primer sets for multiplexes 1 and 2. Allele counts are listed by host of origin (T - *A. texanum*, L - *A. laterale*, X - ambiguous). For Atex74 (an *A. texanum* exclusive locus) alleles are categorized by motif size as determined by stutter band sizes. \* 4-bp alleles for Atex74 went beyond the 500-bp size standard. Any alleles above 500-bp were identified as 500+..... 47

**Table 2.S1 Continued.** Primer sets for multiplexes 3 and 4. Allele counts are listed by host of origin (T - *A. texanum*, L - *A. laterale*, X - ambiguous). One allele size (122-bp) in locus AmmH123 amplified in both *A. texanum* and *A. laterale*, all other alleles appear unambiguous..... 48

**Table 2.S2.** Multiplex reaction mixtures: A) MP1; B) MP2; C) MP3; D) MP4. Mixtures were calculated to 450 uL mixtures and dispense into 96 wells of 5 uL reactions. All reactions start with a 15 min start at 94°C, followed by 40 cycles of 94°C for 30s, T<sub>A</sub>°C temperature for 90s, 72°C for 60s, ending with 30min at 72°C. .... 49

**Table 2.S3.** Total sample size, raw counts, and relative abundances provided. Relative abundances provided in three forms under raw counts, from top to bottom: total relative abundance, relative abundance within unisexuals, and relative abundance within ploidy level. Host species are not provided relative abundance within unisexuals or within ploidy level. The LT genototype, as the only diploid unisexual, is not provided relative abundance within ploidy level. As all unisexuals must maintain at least one L and one T on Pelee, unknown unisexual samples must be at least LT, therefore unknown contributions are labeled with '?'s based on ploidy level. Sites arranged by dissimilarity and cluster order with the Island level ( $\gamma$ -diversity) data on top. Island level data includes all samples, including from sites removed due to sample size (i.e. D6.2 and D2). .... 51

**Table 2.S4.** Probability of false absence assuming relative abundances of 5%, 2%, 1%, and 0.5% of population. Calculated probabilities are listed alongside indicator markers on bullet chart. Grey shading indicates levels of false absence probability, with darker shades indicating lower probability. Operationally, we inferred true absence when we achieved 95% confidence that the true relative abundance of undetected hosts was <5% (indicated by the red line). Only site B3 does not meet the threshold of <5% false absence probability given an assumed true relative abundance of 5%. Cases where the probability of false absence was >10% are marked with squares. .... 53

**Table 2.S5.** Sample sizes, genototype richness, and diversity values provided for unisexual assemblages at each site (See Table 2.S3 for Total counts including host samples). Chao1 richness calculated value with upper range (95% confidence with max of 10) provided, upper range not provided for site C3 as all bootstrap values were '3'. Calculated values with confidence intervals provided under respective 'Observed' columns. Mean and standard deviation of bootstrap runs provided under 'Estimate' columns. Bootstrap value distributions provided as density plots for lambda and V. First

quartile, median, and third quartile provided under distribution figures. Sites arranged by dissimilarity and cluster order..... 54

**Table 3.1.** *Ambystoma* salamander diversity measures for sites across Pelee Island Ontario, arranged by historic geographical upland habitat patch (NW, NE, east, and south). Alphanumeric codes indicate site based on location within a grid (see Fig. 3.3)<sup>157</sup>. Values indicate the total number of multilocus lineages observed, as well as number of private and shared lineage, along with number of genotyped LT samples (N). MLL richness estimates (Chao1) are rounded up to whole numbers. Relative abundance of hosts as well as unisexual genotypes required for the diploidization cycle are presented from Bare et al.<sup>157</sup>, with historic values from Bogart and Licht<sup>156</sup> presented underneath where available..... 75

**Table 3.2.** Results from selection of candidate linear models that predict Bray-Curtis dissimilarity of diploid unisexual lineage composition among *Ambystoma* salamander breeding sites on Pelee Island, Ontario. The Upland model uses a binary variable indicating whether two sites were located within the same patch of historic upland habitat, Geo uses a continuous variable reflecting Euclidean geographic distance between sites, and Resist uses a continuous variable reflecting landscape resistance between pairs of sites based on a resistance map derived from Smith<sup>218</sup>. Null reflects an intercept-only model..... 76

**Table 3.S1.** Counts for each Full MLG ID, Short MLG ID, and MLL ID in total and by site. Full MLG ID are based on all available loci, while Short MLG ID do not consider AjeD283 or AmaD321 due to regular inconsistencies and uncertainties during genotyping. Full MLG ID was determined prior to filtering samples with incomplete loci data..... 91

**Table 3.S2.** Genotypes for each Full MLG per MLL. Loci are arranged by species association. Atex74 has alleles of two different motif sizes, with 4-bp motif alleles designated by “<sub>4bp</sub>”. Atex74 alleles larger than 500 were assigned 503, as it is the next largest allele that would come after the 500-bp limit. Loci AmaD321 and AjeD283 were not used when determining lineage assignments as they are presumed less accurate and are therefore italicized..... 103

**Table 3.S3.** Table of all alleles per locus for each MLL. Loci names are separated and colored based on their host association: *A. laterale* - blue, *A. texanum* - orange, Indeterminant - black. Loci in italics were not used when determining MLL due to inconsistencies and regular uncertainties during genotyping. ....112

**Table 3.S4.** Overall allelic richness for each locus. AmmH123 and Atex74 are separated into two columns to distinguish species-specific alleles and motifs for Amm123 and Atex74, respectively.....117

**Table 3.S4 Continued.** Overall allelic richness for each locus. AmmH123 and Atex74 are separated into two columns to distinguish species-specific alleles and motifs for Amm123 and Atex74, respectively. \*Alleles larger than 500-bp for the 4-basepair motif alleles of

Atex74 are all categorized as 503 as they go beyond the ladder size and 503 is the next largest allele size after the 499-bp allele (e.g. alleles of size 507 or 531 would be classified as 503).....118

**Table 3.S5.** All diversity measures calculated including MLL:N ratios for all samples, private MLL, and shared MLL. Confidence intervals based on 1000 bootstraps of 30 samples per site (excluding B3) are provided under observed diversity metrics. ....119

**Table 3.S5 Continued.** Simpson diversity ( $\lambda$ ), evenness ( $V$ ), Beta Pareto, and the Lineage Diversity Index (LDI) measures as suggested by Arnaud-Haond et al.<sup>108</sup>. Confidence intervals based on 1000 bootstraps of 30 samples per site (excluding B3) are provided under observed diversity metrics. Relative abundance values are provided for hosts and unisexual genotypes (from <sup>157</sup>) which required for the diploidization cycle proposed by Bogart and Bi <sup>137</sup>. \*Historic relative abundances of hosts and genotypes from Bogart and Licht <sup>156</sup> provided underneath contemporary genotype and host relative abundance values. .... 120

**Table 3.S6.** Results from model selection exercise comparing linear models which seek to predict Bray-Curtis dissimilarity of diploid unisexual lineage composition among sites on Pelee Island, Ontario. The Upland model uses a binary variable indicating whether or not two sites were located within the same patch of historic upland habitat, Geo uses a continuous variable reflecting geographic distance between sites, and Resist uses a continuous variable reflecting landscape resistance between pairs of sites based on a resistance map derived from Smith <sup>218</sup>. Null reflects an intercept-only model. Two sets of models are presented, depending on if site B6 is included or not. This is done because lineage composition at site B6 conforms least to our hypothesis but may be the result of alternative explanations that we were unable to test. Site C3 was removed from modeling due to concerns of founder effects. Additionally, model selection criteria, residual values, and F-statistics are all included in this table for complete model representation. .... 121

**Table A.1.** List of citations and associated accession numbers for recognized *Ambystoma* microsatellite loci primer sets. .... 144

**Table A.2.** Locus count per chromosome arm and species where associated accession sequence could be reliably aligned to the axolotl genome. .... 148

**Table A.3.** Total number of primer sets and average alignment metrics for each species. .... 150

**Table A.4.** Successfully aligned loci listed by species of origin. Chromosome arm and alignment statistics provided for each primer. Species ordered by phylogenetic distance <sup>333</sup>. Loci used in this thesis are identified (\*). .... 151

## List of Figures

**Figure 2.1.** Putative pathways for genototype change in unisexual *Ambystoma* showing hypothesized changes in ploidy level. Panel A) represents an assemblage with both *A. laterale* (blue) and *A. texanum* (orange). Panel B) represents an assemblage with one or the other host. These assemblages are unidirectional, remaining exclusive to either *A. laterale* (blue) or *A. texanum* (orange) with non-viable routes faded out. Solid unidirectional arrows indicate genome incorporation, black bidirectional arrows indicate genome replacement by alternative genome (L replaces T or T replaces L), and dotted unidirectional arrow indicates hypothesized route of diploidization. .... 35

**Figure 2.2.** Map of Pelee Island, Ontario, Canada, with each grid square representing a 2 km<sup>2</sup> area. Highlighted squares indicate the location of surveyed sites. Pie charts represent community composition at each site. Sexual species (i.e., *Ambystoma laterale* (LL) and *A. texanum* (TT)) are depicted in blue and orange respectively, and unisexuals are broken up by ploidy (2N, 3N, 4N, and 5N; grayscale). Data from the whole island is presented in the middle of the figure. Sample size and observed unisexual genototype richness (R) are provided within each circle plot. .... 36

**Figure 2.3.** Dendrogram representation of unisexual assemblage composition of ten sites across Pelee Island, Ontario, Canada, based on Bray-Curtis dissimilarity indices calculated using the proportion of each unisexual genototype within each assemblage. Relative abundances and confidence intervals of each host and most influential genotypes are provided (for full assemblage compositions see Fig. 2.S1 and Table 2.S3). Values provided for non-zero abundances for single site clusters (Clusters 1 and 2) and average abundances for multi-site clusters (Clusters 3 and 4). Column colors are by host (blue and orange for *A. laterale* and *A. texanum*, respectively) and unisexual ploidy level (grey scale). .... 37

**Figure 2.4.** A) Richness, diversity ( $\lambda$ ), and evenness (V) across Pelee Island, Ontario Canada. Diversity indices were calculated along with estimated error using a bootstrap procedure based on minimum sample size. Richness point values are based on calculated Chao1 index, lower errors indicate identified genototype richness, and high errors based on Chao1 bootstrap confidence up to a maximum of 10 (maximum number of theoretical genotypes for this system). Sites are arranged by cluster and assemblage similarity shown in Fig. 2.3. See supplementary material (Table 2.S3) for sample sizes and site by site breakdown of genototype and ploidy. B) The relationship between the relative abundance of the bisexual host species, and diversity metrics for unisexual assemblages across Pelee Island, Canada. Curves were generated using locally estimated scatterplot smoothing (LOESS) fit, shaded areas represent 95% confidence regions. Clusters indicated by point shape and colors shown in Fig. 2.3. .... 38

**Figure 2.5.** Principal Coordinate Analysis (PCoA) biplots based on unisexual assemblage dissimilarities showing directional influence of A) most influential unisexual genotypes (e.g., LT, LLT, LTT, and LTTT) and B) correlated influence of host

influence. Relative overall explanatory value for each axis are provided. *Ambystoma laterale* (LL) directionality aligns to that of unisexual genototype LLT while *A. texanum* (TT) has an intermediate directional influence comparable to that of LTT and LTTT suggesting correlation. Genototype LT has an orthogonal influence compared to either host and to the host-associated genotypes (LLT, LTT, and LTTT). Clusters indicated by point shape and colors shown in Figs. 2.3 and 2.4. .... 39

**Figure 2.6.** The relationship between the relative host availability (i.e., the proportion of the total salamander assemblage that is *A. texanum* minus the proportion that is *A. laterale*), and genome bias in unisexual assemblages across Pelee Island, Ontario, Canada. ‘Genome bias’ reflects the total genomic contributions of each host per individual within an assemblage. Assemblages with a positive value have more T-biased genomes (e.g., LTT, LTTT, LTTT, LLTTT), whereas assemblages with a negative value are more L-biased (e.g., LLT, LLLT). *Ambystoma texanum* (TT) was the only host available at most sites. *A. laterale* (LL) was the only host present at site B3, and both hosts were present at site D3.1. Clusters indicated by point shape and colors shown in Figs. 2.3 and 2.4..... 40

**Figure 2.S1.** Relative abundances of both hosts (*A. laterale*, LL; *A. texanum*, TT) and the unisexual genotypes (LT, LLT, LTT, and LTTT) by site arranged in cluster groups. .. 44

**Figure 2.S2.** A) Corplot of all Bray-Curtis similarities (1 - dissimilarity) displayed as pie charts above diagonal and numeric values below diagonal. Site clusters are enclosed in squares. B) Bray-Curtis dendrogram aligned to map along with geographic Mantel test result. Site clusters are colored following the scheme from the corplot (A). ..... 45

**Figure 2.S3.** Screeplot of PCoA proportion of explained variances (solid) and comparative broken stick (dashed) with red line where explained variance fall below broken stick indicating loss of informative value. .... 46

**Figure 3.1.** Three alternative proposed routes for novel diploid lineage formation in unisexual *Ambystoma*. Diploidization (left) requires the presence of *A. laterale* (LL) and one other host (here *A. texanum*; TT) in order to produce a symmetrical tetraploid (e.g. LLTT). The symmetrical tetraploid can then produce ploidy-reduced LT diploids composed of a complete complement of randomly subset L and T chromosomes (e.g.,  $L_{\alpha}T_{\alpha}$ ,  $L_{\beta}T_{\beta}$ ,  $L_{\alpha}T_{\beta}$ ,  $L_{\beta}T_{\alpha}$ )<sup>137</sup>. Replacement (center) requires a progenitor LT diploid, resulting in the complete replacement of one haplome while maintaining hybrid status with an *A. laterale* haplome, L. To date, this has not been demonstrated to occur in diploid unisexuals<sup>136</sup> nor has host genotype (e.g., LL, TT) reconstitution been successful<sup>122,265</sup>. Reduction (right) requires a progenitor triploid (LTT here) producing an unfertilized reduced egg that has lost one complete, but randomized, haplome such that the produced diploid maintains a hybrid nuclear genome. Reduced eggs have been observed<sup>139</sup>, but no ploidy-reduced offspring have been verifiably documented in family studies. Note that only one host is necessary for the replacement and reduction routes. Each mechanism outlined has been proposed in the literature, but no direct evidence is currently available for any of these outcomes. .... 73

**Figure 3.2.** Relative abundance of each multilocus lineage for *Ambystoma* salamander breeding sites across Pelee Island, Ontario. Alphanumeric codes indicate site based on location within a grid (see Fig. 3.3) <sup>157</sup>. Sites are grouped based on the historic upland habitat patches with which they are associated (northwest, NW; northeast, NE; east, E; and south, S). Lineages are arranged to display lineage presence and relative abundance in a nested fashion..... 74

**Figure 3.3.** Maps depicting site distribution of diploid unisexual (LT) *Ambystoma* salamander lineages across Pelee Island, Ontario. Boundaries of historic upland habitat patches are represented in light green. A) Cluster map showing sites that group together based on similarity of diploid unisexual lineage composition. Clustered sites are connected by solid black lines. At each site, composition of multilocus lineages (MLLs) is represented by pie charts with sample size and MLL count displayed underneath. Site C3 is presented but was not included in the clustering analysis due to concerns over founder effects. Samples from private lineages are pooled together under the “Private” label for visualization. B) Map of inferred connectivity among sites based on divMigrate analysis of diploid unisexual lineages across Pelee Island. Stronger relative rates of connectivity (Jost’s D) are represented with thicker lines. Values of D < 0.1 are not represented in this figure for the purpose of clarity. .... 77

**Figure 3.S1.** Chroma images of two case examples of *A. texanum* individuals having two Atex74 (green) alleles with one having a 2-bp motif and the second having a 4-bp motif. Ladder (ROX 500, red) presented extends to 350 bp in image. .... 79

**Figure 3.S2.** Two additional Chroma images of *A. texanum* samples demonstrating a 235-bp allele for the 4-bp motif Atex74 (green) allele (top) and a sample with a 4-bp motif allele but without any 2-bp motif allele (bottom). Ladder (ROX 500, red) depicted out to 350-bp. .... 80

**Figure 3.S3.** Four additional *A. texanum* samples with only 2-bp motif Atex74 (green) alleles. Ladder (ROX 500, red) depicted out to 500-bp..... 81

**Figure 3.S4.** Four examples of Atex74 (green) 4-bp motif alleles extending up to and beyond the 500-bp marker in the ladder (ROX 500, red). .... 82

**Figure 3.S5.** Satellite imagery of Pelee Island (Mar 2020, Google Images) overlaid with outlines of historic uplands (grey) using Google Earth. Upland outlines are based on the 1867 Campbell map (Fig. C.2). Sand bars, particularly in the SW and NE corners, have shifted in the 150 years since the Campbell map was drawn. .... 83

**Figure 3.S6.** Frequency distribution of pairwise distances between all sample pairs, includes samples with the same MLG. Black represents the sample pairs that are identified as the same lineage. Samples were inclusively grouped together into the same MLL so long as each sample was at least within two mutations steps of another sample in the same MLL. A single clonal lineage would be demonstrated by a single peak near the start of the histogram while a purely sexually reproducing population would resemble a normal curve <sup>108</sup>. Multiple peaks indicate multiple distinct lineages as samples of the

same lineage would have a distance close to or at 0 while sample pairs from two different lineages would consistently have similar distances from each other. .... 84

**Figure 3.S7.** Frequency distribution of pairwise distances between unique MLG pairs. Only one sample per MLG is represented in these pairings. Six MLG pairs have a pairwise distance of 0 due to missing allelic data for the second allele of either AjeD422 or AmmH123. Black represents the sample pairs that are identified as the same lineage. Samples were inclusively grouped together into the same MLL so long as each sample was at least within two mutations steps of another sample in the same MLL. .... 85

**Figure 3.S8.** Frequency distribution histograms of pairwise Manhattan distances among all sample pairs for each MLL with more than one sample. Only four MLL have any sample pairs with >6 stepwise mutation differences, all of which are among the five most sampled lineages. Of the top 5 most sampled MLL, only MLL-7 has no sample pairs with more than 3 stepwise mutation separation. .... 86

**Figure 3.S9.** Genotype accumulation curve of all LT genotypes, demonstrating a linear increase in genotype richness with increasing number of loci. AjeD283 and AmaD321 were removed from this assessment, and the two different Atex74 motif alleles were considered as a single locus (see Details on Atex74 above). .... 87

**Figure 3.S10.** Lineage accumulation curves demonstrating that MLL richness plateaus at 36 MLL as loci count increases beyond 6 loci. At minimum, all MLL can be identified using at least 5 loci, while not all MLL could be identified with two sets of 11 loci. .... 88

**Figure 3.S11.** Completeness curves for each site based on rarefaction and extrapolation calculations from iNEXT. Sample coverage estimates the proportion of the total number of individuals in an assemblage that belong to lineages represented by our sample, such that a value of 1 indicates that all individuals from an assemblage are represented by lineages documented. Coverage values have been extrapolated for each site out to a theoretical sample size of 300, with confidence intervals for the entire range of sample sizes. .... 89

**Figure 3.S12.** A) Silhouette widths calculated by kmeans clustering, identifying 4 optimal clusters. B) Total width sum of squares (WSS) calculated by kmeans clustering identifying 4 optimal clusters. .... 90

**Figure A.1.** A) Diagram of intergenomic crossover process. Within a symmetrical tetraploid (blue = *A. laterale*, orange = *A. texanum*), the hypothesized diploidization process could result in four outcomes dependent on if intergenomic crossover occurs between homeologous chromatids. In three outcomes, at least one chromatid is chimeric, possessing regions originating from two different species. B) Assuming two targeted loci map to the same chromosome (Locus 1 – green band, Locus 2 – red band), each of the four offspring have distinct genomic outcomes. Two outcomes (middle) represent a misidentification of genotype (G) due to one locus signaling two copies from one species and the second locus signaling one copy from each species. One outcome

represents a correct genototype (right) but two chimeric chromatids. The last offspring (left) is a ‘true’ LT with intact chromatids. .... 143

**Figure A.2.** Karyotype of the axolotl (*A. mexicanum*) genome. Microsatellite loci are mapped with color depicting species from which loci were originally identified from. Not all loci could be effectively placed due to either low confidence in mapping or multiple placements of equal support. Centromeres are marked as black bars. Chromosome arms are arranged q-arm on the left of the centromere and p-arm to the right. .... 146

**Figure A.3.** Loci locations for 11 of 14 loci used in this PhD thesis. Loci AmmH123 and H123b are the same locus but different primer sets derived from the same published microsatellite sequence. Three loci were unsuccessfully mapped: Atex74 (more than one region with 100% query coverage), AjeD422 (no significant alignment), and AmaD42 (no significant alignment). Chromosomes 5 and 6 each have three loci mapped to them, chromosome 3 has two loci, with chromosomes 10, 9, and 1 each having one locus each. .... 147

**Figure A.4.** Sequence alignment quality measures of matched primer sequences for loci where primer pairs were successfully matched. Species order from left to right goes from closest relative to most distant relative of *A. mexicanum*<sup>334</sup>. More distant relatives had comparably fewer primer pair alignments, with primer pairs derived from the most distant relatives (*A. talpoideum* and *A. maculatum*) generally having lower identity match and higher numbers of mismatched base pairs. .... 149

**Figure A.5.** Some microsatellite sequences would have complete coverage, but in sections along a localized region. AcroD315 for example was separated into four sections that aligned along adjacent sequences, with some (sections b and c) having small degrees of overlap along the repeat region. While the repeat region of interest is fully identified, sections a and d are separated from it by a few hundred bp. Given the close proximity, one might postulate a large insertion event between sections a and b, and a translocation event separating subsection d upstream from the other three subsections. Alignments provided by SequenceServer<sup>340</sup>, figure generated by Kablammo<sup>341</sup> ..... 154

**Figure A.6.** Project flow chart detailing file inputs (grey), outputs (black), intermediary data files (green), data processing steps (orange), data management steps (yellow), and functions (blue). .... 155

**Figure A.7.** Depiction of the general process for this project. A) Microsatellite sequence (gray) from GenBank accession is aligned to the reference genome (black), with the sequence to which the microsatellite is aligned is then pulled out and used as a reference for the alignment of the primer set (green) for that locus. B) Quite commonly, the microsatellite sequence would break alignment along the repeat region (orange) that the primer set is trying to target. Consequently, only a single primer from the pair could properly align. In these situations, the primer set would be removed from consideration in the final analysis because the complementary primer alignment could not be evaluated. .... 156

**Figure B.1.** Collection of spermatophores presumptively left by an *A. texanum* male at site D3.1, found on March 23, 2019. These “sperm gardens” can be found in ponds during breeding season. .... 185

**Figure B.2.** Additional image of a “sperm garden” left by an *Ambystoma texanum* male on March 23, 2019, situated in a shallow pit left behind by a treefall..... 186

**Figure B.3.** Image of a salamander with presumed skeletal deformity found on May 10, 2019 on Pelee Island, Ontario. This individual never straightened out and maintained distorted spinal arrangement when mobile. .... 186

**Figure C.1.** Survey map of Pelee Island, Ontario by P. D. Salter in 1847 <sup>168</sup>. The first known survey map of Pelee Island identifying historic uplands and inland marshes. A ‘Big Spring’ is identified in approximately the same location as site B6 used in this thesis. .... 187

**Figure C.2.** Survey map of Pelee Island, Ontario by Campbell in 1867 <sup>167</sup>. Historic upland demarcations of this reference map, outlined in green, were used in Chapter 3 to identify which sites were associated with each upland..... 188

# Chapter 1: Introduction

## General Introduction

Biological diversity has a multitude of meanings, often dependent on the system being investigated or the scientific questions being asked. For instance, while community or species diversity is typically used to describe what species are present within an ecosystem<sup>1,2</sup>, functional diversity<sup>3,4</sup> and structural diversity<sup>5,6</sup> can each be used to specify how species interact within an ecosystem. Some have taken to referring to “dimensions of diversity” in recognition of the numerous ways biologists categorize diversity<sup>7,8</sup>. Each dimension of diversity can be measured at various spatiotemporal reference frames depending on the scale and resolution of interest<sup>9,10</sup>, with each category being defined by different properties (e.g. richness, evenness, and heterogeneity)<sup>11,12</sup> and scales<sup>13,14</sup>. In this way, diversity can be encompassed by a multitude of metrics, each with a specific interpretation that informs our understanding of ecological systems. As biological and ecological theory advances and the list of analyses and interpretations expands, collectivizing these metrics into separate dimensions of diversity has become more challenging. To better catalog the progression of research and contextualize the analyses, subdivisions of the various dimensions of diversity may be warranted. Critically, while each of these dimensions and their aspects are used to explore fundamentally different questions, they must be considered holistically to fully understand biodiversity<sup>15</sup>, the multitude of ecological dynamics, and the processes through which ecosystems function.

## Community Diversity

Community diversity studies typically measure species variation within an environment but in some cases there may be the need to examine patterns of diversity within one or few related species that form “assemblages”<sup>16</sup>. In theory, such measures of diversity are valuable as they can help infer an ecosystem’s stability, maturity, productivity, evolutionary time, interspecific pressures, and spatial heterogeneity<sup>17</sup>. However, the term “diversity” has become a catch-all due to the varied and disparate ways in which it has been measured, effectively making it a “nonconcept”<sup>18</sup>. In order to disentangle these meanings, The overarching concept may be classified into different scales:  $\alpha$ -,  $\beta$ -, and  $\delta$ -diversity<sup>13,14</sup>.

Many have taken to classifying  $\alpha$ -diversity indices into three forms of information: richness, evenness/equitability, and heterogeneity<sup>11</sup>. Richness is typically based strictly on incidence data. While generally understood as how many species (N) are within a community, researchers have long recognized that the realities of sampling limitations invariably result in an underestimate of true richness<sup>11</sup>. To compensate for this, estimators relying on the number of species with one (Chao1) and/or two (Chao2) incidence recordings in a sample were developed to project the true number of species within a community<sup>19</sup>.

Compared to richness, evenness (sometimes referred to as “equitability”) measures are plentiful with varied interpretations and use cases. In brief, evenness indices describe how uniform a community’s composition is<sup>20</sup> by measuring how equally abundant species are within the community<sup>21</sup>. Despite its seeming simplicity, evenness measurements have practically become a sub-discipline of ecological theory, to the point

where evenness may be defined distinctively from equitability<sup>22</sup> with some arguing for necessary mathematical properties for a metric to be considered a true evenness index<sup>23</sup>. While a multitude of evenness indices exist<sup>21-23</sup>, there are those that appear more regularly in the literature such as Pielou's  $J'$ <sup>24</sup> or Simpson's evenness index,  $V$ <sup>18</sup>.

Heterogeneity can be thought of as the effective number of species<sup>25</sup>, incorporating both species richness and evenness<sup>22</sup>. Much like evenness indices, heterogeneity measures are numerous, though the most common measures of heterogeneity are the Shannon-Wiener index (Shannon diversity or Shannon entropy) or some variant of Simpson index<sup>26</sup>. Each of these metrics have different biases based on species rarity<sup>11</sup>, and therefore distinct interpretations. For instance, the Shannon-Wiener index can be considered as the minimum number of yes/no questions, on average, needed to identify a species<sup>27</sup>, while the Simpson index can be interpreted as the probability that two independently chosen individuals from a population will be the same species<sup>26</sup>. Of these metrics, Simpson's reciprocal is most aligned to the "effective number of species" definition of heterogeneity<sup>27</sup>.

Up to now, this discussion of community diversity has been focused on the assessment of diversity within a single community at one given time point, or  $\alpha$ -diversity. Where  $\alpha$ -diversity can be considered diversity within a designated habitat,  $\beta$ -diversity measures how alike two communities are. For this reason,  $\beta$ -diversity metrics are often referred to as "distances". However, not all are true mathematical distances but rather are "dissimilarities" such as the widely used Bray-Curtis index<sup>28</sup>. A valuable attribute of  $\beta$ -diversity is that it can be used to compare not only spatial, but also temporal patterns of diversity. Each reference frame, spatial or temporal, will provide distinct information and

can be used to assess questions based in either geographic or temporal contexts respectively.

Metacommunity theory, has become widely popular to address the interactions of multiple communities on a landscape level <sup>29,30</sup>. In a metacommunity or meta-assemblage context, temporal processes and spatial dynamics can have strong interactive effects <sup>31-33</sup>. For instance, after an assemblage expands outwards and colonizes a new space, the arrival order of species or lineages can prevent or limit successful colonization of secondary dispersers leaving “priority effects” reflected in the assemblage’s structure <sup>34</sup>. The complement to priority effects may be “legacy effects”, where past events or the presence of a species in the past can leave impacts on contemporary systems <sup>35</sup>. Legacies can come in a multitude of forms, requiring the use of different dimensions of diversity to fully explore their influences <sup>36</sup>. To properly assess the processes leading to contemporary metacommunity structure, the system’s spatiotemporal dynamics must be recognized when drawing conclusions from the data.

Habitat heterogeneity likewise influences spatiotemporal patterns of metapopulation patch occupancy <sup>37</sup> and should be considered to have similar effects for metacommunities or meta-assemblages. Interpatch distance and landscape resistance can influence connectivity patterns across a landscape <sup>38</sup>, though can shift over time as suitable habitat patch size <sup>39</sup>, landscape cover <sup>40</sup>, and structure may change <sup>41</sup>. However, the impacts felt by habitat heterogeneity dynamism will vary depending on the species of concern <sup>37</sup>. As each species responds differently, this further suggests that interspecific interactions may likewise shift in a dynamic fashion following spatiotemporal habitat

changes<sup>42</sup> potentially leading to local extinction events as species become more or less competitive with each other<sup>43,44</sup>.

### **Sexual Parasite Ecology**

The study of alternative reproductive systems has greatly expanded in recent decades as more non-sexually reproducing animal groups have been formally described<sup>45,46</sup>. However, research on the dynamics of these systems lags considerably when compared to closely related sexual species<sup>47,48</sup>. Not only are these systems underutilized resources for ecological and genetic study<sup>49,50</sup>, but their atypical reproduction often interplays with other species resulting in modified ecosystem interactions<sup>51,52</sup> or evolutionary dynamics of more well-understood species<sup>53,54</sup>. To advance ecological theory, and better address conservation concerns specific to these unique systems, alternative reproductive systems require greater investigation into understanding their genetic dynamics and the ecological implications of such dynamics.

Part of the challenge with alternative reproductive systems is the diversity of modes and outcomes (reviewed in<sup>55</sup>). While parthenogenesis (e.g. *Daphnia* sp.<sup>56</sup>) typically requires no partner for reproduction (though see pseudocopulatory behavior in *Aspidoscelis* [*Cnemidophorus*] sp.<sup>57</sup>), many other alternative modes of reproduction do require an additional partner either for egg stimulation (gynogenesis: e.g. *Poeciliopsis monarcha*<sup>58</sup>) or genome replacement (hybridogenesis: e.g. *Pelophylax* [*Rana*] *esculenta*<sup>59</sup>). The necessity of a viable sexually reproducing host leads to resource competition<sup>52,60</sup>. In particular, the competition for sperm between sexual and non-sexually reproducing species has led some to label such groups as “sexual parasites”<sup>48,61</sup>. As many sexual

parasites are all female, they can have greater population growth rates<sup>62</sup> which could lead to the loss of the sexual host due to over competition<sup>63,64</sup>.

Many studies have investigated the consequences of parasitism on host species<sup>65,66</sup> and there is a growing consensus that parasite ecology is far more complex and dynamic than previously appreciated, influencing not just the host but broader ecological processes as well<sup>48,67</sup>. For example, there are many indirect effects parasites may have on the coexistence of multiple hosts. While one host may be a stronger competitor in isolation, the presence of a parasite can give advantage to the weaker competitor if the parasite has unequal influence on the two hosts<sup>68</sup>. Additionally, sexual parasites with multiple hosts exhibit a form of ecological fitting<sup>69</sup> when encountering a novel habitat, as they can rapidly incorporate the locally-adapted genetics of their new host population<sup>70,71</sup>. Therefore, not only can parasites influence host populations<sup>72,73</sup>, but they may also be influenced by host diversity<sup>74,75</sup>.

Furthermore, as hosts are a fundamental aspects of a parasite's habitat, host diversity, distribution, and dispersal can impact a parasite's ecology and diversity<sup>76-79</sup>. For example, host switching can allow the sexual parasite to broaden their range potential beyond that of any single host<sup>80,81</sup>. Intriguingly, this can be reflected in divergent patterns of genetic diversity between the parental haplomes within hybrid sexual parasites<sup>82,83</sup>, once again highlighting how recognition of different dimensions of diversity can advance our understanding of ecological dynamics.

## **Genetic Diversity**

Genetic diversity is broadly understood as a measurement of the genetic variation present within an individual or group of organisms<sup>84</sup>. This dimension of diversity is often

used to assess a population's stability<sup>85-87</sup>, disease and parasite resistance<sup>88,89</sup>, or connectivity to other populations<sup>90,91</sup>, among other uses (reviewed in<sup>92</sup>). While usually reliant on seemingly simple allelic data, the measures of genetic diversity are numerous<sup>84,93</sup>. This is because of a variety of factors such as group size, type of loci, or type of genetic material being assessed<sup>84</sup>. However, this also means that studies into genetic diversity can be highly tailored towards specific, yet expansive, questions<sup>94,95</sup>.

There is increased interest in not just measuring genetic diversity but also assessing the ways in which it is maintained within and among populations. For instance, landscape genetics has become a burgeoning field of study to investigate how landscape structure can influence population genetics<sup>96,97</sup>. While local landscape modifications certainly can impact local populations, broader changes in landscape structure and use can impact connectivity pathways, altering gene flow<sup>98,99</sup> and producing persistent genetic legacy effects, including "founder effects"<sup>100-102</sup>. However, these changes may not leave an immediate impact on genetic structure, causing a lag between the inciting incident and a measurable signal<sup>103,104</sup>. Consequentially, there is growing interest in investigating specifically how such time lags from past events, landscapes, or interactions influence interpretation of genetic diversity<sup>41,105,106</sup>. Furthermore, landscape modifications may result in changes to how populations interact with their environment, leading to shifts in selective pressures that take time to be realized within a population's genetic structure<sup>35,107</sup>. Therefore, genetic diversity, much like community diversity, can be influenced both by contemporary interactions and historic legacies. Importantly, the signal of these distinct driving forces differ, allowing for hypothesis testing.

## Dynamics of Clonality

In the past two decades, strides have been made to formalize and contextualize genetic diversity in clonal systems<sup>108</sup>. The use of multilocus genotypes (MLG) have become a common way to identify genetically distinct individuals<sup>108,109</sup> which can be refined depending on loci count and allelic diversity of loci used. However, due to occasional mutation or scoring errors, individuals may be identified with different MLG even though they are related via clonal reproduction<sup>110</sup>. In such cases, the use of a multilocus lineage (MLL)<sup>108,111</sup> as an aggregation of closely related MLGs may be more practical to avoid over-interpretation of potentially paraphyletic relationships<sup>110</sup>. While individuals within a single MLL would be related by phylogeny, that is not necessarily the case between individuals of two different MLL. In this way, MLL can be considered a specific type of operational taxonomic unit (OTU). As a discrete OTU, metrics typical of community diversity (e.g. alpha diversity and beta diversity) can be used to describe clonal lineage diversity as well<sup>108,112</sup>. The use of MLL can be further extended depending on the sample size and allelic richness found within the loci used. For instance, within-lineage genetic diversity could then be described and used to determine lineage age<sup>113</sup>, connectivity patterns among sites<sup>114,115</sup>, or colonization timelines<sup>116,117</sup> based on mutation rate estimations. While refined interpretations of such metrics require an understanding of the dynamics of the clonal system in question, the use of MLL expands the research potential for clonal systems.

Beyond the genetic consequences of clonality, clonal systems also must interact with their local environment. Intriguingly, clonal lineages can have distinct niches compared to their sexual counterparts due to the overall genetic variability within their

respective populations <sup>118</sup>, making stable coexistence a complex endeavor <sup>53,119</sup>.

Compounding this, different lineages may exhibit distinct niches from one another <sup>120</sup> resulting in more variable competition. Should lineage diversity patterns exist upon a landscape, these divergent niches may also lead to variable competitive pressures among assemblages <sup>101</sup>. In the case of sexual parasites, variable pressures within a meta-assemblage could promote genetic diversity within the sexual hosts <sup>121</sup>.

### **Unisexual *Ambystoma***

Unisexual *Ambystoma* are a monophyletic clade of all-female sexually parasitic nuclear hybrid salamanders that form mixed-ploidy assemblages composed predominantly of genetic clones <sup>122–124</sup>. Mitochondrial genetic data supports a single origin ~5 million years ago <sup>125</sup> from an ancestral population most closely related to *A. barbouri* <sup>126</sup>. This group of unisexual hybrids ranges from the southern tip of Lake Michigan to the east coast of the United States and Canada, including Prince Edward Island, overlapping with the ranges of five known host species: *A. laterale*, *A. jeffersonianum*, *A. texanum*, *A. barbouri*, and *A. tigrinum* <sup>127,128</sup>.

As genetic hybrids, all unisexual *Ambystoma* simultaneously maintain genomic representation from at least two different host species, invariably with at least one full haplome derived from *A. laterale* <sup>123,127</sup>. Individuals are assigned “genomotypes”, a genetic biotype category separate from a “species” classification, that reflects the genomic contributions of each host species and their dosage <sup>129,130</sup>. For instance, a triploid genomotype LTT indicates one complement of *A. laterale* chromosomes and two complements of *A. texanum* chromosomes. To date, 25 genomotypes have been

documented in the wild ranging from diploid to pentaploid with at least one tetraploid also being a tetrahybrid (LTJTi) <sup>128</sup>.

Unisexual *Ambystoma* use a unique reproductive mode referred to as “kleptogenesis” (“birth by theft”) as they are considered to “steal” sperm from a bisexual host species to reproduce <sup>124,131</sup>. Much like gynogenesis, sperm from one of these hosts is required for successful egg development <sup>132,133</sup>. While unisexual offspring are predominantly clones of the mother, offspring produced by kleptogenesis occasionally incorporate the haplome provided by the fertilizing host’s sperm (known as “ploidy elevation”) or may exhibit genome replacement wherein one haplome from the mother is replaced by the sperm-borne haplome <sup>134</sup>, a process more similar to hybridogenesis. Comparatively, genome replacement appears to be relatively rare <sup>135,136</sup> and potentially associated with a novel host <sup>134</sup>. A hypothesized fourth outcome predicts diploid hybrid offspring being produced by symmetrical tetraploid unisexuals <sup>137</sup>, though has not been empirically observed and symmetrical tetraploid individuals appear to be rare. Lastly, some have suggested ploidy reduction as a fifth potential outcome, where the offspring are produced from reduced eggs without the incorporation of the sperm-borne haplome <sup>138–140</sup>. However, when the genetic <sup>140</sup> or isozyme <sup>131</sup> data is reviewed, reported instances appear more likely to result from genotyping error induced by allele dropout or likely hidden dosage effects <sup>141</sup> (E. Bare *personal observation*).

In the wild, unisexual *Ambystoma* populations tend to be heavily triploid biased <sup>142,143</sup>, perhaps suggesting that triploidy offers a balance of the numerous pros and cons to polyploidy for this system, though diploid exclusive populations <sup>136</sup> and higher ploidy level biased populations <sup>142–144</sup> have been documented. Across their range, genotypes

vary in accordance with local host species availability<sup>145,146</sup>. Where multiple hosts are present, such as in the Michigan and Ohio region of their range, unisexual *Ambystoma* can have more varied assemblages with tri- or tetra-hybrid genotypes<sup>128,146</sup>. Even in such cases though, triploid genotypes are overrepresented and genotype diversity is minimal. Genotypic (MLG) diversity is also regularly quite low when compared to local host populations<sup>144,147,148</sup>, with much of the variation present likely being attributable to single-step mutations in microsatellite loci or genome replacement<sup>126,134,136</sup>.

Genotypes seemingly take on intermediate niches based on host genomic contributions<sup>81,146</sup>, reflective of their equivalent genome expression<sup>149</sup>. Periodic bouts of genomic introgression from host populations<sup>150</sup> have seemingly allowed unisexual populations to both rapidly adapt to local environments by “stealing” from the locally adapted population, but also stave off the effects of Muller’s ratchet<sup>151,152</sup> by providing a mechanism by which deleterious mutations may be purged. Introgression is likely facilitated by a lack of sexual selectivity on the part of “pure” males, as documented in *A. texanum* and *A. laterale* by Licht and Bogart<sup>153</sup>. The fact that *A. texanum* males deposit fields of spermatophores accessible to all females further encourages genetic introgression<sup>154,155</sup> (E. Bare *personal observation*; Figure B.1 and Figure B.2).

While quantifying the mechanics of such a complex system is daunting, it also offers a unique opportunity to test various threads of ecological theory across a broad range of disciplines. In the remaining chapters of this thesis, I will demonstrate how this system can be used to explore various axes of genetic diversity and how each axis can individually provide insight into different aspects of ecological theory.

## Pelee Island

In this thesis, I focus specifically on the unisexual complex of Pelee Island, Ontario, Canada, located in the western basin of Lake Erie. Unisexual *Ambystoma* assemblages on Pelee Island are distinct in being predominantly diploid<sup>156,157</sup>, whereas assemblages of unisexual *Ambystoma* are mostly triploid across their range<sup>142,143</sup>. Additionally, Pelee Island has two known host species, *A. laterale* and *A. texanum*<sup>156,158</sup> and is situated at the southern and northern extremes of their respective ranges<sup>127,159</sup>. While *A. laterale* is widespread on mainland Ontario, Pelee Island has the only population of *A. texanum* in Canada and is federally listed as endangered<sup>160,161</sup>. Consequently, the unisexuals on Pelee Island, which are reproductively dependent on *A. texanum*, have now been listed as endangered as well<sup>162,163</sup>.

Pelee Island (41.8 km<sup>2</sup>) is the largest island in the western Lake Erie archipelago and situated roughly 13 km south of mainland Ontario and 19.5 km north of mainland Ohio. The island formed ~5000 years ago following isostatic rebound and the filling of the Erie basin during the Nipissing Transgression<sup>164–166</sup>. Following the Erie basin filling, Pelee Island was structured as four discrete dry uplands<sup>165,166</sup> with uplands separated by one primary marshland (“Big Marsh”) and four smaller marshes (“Lighthouse Marsh”, “Middle Marsh”, “South Marsh”, and “Marsh”; see Figure C.1 and Figure C.2)<sup>167,168</sup>. Following increases in human settlement starting in 1867, the dry uplands of the island that were heavily forested were almost entirely logged for agricultural purposes<sup>169,170</sup>. While records suggest that the marshlands dried up periodically<sup>169</sup>, the two largest marshlands were permanently drained when an internal drainage system that was

completed in 1889<sup>169</sup>. The drainage systems have remained active and were renewed in 2008<sup>171</sup>.

Conservation and restoration efforts have brought Pelee Island back to 32% natural cover<sup>172</sup> with multiple projects aimed at further wetland development and restoration<sup>173</sup>. Three significant ecological spaces of the island have also been maintained for conservation<sup>174</sup>: Lighthouse Point Provincial Nature Reserve (maintained by Ontario Ministry of Natural Resources and Fisheries, OMNRF), Fish Point Provincial Nature Reserve (OMNRF), and the Stone Road Alvar complex (Essex Region Conservation Authority, Ontario Nature, and The Nature Conservancy of Canada, NCC). Additional land parcels have been acquired by the NCC and the Pelee Island Winery<sup>174</sup>, resulting in ~18% of the island as protected environmental lands and an additional ~10% in environmental review<sup>175</sup>. Occasional winter storms have led to significant landscape changes as well. For instance, the erosion of sandbanks that protect wetlands from Lake Erie has been seen following the winter storms of 2018/19 and 2021/22 (E. Bare *personal observation*) and has been of concern for decades<sup>176</sup>.

### **Goals of the thesis:**

In this thesis, I investigate how genetic diversity can be further broken down into deeper axes of diversity. These axes of genetic diversity offer new insights into unisexual *Ambystoma* ecology and their interactions with their host species when viewing their properties across different scales. In Chapter 2:, I focus on the genomotype (“biotype”) axis of unisexual diversity and I show that unisexual genomotype diversity reflects host availability at a local scale, impressing the notion that host species are akin to some definitions of “keystone species”. In Chapter 3:, I demonstrate that the lineage axis in

unisexual *Ambystoma* primarily reveals the impact of historic landscape structure, with some additional contemporaneous influences. Chapter 3: also provides indirect evidence supporting the mechanism of diploidization from symmetrical tetraploids, a previously hypothesized reproductive outcome for unisexual *Ambystoma*. Throughout this thesis I show that unisexual *Ambystoma* assemblage structure is associated with host diversity in different ways depending on the genetics axis(es) that are examined. Lastly, I discuss how the investigation of multiple axes of diversity can improve our understanding of the key ecological processes at play.

## Chapter 2: Diversity and composition of mixed-ploidy unisexual salamander assemblages reflect the key influence of host species

Evan A. Bare<sup>1</sup>, Jim P. Bogart<sup>3</sup>, Chris Wilson<sup>1,4</sup>, Dennis L. Murray<sup>1,2</sup>, Thomas J. Hossie<sup>1,2</sup>

<sup>1</sup> Environmental & Life Sciences Graduate Program, Trent University, Peterborough, ON, K9L 0G2

<sup>2</sup> Biology Department, Trent University, Peterborough, ON, K9L 1Z8

<sup>3</sup> Department of Integrative Biology, University of Guelph, Guelph, ON, N1G 2W1

<sup>4</sup> Aquatic Research and Monitoring Section, Ontario Ministry of Natural Resources and Forestry, Peterborough, ON, Canada

This chapter of the thesis has been published<sup>157</sup>.

### Abstract

Understanding processes that govern and sustain biological diversity is a central goal of community ecology. Unisexual complexes, where reproduction depends on sperm from males of one or more bisexual host species, are rare and the processes driving their diversity and structure remain poorly understood. Unisexual *Ambystoma* salamanders produce distinct biotypes (“genomotypes”) depending on which bisexual species they ‘steal’ sperm from. This reproductive mode should generate distinct assemblages depending on the locally available bisexual host species. Yet, how availability and

---

Author Contributions: EAB, JPB, DLM, and TJH conceived and designed the study. EAB and JPB conducted the genotyping work. EAB and TJH conducted fieldwork. JPB and CW provided advice on lab techniques. EAB analyzed the data and TJH collaborated on statistical analysis. EAB and TJH wrote the manuscript. All authors provided critical feedback and contributed to the final version of the manuscript.

relative abundance of multiple bisexual hosts influences composition and diversity of natural unisexual assemblages at local or regional scales remains unknown. We hypothesize that host identity most directly drives local assemblage composition, with host variation associated with increased beta and gamma diversity within unisexuals. We collected genetic samples from *Ambystoma* salamanders across Pelee Island, Ontario, Canada (2015-2022). Two host species were identified (*A. texanum* and *A. laterale*) with nine sites having a single host and one site having both. Unisexual assemblages were grouped into four clusters by similarity, with host identity being a key determinant. Gamma diversity increased as a result of distinct host-specific assemblages forming at different sites on the island (i.e., high beta diversity). Assemblage composition, but not diversity, was correlated with relative host abundance, which may reflect matching niche requirements between host and unisexual forms they produce. Our results demonstrate that diversity and structure of unisexual assemblages are clearly shaped by their host(s) and such systems may serve as models for studying how biotic interactions shape ecological communities.

**Key Words:** *Ambystoma*, community ecology, kleptogenesis, keystone species, species complex

## Introduction

A central goal of community ecology is to understand processes governing and sustaining biological diversity. Fundamentally, ecological communities are composed of members whose niche requirements are met by prevailing abiotic conditions as well as biotic interactions within the ecosystem<sup>177,178</sup>. Environmental variation undoubtedly plays an important role in determining composition and diversity of ecological communities, and more heterogeneous environments may support higher species diversity because they provide a wider range of available niches<sup>179</sup>. Biotic interactions among community members can also have strong impacts on community composition and diversity<sup>180,181</sup>. Understanding how species interactions influence diversity, as well as the processes driving variation in diversity along spatial and temporal scales, remains a top priority in ecology<sup>182,183</sup>. While environmental conditions may set some of the broad patterns in ecological communities, presence and distribution of certain species across the landscape can dramatically influence the structure of local communities<sup>182,184</sup>. Thus, quantifying the role of biotic interactions in driving community structure remains essential to understanding patterns of diversity.

Broadly speaking, keystone species are recognized as having a disproportionate role in shaping the diversity or structure of an ecological community or assemblage<sup>185</sup>. The loss of such species is expected to cause a large shift in community structure, leading to local extinctions and fundamental changes in biotic interactions across the system<sup>186</sup>. Yet, the effects of keystone species can be context-specific<sup>187</sup>, and distinct keystone effects are generally not interchangeable<sup>188</sup>. Consequently, sympatry of multiple keystone species can elevate species diversity through additive effects on the community

<sup>189–191</sup>. In addition, interactions among two or more members of a community can produce ecosystem- or community-level effects that are greater than those of any individual species (i.e. ‘keystone interactions’)<sup>192</sup>. Although diversity might also be impacted by the abundance of a keystone species <sup>193,194</sup>, it remains unclear whether communities respond to variation in composition of keystone species <sup>185,193,194</sup>.

Unisexual salamanders of the genus *Ambystoma* (henceforth, ‘unisexuals’) are an ancient monophyletic lineage of nuclear allopolyploid genomic hybrids which persist over an extensive range in eastern North America by ‘stealing’ sperm from as many as five sympatric, bisexual species of *Ambystoma* <sup>126,163</sup>. These all-female unisexual salamanders are obligative reproductive parasites of the bisexual species they live alongside <sup>128</sup>. While the majority of unisexual offspring have a genotome identical to their mother, unisexuals may also produce offspring with a variety of distinct genotypes through genome incorporation from sperm provided by locally available host(s) <sup>128,195</sup> (Figure 2.1). All unisexuals possess nuclear genomes derived from at least two contemporary bisexual species and range in ploidy from diploid (2N) to pentaploid (5N) <sup>124,163</sup>. Consequently, unisexual assemblages are composed of individuals with a diversity of ‘genotypes’, which vary in chromosome number and composition <sup>129</sup>. The niche requirements of each genotype may also vary <sup>81,146</sup>, given that genotypes exhibit phenotypic variation reflective of differences in ploidy and proportional genomic contributions of their host species <sup>149</sup>. In treating each genotype as an ‘ecological species’ within the broader unisexual complex <sup>196,197</sup>, this unique system provides an exceptional case for studying the role of biotic interactions in governing patterns of diversity and community composition.

While the reproductive biology of this system is now reasonably well understood, it remains unclear how these interactions are realized under natural conditions to determine the diversity and composition of unisexual assemblages across the landscape. Our contemporary understanding suggests that structure of unisexual assemblages should be determined by identity of the locally available bisexual host, through production of distinct (host-specific) genotypes. Furthermore, when multiple hosts are available, potential for additional genotypes is unlocked and can thereby increase assemblage diversity through additive effects (i.e., other host-specific genotypes), as well as interactive effects (i.e., genotypes which arise only when both hosts are present) (Figure 2.1). The loss of a bisexual host at a given site should halt production of certain genotypes and lead to a dramatic shift in unisexual assemblage composition over time, and eventually, extirpation of the entire assemblage if no other host is available<sup>148</sup>. Thus, each bisexual host species has an ecological role analogous to a keystone host<sup>198</sup> promoting biological diversity by facilitating colonization, establishment, persistence, and formation of several unisexual genotypes.

We investigate variation in the structure and diversity of unisexual assemblages at breeding sites across Pelee Island, Ontario, Canada. Pelee Island provides a rare opportunity to study a unisexual system with isolated assemblages occurring in sites that vary in the number and identity of bisexual host species. Interestingly, historic data from the island suggests substantial variation in assemblage composition, even among sites with a common bisexual host<sup>158,162</sup>. We predict that the composition of unisexual assemblages varies across the island, and that unisexual genotypes present at each site have more copies of the genome associated with the known bisexual host at the site (i.e.,

have a host-associated ‘genome bias’). Accordingly, we expect to observe greater variation in assemblage composition (beta diversity) between sites that differ in host species composition. Further, we predict that assemblages with two bisexual hosts would have the greatest diversity (alpha diversity) of unisexual genotypes. Finally, we use our unique dataset to explore the effect of bisexual host abundance on assemblage diversity and evenness, to investigate the possible impact of host species abundance on diversity. Overall, we seek to understand and quantify the extent to which patterns of alpha, beta, and gamma diversity in unisexual assemblages are driven by biotic interactions with their host(s).

## **Methods**

### Study System

Our study was conducted on Pelee Island (41.8 km<sup>2</sup>) in Lake Erie, Ontario, Canada (41.6 N, -82.6 E). Amphibian populations on Pelee Island were isolated from the mainland following the island’s formation after glacial retreat, around 4000 BP<sup>164</sup>. Unisexual populations on the island are found syntopically with either (or both) *Ambystoma texanum* and *A. laterale*<sup>158,162</sup>. Patches of suitable habitat consist of both terrestrial and aquatic environments sufficient for foraging, dispersal, breeding, and hibernation<sup>162,163</sup>. Across the island, patches are largely isolated from one another due to habitat fragmentation arising from human development (i.e., agriculture, irrigation, roads). Herein we use an existing ‘genotype’ nomenclature where, for example, ‘LTT’ represents a triploid with a single set of *A. laterale* (L) chromosomes, and two sets of chromosomes from *A. texanum* (T)<sup>128,129</sup>. When unisexuals have greater number of chromosome complements from one host species, we refer to it as having a ‘genome bias’

favoring that host. For instance, an LT unisexual has no bias, but an LTT has a T-biased genotype. Previous work found diploid unisexuals (LT) to be abundant on the island<sup>195</sup>, while diploid unisexuals are generally rare elsewhere across the unisexual *Ambystoma* range<sup>142,143,199</sup>.

Unisexuals reproduce by ‘kleptogenesis’, a unique reproductive mode that has four primary outcomes: 1) the offspring is a genetic clone of the mother; 2) the sperm genome is incorporated into an unreduced egg to produce a ploidy-elevated offspring; 3) genome replacement, resulting in an offspring of the same ploidy as the mother but with a novel genotype and potentially different genome; and 4) an hypothesized mechanism where symmetrical tetraploid (e.g. LLTT) mothers produce diploidized unisexual offspring (e.g., LT)<sup>128,137</sup>. With this diversity of potential reproductive outcomes (see Figure 2.1), multiple genotypes can be derived *in situ* and can live sympatrically. Note that parental genotypes (i.e., LL or TT) are never reconstituted from the unisexual lineage<sup>133,136</sup>.

### Salamander Sampling

Between Sept-2015 and Aug-2022, *Ambystoma* salamanders were sampled from sites across Pelee Island (Figure 2.2) using a combination of opportunistic search, coverboard surveys, and minnow trapping during the breeding season (March). Most sites were located on protected lands, with additional sites located on private property where access permission was granted. Two areas with known salamander populations were not sampled because access permission could not be secured. We sought to be as comprehensive as possible in our selection of sites across the island with sites having variable habitat conditions<sup>200</sup>, but additional unsampled sites may exist. Nevertheless, we

suspect that our sample includes >80% of *Ambystoma* breeding areas on Pelee Island. On average, sampled sites were separated by 4.6 km ( $\pm 2.8$  SD, median: 4.4 km, range: 0.6 km – 10.9 km), and all sites were separated from one another by at least 1 km, except for two pairs of sites that were separated by 600 m (D3.1 and D3.2) and 750 m (D3.2 and C3). In all cases sites were separated by a distance greater than twice the reported breeding migration distances for *A. texanum* (125 m)<sup>201</sup> or *A. laterale* (281 m)<sup>202</sup>. Further, distances between almost all site pairs were more than twice that of proposed terrestrial buffer sizes for salamanders: 218 m<sup>203</sup> and 400-450 m for *A. jeffersonianum*<sup>204</sup>. Neither host studied herein is reported to make breeding migrations of such distances, and unisexual *Ambystoma* with elevated ploidy are thought to exhibit lower dispersal capacity compared to their diploid bisexual hosts<sup>130,204,205</sup>. Thus, while nearby sites could periodically exchange individuals, we contend that our collection of samples from distinct sites, as designated here, enabled us to sample distinct assemblages across the island. We further validated this claim by testing for spatial autocorrelation in assemblage composition (see below).

Tail tissue samples were collected and stored in 95% ethanol for DNA extraction and genotyping. Individuals were uniquely marked with visual implant elastomer (VIE) for a concurrent mark-recapture study and to prevent resampling of individuals. All captured salamanders were released back to their point of capture, and all field equipment was disinfected between sites<sup>206</sup>. Morphometric variation is unreliable for species identification<sup>128</sup>, rendering investigators blind to the identification of salamanders at time of sampling. Animals were handled in accordance with Animal Care protocols approved by Trent University and Ontario Ministry of Natural Resources and Forestry (Protocols:

23906, 25301, 25344). Land access permits, Wildlife Scientific Collector's Authorizations (1079527, 1082275, 1085623, 1088782), and a Notice of Activity under the Ontario Endangered Species Act (Confirmation ID: M-102-3802796883, M-102-9225853169, M-102-1254262277) were secured to conduct this work.

### Genotyping for Taxonomic Assessment

Individuals were given a taxonomic assignment (genomotype) which reflects ploidy and genome dosage based on multilocus genotypes (MLGs). Samples collected between 2015 and 2018 were assessed using seven microsatellite loci (*Atex74*, *Atex141*, *AjeD75*, *AjeD94*, *AjeD346*, *AjeD283*, and *AjeD422*) with tetranucleotide motifs that are used in the unisexual *Ambystoma* complex (see protocols in Supplemental and locus details in Table 2.S1 and Table 2.S) <sup>207–209</sup>. An additional seven microsatellite loci (*AjeD23*, *Atex102*, *AmmH123*, *AmaD42*, *AmaD321*, *AmaD367*, and *AcroD315*) were included for samples from 2019 to 2022 <sup>207,209–211</sup>. A subset of 2015–2018 samples (430 of 2202) were rerun with the full set of 14 loci to assess consistency in genomotype assessment. Nine loci were diagnostic, amplifying in one host species or the other, and were used to identify host species contributions: *AjeD346*, *AmaD367*, *AmaD42*, *AcroD315*, and *AjeD94* for *A. laterale*; *Atex74*, *Atex141*, *Atex102*, and *AmaD321* for *A. texanum*. Five loci amplify microsatellite alleles in both *A. laterale* and *A. texanum* genomes: *AjeD23* and *AjeD75* have unambiguous allele size ranges, such that alleles derived from *A. laterale* and *A. texanum* can be distinguished; *AjeD422* and *AjeD283* had alleles that could not be assigned reliably to *A. laterale* or *A. texanum*; and *AmmH123* had only one ambiguous allele. Details for each locus and multiplex reaction are provided in Table 2.S1 and Table 2.S2. Ploidy for each sample was determined either based on the

maximum number of unique alleles in an ambiguous locus (e.g., *AjeD422* or *AjeD283*) or by adding allele count from the two highest species-specific loci (see <sup>124,126,141</sup>).

Occasional cases of *A. texanum* being identified as triploid or tetraploid (20/151) due exclusively to *AjeD283* resulted in the locus being dropped from use for ploidy determination. Samples with low amplification success (>3 failed loci,  $n = 23$ , 1.0% of total) were not counted and those with ambiguity in assigning genomotype ( $n = 66$ , 2.5% of total) were counted but excluded from analyses. One sample was excluded due to DNA contamination.

### Statistical Analysis

We identified ten sites that we considered discrete units supporting independent assemblages of salamanders and assessed unisexual assemblage composition at both the site and regional (i.e., whole-island) level. Samples were collected from two additional locations on the island (within D2 and D6.2, Figure 2.2) but were excluded from site-level analysis due to limited sampling (i.e., nine and six samples, respectively) and unclear association with a breeding pond. Analyses were restricted to samples where genomotype could be unambiguously identified (i.e., 97.5% of total samples). A 95% confidence interval of relative abundance was calculated for each host and the four most abundant genotypes (LT, LTT, LTTT, and LLT) for each site using the `prop.test` function in R <sup>212</sup>. Additionally, probability of false absence for each site was estimated using a binomial distribution model assuming unbiased sampling and true relative abundances of 5%, 2%, 1%, and 0.5%.

We calculated several indices to quantify diversity patterns on the landscape. Specifically, we calculated the observed unisexual genomotype richness (i.e., number of

unique unisexual genotypes,  $S$ ) for each site. Next, we calculated Simpson diversity ( $\lambda$ ), Simpson evenness ( $V$ ), and Chao1 index, as well as their bootstrap confidence intervals, for each unisexual assemblage using the `diversity_ci` function from the R package *poppr* version 2.9.3<sup>213,214</sup>. Spearman rank correlation tests were then used to assess whether relative abundance of bisexual hosts correlated with any of these diversity metrics.

To evaluate beta diversity, we compared unisexual assemblages at each site by calculating Bray-Curtis dissimilarity based on relative abundance of each unisexual genotype, with the `vegdist` function from the R package *vegan*<sup>215</sup>. Using these scores, we then performed hierarchical clustering of these sites using the complete linkage method to group sites with similar unisexual assemblage structure. A Principal Coordinate Analysis (PCoA) was then conducted to better describe how each of the unisexual assemblages varied in their composition. Biplots were constructed to visualize how assemblages were differentiated based on genotype composition, and to examine whether clusters could be differentiated based on the relative abundance of the bisexual host. Patterns of unisexual assemblage composition could be influenced by exchange of individuals between sites, or by gradients in environmental features on the landscape. We therefore assessed whether unisexual assemblage composition across the island was spatially autocorrelated by conducting a Mantel test (with 9999 permutations) based on the Bray-Curtis dissimilarity index and pairwise distances between breeding ponds, using the `mantel.rtest` from the R package *ade4*<sup>216</sup>.

Next, we set out to test whether unisexual genotypes present at each site had more copies of the genome associated with the bisexual host detected at that site (i.e., had

a host-associated “genome bias”). Genome bias in this study reflects the relative genetic input from each bisexual host species within a unisexual assemblage, and was calculated separately for each assemblage and life stage using the following formula:

$$\%T = \frac{1}{n} \sum_i \frac{T_i}{N_i}$$

where  $n$  is the sample size (number of individuals sampled),  $T_i$  is the number of T genomes in individual  $i$ , and  $N_i$  is the ploidy of individual  $i$ . Because all individuals have at least one L and T genome, a normalization factor of 0.5 was subtracted from %T. In this way, an assemblage of all symmetrical hybrids (e.g., LT or LLTT) would have a value of 0, T-biased assemblages would be positive, and L-biased assemblages negative. As an indicator of relative host availability at each site (i.e., dominant host), we subtracted the proportion of *A. laterale* in the total assemblage from the proportion of *A. texanum* in the total assemblage. In this index, a negative value indicates that *A. laterale* is more abundant, while a positive value indicates that *A. texanum* is more abundant. A Spearman rank correlation was then used to test whether unisexual assemblage genome bias was positively correlated with relative host bias. All analyses were conducted in R 212.

## Results

### Overview

During 2015-2022, we collected 2646 adult salamander tissue samples, 2580 of which were successfully genotyped. Bisexual species (*A. texanum*,  $n = 151$ ; *A. laterale*,  $n = 2$ ) made up only 5.8% of all the individuals we sampled. Diploid unisexuals (LT) made up 64.0% of the total sample (Figure 2.2, Figure 2.S1, and Table 2.S3). Nine sites had *A. texanum*, while *A. laterale* was detected at only two non-neighboring sites (Figure 2.2

and Figure 2.S1). Only one site (D3.1) had both *A. texanum* and *A. laterale*. For all sites except B3 we had >95% confidence that non-detection of a host indicated its true absence from the community (Table 2.S4). In total, we observed eight different unisexual genotypes: LT, LLT, LTT, LLLT, LLTT, LTTT, LLTTT, and LTTTT (Figure 2.S1 and Table 2.S3). Diploids (LT) were 69.8% of all unisexual *Ambystoma* at the island-level. Within triploids, the LTT genotype was more common than LLT (21.9% and 2.4% of genotyped unisexual assemblage, respectively). Tetraploids were present at each site and comprised 5.2% (129/2493) of all unisexual *Ambystoma*, though no tetraploid genotype was present at all sites. Pentaploids were especially rare (~0.5%, 12/2493; Figure 2.2 and Table 2.S3).

Ninety percent (385/430) of the samples scored using both seven and 14 microsatellite loci approaches were identified as the same genotype. Eight individuals initially had ambiguous genotypes (e.g., LLT or LTT) using seven loci, of which five were assigned specific genotypes when tested with 14 loci. Two samples were initially identified as LL but were later found to be unisexual LT and LTT. When using the full 14 loci, thirteen samples (3%) were assigned a genotype of a lower ploidy, and 22 (5%) were assigned higher ploidy genotypes, compared to when only seven loci were used. Therefore, apart from modest differences in data resolution, use of seven loci provided results that were comparable with more contemporary techniques with the 14 loci set. Overall, 63 samples (2.5% of all unisexual samples) were excluded from our analysis because they had an ambiguous genotype. Thirty-six of these came from samples genotyped using the 7 loci set (n = 858), and twenty-seven of these were samples genotyped using the full 14 loci (n = 1635).

### Site Diversity

D3.1 was the only site where both host species were detected and also had the highest number of observed unisexual genotypes ( $S = 7$ , Figure 2.2 and Table 2.S3). Overall, three sites (B3, D3.1, and D7) approached the theoretical maximum number of unisexual genotypes possible on the island based on the Chao1 index (Figure 2.4). We were able to confirm that *A. laterale* was present at B3, and our analyses indicate that *A. texanum* could also be present at this site despite going undetected (Table 2.S4). Sites B3 and C3 had the highest Simpson diversity values ( $\lambda$ ), and C3 has the highest evenness score ( $V$ ; Figure 2.4 and Table 2.S5), consistent with its low richness in unisexual genotypes. None of the diversity metrics were correlated with relative host abundance ( $\lambda$ :  $p = 0.23$ ,  $\rho = 0.42$ ;  $V$ :  $p = 0.12$ ,  $\rho = 0.53$ ; Chao:  $p = 0.51$ ,  $\rho = -0.23$ ; Figure 2.4). Interestingly, we detected unisexual genotypes that can only be produced with genetic input from both bisexual hosts at seven of the 10 sites we examined (Figure 2.3 and Figure 2.S1). The three sites lacking such genotypes (C3, D1.1 and D6.1) also had low richness based on the Chao1 index. Symmetrical tetraploids were detected at five of the sites (B3, B6, B8, D3.1 and D7).

Assemblage composition was not influenced by geographic proximity to neighboring communities based on our Mantel test of Bray-Curtis dissimilarity values ( $p = 0.69$ , Figure 2.S2). Bray-Curtis dissimilarities were used for hierarchical clustering (Figure 2.S2) that identified four clusters reflecting unisexual assemblages that were broadly similar in their composition (Figure 2.3 and Figure 2.5). Cluster 1 (site B3) was characterized by a high proportion of LLTs (33%), few LTT (7%), and a modest amount of LTs (53%). Cluster 2 (site C3) was characterized by a comparably high relative

abundance of LTTT (26%), relatively few LT unisexuals (39%). Cluster 3 (sites D1.2, D3.1, D6.1, D7) was characterized by an intermediate number of LT unisexuals (mean = 56%), and an elevated proportion of LTTs (28%). Cluster 4 (sites D1.1, B8, B6, D3.2) was characterized by a large proportion of LTs (mean = 71%), and an intermediate number of LTTs (mean = 16%). Notably, the site where *A. laterale* was the sole host detected (site B3) had the most distinct unisexual assemblage composition, but the assemblage composition at the site where both host species were detected (D3.1) was not substantially different from other sites in Cluster 3 (Figure 2.3 and Figure 2.5). While *A. laterale* was not detected elsewhere, it remains possible that they were present and not detected (Table 2.S4). However, if *A. laterale* was present at these sites it would be at lower relative abundance (Figure 2.3 and Table 2.S4), making *A. texanum* by far the dominant host (Figure 2.3) with unlikely exceptions being at sites B6 and D6.1.

The PCoA based on Bray-Curtis dissimilarities found only the first two coordinates to be informative, explaining 46% and 32% of the variance, respectively (Figure 2.5 and Figure 2.S3). PCoA Axis 1 corresponded with differences in the relative abundance diploid vs. ploidy-elevated unisexuals in the assemblage (i.e., reflected mean ploidy), whereas Axis 2 corresponded with differences in the genome bias of the assemblage (Figure 2.5 and Figure 2.6). The relative abundance of *A. texanum* corresponded with a larger Axis 1 value and smaller Axis 2 value, indicating that assemblages with more *A. texanum* also tended to have higher ploidy and T-biased genotypes (Figure 2.5B).

### Genome Bias

As predicted, unisexual assemblages had a genome-bias favoring their dominant host ( $\rho = 0.83$ ,  $p = 0.006$ ; Figure 2.6). Site B3 was the only case where the unisexual assemblage skewed towards L-biased genotypes and was also the only site where *A. laterale* was the sole host we detected (Figure 2.3 and Figure 2.S1). Although site D3.1 had both bisexual hosts, *A. texanum* was much more abundant than *A. laterale* at that site and the unisexual assemblage showed a strong genome bias favoring T-biased genotypes (Figure 2.6).

### **Discussion**

We investigated patterns in the structure and diversity of unisexual *Ambystoma* salamander assemblages across Pelee Island, Ontario, where the bisexual hosts on which they are reproductively dependent vary in both abundance and identity. These assemblages differ dramatically from analogous mainland systems in that they are dominated by diploid unisexuals, have up to seven distinct genotypes, and vary substantially in composition across a relatively small regional scale. Consistent with expectations, unisexual assemblage structure appears to be governed primarily by the locally available host(s). Specifically, the genome bias of each unisexual assemblage closely matches relative host availability at each site, and assemblages contrast most among sites which differ in the identity and relative abundance of the host. However, while the site where both hosts are present (D3.1) has very high richness in unisexual genotypes, two other sites (B3, D7) have comparably high richness despite only a single host being identified. Further, we find no support for a relationship between relative host abundance and any diversity metrics. Our work indicates that the diversity

and composition of unisexual assemblages across local and regional scales is broadly dependent on the identity of available bisexual hosts, following the contemporary understanding of unisexual reproduction, but that unisexual assemblages may also be shaped by underappreciated metacommunity dynamics, legacy effects of extirpated hosts, and/or local selective pressures.

Unisexual assemblages are composed primarily of individuals with genotypes governed by relative abundance of the more prevalent host, resulting in an assemblage-level genome bias that follows relative host availability. The nine assemblages where *A. texanum* is the dominant (or only) host take one of three forms (i.e., Clusters 2-4), and clusters with more *A. texanum* also have fewer LT unisexuals and more T-biased polyploid unisexuals. If warmer ponds are favorable to *A. texanum* it could generate the observed pattern as warmer breeding waters can also lead to higher rates of ploidy-elevation<sup>217</sup>. Alternatively, T-biased genotypes (e.g., LTT, LTTT) might also have higher relative fitness in habitats best suited for *A. texanum*. Indeed, the distribution of unisexual *Ambystoma* across Ontario similarly indicates that environmental niche of unisexual *Ambystoma* is governed primarily by their hybrid nuclear genome<sup>81</sup>. Further, Greenwald et al.<sup>146</sup> found that unisexual *Ambystoma* in Ohio had greater niche overlap with the host having closest genetic similarity. Quantifying specific patterns in genotype survival and reproductive output across variable habitats is a clear next step towards understanding factors driving unisexual assemblage composition.

At several sites we detect unisexuals with genotypes which, in theory, could not have been produced *in situ* given contemporary host availability (e.g., LLT at a site with only TT hosts, or LLTT where only one host was present). Three processes could

explain these patterns: 1) sampling effort was insufficient to detect the alternate host, 2) individuals immigrated from a site with one host to a site with the alternate host, or 3) mismatched genotypes are able to persist for a prolonged period after a host is lost (i.e., legacy effects). We have reasonably high confidence that the hosts currently available at each site were detected (Table 2.S4), apart from site B3 where we acknowledge that *A. texanum* may be present. Importantly, we contend that even if a host species was missed it would be of such low relative abundance that its effect on the overall unisexual assemblage structure would be limited due to the difference in reproductive potential. Occasional immigration from neighboring sites may be possible. For instance, sites B3 and C3 are both locations where artificial breeding sites were constructed and subsequently colonized through natural immigration. It is conceivable that assemblage structure at some sites (e.g., B3) is a consequence of differential immigration rates between adjacent L-biased and T-biased source assemblages. However, immigration is likely rare at most sites given the distance between them and the low suitability of intervening landscape on Pelee Island<sup>218</sup>. Further, mismatched genotypes are largely L-biased polyploids at sites distant from assemblages where *A. laterale* is likely to be present. Thus, we suspect that in most cases mismatched genotypes were produced *in situ* prior to recent extirpations of *A. laterale* (i.e., legacy effects), such as at site D6.1 which has the highest relative abundance of LLT outside of B3, but have persisted due to the high rate of clonal reproduction. Such a scenario has been proposed for a site in Ohio where *A. barbouri* is the only known host for a J-biased unisexual assemblage<sup>126</sup>. Indeed, *A. laterale* were known to be present at both B6 and D6.1 as recently as 1984-1991<sup>160</sup>, but can no longer be found despite extensive sampling.

Interestingly, sites C3, D3.1, and D3.2 are the closest neighboring assemblages we sampled, connected by routes with relatively low resistance to dispersal (Smith et al., *in review*), and yet each presents a distinct assemblage composition. This suggests that while dispersal may play a role in structuring unisexual assemblages, assemblage composition on Pelee Island is better explained as a consequence of host species relative abundance. Furthermore, historical sampling on Pelee Island from over three decades ago found an L-biased unisexual assemblage associated with a large relative abundance of *A. laterale* (~16%) in the northwest corner of the island (region A2 in Figure 2.2) that we were not able to sample<sup>160</sup>. Consistent with our results depicted in Figure 2.6, this assemblage would have been even more L-biased than what we observed at B3 (i.e., genome bias of unisexual assemblage = -0.14). Future work will leverage our genetic data to better understand historic and/or contemporary connectivity among sites across the island, as well as possible changes in these assemblage compositions over time.

Theory holds that diploid unisexuals can only be produced clonally or by symmetrical tetraploids (e.g., LLTT genotypes) which requires genetic input from both *A. laterale* and another suitable host<sup>137</sup>. Consistent with this, diploid unisexual *Ambystoma* are uncommon elsewhere in their range where only a single host is available<sup>143,144</sup>. The surprisingly high abundance of diploid unisexuals on Pelee Island, including at sites where only one host was detected, may indicate that diploid unisexuals have higher relative fitness than ploidy-elevated conspecifics and can therefore persist longer and proliferate faster than other genotypes once produced. This is consistent with previous research showing that higher ploidy unisexual salamanders have lower survival across all life stages<sup>219</sup>, though the exact reason why is unclear. Future work is required

to identify the specific mechanisms which might lead to survival and fitness differences among unisexual genotypes<sup>130,146,220</sup>.

To our knowledge this is the first study to directly investigate the effects of multi-host interactions on the composition and diversity of naturally occurring unisexual assemblages. We report levels of diversity in unisexual assemblages on an isolated 42 km<sup>2</sup> island which are higher than any of the corresponding mainland systems investigated to date. We attribute this primarily to the presence of multiple bisexual hosts on the island following from our contemporary understanding of the kleptogenic reproductive mode<sup>128,137,163</sup> (Figure 2.1). Importantly, while the composition of unisexual assemblages appears strongly influenced by host identity and correlated with relative host abundance, the diversity of unisexual genotypes within an assemblage does not appear to be a function of relative host abundance. The processes which underpin additional temporal or spatial variation in assemblage composition remain poorly understood and require further investigation. More generally, it remains unclear how unisexual salamander assemblages are maintained, or whether they are stable over the long term. These questions are beyond the scope of this study; however, some proposed mechanisms related to extinction-colonization dynamics or demographic costs analogous to the cost of producing males offer partial explanation<sup>64,205</sup>. More broadly, variation in host availability increased beta and gamma diversity in a way that is analogous to a 'keystone species'. Unisexual complexes may therefore provide a valuable model for studying the role of biotic interactions and facilitation in dictating the patterns of diversity that we observe in natural systems.

## Tables and Figures

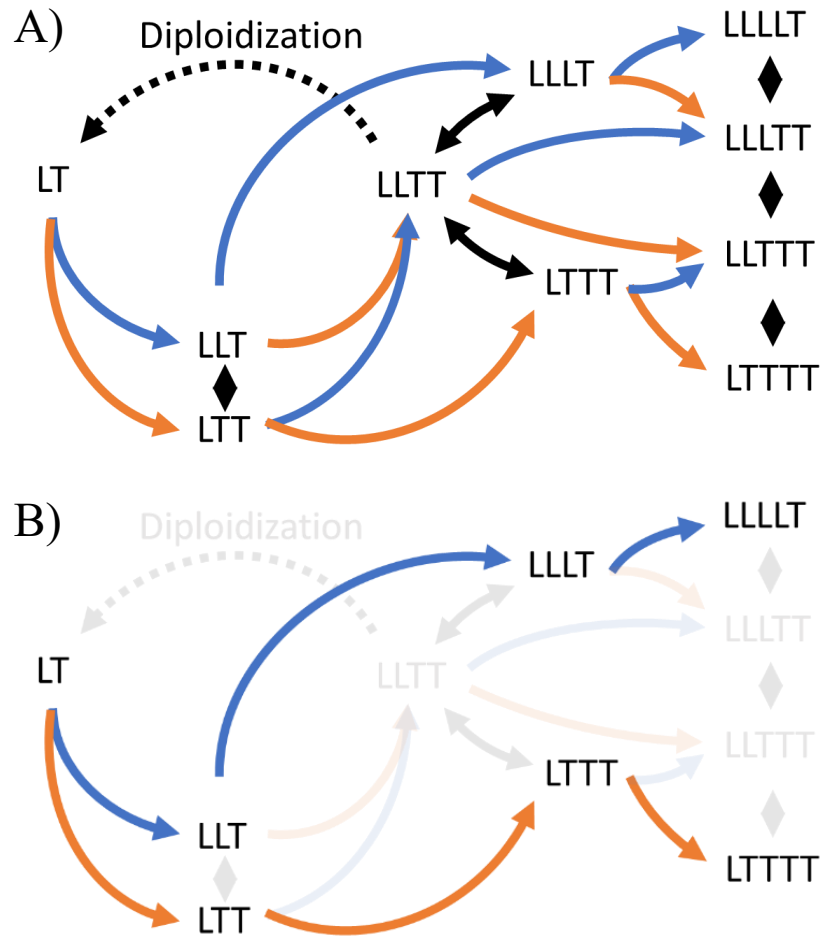


**Figure 2.1.** Putative pathways for genotypic change in unisexual *Ambystoma* showing hypothesized changes in ploidy level. Panel A) represents an assemblage with both *A. laterale* (blue) and *A. texanum* (orange). Panel B) represents an assemblage with one or the other host. These assemblages are unidirectional, remaining exclusive to either *A. laterale* (blue) or *A. texanum* (orange) with non-viable routes faded out. Solid unidirectional arrows indicate genome incorporation, black bidirectional arrows indicate genome replacement by alternative genome (L replaces T or T replaces L), and dotted unidirectional arrow indicates hypothesized route of diploidization.

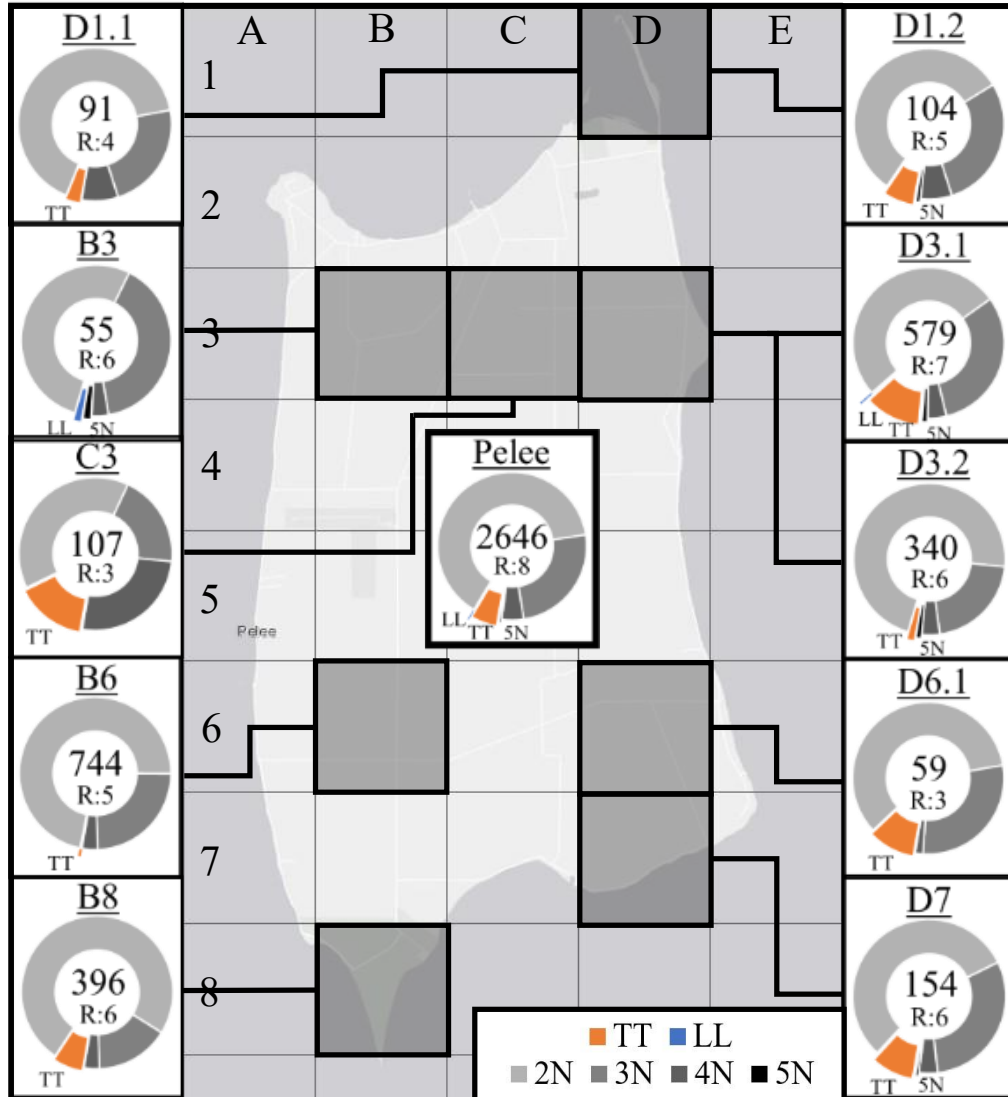


**Figure 2.2.** Map of Pelee Island, Ontario, Canada, with each grid square representing a 2 km<sup>2</sup> area. Highlighted squares indicate the location of surveyed sites. Pie charts represent community composition at each site. Sexual species (i.e., *Ambystoma laterale* (LL) and *A. texanum* (TT)) are depicted in blue and orange respectively, and unisexuals are broken up by ploidy (2N, 3N, 4N, and 5N; grayscale). Data from the whole island is presented in the middle of the figure. Sample size and observed unisexual genotype richness (R) are provided within each circle plot.

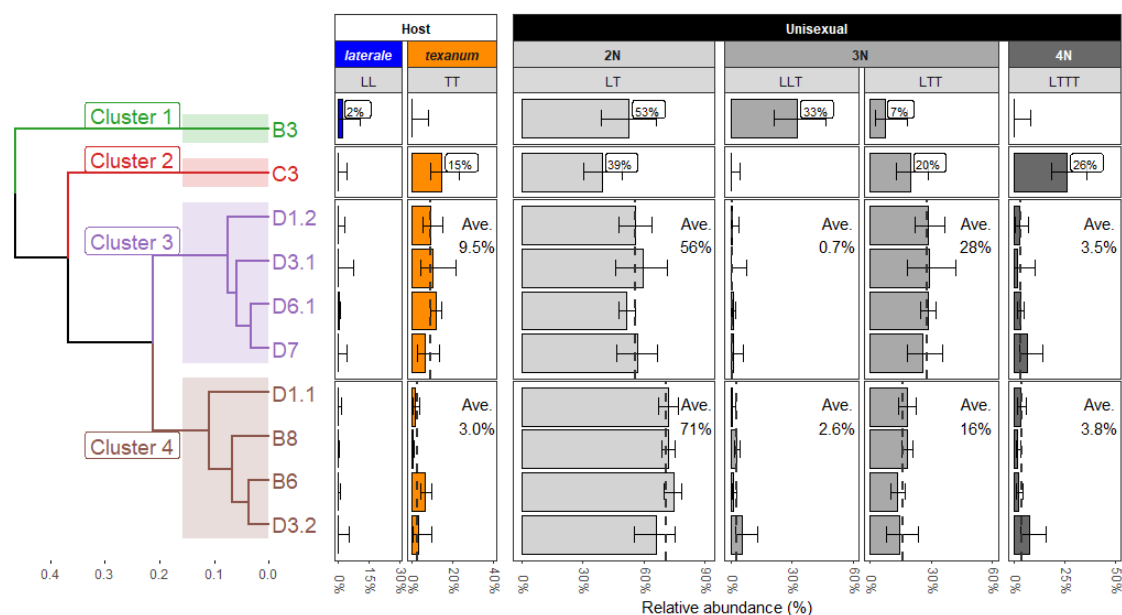


**Figure 2.3.** Dendrogram representation of unisexual assemblage composition of ten sites across Pelee Island, Ontario, Canada, based on Bray-Curtis dissimilarity indices calculated using the proportion of each unisexual genotype within each assemblage. Relative abundances and confidence intervals of each host and most influential genotypes are provided (for full assemblage compositions see Figure 2.S1 and Table 2.S3). Values provided for non-zero abundances for single site clusters (Clusters 1 and 2) and average abundances for multi-site clusters (Clusters 3 and 4). Column colors are by host (blue and orange for *A. laterale* and *A. texanum*, respectively) and unisexual ploidy level (grey scale).

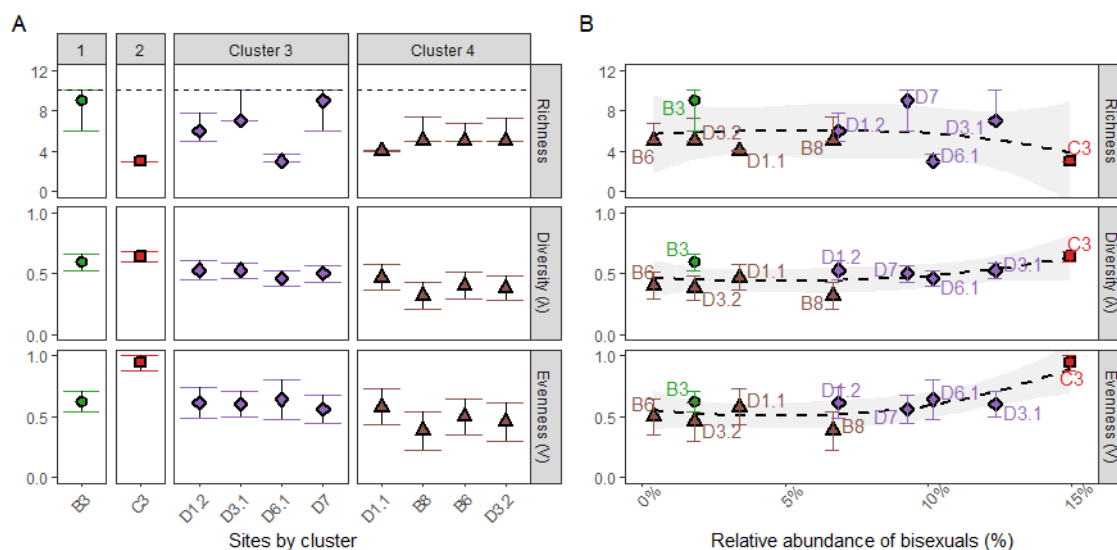


**Figure 2.4.** A) Richness, diversity ( $\lambda$ ), and evenness (V) across Pelee Island, Ontario Canada. Diversity indices were calculated along with estimated error using a bootstrap procedure based on minimum sample size. Richness point values are based on calculated Chao1 index, lower errors indicate identified genotype richness, and high errors based on Chao1 bootstrap confidence up to a maximum of 10 (maximum number of theoretical genotypes for this system). Sites are arranged by cluster and assemblage similarity shown in Figure 2.3. See supplementary material (Table 2.S3) for sample sizes and site by site breakdown of genotype and ploidy. B) The relationship between the relative abundance of the bisexual host species, and diversity metrics for unisexual assemblages across Pelee Island, Canada. Curves were generated using locally estimated scatterplot smoothing (LOESS) fit, shaded areas represent 95% confidence regions. Clusters indicated by point shape and colors shown in Figure 2.3.

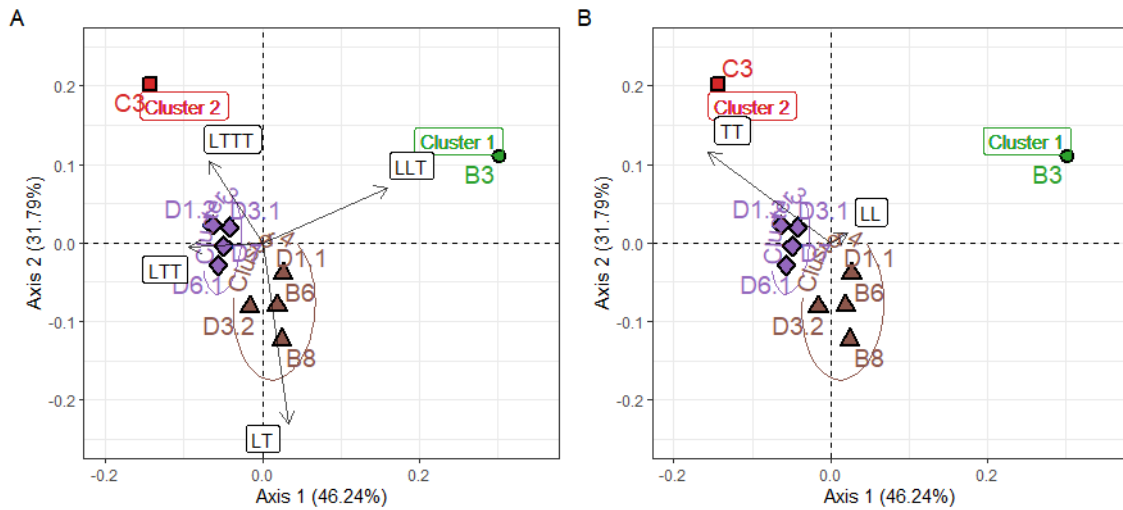


**Figure 2.5.** Principal Coordinate Analysis (PCoA) biplots based on unisexual assemblage dissimilarities showing directional influence of A) most influential unisexual genotypes (e.g., LT, LLT, LTT, and LTTT) and B) correlated influence of host influence. Relative overall explanatory value for each axis are provided. *Ambystoma laterale* (LL) directionality aligns to that of unisexual genotype LLT while *A. texanum* (TT) has an intermediate directional influence comparable to that of LTT and LTTT suggesting correlation. Genotype LT has an orthogonal influence compared to either host and to the host-associated genotypes (LLT, LTT, and LTTT). Clusters indicated by point shape and colors shown in Figure 2.3 and Figure 2.4.

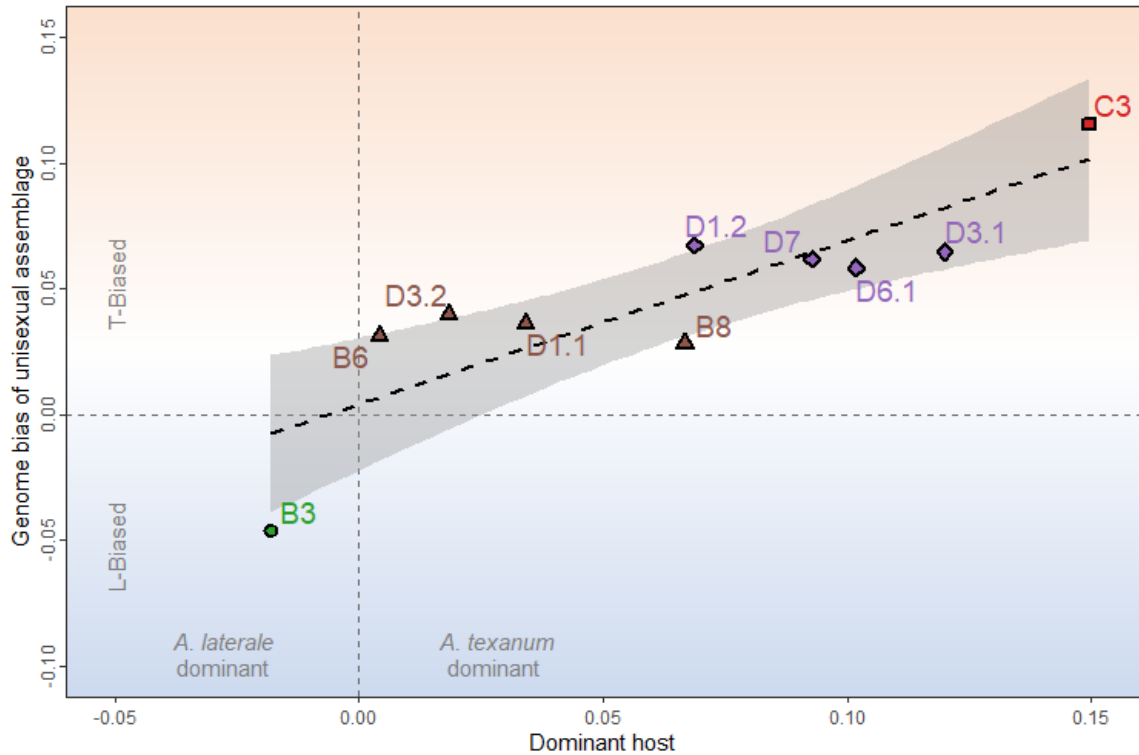


**Figure 2.6.** The relationship between the relative host availability (i.e., the proportion of the total salamander assemblage that is *A. texanum* minus the proportion that is *A. laterale*), and genome bias in unisexual assemblages across Pelee Island, Ontario, Canada. ‘Genome bias’ reflects the total genomic contributions of each host per individual within an assemblage. Assemblages with a positive value have more T-biased genomes (e.g., LTT, LTTT, LTTTT, LLTTT), whereas assemblages with a negative value are more L-biased (e.g., LLT, LLLT). *Ambystoma texanum* (TT) was the only host available at most sites. *A. laterale* (LL) was the only host present at site B3, and both hosts were present at site D3.1. Clusters indicated by point shape and colors shown in Figure 2.3 and Figure 2.4.

## Supplemental

### Procedures

#### *7-loci Amplification Procedure*

DNA extractions were done using the protocol provided with a Promega Wizard Genomic DNA Purification kit. Extracted DNA was re-hydrated in 100  $\mu$ l of water and stored at  $-20^{\circ}\text{C}$  prior to being used for PCR amplification of microsatellite DNA alleles.

Forward primers for each locus were fluorescently labeled with tetramethyl rhodamine (TET). The 25.5  $\mu$ l PCR reaction mix for each sample consisted of 1.5  $\mu$ l of the hydrated DNA extraction, 1.0  $\mu$ l (10 pmol/ $\mu$ l) each of labeled forward and unlabeled reverse primers, 0.6  $\mu$ l dNTP (10 mM of each dNTP: Roche Diagnostics), 0.15  $\mu$ l Taq polymerase (New England Biolabs), 2.5  $\mu$ l homemade PCR Buffer [each ml consisted of 25  $\mu$ l 1M  $\text{MgCl}_2$ , 100  $\mu$ l 1M Tris (pH 8.3), 500  $\mu$ l 1M KCl, 80  $\mu$ l Bovine Serum Albumin (BSA: 10 mg/mL: Sigma), 50  $\mu$ l 2% gelatin (Sigma), 245  $\mu$ l water], and 18.75  $\mu$ l water. The PCR reaction was initiated with a 1 min denaturation at  $94^{\circ}\text{C}$  followed by 30 cycles of  $94^{\circ}\text{C}$  (45 sec) / annealing temperature of  $56^{\circ}\text{C}$  [Atex102, Atex141],  $57^{\circ}\text{C}$  [AjeD94, AjeD346, AjeD422, Atex74] or  $58^{\circ}\text{C}$  [AjeD283] (45 sec) /  $72^{\circ}\text{C}$  extension (30 sec). PCR products were electrophoresed on vertical, 6 % denaturing polyacrylamide gels alongside a Genescan<sup>TM</sup>-350 TAMRA size standard ladder. Gels were scanned with a Hitachi FMBioIII imager and the PCR products (bands) were scored relative to the ladder using Hitachi FMBioIII imaging software. PCR reactions of the same samples were repeated, and the position of the samples on the gel was changed to minimize possible scoring errors.

### *14-loci Amplification Procedure*

DNA extractions were done following a standard ethanol precipitation procedure. Extracted DNA was re-hydrated in 200 µl of water and stored at -20°C prior to being used for PCR amplification of microsatellite DNA alleles.

In addition to the previous seven loci used in the 7-loci procedure, seven more loci were chosen to further enhance genotype resolution. Of the additional loci, Atex102 and AmaD321 were *A. texanum* specific; AmaD42, AmaD367, and AcroD315 were *A. laterale* specific; AjeD23 and AjeD75 were monomorphic in *A. texanum* and varied in *A. laterale*; and AmmH123 had multiple alleles for both hosts. AmaD321 appears to have undergone a duplication event as diploid *A. texanum* regularly had three, and sometimes four, distinct alleles. Atex141 was found to primarily have 2-bp long stutter bands with some alleles having 4-bp stutter bands, though do not appear to be from different locations on the genome – these traits were considered informative and identified for each sample. Allele size ranges and overall allele richness are provided in Supp. 4.

Forward primers for each locus were fluorescently tagged with one of four labels: NED, HEX, 6-FAM, or ROX. Four multiplex reactions (detailed in Table 2.S2) were developed and optimized based on protocols provided by QIAGEN Multiplex Kit (cat. 206145) to avoid allele size overlap of loci with identical tags (Table 2.S1). All multiplexes were initiated with a 15 min denaturation at 94°C, followed by 40 cycles of 94°C (30 sec) / annealing temperature of 53°C [multiplex 3], 55°C [multiplex 1], or 56°C [multiplexes 2 and 4] (90 sec) / 72°C extension (60 sec). A final extension step was run at 72°C for 30 min. PCR outputs were read using an Applied Biosystems 3730xl sequence analyzer with either GeneScan™ 500 ROX™ size standard [multiplexes 1 and 2] or

GeneScan™ 500 LIZ™ size standard [multiplexes 3 and 4]. Trace reads were screened using Geneious 2022.2.

Supplemental Tables and Figures

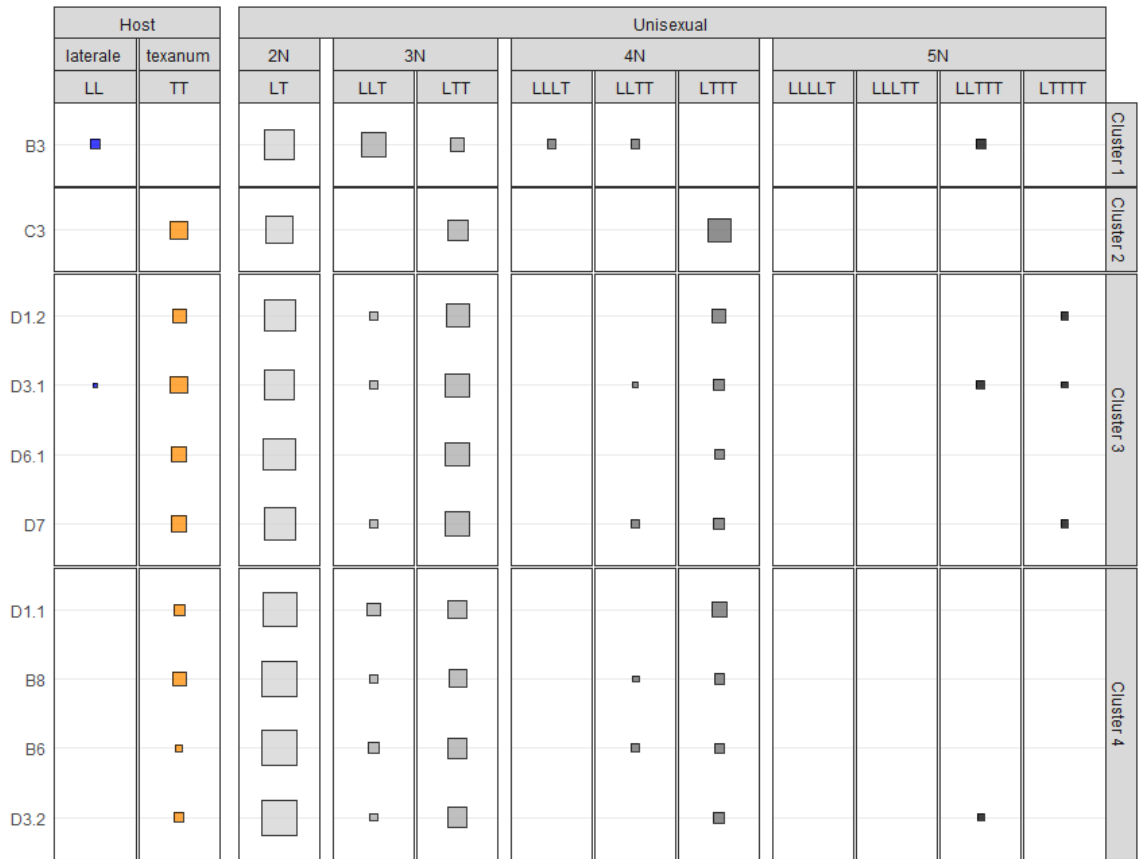


**Figure 2.S1.** Relative abundances of both hosts (*A. laterale*, LL; *A. texanum*, TT) and the unisexual genotypes (LT, LLT, LTT, and LTTT) by site arranged in cluster groups.

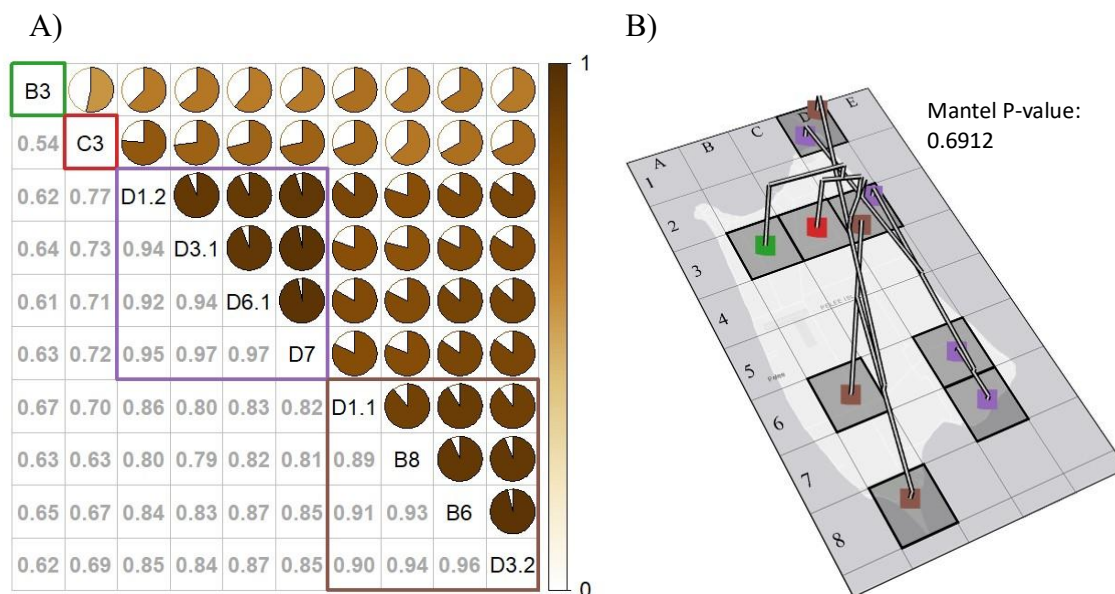


**Figure 2.S2.** A) Corrplot of all Bray-Curtis similarities (1 - dissimilarity) displayed as pie charts above diagonal and numeric values below diagonal. Site clusters are enclosed in squares. B) Bray-Curtis dendrogram aligned to map along with geographic Mantel test result. Site clusters are colored following the scheme from the corrplot (A).

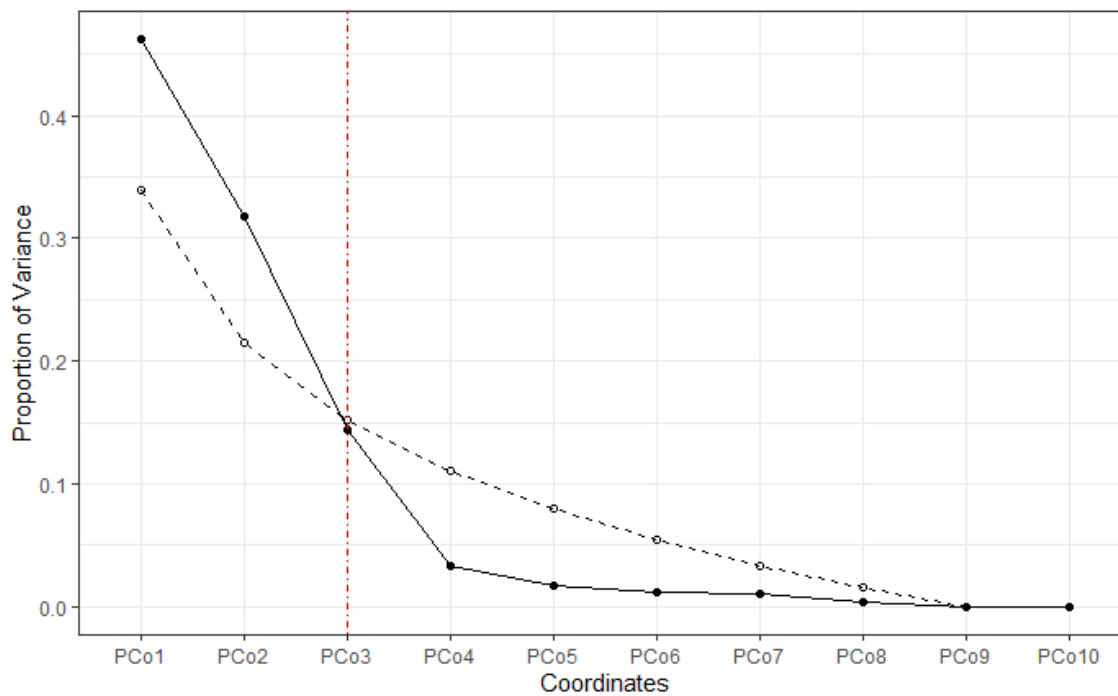


**Figure 2.S3.** Screplot of PCoA proportion of explained variances (solid) and comparative broken stick (dashed) with red line where explained variance fall below broken stick indicating loss of informative value.

**Table 2.S1.** Primer sets for multiplexes 1 and 2. Allele counts are listed by host of origin (T - *A. texanum*, L - *A. laterale*, X - ambiguous). For Atex74 (an *A. texanum* exclusive locus) alleles are categorized by motif size as determined by stutter band sizes. \* 4-bp alleles for Atex74 went beyond the 500-bp size standard. Any alleles above 500-bp were identified as 500+.

	Primer	Sequence (5' -> 3')	Tag	Alleles	Richness
Multiplex 1	Atex74 - F	TCAACGAAAGAGGTGTTGGGT	HEX	2-bp: 219, 221, 223, 225, 229, 231, 233, 237, 241	T-2bp: 9
	Atex74 - R	TCCAACGACAGCGGTATAAA		4-bp*: 235, 239, 243, 247, 251, 267, 271, 275, 279, 295, 307, 311, 315, 319, 323, 331, 335, 339, 343, 347, 351, 355, 359, 363, 367, 371, 379, 393, 401, 405, 409, 413, 417, 421, 425, 429, 433, 437, 441, 445, 449, 471, 475, 479, 483, 487, 491, 495, 499, *500+	T-4bp: 51+
	Atex102 - F	TTCAGGTGGATTCACAGTGC	NED	128, 132, 148, 152, 156, 160, 164, 168, 172, 176, 180, 184, 188,	T: 18
	Atex102 - R	CTGTGTTAGGGGTTTCCTG		192, 196, 200, 204, 208	
	Atex141 - F	GCTTCTTTTGCTTGCTGTT	6FAM	220, 224, 228, 232, 236, 240, 256, 260, 264, 268, 272, 276, 280,	T: 19
	Atex141 - R	TTTCGCAATTGCTGATAAGG		284, 288, 292, 296, 300, 304	
Multiplex 2	AjeD94 - F	ATATCCCATTCCATTGTTTCTG	HEX	146, 150, 154	L: 3
	AjeD94 - R	ATGGACATTCACATGATCACC			
	AjeD283 - F	TTGCACCCTTGGCAGATG	NED	116, 128, 132, 136, 140, 144, 148, 152, 156, 160, 164, 168, 172,	X: 26
	AjeD283 - R	TGTAATGGGTCAGGCAATAATC		176, 180, 184, 188, 192, 196, 200, 204, 208, 212, 216, 220, 236	
	AjeD346 - F	AGCAGGATTAGTGCTTAGATGC	6FAM	246, 250, 262, 266, 270, 274, 278, 282, 286, 290	L: 10
	AjeD346 - R	TGGCAATGTTTACCTAAGAGAG			
	AjeD422 - F	CAAGGTGCTCAAGTTACTGTTC	HEX	202, 206, 210, 226, 230, 234, 238, 242, 246, 250, 254, 258, 262,	X: 21
	AjeD422 - R	CAAATTCTGTACCTGACTGCTG		266, 270, 274, 278, 282, 286, 290, 302	
AjeD75 - F	TTATATGTAGTGCCTGGATGCC	6FAM	L: 102, 106, 110, 114, 118, 122, 126, 130, 134, 138	L: 10	
AjeD75 - R	ATGTCAGTGCAGCTATTTTGC		T: 150, 154, 158, 162, 166	T: 5	

**Table 2.S1 Continued.** Primer sets for multiplexes 3 and 4. Allele counts are listed by host of origin (T - *A. texanum*, L - *A. laterale*, X - ambiguous). One allele size (122-bp) in locus AmmH123 amplified in both *A. texanum* and *A. laterale*, all other alleles appear unambiguous

	Primer	Sequence (5' -> 3')	Tag	Alleles	Richness
Multiplex 3	AmaD321 - F	TGGTGCATCTATATTCCTCAAG	<b>6FAM</b>	138, 142, 146, 150, 154, 158, 162, 166, 170, 174, 178, 182, 186, 190, 194, 198, 202, 206, 210	T: 19
	AmaD321 - R	GATGCCTTGAAACTTGTTCTTC			
	AmaD367 - F	TTCCTCTTAATGTTTTCCGTTG	<b>HEX</b>	138, 142, 146, 150, 158, 162, 166, 170, 174, 178, 186, 194	L: 12
	AmaD367 - R	GTCTTCTCTCCACATGGTTTTG			
	AmaD42 - F	TAACTAGCTGTCAATCGCTCTC	<b>ROX</b>	166, 170, 174, 178, 182, 186, 190, 206, 210, 218, 222, 226, 230	L: 13
	AmaD42 - R	GATGGAAAATCAATCAAGTGTG			
Multiplex 4	AjeD23 - F	GAACACAGGCTACTAACAACAGG	<b>6FAM</b>	T: 174	T: 1
	AjeD23 - R	AAAACCTCTGGAGAAACATGAG		L: 202, 210, 214, 218, 222, 226, 230, 234, 238, 250	L: 10
	AmmH123 - F	ACAAACCCACTGACAACTTTGGAC	<b>HEX</b>	T: 78, 82, 86, 90, 94, 98, 122	T: 7
	AmmH123 - R	GGTTGCCTCCTGAGAACTTTATTTTC		L: 114, 118, 122, 126, 130, 134, 138, 142, 146, 150, 162, 170	L: 12
	AcroD315 - F	AATACGTTTCTTTTGTGTGAGC	<b>ROX</b>	166, 170, 174, 178, 182, 186, 198, 202, 262, 266, 270, 274	L: 12
	AcroD315 - R	AGAACAAATAACAGTGAAAGAGAGC			

**Table 2.S2.** Multiplex reaction mixtures: A) MP1; B) MP2; C) MP3; D) MP4. Mixtures were calculated to 450 uL mixtures and dispense into 96 wells of 5 uL reactions. All reactions start with a 15 min start at 94°C, followed by 40 cycles of 94°C for 30s, T<sub>A</sub>°C temperature for 90s, 72°C for 60s, ending with 30min at 72°C.

A) T <sub>A</sub> =55		Cycles = 40				Per Well	# Samples
QIAGEN multiplex UniSal MP1						5 µL	100
Reagent	Stock	Units	Desired	Units	Vol	Total vol	
ddH2O			To fill		0.4	40	
Q-Solution	5		1		1	100	
Buffer	2		1		2.5	250	
HEX	Atex74-F	10 µM	0.2	µM	0.1	10	
	Atex74-R	10 µM	0.2	µM	0.1	10	
NED	Atex102-F	10 µM	0.2	µM	0.1	10	
	Atex102-R	10 µM	0.2	µM	0.1	10	
6FAM	Atex141-F	10 µM	0.2	µM	0.1	10	
	Atex141-R	10 µM	0.2	µM	0.1	10	
	DNA		ng/µL		0.5		
						5	450
B) T <sub>A</sub> =56		Cycles = 40				Per Well	# Samples
QIAGEN multiplex UniSal MP2						5 µL	100
Reagent	Stock	Units	Desired	Units	Vol	Total vol	
ddH2O			To fill		0.52	52	
Q-Solution	5		1		1	100	
Buffer	2		1		2.5	250	
HEX	AjeD94-F	10 uM	0.2	uM	0.05	5	
	AjeD94-R	10 uM	0.2	uM	0.05	5	
NED	AjeD283-F	10 uM	0.2	uM	0.05	5	
	AjeD283-R	10 uM	0.2	uM	0.05	5	
6FAM	AjeD346-F	10 uM	0.2	uM	0.05	5	
	AjeD346-R	10 uM	0.2	uM	0.05	5	
HEX	AjeD422-F	10 uM	0.2	uM	0.05	5	
	AjeD422-R	10 uM	0.2	uM	0.05	5	
6FAM	AjeD75-F	10 uM	0.16	uM	0.04	4	
	AjeD75-R	10 uM	0.16	uM	0.04	4	
	DNA		ng/µL		0.5		
						5.0	450.0

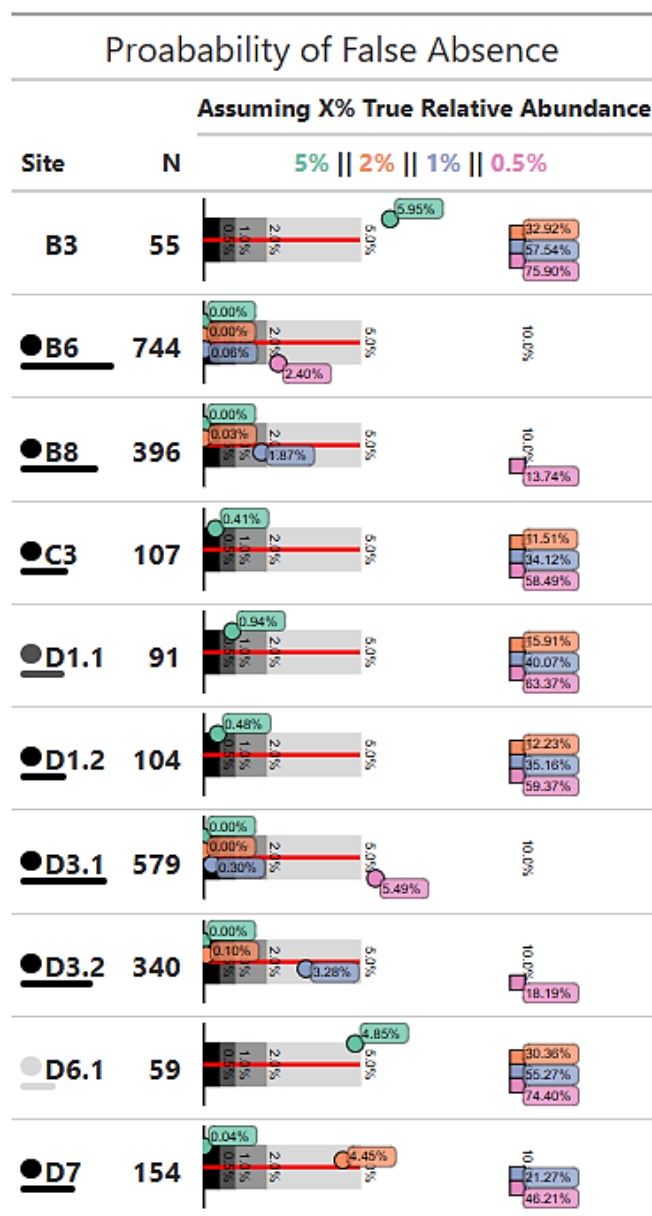
Table 2.S2 *Continued.*

C) T <sub>A</sub> =53		Cycles = 40				Per Well	# Samples
QIAGEN multiplex UniSal MP3						5 µL	100
Reagent	Stock	Units	Desired	Units	Vol	Total vol	
ddH2O			To fill		0.84	84	
Q-Solution	5		1		1	100	
Buffer	2		1		2.5	250	
HEX ROX	AmaD42-F	10 µM	0.16	µM	0.020	2	
	AmaD42-R	10 µM	0.16	µM	0.020	2	
HEX	AmaD367-F	10 µM	0.24	µM	0.030	3	
	AmaD367-R	10 µM	0.24	µM	0.030	3	
6FAM	AmaD321-F	10 µM	0.24	µM	0.030	3	
	AmaD321-R	10 µM	0.24	µM	0.030	3	
DNA			ng/µL		0.5		
						5	450
D) T <sub>A</sub> =56		Cycles = 40				Per Well	# Samples
QIAGEN multiplex UniSal MP4						5 µL	100
Reagent	Stock	Units	Desired	Units	Vol	Total vol	
ddH2O			to fill		0.86	86	
Q-Solution	5		1		1	100	
Buffer	2		1		2.5	250	
6FAM	AjeD23-F	10 µM	0.16	µM	0.02	2	
	AjeD23-R	10 µM	0.16	µM	0.02	2	
HEX	AmmH123-F	10 µM	0.20	µM	0.025	2.5	
	AmmH123-R	10 µM	0.20	µM	0.025	2.5	
ROX	AcroD315-F	10 µM	0.20	µM	0.025	2.5	
	AcroD315-R	10 µM	0.20	µM	0.025	2.5	
DNA			ng/µL		0.5		
						5.0	450

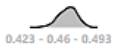
**Table 2.S3.** Total sample size, raw counts, and relative abundances provided. Relative abundances provided in three forms under raw counts, from top to bottom: total relative abundance, relative abundance within unisexuals, and relative abundance within ploidy level. Host species are not provided relative abundance within unisexuals or within ploidy level. The LT genomotype, as the only diploid unisexual, is not provided relative abundance within ploidy level. As all unisexuals must maintain at least one L and one T on Pelee, unknown unisexual samples must be at least LT, therefore unknown contributions are labeled with '?'s based on ploidy level. Sites arranged by dissimilarity and cluster order with the Island level ( $\gamma$ -diversity) data on top. Island level data includes all samples, including from sites removed due to sample size (i.e. D6.2 and D2).

	Total Sample		Hosts		Unisexuals															
	Hosts    Unisexuals		A. lat	A. tex	2N		3N			4N				5N						
	LL    TT    2N    3N    4N    5N		LL	TT	LT	LLT	LTT	LT?	LLLT	LLTT	LTTT	LT??	LLLL	LLTT	LT??	LT???	LLLLL	LLTTT	LT???	LLLLL    LLLTT    LLTTT    LTTT    LT???
<b>ISLAND</b>																				
<b>Pelee</b>		2	151	1693	61	547	49	657	1	14	99	15	129	0	0	8	4	2	14	
		0.1%	5.7%	64.0%	2.3%	20.7%	1.9%	0.0%	0.0%	0.5%	3.7%	0.6%	0.0%	0.0%	0.3%	0.2%	0.1%	0.0%	0.1%	
		NA	NA	67.9%	2.4%	21.9%	2.0%	0.0%	0.0%	0.6%	4.0%	0.6%	0.0%	0.0%	0.3%	0.2%	0.1%	0.0%	0.1%	
		NA	NA	NA	9.3%	83.3%	7.2%	61 - 547 - 49	0.8%	10.9%	76.7%	11.6%	1 - 14 - 99 - 15	0.0%	0.0%	97.1%	28.6%	14.3%	0 - 0 - 8 - 4 - 2	
<b>CLUSTER 1</b>																				
<b>B3</b>		1	0	29	18	4	0	22	1	1	0	0	2	0	0	1	0	0	1	
		1.8%	0.0%	52.7%	32.7%	7.3%	0.0%	0.0%	1.8%	1.8%	0.0%	0.0%	0.0%	0.0%	1.8%	0.0%	0.0%	0.0%	0.0%	
		NA	NA	53.7%	33.3%	7.4%	0.0%	18 - 4 - 0	1.9%	1.9%	0.0%	0.0%	0.0%	0.0%	1.9%	0.0%	0.0%	0.0%	0.0%	
		NA	NA	NA	81.8%	18.2%	0.0%	50.0%	50.0%	0.0%	0.0%	0.0%	1 - 1 - 0 - 0	0.0%	0.0%	100.0%	0.0%	0.0%	0 - 0 - 1 - 0 - 0	
<b>CLUSTER 2</b>																				
<b>C3</b>		0	16	42	0	21	0	21	0	0	28	0	28	0	0	0	0	0	0	
		0.0%	13.9%	33.3%	0.0%	19.0%	0.0%	0.0%	0.0%	0.0%	23.2%	0.0%	0.0%	0.0%	0.0%	0.0%	0.0%	0.0%	0.0%	
		NA	NA	46.2%	0.0%	23.1%	0.0%	0 - 21 - 0	0.0%	0.0%	30.8%	0.0%	0.0%	0.0%	0.0%	0.0%	0.0%	0.0%	0.0%	
		NA	NA	NA	0.0%	100.0%	0.0%	0.0%	0.0%	100.0%	0.0%	0.0%	0 - 0 - 28 - 0	0.0%	0.0%	0.0%	0.0%	0.0%	0 - 0 - 0 - 0 - 0	
<b>CLUSTER 3</b>																				
<b>D1.2</b>		0	7	59	1	27	2	30	0	0	7	0	7	0	0	0	1	0	1	
		0.0%	6.7%	56.7%	1.0%	26.0%	1.0%	0.0%	0.0%	0.0%	6.7%	0.0%	0.0%	0.0%	0.0%	0.0%	1.0%	0.0%	0.0%	
		NA	NA	60.8%	1.0%	27.8%	2.1%	1 - 27 - 2	0.0%	0.0%	7.2%	0.0%	0.0%	0.0%	0.0%	0.0%	1.0%	0.0%	0 - 0 - 0 - 1 - 0	
		NA	NA	NA	3.3%	90.0%	6.7%	0.0%	0.0%	100.0%	0.0%	0.0%	0 - 0 - 7 - 0	0.0%	0.0%	0.0%	100.0%	0.0%	0.0%	
<b>D3.1</b>		1	69	299	6	165	8	179	0	2	18	4	24	0	0	5	2	0	7	
		0.2%	11.9%	11.9%	1.0%	25.9%	1.0%	0.0%	0.0%	0.3%	3.1%	0.7%	0.0%	0.0%	0.9%	0.3%	0.0%	0.0%		
		NA	NA	58.7%	1.2%	32.4%	1.6%	6 - 165 - 8	0.0%	0.4%	3.5%	0.8%	0.0%	0.0%	1.0%	0.4%	0.0%	0.0%		
		NA	NA	NA	3.4%	92.2%	4.5%	0.0%	8.3%	75.0%	16.7%	0.0%	0 - 2 - 18 - 4	0.0%	0.0%	71.4%	28.6%	0.0%	0 - 0 - 5 - 2 - 0	
<b>D6.1</b>		0	6	35	0	17	0	17	0	0	1	0	1	0	0	0	0	0	0	
		0.0%	10.2%	39.3%	0.0%	28.0%	0.0%	0.0%	0.0%	0.0%	1.7%	0.0%	0.0%	0.0%	0.0%	0.0%	0.0%	0.0%		
		NA	NA	66.0%	0.0%	32.1%	0.0%	0 - 17 - 0	0.0%	0.0%	1.9%	0.0%	0.0%	0.0%	0.0%	0.0%	0.0%	0.0%		
		NA	NA	NA	0.0%	100.0%	0.0%	0.0%	0.0%	100.0%	0.0%	0.0%	0 - 0 - 1 - 0	0.0%	0.0%	0.0%	0.0%	0.0%	0 - 0 - 0 - 0 - 0	
<b>D7</b>		0	14	86	1	44	2	47	0	1	4	1	6	0	0	0	1	0	1	
		0.0%	9.1%	55.8%	0.6%	28.6%	1.3%	0.0%	0.0%	0.6%	2.6%	0.6%	0.0%	0.0%	0.0%	0.6%	0.0%	0.0%		
		NA	NA	61.4%	0.7%	31.4%	1.4%	1 - 44 - 2	0.0%	0.7%	3.9%	0.7%	0.0%	0.0%	0.0%	0.7%	0.0%	0.0%		
		NA	NA	NA	2.1%	93.6%	4.3%	0.0%	16.7%	66.7%	16.7%	0.0%	0 - 1 - 4 - 1	0.0%	0.0%	0.0%	100.0%	0.0%	0 - 0 - 0 - 1 - 0	
<b>CLUSTER 4</b>																				
<b>D1.1</b>		0	3	60	5	13	3	21	0	0	7	0	7	0	0	0	0	0	0	
		0.0%	3.3%	62.5%	5.9%	14.3%	3.3%	0.0%	0.0%	0.0%	7.7%	0.0%	0.0%	0.0%	0.0%	0.0%	0.0%	0.0%		
		NA	NA	68.2%	5.7%	14.8%	3.4%	5 - 13 - 3	0.0%	0.0%	8.0%	0.0%	0.0%	0.0%	0.0%	0.0%	0.0%	0.0%		
		NA	NA	NA	23.8%	61.9%	14.3%	0.0%	0.0%	100.0%	0.0%	0.0%	0 - 0 - 7 - 0	0.0%	0.0%	0.0%	0.0%	0.0%	0 - 0 - 0 - 0 - 0	
<b>B8</b>		0	26	295	5	53	4	62	0	2	9	2	13	0	0	0	0	0	0	
		0.0%	6.6%	74.5%	1.3%	18.3%	1.0%	0.0%	0.0%	0.5%	2.3%	0.5%	0.0%	0.0%	0.0%	0.0%	0.0%	0.0%		
		NA	NA	79.7%	1.4%	14.3%	1.1%	5 - 53 - 4	0.0%	0.5%	2.4%	0.5%	0.0%	0.0%	0.0%	0.0%	0.0%	0.0%		
		NA	NA	NA	8.1%	85.5%	6.5%	0.0%	15.4%	69.2%	15.4%	0.0%	0 - 2 - 9 - 2	0.0%	0.0%	0.0%	0.0%	0.0%	0 - 0 - 0 - 0 - 0	
<b>B6</b>		0	3	535	23	135	21	179	0	8	14	5	27	0	0	0	0	0	0	
		0.0%	0.4%	71.9%	3.1%	18.1%	2.8%	0.0%	0.0%	1.1%	1.9%	0.7%	0.0%	0.0%	0.0%	0.0%	0.0%	0.0%		
		NA	NA	72.2%	3.1%	18.2%	2.8%	23 - 135 - 21	0.0%	1.1%	1.9%	0.7%	0.0%	0.0%	0.0%	0.0%	0.0%	0.0%		
		NA	NA	NA	12.8%	75.4%	11.7%	0.0%	29.6%	51.9%	18.5%	0.0%	0 - 8 - 14 - 5	0.0%	0.0%	0.0%	0.0%	0.0%	0 - 0 - 0 - 0 - 0	
<b>D3.2</b>		0	6	245	2	61	9	72	0	0	11	2	13	0	0	2	0	2	4	
		0.0%	1.8%	72.1%	0.6%	17.9%	2.6%	0.0%	0.0%	0.0%	3.2%	0.6%	0.0%	0.0%	0.6%	0.0%	0.6%	0.0%		
		NA	NA	73.4%	0.6%	18.3%	2.7%	2 - 61 - 9	0.0%	0.0%	3.3%	0.6%	0.0%	0.0%	0.6%	0.0%	0.6%	0.0%		
		NA	NA	NA	2.8%	84.7%	12.9%	0.0%	0.0%	84.6%	15.4%	0.0%	0 - 0 - 11 - 2	0.0%	0.0%	50.0%	0.0%	50.0%	0 - 0 - 2 - 0 - 2	

**Table 2.S4.** Probability of false absence (presented as percentages) assuming relative abundances of 5%, 2%, 1%, and 0.5% of population. Calculated probabilities are listed alongside indicator markers on bullet chart. Grey shading indicates levels of false absence probability, with darker shades indicating lower probability. Operationally, we inferred true absence when we achieved 95% confidence that the true relative abundance of undetected hosts was <5% (indicated by the red line). Only site B3 does not meet the threshold of <5% false absence probability given an assumed true relative abundance of 5%. Cases where the probability of false absence was >10% are marked with squares.



**Table 2.S5.** Sample sizes, genototype richness, and diversity values provided for unisexual assemblages at each site (See Table 2.S3 for Total counts including host samples). Chao1 richness calculated value with upper range (95% confidence with max of 10) provided, upper range not provided for site C3 as all bootstrap values were '3'. Calculated values with confidence intervals provided under respective 'Observed' columns. Mean and standard deviation of bootstrap runs provided under 'Estimate' columns. Bootstrap value distributions provided as density plots for lambda and V. First quartile, median, and third quartile provided under distribution figures. Sites arranged by dissimilarity and cluster order.

	Richness			Lambda (Diversity)			V (Evenness)		
	N	Genos	Chao1	Observed	Estimate	Density	Observed	Estimate	Density
<b>ISLAND</b>									
<b>Pelee</b>	2427	8	8-10	0.46 ± 0.10	0.46 ± 0.05		0.52 ± 0.14	0.53 ± 0.07	
<b>CLUSTER 1</b>									
<b>B3</b>	54	6	9-10	0.59 ± 0.07	0.59 ± 0.03		0.62 ± 0.08	0.68 ± 0.04	
<b>CLUSTER 2</b>									
<b>C3</b>	91	3	3	0.64 ± 0.04	0.63 ± 0.02		0.94 ± 0.06	0.93 ± 0.03	
<b>CLUSTER 3</b>									
<b>D1.2</b>	95	5	6-8	0.53 ± 0.08	0.52 ± 0.04		0.61 ± 0.13	0.65 ± 0.06	
<b>D3.1</b>	497	7	7-10	0.53 ± 0.07	0.52 ± 0.04		0.60 ± 0.11	0.62 ± 0.06	
<b>D6.1</b>	53	3	3-4	0.46 ± 0.07	0.45 ± 0.04		0.64 ± 0.17	0.70 ± 0.10	
<b>D7</b>	137	6	9-10	0.50 ± 0.07	0.50 ± 0.04		0.56 ± 0.12	0.61 ± 0.06	
<b>CLUSTER 4</b>									
<b>D1.1</b>	85	4	4-4	0.47 ± 0.10	0.46 ± 0.05		0.58 ± 0.15	0.58 ± 0.08	
<b>B8</b>	364	5	5-7	0.32 ± 0.11	0.32 ± 0.05		0.38 ± 0.16	0.37 ± 0.08	
<b>B6</b>	715	5	5-7	0.40 ± 0.11	0.40 ± 0.05		0.50 ± 0.14	0.46 ± 0.07	
<b>D3.2</b>	321	5	5-7	0.38 ± 0.10	0.38 ± 0.05		0.46 ± 0.16	0.47 ± 0.08	

## **Chapter 3: Lineage diversity in unisexual salamander assemblages reveals the influence of historic landscape and biotic interactions**

Evan A. Bare<sup>1</sup>, Jim P. Bogart<sup>2</sup>, Chris Wilson<sup>1,3</sup>, Dennis L. Murray<sup>1,4</sup>, Thomas J. Hossie<sup>1,4</sup>

<sup>1</sup> Environmental & Life Sciences Graduate Program, Trent University, Peterborough, ON, K9L 0G2

<sup>2</sup> Department of Integrative Biology, University of Guelph, Guelph, ON, N1G 2W1

<sup>3</sup> Aquatic Research and Monitoring Section, Ontario Ministry of Natural Resources and Forestry, Peterborough, ON, Canada

<sup>4</sup> Biology Department, Trent University, Peterborough, ON, K9L 1Z8

### **Abstract**

*Background:* Past environmental events and biological interactions can have long-lasting impacts on biodiversity. Failing to consider how historic environments have shaped contemporary patterns (i.e., legacy effects) hinders our ability to identify the ecological factors which structure metacommunities and shape patterns of diversity, particularly in long-lived organisms and communities with slow rates of turnover. Herein, we examine how past landscape structure and interspecific interactions with sexual host species have shaped diversity and distribution of clonal lineages in a unisexual salamander complex across a heavily modified environment on Pelee Island, Ontario, Canada.

---

Author Contributions: EAB, JPB, DLM, and TJH conceived and designed the study. EAB and JPB conducted the genotyping work. EAB and TJH conducted fieldwork. JPB and CW provided advice on lab techniques. EAB analyzed the data and TJH collaborated on statistical analysis. EAB and TJH wrote the manuscript. All authors provided critical feedback and contributed to the final version of the manuscript.

*Results:* We genotyped a total of 1007 individuals, representing 36 distinct genetic lineages. Sample sites clustered into four groups based on lineage composition, with site clusters generally aligning with the boundaries of historic upland patches. Modeling also found that co-occurrence in areas associated with historic upland patches explained beta diversity patterns better than either geographic distance or landscape resistance.

Migration rate estimates suggest some contemporary connectivity between historic uplands, but only in cases involving recently constructed or disturbed breeding sites.

Total and private lineage richness were remarkably high and best explained as a genetic legacy of biotic interactions with both sexual hosts, with novel lineages produced through the previously hypothesized mechanism of diploidization.

*Conclusion:* Despite prolonged and widespread disturbance, this small island supports tremendous lineage diversity. Lineage distribution appears to reflect the pre-drainage structure of the island landscape, although the distribution of specific lineages suggests a deeper landscape legacy predating island formation.

**Keywords:** Landscape genetics, *Ambystoma*, species complex, lineage diversity, clonality, historic ecology

## Introduction

Ecologists have long recognized that both the physical environment and local interspecific interactions can strongly influence population dynamics, genetic diversity, and community structure <sup>35,221,222</sup>. In some cases, these effects on ecosystem structure and composition persist long after the causal influence has ended <sup>35</sup>. Failing to recognize how historic factors have shaped contemporary populations or communities (i.e., ‘legacy effects’) limits our ability to accurately identify and understand the ecological processes that shape natural systems <sup>107</sup>. This historical context is also critical for gaining a robust understanding of contemporary patterns of habitat connectivity, genetic linkages among populations, and genetic diversity <sup>223</sup>. Increasingly, uncovering the role of historic processes has become important for understanding the impacts of habitat loss, fragmentation, and range shifts on natural populations <sup>42,223</sup>. Given the significant losses of biodiversity occurring alongside rapid and dramatic changes to our ecosystems, it is essential that ecologists seek to quantify the effects of both historic and contemporary environments to better understand the key drivers of vulnerable ecological systems.

Historic environments and interactions can leave a variety of long-lasting effects on populations and communities <sup>35</sup>. For instance, legacies of historic diversity can have conflicting influences on the richness of contemporary communities <sup>36</sup>, and past inhabitants can enhance productivity of contemporary community members through various feedback interactions within an ecosystem <sup>224</sup>. Additionally, past events may leave legacies that lead to extinction debts and immigration credits which are realized over various timeframes <sup>225</sup>. Meanwhile, legacies arising from the population’s colonization history can lead to founder and priority effects that can influence long-term genetic and

community structure<sup>34</sup>. Importantly, the prolonged or time-lagged responses of legacy effects on genetic diversity can continue to influence contemporary dynamics as a consequence of systemic changes to a population<sup>106,226</sup>. In such cases, entire ecosystem functions may be impacted<sup>227</sup> or have delayed responses to ecosystem change<sup>228</sup>. Therefore, understanding how and why the past influences present ecosystems is imperative to the development of management policies<sup>229,230</sup> and efforts to mediate detrimental legacies<sup>231</sup>.

A primary challenge to measuring the influence of historic processes is teasing apart the signal of legacy effects from the backdrop of contemporary dynamics<sup>107</sup>, and separating the impacts of distinct legacy effects from one another<sup>232</sup>. For example, when dispersal routes are dynamic it can be challenging to disentangle the effects of large-scale historic disturbance on connectivity networks and gene flow from those arising due to contemporary immigration and emigration<sup>233,234</sup>. Similarly, distinguishing between the impacts of historic and contemporary biotic interactions is made difficult when hard-to-detect<sup>76</sup> or extirpated constituents<sup>222,235</sup> of the community have had an outsized impact on community or assemblage structure. Having time series data documenting community structure and a known history of landscape alterations are therefore key assets when seeking to distinguish legacy effects from contemporary processes.

Pelee Island is one such case where key temporal changes in both the landscape and assemblage structure are documented. This 42 km<sup>2</sup> island located in Lake Erie, Ontario, Canada (41.6 N, 82.6 E) has been isolated from the mainland for ~ 4000-5000 years<sup>165</sup>. A large central marsh once separated four distinct 'sub-islands' comprised of upland habitat intermittently connected by sandbars<sup>167,169</sup> (Figure 3.S5 and Figure C.2),

each of which may have supported discrete salamander assemblages. In the 1890's approximately 20 km<sup>2</sup> of marshlands were drained across the island leading to permanent dry-land connections across all historic patches of upland habitat <sup>169</sup>. In addition, the island was extensively logged, with ~75% of the natural woodlands being cleared <sup>170</sup>. Today, >60% of the island is used for agriculture with < 20% constituting protected ecological space <sup>175</sup>. This island is home to a salamander complex composed of unisexual *Ambystoma* and two sexual host species: small-mouthed salamanders (*A. texanum*) and blue-spotted salamanders (*A. laterale*) <sup>156,157</sup>. *Ambystoma* salamanders occur in legacy habitat patches as well as newer areas with secondary succession forest and constructed wetlands, suggesting that natural dispersal between patches may be occurring <sup>157,200</sup>. These features make Pelee Island a valuable location to evaluate how legacy effects and contemporary landscape structure have shaped contemporary patterns of diversity.

The unique reproductive biology of unisexual *Ambystoma* makes them an interesting system for studying legacy effects. Specifically, unisexual *Ambystoma* are a group of predominantly clonal salamanders that require sperm from a viable host species in a fashion akin to gynogenesis <sup>124,128</sup>. Within this monophyletic group <sup>236</sup>, distinct clonal lineages are readily identifiable with microsatellite markers targeting their nuclear genomes <sup>134</sup>. Unlike gynogenesis however, new lineages can arise from a variety of hypothesized reproductive outcomes <sup>137,157</sup> (Figure 3.1). Contemporary theory predicts that when unisexual *Ambystoma* can access sperm from multiple hosts there should be increased opportunity for novel unisexual lineages to be produced through diploidization (Figure 3.1; <sup>137</sup>). Two additional processes may also occasionally create new lineages independent of which or how many host species are present (i.e., genome replacement <sup>135</sup>,

ploidy reduction<sup>140,219</sup>) (Figure 3.1). Due to presumed differences in lineage production rate associated with each process, a genetic legacy of elevated unisexual lineage diversity may be identifiable at sites where both *A. laterale* and one other host species (e.g. *A. texanum*) were once present.

Herein, we examine the diversity and distribution of unisexual *Ambystoma* lineages across Pelee Island to address whether legacy effects arising from historic landscape structure and community composition help explain contemporary patterns of unisexual *Ambystoma* diversity. Consistent with the diploidization hypothesis, we predicted that sites with historic or contemporary presence of both sexual hosts would have greater private lineage richness. Additionally, we test three potential hypotheses to explain spatial patterns in the similarity of salamander lineage assemblages across the landscape: similarity-by-distance, similarity-by-resistance, and similarity-by-upland. If contemporary dispersal plays a primary role in governing lineage composition of unisexual *Ambystoma* assemblages, then similarity among these assemblages should be best explained by models of similarity-by-distance or similarity-by-resistance. However, if a legacy effect from historic upland boundaries from the pre-drainage landscape has shaped contemporary lineage assemblages, then the similarity-by-upland model should provide the greatest explanatory power. Finally, support the null model would demonstrate a lack of detectable spatial pattern in assemblage structure indicating an absence of dispersal barriers across the historic inland marsh and/or high contemporary lineage turnover rates across sites. After >100 years since the major wetland drainage event, we predict that the contemporary composition of unisexual *Ambystoma* lineages

remains aligned with historic upland structure, reflecting a legacy effect of the historic landscape.

## **Methods**

### Salamander Sampling

We collected salamander tissue samples between March 2019 and August 2022. Focal sampling sites were separated by >600 m, which is >2x the maximum reported breeding migration distances of *A. laterale*<sup>202</sup> and *A. texanum*<sup>201</sup>, each of which are considered to have greater movement capacity compared to unisexual *Ambystoma*<sup>205</sup>. Sampled sites span the entire island but exclude two known *Ambystoma* breeding areas (>1.4 km from other known sites) located in areas we could not access. Site naming conventions follow those used in Bare et al.<sup>157</sup>. Tail tissue was non-lethally collected from captured salamanders and stored in 95% ethanol for DNA extraction<sup>157</sup>. Individuals were marked using visible implant elastomer, and field equipment was disinfected between sites. Animals were handled in accordance with Animal Care protocols approved by Trent University and Ontario Ministry of Natural Resources (Protocols: 23906, 25301, 25344). Samples were genotyped using 14 loci and assigned genotypes based on their multilocus genotype (MLG) (Table 3.S2)<sup>157</sup>.

### Lineage Assignment

Diploid LT unisexuals are the most abundant genotype on Pelee Island (67.9%) and comprise >50% of unisexuals at most sampled sites (range: 46% - 80%<sup>157</sup>). By focusing our analysis on LT diploids, we avoid ambiguity in lineage assignments for polyploid unisexuals with minimal data loss. We defined a unique diploid lineage as any

set of organisms sharing ancestry exclusively through reproductive outcomes, where the entirety of the diploid set of chromosomes is passed from mother to offspring. To identify diploid lineages, Manhattan genetic distances were calculated between each pair of diploid LT individuals using modified code for the Bruvo.distance function used in the meandistance.matrix function of the *polysat* R package<sup>237</sup>. Diploid LT individuals were clustered using the “single” algorithm of the hclust function<sup>212</sup> and assigned to multilocus lineages (MLL) using the cutree function in the *dendextend* R package (ver. 1.17.1)<sup>238</sup> with a cut height of 2 determined by the first peak of the frequency distribution of distances<sup>108</sup> (Figure 3.S6 - Figure **3.S8**). Accumulation curves were developed for both MLG and MLL to assess sufficiency of available loci to distinguish unique MLGs and MLLs using the genotype\_curve function from *poppr* (ver. 2.9.4)<sup>213,214</sup>. For the MLL genotype curve, we used the most prevalent MLG of each MLL as a representative of the MLL. Two microsatellite loci were excluded from analyses: *AmaD321* was removed from distance calculations due to presence of apparent paralogs, and *AjeD283* was removed due to inconsistent amplification<sup>157</sup>. Allele calls for *Atex74* were modified prior to distance calculations due to unforeseen complications (see Supplemental and Figure 3.S1 - Figure **3.S4**).

### Statistical Analysis

#### *Completeness and Coverage*

Completeness curves for each site were constructed to ensure that our sampling effort was sufficient to adequately assess lineage diversity. Rarefaction and extrapolation curves were calculated using the iNEXT function of the iNEXT R package<sup>239,240</sup>, with an endpoint of 300 samples. This analysis calculates estimated richness values, sample

coverage of the total assemblage, and confidence intervals based on the sampling effort. We then extrapolated these values to the endpoint sample size.

### *Diversity*

To quantify lineage diversity at each site we used alpha diversity metrics including MLL count, Chao1 estimation of true MLL richness, the complement of Simpson index ( $1 - \lambda$ ), and a lineage diversity index (LDI) (i.e.,  $(\text{MLL} - 1)/(\text{N} - 1)$  from Dorken and Eckert<sup>241</sup>). Calculations and associated bootstrap confidence intervals were obtained from the `diversity_ci` function in the R package *poppr* (ver. 2.9.4)<sup>213,214</sup>, with data rarefied to 30 samples. Further, we quantified the number of private MLL and sample sizes of each private MLL at each site.

Among-site diversity ( $\beta$  diversity) was calculated using the Bray-Curtis index based on lineage relative abundance data from each site<sup>28</sup>. We then constructed statistical models to examine whether dissimilarity in lineage composition was best predicted by geographical distance between sites (calculated by the `st_as_sf` function from the *sf* R package (ver. 1.0-14)<sup>242</sup>, landscape resistance between sites based on modeling outputs from Smith<sup>218</sup>, or a binary variable identifying whether sites would have shared the same historic patch of upland habitat. These candidate models and an intercept-only null model were compared using AICc and the weight of support for each model was estimated by calculating the AICc weight<sup>243</sup>. We considered models with  $\Delta\text{AICc} < 2$  to be statistically indistinguishable<sup>244</sup>.

We further assessed site-level patterns in lineage composition using principal coordinate analysis (PCoA) of the Bray-Curtis values for each site. The PCoA results were then used to determine the optimal number of site clusters using the `fviz_nbclust`

function from the *factoextra* R package (ver. 1.0.7) <sup>245</sup> with the kmeans algorithm, and methods set for both “silhouette” and “wss”. The hypothesized effect of historic landscape influence would be supported if the optimal number of clusters matched number of historic patches of upland habitat, and if sites clustered together based on location of historic upland patches. To visualize spatial relation of identified clusters, an unrooted neighbor-joining tree based on Bray-Curtis complement values was constructed using the nj function from the *ape* R package (ver. 5.7-1) <sup>246</sup> and projected onto a map of Pelee Island. Site C3 was excluded from modeling and PCoA because it was constructed just prior to the end of our fieldwork in 2021 and was therefore uninformative for our overarching goal of examining legacy effects.

### *Connectivity*

We used a modified version of the divmigRate method <sup>247</sup> from the *diveRcity* R package (ver. 1.9.90) <sup>248</sup> to measure asymmetric patterns of connectivity among sites. This method was originally designed for genetic data from sexually reproducing diploid systems, but we used a version for haploid data developed by Kling and Ackerly <sup>249</sup>, calculating Jost’s D metric of differentiation <sup>93</sup>. Furthermore, this analysis used lineage assignment rather than allele data to account for complete genetic linkage in this predominantly clonal system.

## **Results**

### Overview

We used 1007 unisexual LT samples in our lineage assessment and identified 36 distinct MLL (Table 3.S1 and Table 3.S2), of which 22 were private to specific sites (Figure 3.2 and Table 3.S5). Histograms of MLG pairwise distances presented multiple

distinct peaks suggestive of distinct lineages (Figure 3.S6 and Figure 3.S7), with all within-MLL MLG pairs being within 7 mutation steps (Figure 3.S8). Nine MLLs had >10 total occurrences in our dataset, and only three had >100. Two sites had <20 samples (D2: n = 5; D6.1: n = 3) and were therefore excluded from further analyses; no identified MLLs from these sites were private. A genotype accumulation curve demonstrated linear increase in MLG with loci count (Figure 3.S9). Comparatively, MLL accumulation plateaued at 36 MLL and showed that each MLL could be identified using a minimum of 5 loci, but up to 10 loci were necessary for all MLLs to be consistently identified assuming random loci choice (Figure 3.S10). Completeness curves indicate that >95% of all lineages, sampled and unsampled, belong to lineages represented in our sample set for each site, except for B3 which had a coverage estimate of 91.6% (Figure 3.S11). Based on these curves, any missing unidentified lineages are likely of low relative abundance and unlikely to strongly influence our results.

Three of 10 sites had more than 10 identified MLLs, while only two had fewer than five (Table 3.1). Notably, site B6 had 20 identified MLLs, but with correspondingly high sampling effort. Six sites had multiple private MLLs, with two sites having sixteen and five private MLLs (B6 and B8, respectively; Table 3.1). Furthermore, seven private MLLs each had more than one representative sample and were exclusive to either B6 or B8.

### Lineage Diversity

LDI values ranged from 0.10 to 0.22 across all sites, with two sites (B6 and B8) having LDI confidence intervals extending >0.25. Only three sites (D3.1, B6, and B8)

had an estimated lineage richness (Chao1)  $>9$ , with five sites (D3.1, D3.2, B6, B8, D7) having an upper range of  $>14$  estimated lineages (Table 3.S5).

While not monoclonal, sites typically appear to be dominated by relatively few MLLs (Figure 3.2A). Southern sites (except for B6) had two dominant MLLs (representing between 60-25% representation), with MLL-8 always being dominant. Comparatively, northern sites each had one lineage with  $>60\%$  representation (Figure 3.2 and Figure 3.3), except for sites D1.1 and C3 which were instead found to be highly heterogeneous, with a Simpson index  $>0.75$  (Table 3.S5). Only sites B3 and D3.2 had a Simpson index  $< 0.4$ .

Both the silhouette and WSS methods for kmeans clustering optimally clustered sites into four groups based on Bray-Curtis dissimilarity (Figure 3.S12). Sites grouped together following expectations based on historic upland patches, except for site B6 which clustered with sites from the Eastern upland patch rather than the Southern upland (Figure 3.3A). Site B3 was the most distinct from other sites, while sites D3.1, D3.2, and B6 were more similar to one another than any other site groupings. Except for B6, these clusters based on unisexual lineage composition align with the historic landscape structure of Pelee Island.

#### Lineage Composition Dissimilarity

Our model selection exercise found that only the Upland model outperformed the null model ( $\Delta AICc > 2$ ; Table 3.2) and best explained variation in MLL assemblage dissimilarity ( $p = 0.039$ ). By comparison, neither geographic distance nor landscape resistance reasonably predicted MLL assemblage dissimilarity (Table 3.2). These results

further support the hypothesized role of historic island landscape structure as having influenced genetic structure of unisexual assemblages on Pelee Island.

### Connectivity

Results from our connectivity analysis further illustrate that relatively high rates of immigration occurred on sites D3.1, D3.2, and B6 (Figure 3.3B), all of which were also grouped together by kmeans clustering. Additionally, sites D1.1 and D1.2 had moderate connectivity while site B3 had the lowest connectivity of all the sites that we sampled; this was consistent with our calculated Bray-Curtis indices. Contrary to prediction, some site pairs from different uplands appear to be connected, specifically B6 to D7 and D7 to D1.1. While these connections are relatively weak, they are still stronger than the connection from D1.1 to D1.2 which are in close physical proximity and on the NW upland (Figure 3.3B).

### **Discussion**

Our analyses support the hypothesis that legacy effects have played a major role in determining the diversity and distribution of unisexual salamander lineages across a human-impacted landscape. Specifically, the distribution of diploid unisexual lineages across Pelee Island was best explained by the location of historic patches of upland habitat that occurred prior to extensive wetland draining >100 years ago. Importantly, the observed patterns could not be explained by models of isolation-by-distance or isolation-by-resistance, suggesting that contemporary dispersal has played only a secondary role. In addition, the enhanced diversity of private unisexual lineages at sites where both sexual hosts were historically present is consistent with the proposed mechanism of diploidization<sup>137</sup>, and supports our hypothesis of a genetic legacy effect arising from past

biotic interactions. Our analysis also suggests patterns of historic or contemporary connectivity among some nearby populations given that some disturbed sites and sites with constructed ponds demonstrate connectivity with sites on different historic uplands.

#### Legacy Effect of the Historic Landscape

The genetic structure of unisexual *Ambystoma* across Pelee Island supports our hypothesis that historic upland habitat patches supported distinct populations, characterized by distinct patterns in lineage diversity that remain detectable today. Across Pelee Island, historic upland patches were each dominated by a different major LT lineage (Figure 3.2). Additionally, lineage composition patterns clustered sites into groups that aligned with the borders of pre-drainage upland patches, with exception of one site (Figure 3.3A). This conclusion was also supported by the superior fit of a model that explained assemblage dissimilarity based on historic upland patch (Table 3.2). These results also make clear that contemporary gene flow, if present, has been insufficient to dilute this historic legacy of a pre-drainage landscape.

Strong geographical structuring of clonal systems is not uncommon, often associated with location of lineage origin<sup>250–252</sup> or founder effects<sup>100,253,254</sup>. However, similar studies often involve polyphyletic clonal systems or greater spatiotemporal scales where mitochondrial lineages can provide sufficient resolution. The use of nuclear genetic lineages in clonal systems provides greater resolution to address specific system dynamics or more refined ecological processes over shorter time scales<sup>100,253</sup>. While our findings support the hypothesis of historically isolated patches of upland habitat, the use of nuclear genetic lineages ensured that our inference was robust, and we contend that

other means of quantifying genetic diversity would have been insufficient to rigorously address our hypotheses.

Intriguingly, incidental departures from the overall trend related to historic upland patches suggest important secondary influences. For instance, only site B6 fell outside of their expected upland patch, grouping with Eastern upland sites located ~6 km away instead of site B8 which was located on the same historic upland patch, was geographically closer, and had traversable intervening forested habitat. We cannot rule out incidental or purposeful human translocation of animals as a possible explanation<sup>255,256</sup>, or that undocumented historical stepping-stone populations might have once connected B6 to the Eastern upland. The presence of MLL-33 at opposite corners of the island (Figure 3.2 and Figure 3.3A), as well as its occurrence at weakly connected sites without shorter stepping-stones at intervening sites (Figure 3.3B), seem unlikely to have resulted from contemporary dispersal. Rather, these patterns may suggest that some lineages were historically more widely distributed across the island<sup>257,258</sup>. Indeed, two of the lineages we identified occurred at all sites, and five others occurred at half of the sites. Similar patterns in other systems have been explained by phases of allopatric divergence followed by secondary admixture<sup>259</sup> or complex interactions of more ancient geological changes<sup>260</sup>. If the major salamander lineages we identified were present on historical uplands prior to the flooding of the Erie basin<sup>165</sup>, it stands to reason that they could have been more widely distributed at the formation of Pelee Island. Thus, while our study focused on a more recent landscape legacy left by the now-drained marshlands, an underlying landscape legacy predating the island's isolation from the mainland may

explain some of the observed patterns. Additional lineage-level study of salamanders from other Lake Erie islands would shed light on this hypothesis.

### Genetic Legacy Effects

Consistent with a legacy effect of historic biotic interactions, we found private lineage richness was highest at the site where both sexual hosts were historically present, but only one host currently remains (Site B6; Table 3.1). A species-hybrid complex in cyprinid fishes (*Squalius alburnoides* complex) shows a similar pattern in that genetic diversity of each genome is greater where both parental species are present<sup>261</sup>. Both systems illustrate an important synergistic effect for hybrid genetic diversity where multiple paternal species are present. More generally, we identified 36 distinct unisexual lineages across 10 sites in an isolated landscape less than 50 km<sup>2</sup>. This degree of MLL richness is high for clonal<sup>250,262</sup> or hemi-clonal systems<sup>263</sup>, and unprecedented in unisexual *Ambystoma*<sup>136,264</sup>, particularly given the comparable genetic resolution and limited spatial scale of our study system. Taken together with the fact that diploids currently make up 68% of all unisexuals on Pelee Island (i.e., a system with two sexual hosts) this system provides strong indirect evidence in support of the diploidization mechanism proposed by Bogart and Bi<sup>137</sup>. Importantly, the observed prevalence of diploid unisexuals and diversity of LT lineages occurs despite a dramatic decline in the apparent abundance and distribution of *A. laterale* across the island<sup>156,157</sup>. Thus, contemporary assemblage structure on Pelee Island more broadly may reflect a genetic legacy of biotic interactions with *A. laterale* from a time when that species was more abundant and widely distributed on the island.

Interestingly, site B8 showed high private lineage richness, despite the apparent absence of *A. laterale* in historic and contemporary sampling<sup>156,157</sup>. Historically, LLT genotypes were relatively abundant at this site (~12% of the unisexuals) as was *A. texanum*<sup>156</sup>. Under these conditions, symmetrical tetraploid genotypes (LLTT) could theoretically be produced at a higher rate compared to other sites (Fig. 2 in<sup>137</sup>). Thus, even the patterns we observed at this site are consistent with the proposed diploidization mechanism. It seems likely that the LLTs at B8 were produced by historic biotic interactions with *A. laterale* at a time prior to historic sampling, possibly reflecting the long timescales through which biotic interactions can impact assemblage composition.

Notably, even without immediate sympatry or temporal separation of the sexual hosts, diploidization may still occur across the landscape when triploid individuals migrate between sites where alternate sexual hosts are present. Such is the case in hybridogenetic water frogs (*Pelophylax esculentus*), where genetic variability for each genome increased independently based on host proximity<sup>82</sup>. This highlights that spatial separation of hosts is not necessarily an impediment to hybrid genetic diversity. Therefore, while our genetic resolution is insufficient to conclusively discern the origins of diploid lineages identified (Figure 3.1), the diploidization pathway is the only available hypothesis consistent with the heightened level of lineage diversity observed on Pelee Island as well as the observed richness of private lineages at specific sites.

## **Conclusion**

Our findings support the influence of two distinct legacy effects occurring in tandem. First, the high lineage richness of unisexual *Ambystoma* and distribution of private novel lineages support the hypothesis of a prevailing genetic legacy resulting

from historic biotic interactions with multiple host species. These results provide strong indirect evidence of novel lineage formation through diploidization in unisexual *Ambystoma*. Second, the contemporary lineage distribution we observed was best explained by a landscape legacy effect reflecting the historic structure of Pelee Island as four isolated upland patches. Additionally, the presence of at least two lineages at all the sites we sampled may indicate a deeper landscape legacy from before the formation of Pelee Island, but further investigation is required. Lastly, results suggest contemporary connectivity between historic uplands, but this connectivity appears to have little influence on assemblages in natural habitat patches. Critically, typical assessments of unisexual *Ambystoma* diversity using genomotype-level analyses or allelic diversity would not have been able to test our hypotheses. Our lineage-level analyses provide unique and novel insight into the biology and ecological dynamics of a poorly understood, and federally endangered, mixed-ploidy salamander complex, demonstrating long-term persistence of lineage diversity on a heavily disturbed landscape with important implications for the management of these animals. Future studies should similarly capitalize on lineage-level analyses to assess contemporary connectivity networks or interspecific interactions between unisexual *Ambystoma* and their hosts.

## Tables and Figures

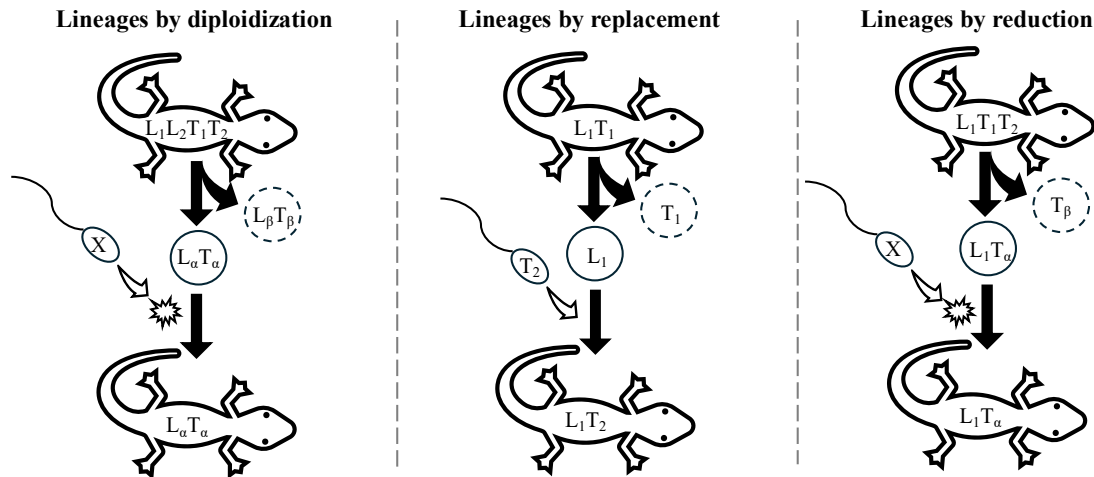


**Figure 3.1.** Three alternative proposed routes for novel diploid lineage formation in unisexual *Ambystoma*. Diploidization (left) requires the presence of *A. laterale* (LL) and one other host (here *A. texanum*; TT) in order to produce a symmetrical tetraploid (e.g. LLTT). The symmetrical tetraploid can then produce ploidy-reduced LT diploids composed of a complete complement of randomly subset L and T chromosomes (e.g.,  $L_{\alpha}T_{\alpha}$ ,  $L_{\beta}T_{\beta}$ ,  $L_{\alpha}T_{\beta}$ ,  $L_{\beta}T_{\alpha}$ )<sup>137</sup>. Replacement (center) requires a progenitor LT diploid, resulting in the complete replacement of one haplome while maintaining hybrid status with an *A. laterale* haplome, L. To date, this has not been demonstrated to occur in diploid unisexuals<sup>136</sup> nor has host genotype (e.g., LL, TT) reconstitution been successful<sup>122,265</sup>. Reduction (right) requires a progenitor triploid (LTT here) producing an unfertilized reduced egg that has lost one complete, but randomized, haplome such that the produced diploid maintains a hybrid nuclear genome. Reduced eggs have been observed<sup>139</sup>, but no ploidy-reduced offspring have been verifiably documented in family studies. Note that only one host is necessary for the replacement and reduction routes. Each mechanism outlined has been proposed in the literature, but no direct evidence is currently available for any of these outcomes.

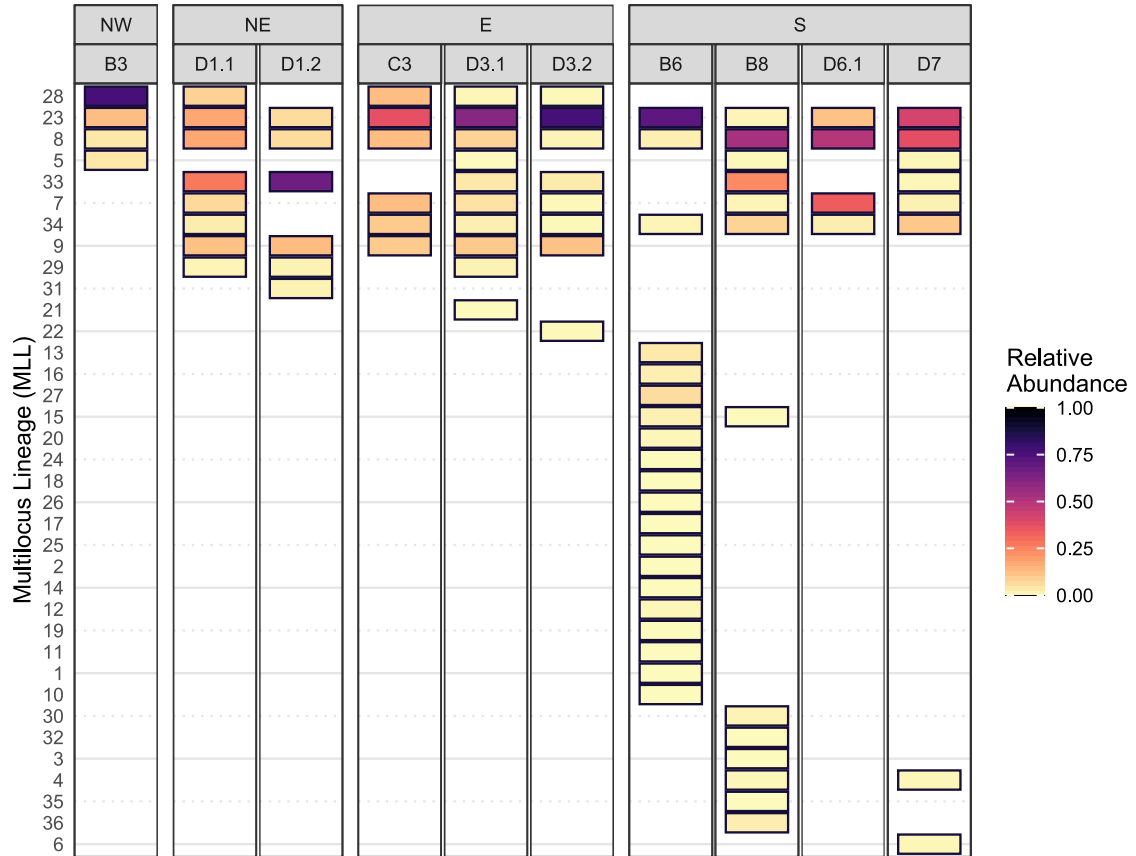


**Figure 3.2.** Relative abundance of each multilocus lineage for *Ambystoma* salamander breeding sites across Pelee Island, Ontario. Alphanumeric codes indicate site based on location within a grid (see Figure 3.3) <sup>157</sup>. Sites are grouped based on the historic upland habitat patches with which they are associated (northwest, NW; northeast, NE; east, E; and south, S). Lineages are arranged to display lineage presence and relative abundance in a nested fashion.

**Table 3.1.** *Ambystoma* salamander diversity measures for sites across Pelee Island Ontario, arranged by historic geographical upland habitat patch (NW, NE, east, and south). Alphanumeric codes indicate site based on location within a grid (see Figure 3.3) <sup>157</sup>. Values indicate the total number of multilocus lineages observed, as well as number of private and shared lineage, along with number of genotyped LT samples (N). MLL richness estimates (Chao1) are rounded up to whole numbers. Relative abundance of hosts as well as unisexual genotypes required for the diploidization cycle are presented from Bare et al. <sup>157</sup>, with historic values from Bogart and Licht <sup>156</sup> presented underneath where available.

		Multilocus Lineages				Sample Size			Host Presence		Genomotype		
		Total	Private	Shared	Chao1	N	Private MLL	Shared MLL	LL	TT	LLT	LTT	LLTT
NW	<b>B3</b>	4	0	4	5	22	0	22	1.8%	0%	32.7%	7.3%	1.8%
	<i>Historic</i>								16.3%	0%	67.3%	0.4%	2.6%
NE	<b>D1.1</b>	8	0	8	9	54	0	54	0%	3.3%	5.5%	14.3%	0%
	<b>D1.2</b>	6	1	5	7	43	1	42	0%	6.7%	1.0%	26.0%	0%
	<i>Historic</i>								0%	78.9%	5%	5%	0%
E	<b>C3</b>	6	0	6	6	37	0	37	0%	15.0%	0%	19.6%	0%
	<b>D3.1</b>	10	1	9	12	169	1	168	0.2%	11.9%	1.0%	28.5%	0.3%
	<b>D3.2</b>	8	1	7	16	103	1	102	0%	1.8%	0.6%	17.9%	0%
S	<b>B6</b>	20	16	4	75	236	34	202	0%	0.4%	3.1%	18.1%	1.1%
	<i>Historic</i>								0.3%	1.4%	31.1%	30.8%	4.0%
	<b>B8</b>	13	5	8	21	225	15	210	0%	6.6%	1.3%	13.4%	0.5%
	<i>Historic</i>								0%	28.1%	8.4%	28.8%	0%
	<b>D6.1</b>	4	0	4	4	32	0	32	0%	10.2%	0%	28.8%	0%
	<i>Historic</i>								1.0%	58.3%	4.2%	15.6%	0%
	<b>D7</b>	8	1	7	16	78	1	77	0%	9.1%	0.6%	28.6%	0.6%

**Table 3.2.** Results from selection of candidate linear models that predict Bray-Curtis dissimilarity of diploid unisexual lineage composition among *Ambystoma* salamander breeding sites on Pelee Island, Ontario. The *Upland* model uses a binary variable indicating whether two sites were located within the same patch of historic upland habitat, *Geo* uses a continuous variable reflecting Euclidean geographic distance between sites, and *Resist* uses a continuous variable reflecting landscape resistance between pairs of sites based on a resistance map derived from Smith<sup>218</sup>. *Null* reflects an intercept-only model.

Model	Variables				Model Selection Criteria		
	Intercept	Geographic Distance	Shared Upland	Resistance	K	AICc	Δ AICc
<i>* UPLAND</i>	0.70 *** <0.001	-	-0.17 * 0.039	-	3	-10.13	0
<i>NULL</i>	0.66 *** <0.001	-	-	-	2	-7.94	2.19
<i>GEO</i>	0.57 *** <0.001	0.02 0.21	-	-	3	-7.28	2.85
<i>RESIST</i>	0.62 *** <0.001	-	-	0.0094 0.68	3	-5.74	4.39

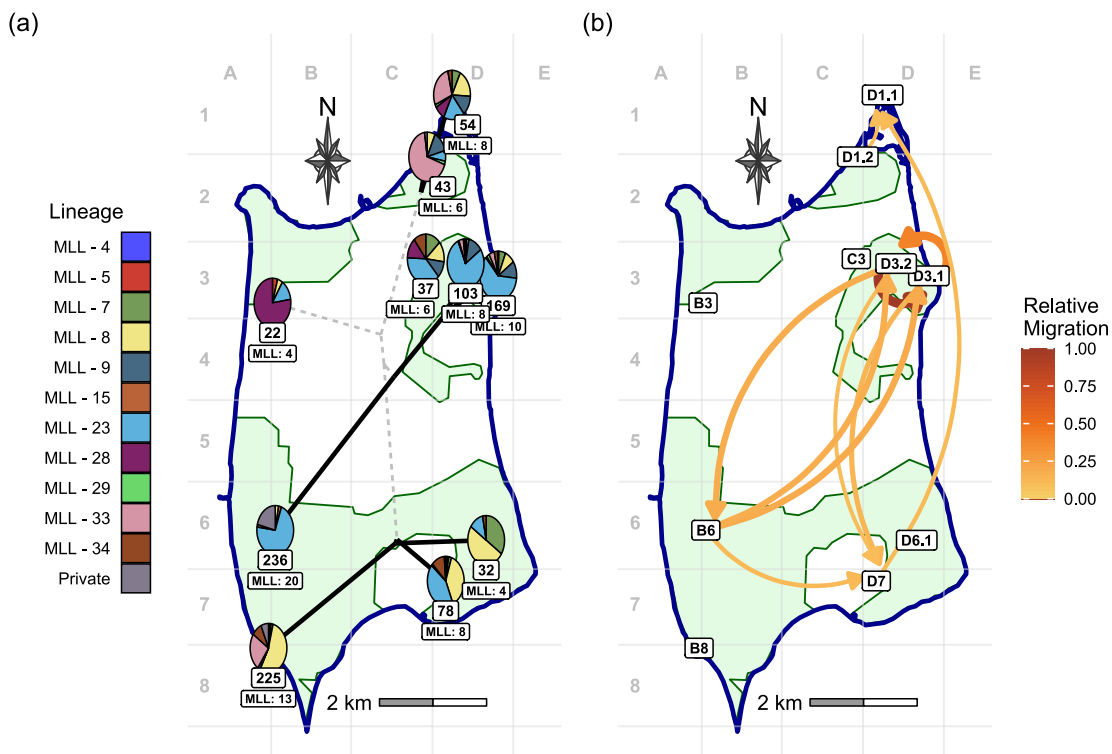


**Figure 3.3.** Maps depicting site distribution of diploid unisexual (*LT*) *Ambystoma* salamander lineages across Pelee Island, Ontario. Boundaries of historic upland habitat patches are represented in light green. A) Cluster map showing sites that group together based on similarity of diploid unisexual lineage composition. Clustered sites are connected by solid black lines. At each site, composition of multilocus lineages (MLLs) is represented by pie charts with sample size and MLL count displayed underneath. Site C3 is presented but was not included in the clustering analysis due to concerns over founder effects. Samples from private lineages are pooled together under the “Private” label for visualization. B) Map of inferred connectivity among sites based on divMigrate analysis of diploid unisexual lineages across Pelee Island. Stronger relative rates of connectivity (Jost’s  $D$ ) are represented with thicker lines. Values of  $D < 0.1$  are not represented in this figure for the purpose of clarity.

## Supplemental

### Details on Atex74

*Atex74* appears to have alleles with either 2-bp motifs or 4-bp motifs. These alleles appear to be of the same locus in the genome as there were never any instances of diploid bisexual *A. texanum* having three *Atex74* alleles. There were, however, instances of *A. texanum* samples having two 2-bp motif alleles, two 4-bp motif alleles, and cases with one of each.

To account for this complexity, all 2-bp motif alleles had their allele size dropped by 200 and then doubled when calculating Manhattan distances. By doing so we ensured that all 2-bp motif alleles were treated as if they had 4-bp motifs but were distant enough from the true 4-bp motif alleles that the calculated Manhattan distance would also be sufficient to place them in distinct lineages.

Additionally, some 4-bp motif alleles for *Atex74* were larger than our ladder (ROX 500) and were therefore coded as 500-bp, as accurate size could not be determined beyond that.

## Supplemental Tables and Figures

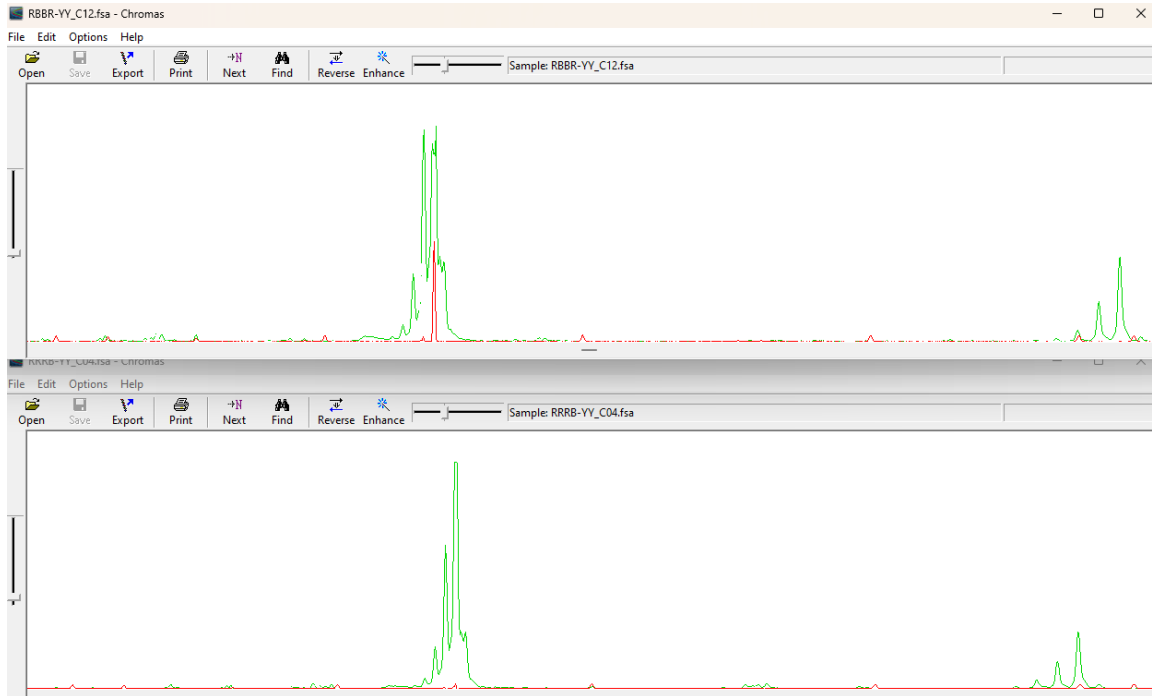


**Figure 3.S1.** Chroma images of two case examples of *A. texanum* individuals having two Atex74 (green) alleles with one having a 2-bp motif and the second having a 4-bp motif. Ladder (ROX 500, red) presented extends to 350 bp in image.

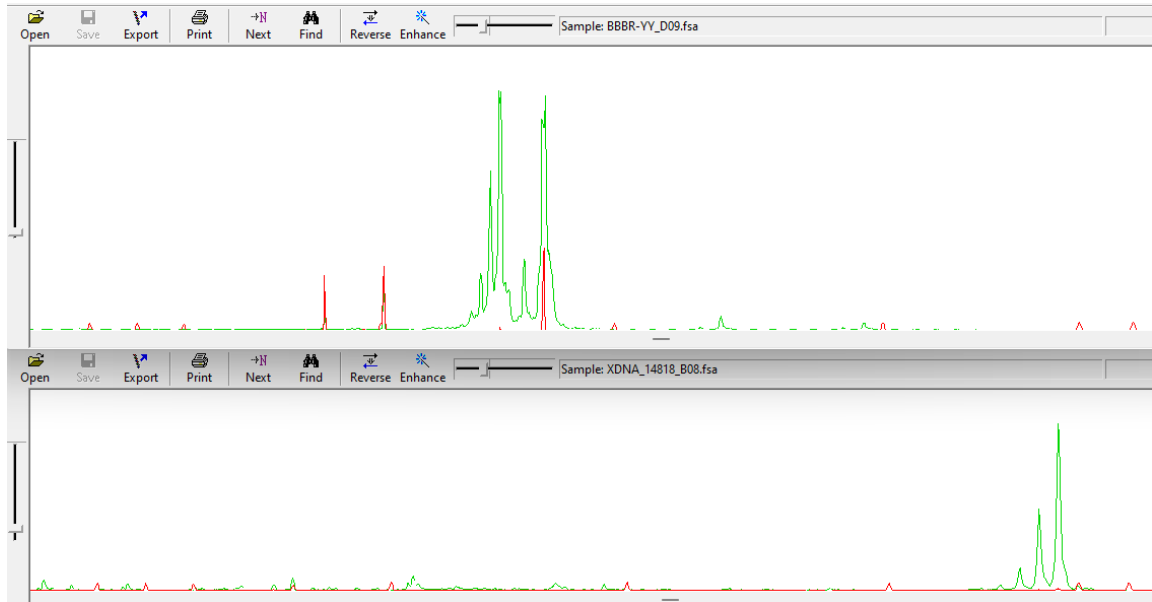


**Figure 3.S2.** Two additional Chroma images of *A. texanum* samples demonstrating a 235-bp allele for the 4-bp motif Atex74 (green) allele (top) and a sample with a 4-bp motif allele but without any 2-bp motif allele (bottom). Ladder (ROX 500, red) depicted out to 350-bp.

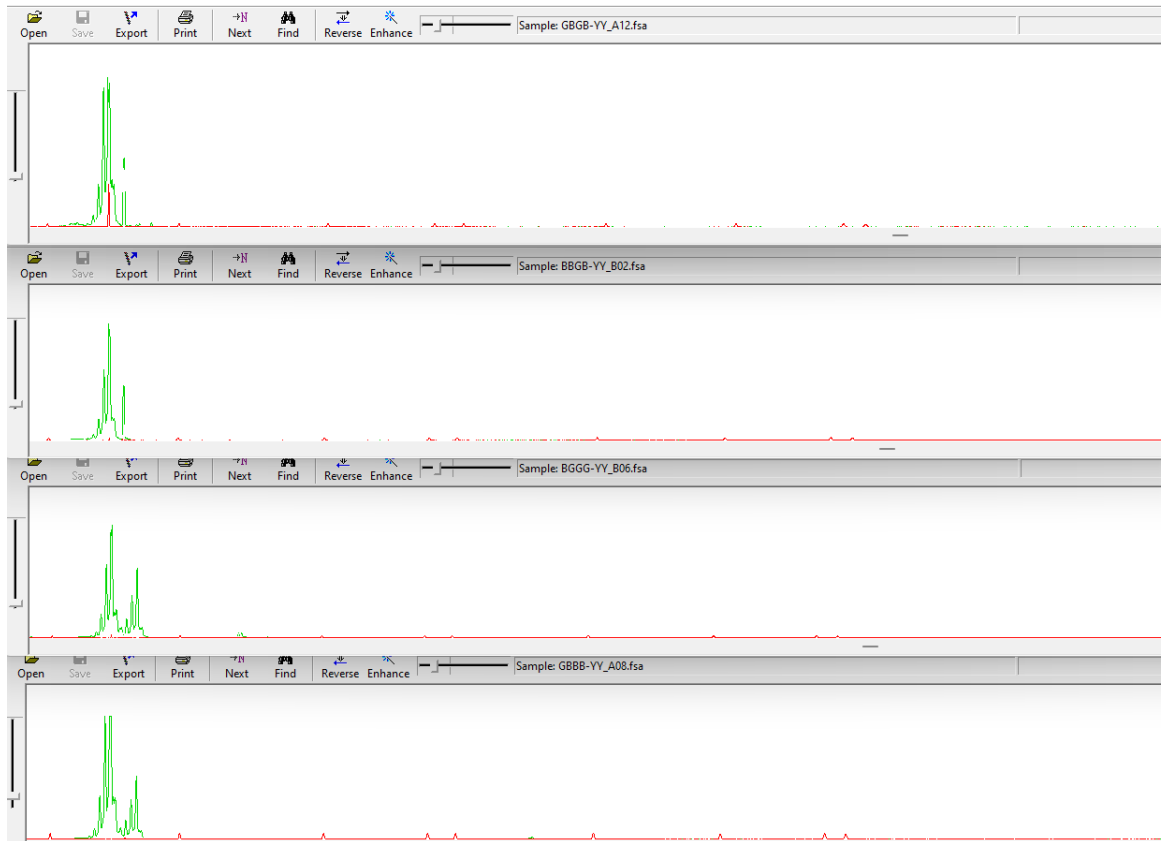


**Figure 3.S3.** Four additional *A. texanum* samples with only 2-bp motif Atex74 (green) alleles. Ladder (ROX 500, red) depicted out to 500-bp.

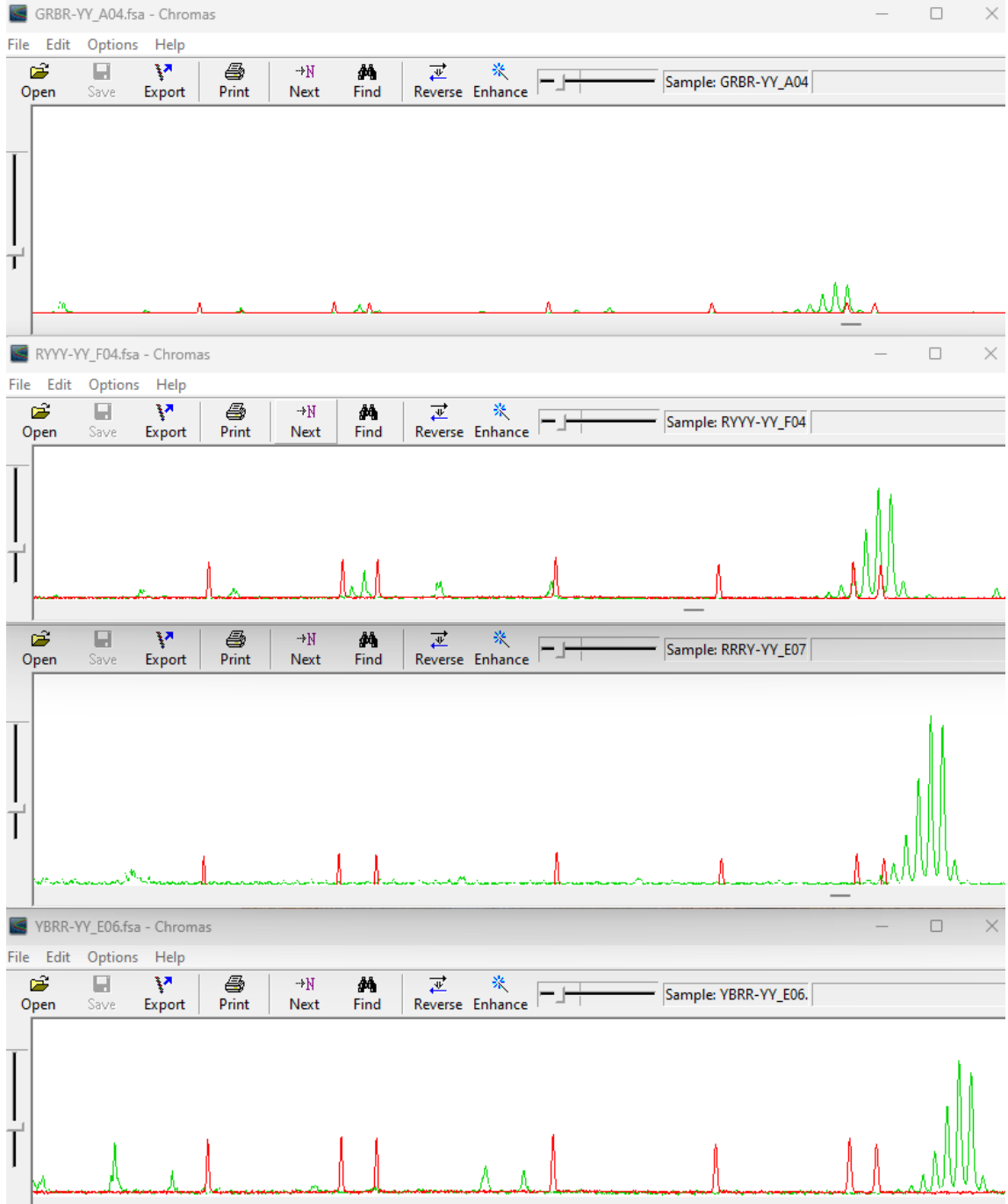


**Figure 3.S4.** Four examples of Atex74 (green) 4-bp motif alleles extending up to and beyond the 500-bp marker in the ladder (ROX 500, red).



**Figure 3.S5.** Satellite imagery of Pelee Island (Mar 2020, Google Images) overlaid with outlines of historic uplands (grey) using Google Earth. Upland outlines are based on the 1867 Campbell map (Figure C.2). Sand bars, particularly in the SW and NE corners, have shifted in the 150 years since the Campbell map was drawn.

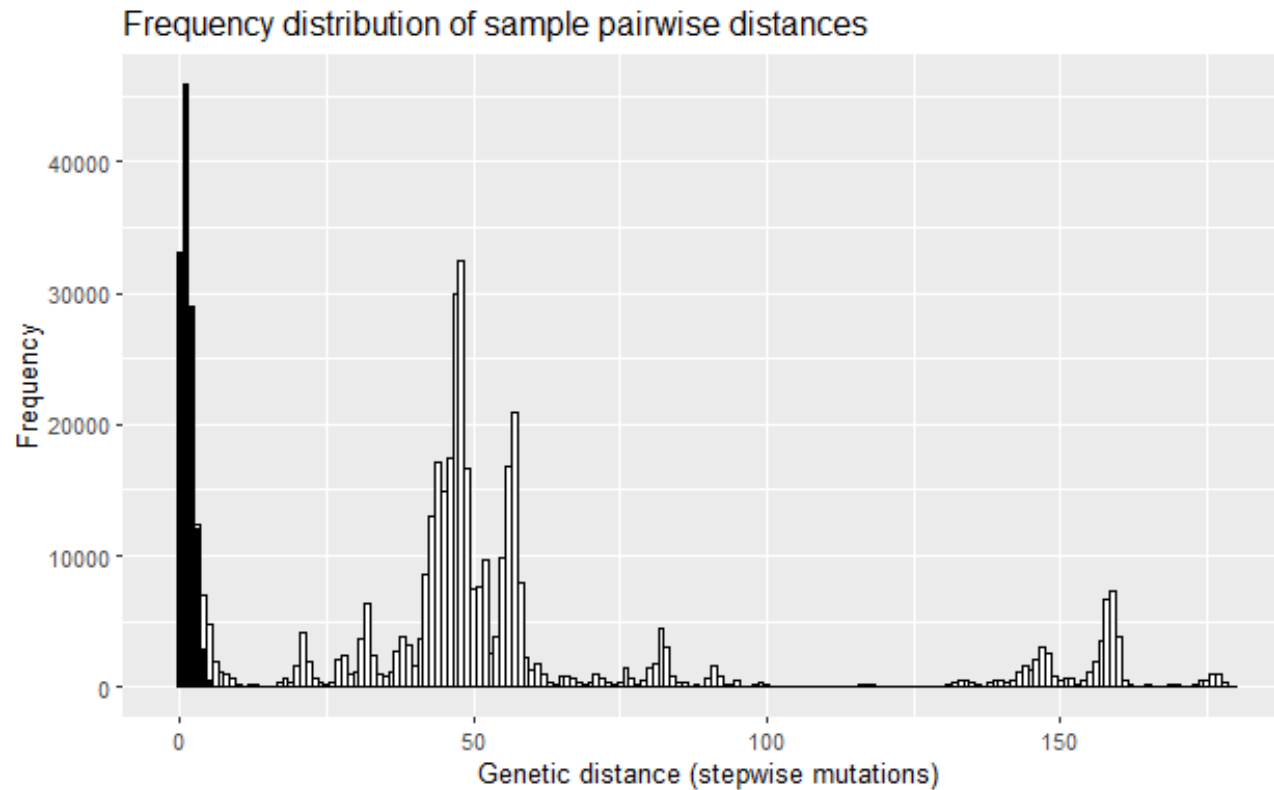


**Figure 3.S6.** Frequency distribution of pairwise distances between all sample pairs, includes samples with the same MLG. Black represents the sample pairs that are identified as the same lineage. Samples were inclusively grouped together into the same MLL so long as each sample was at least within two mutations steps of another sample in the same MLL. A single clonal lineage would be demonstrated by a single peak near the start of the histogram while a purely sexually reproducing population would resemble a normal curve<sup>108</sup>. Multiple peaks indicate multiple distinct lineages as samples of the same lineage would have a distance close to or at 0 while sample pairs from two different lineages would consistently have similar distances from each other.

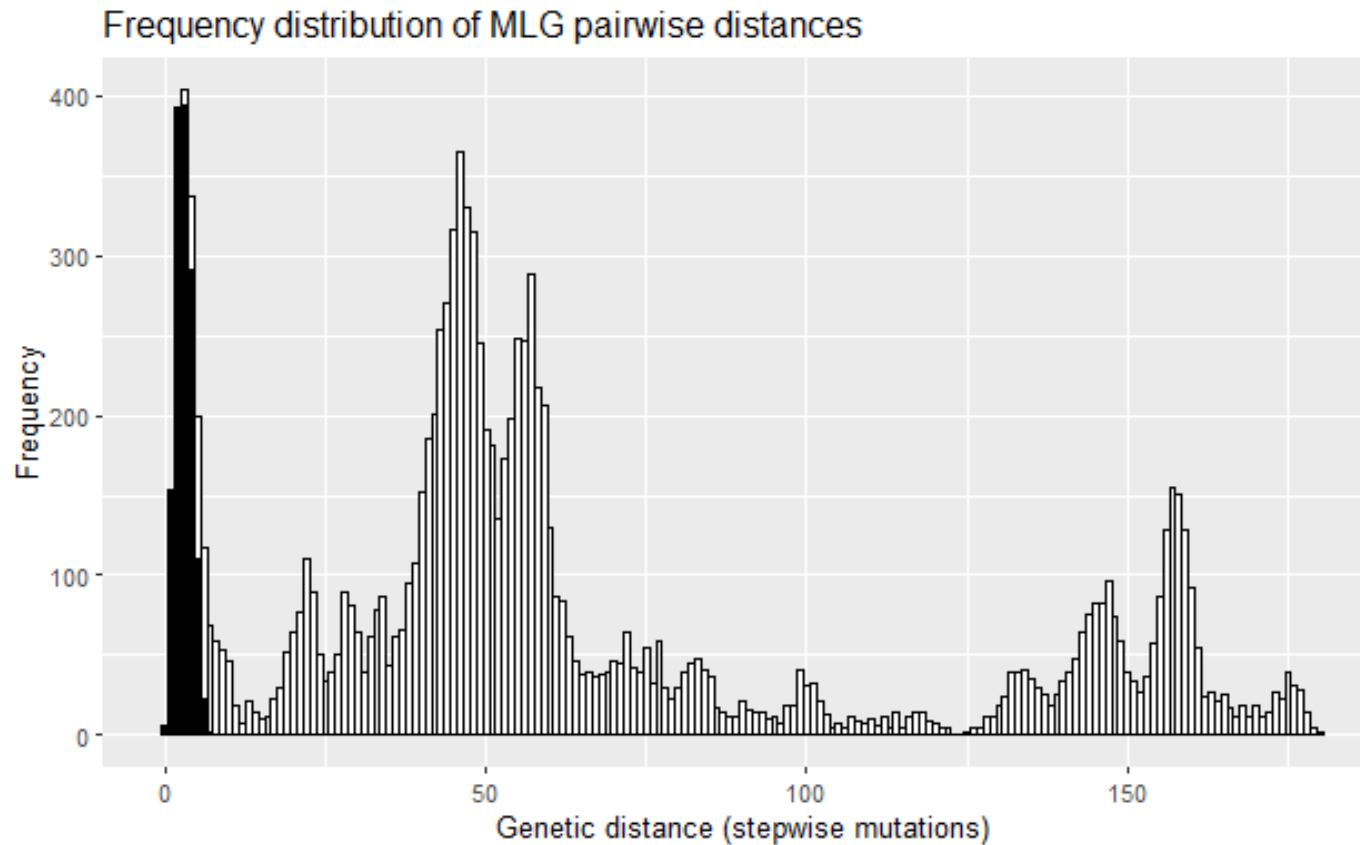


**Figure 3.S7.** Frequency distribution of pairwise distances between unique MLG pairs. Only one sample per MLG is represented in these pairings. Six MLG pairs have a pairwise distance of 0 due to missing allelic data for the second allele of either AjeD422 or AmmH123. Black represents the sample pairs that are identified as the same lineage. Samples were inclusively grouped together into the same MLL so long as each sample was at least within two mutations steps of another sample in the same MLL.

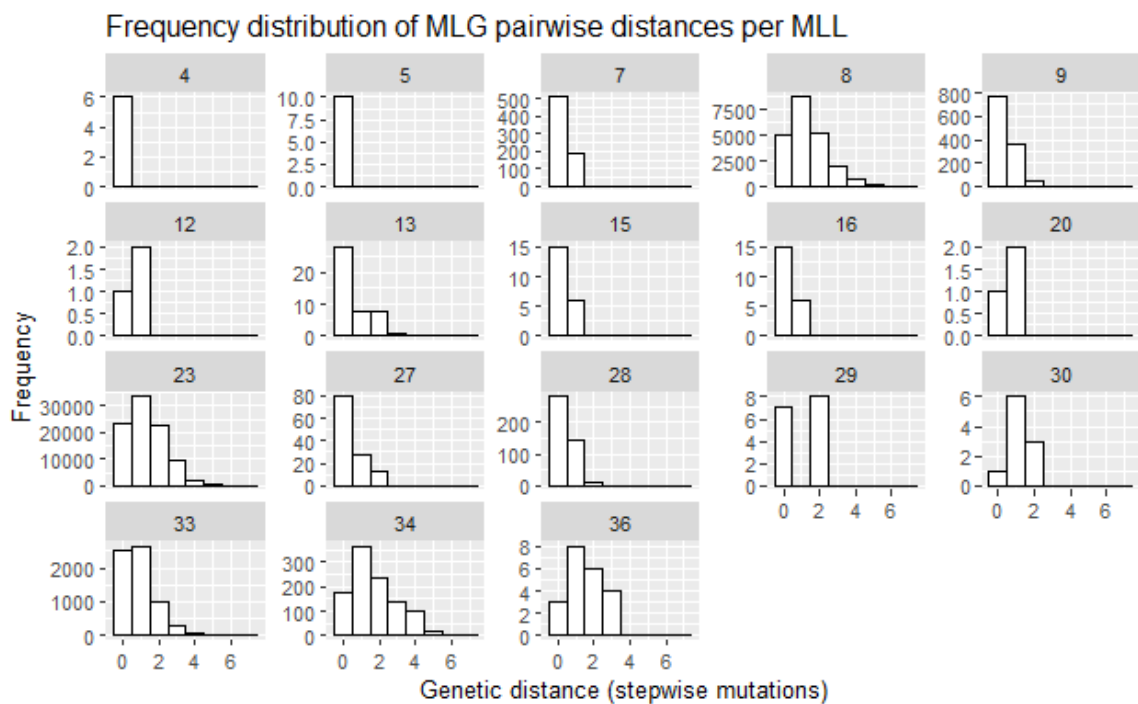


**Figure 3.S8.** Frequency distribution histograms of pairwise Manhattan distances among all sample pairs for each MLL with more than one sample. Only four MLL have any sample pairs with >6 stepwise mutation differences, all of which are among the five most sampled lineages. Of the top 5 most sampled MLL, only MLL-7 has no sample pairs with more than 3 stepwise mutation separation.

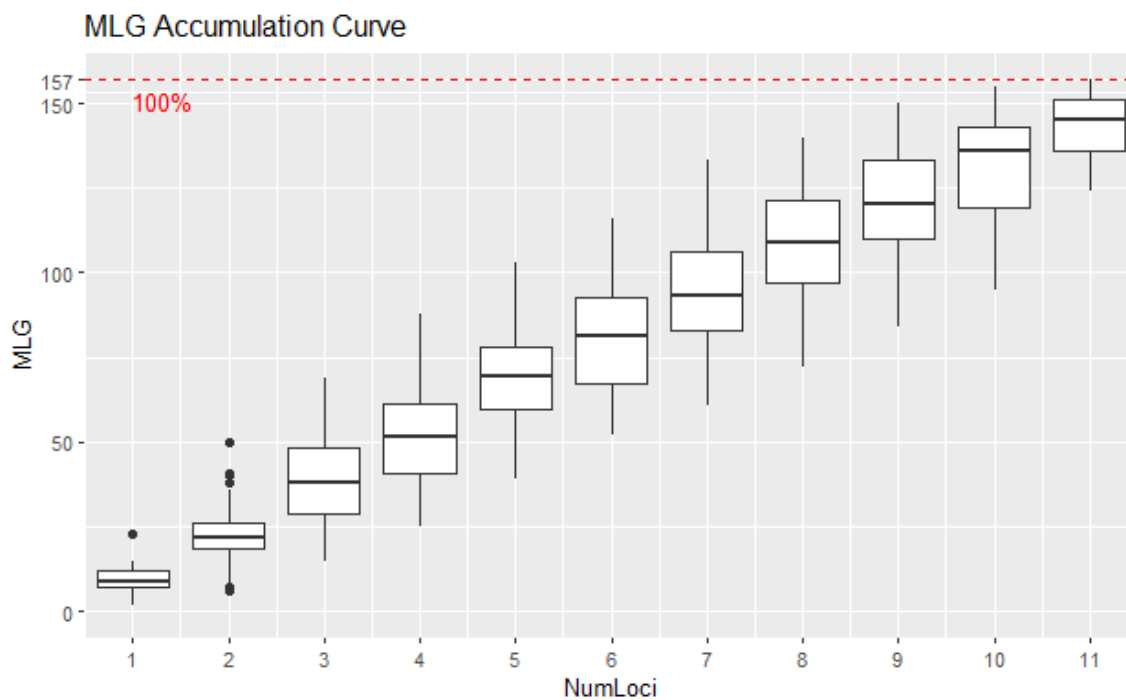


**Figure 3.S9.** Genotype accumulation curve of all LT genotypes, demonstrating a linear increase in genotype richness with increasing number of loci. AjeD283 and AmaD321 were removed from this assessment, and the two different Atex74 motif alleles were considered as a single locus (see above).

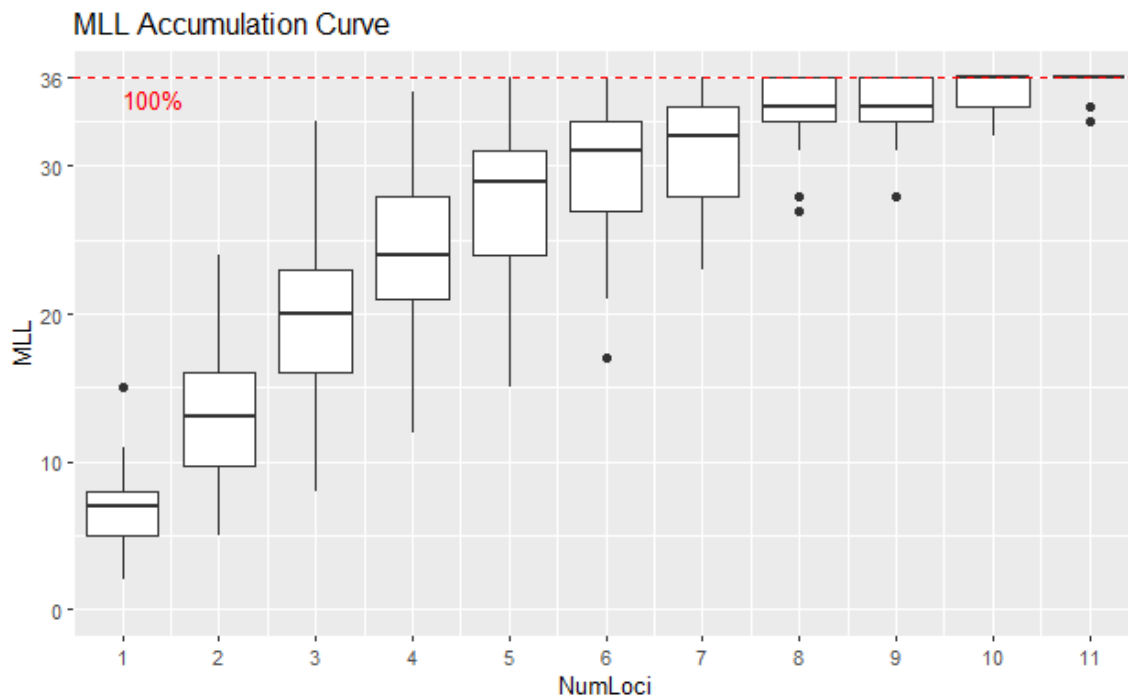


**Figure 3.S10.** Lineage accumulation curves demonstrating that MLL richness plateaus at 36 MLL as loci count increases beyond 6 loci. At minimum, all MLL can be identified using at least 5 loci, while not all MLL could be identified with two sets of 11 loci.

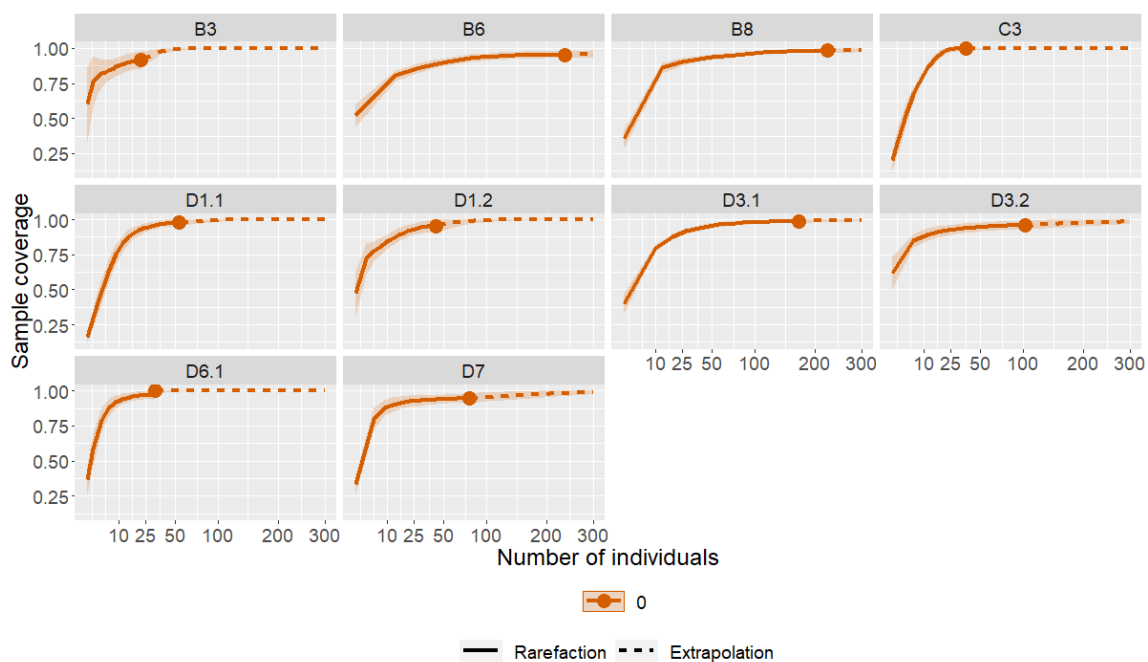


**Figure 3.S11.** Completeness curves for each site based on rarefaction and extrapolation calculations from *iNEXT*. Sample coverage estimates the proportion of the total number of individuals in an assemblage that belong to lineages represented by our sample, such that a value of 1 indicates that all individuals from an assemblage are represented by lineages documented. Coverage values have been extrapolated for each site out to a theoretical sample size of 300, with confidence intervals for the entire range of sample sizes.

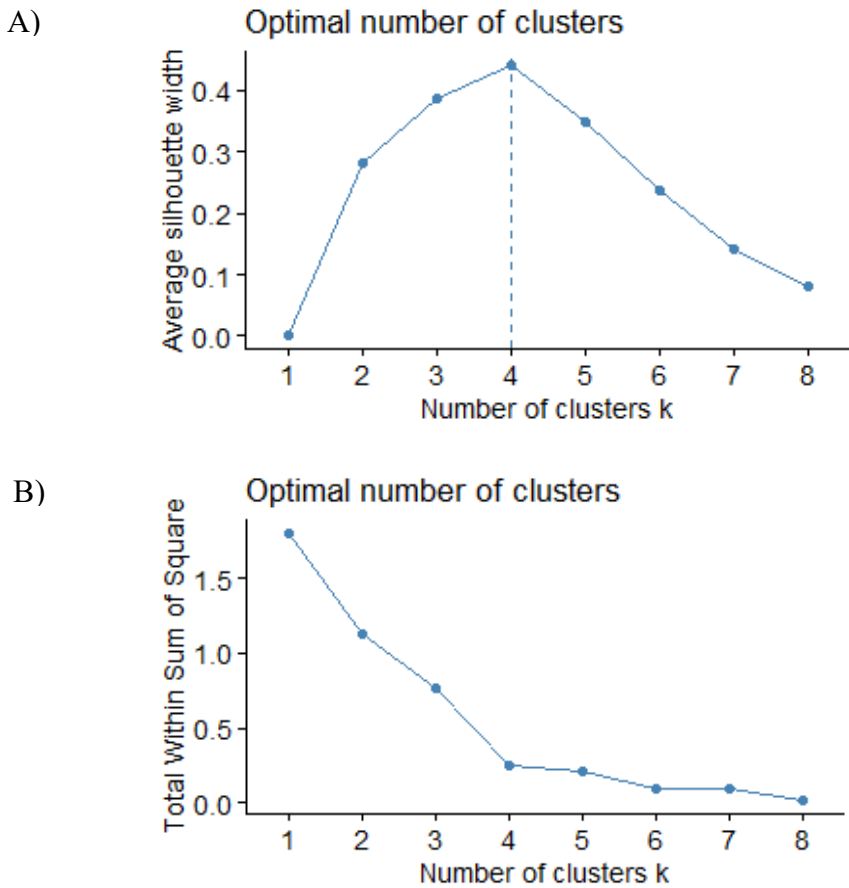


**Figure 3.S12.** A) Silhouette widths calculated by kmeans clustering, identifying 4 optimal clusters. B) Total width sum of squares (WSS) calculated by kmeans clustering identifying 4 optimal clusters.

**Table 3.S1.** Counts for each Full MLG ID, Short MLG ID, and MLL ID in total and by site. Full MLG ID are based on all available loci, while Short MLG ID do not consider AjeD283 or AmaD321 due to regular inconsistencies and uncertainties during genotyping. Full MLG ID was determined prior to filtering samples with incomplete loci data.

Site Details			Full MLG			Short MLG			MLL		
Site	HighGround	Site Count	ID	Count	Site Count	ID	Count	Site Count	ID	Count	Site Count
B6	S	236	197	1	1	89	1	1	1	1	1
B6	S	236	154	1	1	68	1	1	2	1	1
B8	S	225	43	1	1	10	1	1	3	1	1
B8	S	225	47	3	3	13	4	3	4	4	3
D7	S	78	48	1	1	13	4	1	4	4	1
D3.1	E	169	26	5	1	1	5	1	5	5	1
B3	NW	22	26	5	1	1	5	1	5	5	1
B8	S	225	26	5	2	1	5	2	5	5	2
D7	S	78	26	5	1	1	5	1	5	5	1
D7	S	78	69	1	1	27	1	1	6	1	1
C3	E	37	175	29	5	77	32	5	7	38	5
D3.1	E	169	163	1	1	77	32	10	7	38	10
D3.1	E	169	175	29	9	77	32	10	7	38	10
D3.2	E	103	176	1	1	78	1	1	7	38	1
D1.1	NE	54	175	29	4	77	32	4	7	38	4
B8	S	225	138	5	1	60	5	1	7	38	4
B8	S	225	160	1	1	77	32	3	7	38	4
B8	S	225	175	29	2	77	32	3	7	38	4
D6.1	S	32	138	5	3	60	5	3	7	38	11
D6.1	S	32	175	29	7	77	32	8	7	38	11
D6.1	S	32	179	1	1	77	32	8	7	38	11
D6.2	S	3	138	5	1	60	5	1	7	38	1
D7	S	78	175	29	2	77	32	2	7	38	2

Table 3.S1 *Continued.*

Site Details			Full MLG			Short MLG			MLL		
Site	HighGround	Site Count	ID	Count	Site Count	ID	Count	Site Count	ID	Count	Site Count
C3	E	37	171	83	2	73	93	2	8	210	5
C3	E	37	182	29	3	79	32	3	8	210	5
D3.1	E	169	136	18	1	58	20	1	8	210	15
D3.1	E	169	137	1	1	59	1	1	8	210	15
D3.1	E	169	142	9	1	62	11	1	8	210	15
D3.1	E	169	148	1	1	66	1	1	8	210	15
D3.1	E	169	167	1	1	73	93	7	8	210	15
D3.1	E	169	171	83	6	73	93	7	8	210	15
D3.1	E	169	182	29	4	79	32	4	8	210	15
D3.2	E	103	171	83	2	73	93	2	8	210	2
D1.1	NE	54	141	2	1	62	11	2	8	210	10
D1.1	NE	54	142	9	1	62	11	2	8	210	10
D1.1	NE	54	145	1	1	64	4	3	8	210	10
D1.1	NE	54	146	3	2	64	4	3	8	210	10
D1.1	NE	54	147	1	1	65	1	1	8	210	10
D1.1	NE	54	164	2	1	73	93	1	8	210	10
D1.1	NE	54	182	29	1	79	32	1	8	210	10
D1.1	NE	54	185	1	1	81	1	1	8	210	10
D1.1	NE	54	218	1	1	103	1	1	8	210	10
D1.2	NE	43	142	9	1	62	11	1	8	210	3
D1.2	NE	43	171	83	2	73	93	2	8	210	3
B3	NW	22	136	18	1	58	20	1	8	210	1
B6	S	236	171	83	4	73	93	4	8	210	7
B6	S	236	182	29	2	79	32	2	8	210	7
B6	S	236	187	1	1	83	1	1	8	210	7

Table 3.S1 *Continued.*

Site Details			Full MLG			Short MLG			MLL		
Site	HighGround	Site Count	ID	Count	Site Count	ID	Count	Site Count	ID	Count	Site Count
B8	S	225	39	1	1	6	1	1	8	210	121
B8	S	225	134	1	1	58	20	9	8	210	121
B8	S	225	136	18	8	58	20	9	8	210	121
B8	S	225	140	1	1	63	2	2	8	210	121
B8	S	225	142	9	5	62	11	5	8	210	121
B8	S	225	143	1	1	63	2	2	8	210	121
B8	S	225	144	1	1	61	1	1	8	210	121
B8	S	225	151	1	1	67	8	8	8	210	121
B8	S	225	152	6	6	67	8	8	8	210	121
B8	S	225	153	1	1	67	8	8	8	210	121
B8	S	225	155	1	1	69	7	7	8	210	121
B8	S	225	156	4	4	69	7	7	8	210	121
B8	S	225	157	2	2	69	7	7	8	210	121
B8	S	225	159	2	1	73	93	68	8	210	121
B8	S	225	161	1	1	73	93	68	8	210	121
B8	S	225	162	1	1	73	93	68	8	210	121
B8	S	225	168	1	1	70	1	1	8	210	121
B8	S	225	169	1	1	71	1	1	8	210	121
B8	S	225	171	83	62	73	93	68	8	210	121
B8	S	225	172	1	1	74	1	1	8	210	121
B8	S	225	174	2	2	76	2	2	8	210	121
B8	S	225	177	2	2	73	93	68	8	210	121
B8	S	225	178	1	1	73	93	68	8	210	121
B8	S	225	182	29	7	79	32	7	8	210	121
B8	S	225	186	1	1	82	1	1	8	210	121
B8	S	225	190	1	1	85	10	7	8	210	121
B8	S	225	191	7	5	85	10	7	8	210	121
B8	S	225	193	1	1	85	10	7	8	210	121

Table 3.S1 *Continued.*

Site Details			Full MLG			Short MLG			MLL		
Site	HighGround	Site Count	ID	Count	Site Count	ID	Count	Site Count	ID	Count	Site Count
D1.1	NE	54	244	2	1	123	38	7	9	49	7
D3.2	E	103	232	1	1	114	1	1	9	49	13
D3.2	E	103	243	7	1	122	7	1	9	49	13
D3.2	E	103	247	34	11	123	38	11	9	49	13
D1.1	NE	54	245	1	1	123	38	7	9	49	7
D1.1	NE	54	247	34	5	123	38	7	9	49	7
D1.2	NE	43	239	1	1	119	1	1	9	49	6
D1.2	NE	43	246	1	1	123	38	5	9	49	6
D1.2	NE	43	247	34	4	123	38	5	9	49	6
B6	S	236	28	1	1	3	1	1	10	1	1
B6	S	236	220	1	1	104	1	1	11	1	1
B6	S	236	230	1	1	112	1	1	12	3	3
B6	S	236	231	2	2	113	2	2	12	3	3
B6	S	236	277	8	8	145	8	8	13	10	10
B6	S	236	278	1	1	146	1	1	13	10	10
B6	S	236	286	1	1	152	1	1	13	10	10
B6	S	236	225	1	1	108	1	1	14	1	1
B6	S	236	223	5	5	107	6	6	15	7	6
B6	S	236	224	1	1	107	6	6	15	7	6
B8	S	225	222	1	1	106	1	1	15	7	1
B6	S	236	40	6	6	7	6	6	16	7	7
B6	S	236	41	1	1	8	1	1	16	7	7
B6	S	236	46	1	1	12	1	1	17	1	1
B6	S	236	37	1	1	4	1	1	18	1	1
B6	S	236	38	1	1	5	1	1	19	1	1
B6	S	236	195	2	2	87	2	2	20	3	3
B6	S	236	196	1	1	88	1	1	20	3	3
D3.1	E	169	42	1	1	9	1	1	21	1	1
D3.2	E	103	70	1	1	28	1	1	22	1	1

Table 3.S1 *Continued.*

Site Details			Full MLG			Short MLG			MLL		
Site	HighGround	Site Count	ID	Count	Site Count	ID	Count	Site Count	ID	Count	Site Count
C3	E	37	67	2	1	25	2	1	23	428	14
C3	E	37	85	2	1	34	2	1	23	428	14
C3	E	37	89	164	6	37	181	6	23	428	14
C3	E	37	90	7	2	38	7	2	23	428	14
C3	E	37	107	17	1	42	17	1	23	428	14
C3	E	37	108	101	2	43	112	2	23	428	14
C3	E	37	124	1	1	51	1	1	23	428	14
D2	E	5	67	2	1	25	2	1	23	428	2
D2	E	5	89	164	1	37	181	1	23	428	2
D3.1	E	169	45	5	3	11	5	3	23	428	104
D3.1	E	169	62	2	1	20	3	1	23	428	104
D3.1	E	169	63	2	2	21	2	2	23	428	104
D3.1	E	169	65	1	1	23	1	1	23	428	104
D3.1	E	169	66	19	1	24	19	1	23	428	104
D3.1	E	169	68	9	4	26	9	4	23	428	104
D3.1	E	169	73	6	6	31	6	6	23	428	104
D3.1	E	169	75	1	1	37	181	53	23	428	104
D3.1	E	169	84	1	1	33	1	1	23	428	104
D3.1	E	169	86	2	2	35	2	2	23	428	104
D3.1	E	169	89	164	51	37	181	53	23	428	104
D3.1	E	169	90	7	2	38	7	2	23	428	104
D3.1	E	169	94	1	1	37	181	53	23	428	104
D3.1	E	169	105	1	1	40	1	1	23	428	104
D3.1	E	169	106	1	1	41	1	1	23	428	104
D3.1	E	169	107	17	8	42	17	8	23	428	104
D3.1	E	169	108	101	11	43	112	12	23	428	104
D3.1	E	169	109	2	1	44	3	1	23	428	104
D3.1	E	169	115	1	1	43	112	12	23	428	104

Table 3.S1 *Continued.*

Site Details			Full MLG			Short MLG			MLL		
Site	HighGround	Site Count	ID	Count	Site Count	ID	Count	Site Count	ID	Count	Site Count
D3.1	E	169	118	1	1	48	1	1	23	428	104
D3.1	E	169	125	2	1	52	2	1	23	428	104
D3.1	E	169	130	3	3	54	28	3	23	428	104
D3.2	E	103	45	5	1	11	5	1	23	428	80
D3.2	E	103	64	2	2	22	2	2	23	428	80
D3.2	E	103	66	19	16	24	19	16	23	428	80
D3.2	E	103	89	164	17	37	181	17	23	428	80
D3.2	E	103	102	1	1	43	112	34	23	428	80
D3.2	E	103	107	17	8	42	17	8	23	428	80
D3.2	E	103	108	101	26	43	112	34	23	428	80
D3.2	E	103	112	1	1	43	112	34	23	428	80
D3.2	E	103	114	6	6	43	112	34	23	428	80
D3.2	E	103	121	1	1	50	1	1	23	428	80
D3.2	E	103	128	25	1	54	28	1	23	428	80
D1.1	NE	54	76	1	1	37	181	7	23	428	10
D1.1	NE	54	77	1	1	37	181	7	23	428	10
D1.1	NE	54	82	3	3	37	181	7	23	428	10
D1.1	NE	54	89	164	2	37	181	7	23	428	10
D1.1	NE	54	103	1	1	44	3	1	23	428	10
D1.1	NE	54	108	101	1	43	112	1	23	428	10
D1.1	NE	54	116	1	1	46	1	1	23	428	10
D1.2	NE	43	89	164	1	37	181	1	23	428	3
D1.2	NE	43	92	1	1	32	1	1	23	428	3
D1.2	NE	43	109	2	1	44	3	1	23	428	3
B3	NW	22	66	19	2	24	19	2	23	428	3
B3	NW	22	89	164	1	37	181	1	23	428	3

Table 3.S1 *Continued.*

Site Details			Full MLG			Short MLG			MLL		
Site	HighGround	Site Count	ID	Count	Site Count	ID	Count	Site Count	ID	Count	Site Count
B6	S	236	27	1	1	2	1	1	23	428	169
B6	S	236	61	1	1	20	3	2	23	428	169
B6	S	236	62	2	1	20	3	2	23	428	169
B6	S	236	68	9	5	26	9	5	23	428	169
B6	S	236	71	1	1	29	1	1	23	428	169
B6	S	236	72	1	1	30	1	1	23	428	169
B6	S	236	85	2	1	34	2	1	23	428	169
B6	S	236	88	3	3	36	4	4	23	428	169
B6	S	236	89	164	68	37	181	75	23	428	169
B6	S	236	90	7	3	38	7	3	23	428	169
B6	S	236	91	1	1	39	1	1	23	428	169
B6	S	236	93	1	1	37	181	75	23	428	169
B6	S	236	95	2	2	37	181	75	23	428	169
B6	S	236	96	1	1	37	181	75	23	428	169
B6	S	236	97	1	1	36	4	4	23	428	169
B6	S	236	98	1	1	37	181	75	23	428	169
B6	S	236	100	1	1	37	181	75	23	428	169
B6	S	236	101	1	1	37	181	75	23	428	169
B6	S	236	108	101	43	43	112	44	23	428	169
B6	S	236	110	1	1	45	1	1	23	428	169
B6	S	236	113	1	1	43	112	44	23	428	169
B6	S	236	117	1	1	47	1	1	23	428	169
B6	S	236	119	1	1	49	1	1	23	428	169
B6	S	236	125	2	1	52	2	1	23	428	169
B6	S	236	127	1	1	53	1	1	23	428	169
B6	S	236	128	25	24	54	28	24	23	428	169
B6	S	236	129	3	2	55	4	2	23	428	169
B8	S	225	89	164	1	37	181	1	23	428	4
B8	S	225	108	101	2	43	112	2	23	428	4

Table 3.S1 *Continued.*

Site Details			Full MLG Details			Short MLG Details			MLL Details		
Site	HighGround	Site Count	ID	Count	Site Count	ID	Count	Site Count	ID	Count	Site Count
B8	S	225	133	1	1	57	1	1	23	428	4
D6.1	S	32	99	1	1	37	181	1	23	428	4
D6.1	S	32	108	101	2	43	112	3	23	428	4
D6.1	S	32	111	1	1	43	112	3	23	428	4
D6.2	S	3	89	164	1	37	181	1	23	428	2
D6.2	S	3	108	101	1	43	112	1	23	428	2
D7	S	78	45	5	1	11	5	1	23	428	33
D7	S	78	80	1	1	37	181	17	23	428	33
D7	S	78	81	1	1	37	181	17	23	428	33
D7	S	78	89	164	15	37	181	17	23	428	33
D7	S	78	108	101	13	43	112	13	23	428	33
D7	S	78	129	3	1	55	4	2	23	428	33
D7	S	78	131	1	1	55	4	2	23	428	33
B6	S	236	132	1	1	56	1	1	24	1	1
B6	S	236	194	1	1	86	1	1	25	1	1
B6	S	236	235	1	1	117	1	1	26	1	1
B6	S	236	226	2	2	109	2	2	27	16	16
B6	S	236	227	1	1	110	1	1	27	16	16
B6	S	236	228	13	13	111	13	13	27	16	16
C3	E	37	56	19	3	17	24	4	28	30	5
C3	E	37	57	1	1	18	1	1	28	30	5
C3	E	37	58	1	1	17	24	4	28	30	5
D3.1	E	169	56	19	2	17	24	2	28	30	2
D3.2	E	103	56	19	1	17	24	1	28	30	1
D1.1	NE	54	52	1	1	16	1	1	28	30	5
D1.1	NE	54	56	19	4	17	24	4	28	30	5
B3	NW	22	54	1	1	17	24	13	28	30	17
B3	NW	22	55	3	3	17	24	13	28	30	17
B3	NW	22	56	19	9	17	24	13	28	30	17

Table 3.S1 *Continued.*

Site Details			Full MLG Details			MLG Details			MLL Details		
Site	HighGround	Site Count	ID	Count	Site Count	ID	Count	Site Count	ID	Count	Site Count
B3	NW	22	59	4	4	19	4	4	28	30	17
D3.1	E	169	49	1	1	14	2	2	29	6	4
D3.1	E	169	50	1	1	14	2	2	29	6	4
D3.1	E	169	51	4	2	15	4	2	29	6	4
D1.1	NE	54	51	4	1	15	4	1	29	6	1
D1.2	NE	43	51	4	1	15	4	1	29	6	1
B8	S	225	279	1	1	147	1	1	30	5	5
B8	S	225	280	1	1	149	2	2	30	5	5
B8	S	225	281	1	1	149	2	2	30	5	5
B8	S	225	283	1	1	148	1	1	30	5	5
B8	S	225	284	1	1	150	1	1	30	5	5
D1.2	NE	43	240	1	1	120	1	1	31	1	1
B8	S	225	250	1	1	126	1	1	32	1	1
D2	E	5	221	1	1	105	1	1	33	115	3
D2	E	5	265	64	1	133	70	1	33	115	3
D2	E	5	266	3	1	134	3	1	33	115	3
D3.1	E	169	233	4	1	115	4	1	33	115	8
D3.1	E	169	251	1	1	127	1	1	33	115	8
D3.1	E	169	253	4	2	129	4	2	33	115	8
D3.1	E	169	264	1	1	132	2	1	33	115	8
D3.1	E	169	265	64	1	133	70	1	33	115	8
D3.1	E	169	267	2	1	135	2	1	33	115	8
D3.1	E	169	275	2	1	143	2	1	33	115	8
D3.2	E	103	233	4	1	115	4	1	33	115	4
D3.2	E	103	262	1	1	132	2	1	33	115	4
D3.2	E	103	265	64	2	133	70	2	33	115	4
D1.1	NE	54	233	4	1	115	4	1	33	115	15

Table 3.S1 *Continued.*

Site Details			Full MLG Details			MLG Details			MLL Details		
Site	HighGround	Site Count	ID	Count	Site Count	ID	Count	Site Count	ID	Count	Site Count
D1.1	NE	54	234	1	1	116	1	1	33	115	15
D1.1	NE	54	252	1	1	128	1	1	33	115	15
D1.1	NE	54	253	4	1	129	4	1	33	115	15
D1.1	NE	54	254	1	1	130	1	1	33	115	15
D1.1	NE	54	258	1	1	133	70	9	33	115	15
D1.1	NE	54	259	1	1	136	1	1	33	115	15
D1.1	NE	54	265	64	8	133	70	9	33	115	15
D1.2	NE	43	233	4	1	115	4	1	33	115	29
D1.2	NE	43	253	4	1	129	4	1	33	115	29
D1.2	NE	43	265	64	22	133	70	22	33	115	29
D1.2	NE	43	266	3	2	134	3	2	33	115	29
D1.2	NE	43	267	2	1	135	2	1	33	115	29
D1.2	NE	43	271	1	1	139	1	1	33	115	29
D1.2	NE	43	274	1	1	142	1	1	33	115	29
B8	S	225	249	1	1	125	1	1	33	115	55
B8	S	225	256	1	1	133	70	35	33	115	55
B8	S	225	257	1	1	133	70	35	33	115	55
B8	S	225	260	1	1	133	70	35	33	115	55
B8	S	225	261	1	1	133	70	35	33	115	55
B8	S	225	263	1	1	131	1	1	33	115	55
B8	S	225	265	64	30	133	70	35	33	115	55
B8	S	225	268	1	1	133	70	35	33	115	55
B8	S	225	269	1	1	137	1	1	33	115	55
B8	S	225	270	13	13	138	13	13	33	115	55
B8	S	225	273	1	1	141	1	1	33	115	55
B8	S	225	275	2	1	143	2	1	33	115	55
B8	S	225	276	1	1	144	1	1	33	115	55
B8	S	225	285	1	1	151	1	1	33	115	55
D7	S	78	272	1	1	140	1	1	33	115	1

Table 3.S1 *Continued.*

Site Details			Full MLG Details			MLG Details			MLL Details		
Site	HighGround	Site Count	ID	Count	Site Count	ID	Count	Site Count	ID	Count	Site Count
C3	E	37	211	14	2	98	16	2	34	46	4
C3	E	37	213	9	2	100	10	2	34	46	4
D3.1	E	169	211	14	2	98	16	2	34	46	5
D3.1	E	169	212	2	1	99	3	1	34	46	5
D3.1	E	169	213	9	2	100	10	2	34	46	5
D3.2	E	103	217	1	1	102	1	1	34	46	1
D1.1	NE	54	205	2	1	96	2	1	34	46	2
D1.1	NE	54	211	14	1	98	16	1	34	46	2
B6	S	236	211	14	4	98	16	4	34	46	4
B8	S	225	198	3	3	90	3	3	34	46	20
B8	S	225	199	1	1	91	1	1	34	46	20
B8	S	225	200	2	1	92	2	1	34	46	20
B8	S	225	201	1	1	93	1	1	34	46	20
B8	S	225	202	1	1	94	1	1	34	46	20
B8	S	225	203	1	1	95	2	2	34	46	20
B8	S	225	204	1	1	95	2	2	34	46	20
B8	S	225	205	2	1	96	2	1	34	46	20
B8	S	225	207	1	1	98	16	5	34	46	20
B8	S	225	209	1	1	99	3	2	34	46	20
B8	S	225	210	1	1	98	16	5	34	46	20
B8	S	225	211	14	3	98	16	5	34	46	20
B8	S	225	212	2	1	99	3	2	34	46	20
B8	S	225	214	1	1	101	3	3	34	46	20
B8	S	225	215	1	1	101	3	3	34	46	20
B8	S	225	216	1	1	101	3	3	34	46	20

Table 3.S1 *Continued.*

Site Details			Full MLG Details			MLG Details			MLL Details		
Site	HighGround	Site Count	ID	Count	Site Count	ID	Count	Site Count	ID	Count	Site Count
D6.1	S	32	211	14	1	98	16	1	34	46	1
D7	S	78	200	2	1	92	2	1	34	46	9
D7	S	78	206	1	1	97	1	1	34	46	9
D7	S	78	208	1	1	100	10	6	34	46	9
D7	S	78	211	14	1	98	16	1	34	46	9
D7	S	78	213	9	5	100	10	6	34	46	9
B8	S	225	236	1	1	118	1	1	35	1	1
B8	S	225	287	1	1	153	1	1	36	7	7
B8	S	225	288	1	1	154	1	1	36	7	7
B8	S	225	289	2	2	155	3	3	36	7	7
B8	S	225	290	1	1	155	3	3	36	7	7
B8	S	225	291	1	1	156	1	1	36	7	7
B8	S	225	292	1	1	157	1	1	36	7	7

**Table 3.S2.** Genotypes for each Full MLG per MLL. Loci are arranged by species association. Atex74 has alleles of two different motif sizes, with 4-bp motif alleles designated by “<sub>4bp</sub>”. Atex74 alleles larger than 500 were assigned 503, as it is the next largest allele that would come after the 500-bp limit. Loci AmaD321 and AjeD283 were not used when determining lineage assignments as they are presumed less accurate and are therefore italicized.

	<i>A. laterale</i>							<i>A. texanum</i>				Both Hosts		
	AcroD315	AjeD23	AjeD75	AjeD94	AjeD346	AmaD42	AmaD367	Atex74	Atex102	Atex141	<i>AmaD321</i>	<i>AjeD283</i>	AjeD422	AmmH123
<b>MLL-1</b>														
197	270	234	122	150	270	186	186	275 <sub>4bp</sub>	176	228	<i>158/170</i>	<i>152/180</i>	238/274	86/122
<b>MLL-2</b>														
154	182	226	106	150	278	166	170	223	200	228	<i>162/170</i>	<i>172</i>	234/254	94/118
<b>MLL-3</b>														
43	182	226	106	150	278	166	170	223	172	228	<i>162/170</i>	<i>172</i>	234/274	94/118
<b>MLL-4</b>														
47	182	226	106	150	278	166	170	223	180	228	<i>162/170</i>	<i>172</i>	234/270	94/118
48	182	226	106	150	278	166	170	223	180	228	<i>162</i>	<i>172</i>	234/270	94/118
<b>MLL-5</b>														
26	182	226	106	150	282	166	170	223	200	220	<i>162/170</i>	<i>172</i>	234/278	94/118
<b>MLL-6</b>														
69	182	226	106	150	278	166	170	223	184	228	<i>162/170</i>	<i>172/180</i>	234/278	94/118
<b>MLL-7</b>														
138	182	214	106	150	278	166	174	223	196	228	<i>162/170</i>	<i>172</i>	234/274	94/118
160	182	214	106	150	278	166	174	223	200	228	<i>162/170</i>	<i>152/172</i>	234/274	94/118
163	182	214	106	150	278	166	174	223	200	228	<i>162/170</i>	<i>168</i>	234/274	94/118
175	182	214	106	150	278	166	174	223	200	228	<i>162/170</i>	<i>172</i>	234/274	94/118
176	186	214	106	150	278	166	174	223	200	228	<i>162/170</i>	<i>172</i>	234/274	94/118
179	182	214	106	150	278	166	174	223	200	228	<i>162/170</i>	<i>176</i>	234/274	94/118
<b>MLL-8</b>														
39	182	226	106	150	274	166	170	221	200	228	<i>162/170</i>	<i>172</i>	234/274	94/118
134	182	226	106	150	278	166	170	223	196	228	<i>162/170</i>	<i>172/176</i>	234/274	94/118
136	182	226	106	150	278	166	170	223	196	228	<i>162/170</i>	<i>172</i>	234/274	94/118
137	186	226	106	150	278	166	170	223	196	228	<i>162/170</i>	<i>172</i>	234/274	94/118
139	182	226	106	150	278	166	170	223	196	228	<i>162/174</i>	<i>172</i>	234/274	94/118
140	182	230	106	150	278	166	170	223	196	228	<i>162/170</i>	<i>148/172</i>	234/278	94/118

Table 3.S2 *Continued.*

	<i>A. laterale</i>							<i>A. texanum</i>				Both Hosts		
	AcroD315	AjeD23	AjeD75	AjeD94	AjeD346	AmaD42	AmaD367	Atex74	Atex102	Atex141	<i>AmaD321</i>	<i>AjeD283</i>	AjeD422	AmmH123
<b>MLL-8</b>														
141	182	226	106	150	278	166	170	223	196	228	162/170	152/172	234/278	94/118
142	182	226	106	150	278	166	170	223	196	228	162/170	172	234/278	94/118
143	182	230	106	150	278	166	170	223	196	228	162/170	172	234/278	94/118
144	182	222	106	150	278	166	170	223	196	228	162	172	234/278	94/118
145	182	226	110	150	278	166	170	223	196	228	162/170	172/176	234/270	94/118
146	182	226	110	150	278	166	170	223	196	228	162/170	172	234/270	94/118
147	182	226	110	150	278	166	174	223	196	228	162/170	172	234/270	94/118
148	182	226	110	150	278	166	170	223	196	228	162/170	172	234/274	94/118
151	182	226	106	150	274	166	170	223	200	228	162/170	140/172	234/274	94/118
152	182	226	106	150	274	166	170	223	200	228	162/170	172	234/274	94/118
153	182	226	106	150	274	166	170	223	200	228	162	172	234/274	94/118
155	182	226	106	150	278	166	170	223	200	228	162/170	144/172	234/270	94/118
156	182	226	106	150	278	166	170	223	200	228	162/166	172	234/270	94/118
157	182	226	106	150	278	166	170	223	200	228	162/170	172	234/270	94/118
159	182	226	106	150	278	166	170	223	200	228	162/170	144/172	234/274	94/118
161	182	226	106	150	278	166	170	223	200	228	154/170	164/172	234/274	94/118
162	182	226	106	150	278	166	170	223	200	228	162/170	164/172	234/274	94/118
164	182	226	106	150	278	166	170	223	200	228	162/170	172/176	234/274	94/118
167	182	226	106	150	278	166	170	223	200	228	162/166	172	234/274	94/118
168	182	222	106	150	278	166	170	223	200	228	162/170	172	234/274	94/118
169	182	226	106	150	278	166	170	223	200	228	162/170	172	234/274	94/114
170	178	226	106	150	278	166	170	223	200	228	162/170	172	234/274	94/118
171	182	226	106	150	278	166	170	223	200	228	162/170	172	234/274	94/118
172	186	226	106	150	278	166	170	223	200	228	162/170	172	234/274	94/118
173	182	226	106	150	278	166	170	223	200	228	162/170	172	234/274	94/122
174	182	230	106	150	278	166	170	223	200	228	162/170	172	234/274	94/118
177	182	226	106	150	278	166	170	223	200	228	162	172	234/274	94/118
178	182	226	106	150	278	166	170	223	200	228	166/170	172	234/274	94/118
181	182	226	106	150	278	166	170	223	200	228	162/170	168/172	234/278	94/118
182	182	226	106	150	278	166	170	223	200	228	162/170	172	234/278	94/118
183	182	226	106	150	278	166	170	223	200	228	162	172	234/278	94/118
184	182	226	106	150	278	166	170	223	200	228	162/170	172	234/282	94/118

Table 3.S2 *Continued.*

	<i>A. laterale</i>							<i>A. texanum</i>				Both Hosts		
	AcroD315	AjeD23	AjeD75	AjeD94	AjeD346	AmaD42	AmaD367	Atex74	Atex102	Atex141	AmaD321	AjeD283	AjeD422	AmmH123
<b>MLL-8</b>														
185	186	226	106	150	278	166	170	223	200	228	162/170	172	238/274	94/118
186	182	226	106	150	282	166	166	223	200	228	162/170	172	234/274	94/118
187	182	226	114	150	278	166	170	223	200	228	162/170	172	234/278	94/118
189	182	226	106	150	278	166	170	223	204	228	162/166	148/172	234/274	94/118
190	182	226	106	150	278	166	170	223	204	228	162/170	172/176	234/274	94/118
191	182	226	106	150	278	166	170	223	204	228	162/170	172	234/274	94/118
192	182	226	106	150	278	166	166	223	204	228	162	172	234/274	94/118
193	182	226	106	150	278	166	170	223	204	228	162	172	234/274	94/118
218	182	226	106	150	278	166	170	223	196	232	162/166	172	234/270	94/118
<b>MLL-9</b>														
232	266	214	126	150	278	218	146	223	172	276	142	172	238/262	86/150
239	266	214	126	150	278	218	146	221	172	280	142	172	238/262	86/150
242	266	214	126	150	274	218	146	223	168	280	142	172	238/262	86/150
243	266	214	126	150	278	218	146	223	168	280	142	172	238/262	86/150
244	266	214	126	150	278	218	146	223	172	280	142	144/172	238/262	86/150
245	266	214	126	150	278	218	146	223	172	280	142	148/172	238/262	86/150
246	266	214	126	150	278	218	146	223	172	280	142	172/176	238/262	86/150
247	266	214	126	150	278	218	146	223	172	280	142	172	238/262	86/150
248	266	214	126	150	278	218	146	223	172	280	142	172	238/262	86
<b>MLL-10</b>														
28	270	234	122	150	270	186	186	241	132	224	158/170	152	242/274	86/122
<b>MLL-11</b>														
220	270	234	122	150	274	222	170	221	188	272	158/170	140	238/254	86/138
<b>MLL-12</b>														
230	270	234	122	150	270	222	170	235	188	272	158/170	140/176	238/270	86/138
231	270	234	122	150	270	222	170	235	188	272	158/170	140/176	238/274	86/138
<b>MLL-13</b>														
277	270	226	122	150	274	186	170	221	176	284	158/170	140/176	238/274	86/138
278	274	226	122	150	274	186	170	221	176	284	158/170	140/176	238/274	86/138
286	270	226	122	150	274	186	170	223	176	288	158/170	140/176	238/274	86/138

Table 3.S2 *Continued.*

	<i>A. laterale</i>							<i>A. texanum</i>				Both Hosts		
	AcroD315	AjeD23	AjeD75	AjeD94	AjeD346	AmaD42	AmaD367	Atex74	Atex102	Atex141	AmaD321	AjeD283	AjeD422	AmmH123
<b>MLL-14</b>														
225	270	234	122	150	274	186	170	223	188	272	158/170	140/176	238/274	86/122
<b>MLL-15</b>														
222	270	234	122	150	274	186	170	223	184	272	158/170	140/176	238/254	86/122
223	270	234	122	150	274	186	170	223	188	272	158/170	140/176	238/254	86/122
224	270	234	122	150	274	186	170	223	188	272	158	152/176	238/254	86/122
<b>MLL-16</b>														
40	270	234	122	150	270	222	170	223	132	228	158/170	152/176	242/274	86/122
41	270	234	122	150	270	222	170	223	132	228	158/170	152/176	242/274	86/126
<b>MLL-17</b>														
46	274	234	122	150	274	222	170	223	176	228	158/170	140/176	238/274	86/122
<b>MLL-18</b>														
37	270	234	122	150	274	186	170	221	176	228	170	140/176	238/254	86/122
<b>MLL-19</b>														
38	270	234	122	150	274	186	170	221	176	228	170	140/176	238/274	86/122
<b>MLL-20</b>														
195	270	234	122	150	274	186	170	235	184	228	178	140/176	238/274	86/138
196	270	234	122	150	274	186	170	235	188	228	158/170	152/176	238/274	86/138
<b>MLL-21</b>														
42	270	234	122	150	270	186	170	223	164	228	158/170	176	238/270	86/138
<b>MLL-22</b>														
70	270	234	110	150	270	186	170	223	184	228	158/170	152/176	238/274	86/138
<b>MLL-23</b>														
27	270	234	122	150	270	186	170	223	184	224	158/170	152/176	238/270	86/138
45	270	234	122	150	270	186	170	223	176	228	158/170	152/176	238/274	86/138
61	270	234	122	150	270	186	170	223	180	228	158/170	152/172	238/270	86/138
62	270	234	122	150	270	186	170	223	180	228	158/170	152/176	238/270	86/138
63	274	234	122	150	270	186	170	223	180	228	158/170	152/176	238/270	86/138
64	270	230	122	150	270	186	170	223	180	228	158/170	152/176	238/274	86/138
65	262	234	122	150	270	186	170	223	180	228	158/170	152/176	238/274	86/138

Table 3.S2 *Continued.*

	<i>A. laterale</i>						<i>A. texanum</i>				Both Hosts			
	AcroD315	AjeD23	AjeD75	AjeD94	AjeD346	AmaD42	AmaD367	Atex74	Atex102	Atex141	AmaD321	AjeD283	AjeD422	AmmH123
<b>MLL-23</b>														
66	270	234	122	150	270	186	170	223	180	228	158/170	152/176	238/274	86/138
67	270	238	122	150	270	186	170	223	180	228	158/170	152/176	238/274	86/138
68	270	234	122	150	270	186	170	223	180	228	158/170	152/176	238/278	86/138
71	270	234	118	150	270	186	170	223	184	228	158	152/176	238/270	86/138
72	270	234	122	150	270	186	170	223	184	228	158/170	152/176	238/266	86/138
73	270	238	122	150	270	186	170	223	184	228	158/170	152/176	238/266	86/138
75	270	234	122	150	270	186	170	223	184	228	158/170	144/176	238/270	86/138
76	270	234	122	150	270	186	170	223	184	228	166	148/176	238/270	86/138
77	270	234	122	150	270	186	170	223	184	228	158/170	152/172	238/270	86/138
80	270	234	122	150	270	186	170	223	184	228	154/170	152/176	238/270	86/138
81	270	234	122	150	270	186	170	223	184	228	158/162	152/176	238/270	86/138
82	270	234	122	150	270	186	170	223	184	228	158/166	152/176	238/270	86/138
84	270	230	122	150	270	186	170	223	184	228	158/170	152/176	238/270	86/138
85	270	234	122	150	270	186	170	223	184	228	158/170	152/176	238/270	86/130
86	274	234	122	150	270	186	170	223	184	228	158/170	152/176	238/270	86/130
88	266	234	122	150	270	186	170	223	184	228	158/170	152/176	238/270	86/138
89	270	234	122	150	270	186	170	223	184	228	158/170	152/176	238/270	86/138
90	274	234	122	150	270	186	170	223	184	228	158/170	152/176	238/270	86/138
91	270	238	122	150	270	186	170	223	184	228	158/170	152/176	238/270	86/138
92	270	234	122	150	270	182	170	223	184	228	158/174	152/176	238/270	86/138
93	270	234	122	150	270	186	170	223	184	228	158	152/176	238/270	86/138
94	270	234	122	150	270	186	170	223	184	228	166/170	152/176	238/270	86/138
95	270	234	122	150	270	186	170	223	184	228	170	152/176	238/270	86/138
96	270	234	122	150	270	186	170	223	184	228	158/170	152/180	238/270	86/138
97	266	234	122	150	270	186	170	223	184	228	158/170	152	238/270	86/138
98	270	234	122	150	270	186	170	223	184	228	158/170	152	238/270	86/138
99	270	234	122	150	270	186	170	223	184	228	158/170	164/176	238/270	86/138
100	270	234	122	150	270	186	170	223	184	228	158/170	172	238/270	86/138
101	270	234	122	150	270	186	170	223	184	228	158/170	180	238/270	86/138
102	270	234	122	150	270	186	170	223	184	228	154/170	152/176	238/274	86/138
103	274	234	122	150	270	186	170	223	184	228	154/170	152/176	238/274	86/138

Table 3.S2 *Continued.*

	<i>A. laterale</i>							<i>A. texanum</i>				Both Hosts		
	AcroD315	AjeD23	AjeD75	AjeD94	AjeD346	AmaD42	AmaD367	Atex74	Atex102	Atex141	AmaD321	AjeD283	AjeD422	AmmH123
<b>MLL-23</b>														
105	266	234	122	150	270	186	170	223	184	228	158/170	152/176	238/274	86/134
106	262	234	122	150	270	186	170	223	184	228	158/170	152/176	238/274	86/138
107	266	234	122	150	270	186	170	223	184	228	158/170	152/176	238/274	86/138
108	270	234	122	150	270	186	170	223	184	228	158/170	152/176	238/274	86/138
109	274	234	122	150	270	186	170	223	184	228	158/170	152/176	238/274	86/138
110	270	238	122	150	270	186	170	223	184	228	158/170	152/176	238/274	86/138
111	270	234	122	150	270	186	170	223	184	228	158/174	152/176	238/274	86/138
112	270	234	122	150	270	186	170	223	184	228	158	152/176	238/274	86/138
113	270	234	122	150	270	186	170	223	184	228	158/170	152/184	238/274	86/138
114	270	234	122	150	270	186	170	223	184	228	154/170	156/176	238/274	86/138
115	270	234	122	150	270	186	170	223	184	228	158/170	164/176	238/274	86/138
116	270	234	122	150	270	186	170	223	184	228	158/166	152/176	238	86/138
117	274	234	122	150	270	186	170	223	184	228	158/170	152/176	238	86/138
118	270	234	126	150	270	186	170	223	184	228	158/170	152/176	238/270	86/138
119	270	234	126	150	270	186	170	223	184	228	158/170	152/176	238/274	86/138
121	270	234	130	150	270	186	174	223	184	228	158/170	152/176	238/274	86/138
124	266	234	122	150	270	186	170	223	188	228	158/170	152/176	238/270	86/138
125	270	234	122	150	270	186	170	223	188	228	158/170	152/176	238/270	86/138
127	270	234	122	150	270	186	166	223	188	228	158/170	152/176	238/274	86/138
128	270	234	122	150	270	186	170	223	188	228	158/170	152/176	238/274	86/138
129	274	234	122	150	270	186	170	223	188	228	158/170	152/176	238/274	86/138
130	270	234	122	150	270	186	170	223	188	228	162/170	152/176	238/274	86/138
131	274	234	122	150	270	186	170	223	188	228	162/170	152/176	238/274	86/138
133	270	234	122	150	274	186	170	223	188	228	158/170	152/176	238/274	86/138
<b>MLL-24</b>														
132	270	234	122	150	274	222	186	223	188	228	158/170	140/176	230/254	86/138
<b>MLL-25</b>														
194	270	234	122	150	270	222	186	235	184	228	158/170	140/176	238/254	86/122
<b>MLL-26</b>														
235	270	234	122	150	270	222	186	233	148	276	158/170	152/172	230/274	86/138

Table 3.S2 *Continued.*

	<i>A. laterale</i>							<i>A. texanum</i>				Both Hosts		
	AcroD315	AjeD23	AjeD75	AjeD94	AjeD346	AmaD42	AmaD367	Atex74	Atex102	Atex141	AmaD321	AjeD283	AjeD422	AmmH123
<b>MLL-27</b>														
226	270	234	122	150	270	222	170	235	128	272	158/170	152	238/254	86/138
227	270	234	122	150	274	222	170	235	128	272	158/170	152	238/254	86/138
228	270	234	122	150	270	222	170	235	132	272	158/170	152	238/254	86/138
<b>MLL-28</b>														
52	202	226	122	150	262	218	170	223	180	228	158/170	152/176	234/274	86/134
54	202	226	122	150	262	218	170	223	180	228	158/170	152/160	238/274	86/134
55	202	226	122	150	262	218	170	223	180	228	158/170	152/172	238/274	86/134
56	202	226	122	150	262	218	170	223	180	228	158/170	152/176	238/274	86/134
57	202	226	122	150	262	218	174	223	180	228	158/170	152/176	238/274	86/134
58	202	226	122	150	262	218	170	223	180	228	162/170	152/176	238/274	86/134
59	202	226	122	150	262	218	170	223	180	228	158/170	152/176	238/278	86/134
<b>MLL-29</b>														
49	178	230	114	150	266	186	146	223	180	228	158/170	160/164	242/278	86/138
50	178	230	114	150	266	186	146	223	180	228	158/170	164	242/278	86/138
51	178	234	114	150	266	186	146	223	180	228	158/170	164	242/282	86/138
<b>MLL-30</b>														
279	178	230	110	150	266	186	142	223	152	284	142	164	242/278	86/138
280	178	230	114	150	266	186	142	223	152	284	142	160/164	242/278	86/138
281	178	230	114	150	266	186	142	223	152	284	142/154	164	242/278	86/138
283	178	230	114	150	266	182	142	223	152	284	142	164	242/278	86/138
284	182	230	114	150	266	186	142	223	152	284	142	164	242/278	86/138
<b>MLL-31</b>														
240	170	234	122	150	278	186	146	221	180	280	142	164/176	242/282	86/122
<b>MLL-32</b>														
250	170	234	114	150	266	186	146	223	180	280	142	172	242/286	86/122

Table 3.S2 *Continued.*

	<i>A. laterale</i>						<i>A. texanum</i>				Both Hosts			
	AcroD315	AjeD23	AjeD75	AjeD94	AjeD346	AmaD42	AmaD367	Atex74	Atex102	Atex141	AmaD321	AjeD283	AjeD422	AmmH123
<b>MLL-33</b>														
221	170	234	114	150	278	186	146	223	180	272	142	172	242/282	86/122
233	170	234	114	150	278	186	146	223	180	276	142	172	242/282	86/122
234	170	234	114	150	282	186	146	223	180	276	142	172	246/282	86/122
249	170	234	110	150	278	186	146	223	180	280	142	172	242/282	86/122
251	170	234	114	150	278	186	146	223	180	280	142	172	238/282	86/122
252	170	234	114	150	278	186	146	223	180	280	142	172	242/274	86/122
253	170	234	114	150	278	186	146	223	180	280	142	172	242/278	86/122
254	170	234	114	150	278	186	150	223	180	280	142	172	242/278	86/122
256	170	234	114	150	278	186	146	223	180	280	142	132/172	242/282	86/122
257	170	234	114	150	278	186	146	223	180	280	142	140/172	242/282	86/122
258	170	234	114	150	278	186	146	223	180	280	142	144/172	242/282	86/122
259	170	238	114	150	278	186	146	223	180	280	142	172/176	242/282	86/122
260	170	234	114	150	278	186	146	223	180	280	142/146	172	242/282	86/122
261	170	234	114	150	278	186	146	223	180	280	142/170	172	242/282	86/122
262	170	234	114	150	278	186	146	223	180	280	142/174	172	242/282	86/118
263	170	230	114	150	278	186	146	223	180	280	142	172	242/282	86/122
264	170	234	114	150	278	186	146	223	180	280	142	172	242/282	86/118
265	170	234	114	150	278	186	146	223	180	280	142	172	242/282	86/122
266	174	234	114	150	278	186	146	223	180	280	142	172	242/282	86/122
267	170	234	114	150	278	186	146	223	180	280	142	172	242/282	86/126
268	170	234	114	150	278	186	146	223	180	280	142	176	242/282	86/122
269	170	234	114	150	278	186	150	223	180	280	142	176	242/282	86/122
270	170	234	114	150	278	186	146	223	180	280	142	172	242/286	86/122
271	170	234	114	150	278	186	146	223	180	280	142	172	242/290	86/122
272	170	234	114	150	282	186	146	223	180	280	142/150	132/172	242/282	86/122
273	170	234	110	150	278	186	146	223	184	280	138/142	172	242/286	86/122
274	170	234	114	150	278	186	146	223	184	280	142/178	172	242/278	86/122
275	170	234	114	150	278	186	146	223	184	280	142	172	242/282	86/122
276	170	234	114	150	278	186	146	223	184	280	142	172	242/286	86/122
285	170	234	114	150	278	186	146	223	180	284	142	172	242/282	86/122

Table 3.S2 *Continued.*

	<i>A. laterale</i>							<i>A. texanum</i>				Both Hosts		
	AcroD315	AjeD23	AjeD75	AjeD94	AjeD346	AmaD42	AmaD367	Atex74	Atex102	Atex141	<i>AmaD321</i>	<i>AjeD283</i>	AjeD422	AmmH123
<b>MLL-34</b>														
198	178	238	122	150	278	218	162	491 <sub>4bp</sub>	204	228	158/170	140/180	230/278	86/138
199	182	238	122	150	278	218	162	491 <sub>4bp</sub>	204	228	158	140/180	230/278	86/138
200	178	238	122	150	278	218	162	495 <sub>4bp</sub>	204	228	158/170	140/180	230/278	86/138
201	178	238	122	150	278	218	162	495 <sub>4bp</sub>	204	228	158/170	140/180	230/278	86/142
202	178	238	122	150	278	218	162	495 <sub>4bp</sub>	204	228	158/170	140/180	230/282	86/138
203	178	238	122	150	278	218	162	499 <sub>4bp</sub>	204	228	158/170	140/180	230/278	86/138
204	178	238	122	150	278	218	162	499 <sub>4bp</sub>	204	228	162/170	140/180	230/278	86/138
205	178	238	122	150	278	218	162	503 <sub>4bp</sub>	200	228	158/170	140/180	230/278	86/138
206	178	238	122	150	278	218	162	503 <sub>4bp</sub>	200	228	158/174	140/180	230/278	86/142
207	178	238	122	150	278	218	162	503 <sub>4bp</sub>	204	228	158/170	140/176	230/278	86/138
208	178	238	122	150	278	218	162	503 <sub>4bp</sub>	204	228	158/170	140/176	230/278	86/142
209	182	238	122	150	278	218	162	503 <sub>4bp</sub>	204	228	130/174	140/180	230/278	86/138
210	178	238	122	150	278	218	162	503 <sub>4bp</sub>	204	228	158/162	140/180	230/278	86/138
211	178	238	122	150	278	218	162	503 <sub>4bp</sub>	204	228	158/170	140/180	230/278	86/138
212	182	238	122	150	278	218	162	503 <sub>4bp</sub>	204	228	158/170	140/180	230/278	86/138
213	178	238	122	150	278	218	162	503 <sub>4bp</sub>	204	228	158/170	140/180	230/278	86/142
214	178	238	122	150	282	218	162	503 <sub>4bp</sub>	204	228	158/166	140/180	230/278	86/138
215	178	238	122	150	282	218	162	503 <sub>4bp</sub>	204	228	158/170	140/180	230/278	86/138
216	178	238	122	150	282	218	162	503 <sub>4bp</sub>	204	228	162	140/180	230/278	86/138
217	178	238	122	150	278	218	162	503 <sub>4bp</sub>	208	228	158/170	140/180	230/278	86/138
<b>MLL-35</b>														
236	178	210	114	146	282	218	138	339 <sub>4bp</sub>	180	276	162/166	160/184	242/282	86/138
<b>MLL-36</b>														
287	174	210	114	146	282	218	138	335 <sub>4bp</sub>	180	288	162/166	160/180	242/282	86/138
288	178	210	114	146	282	218	138	335 <sub>4bp</sub>	180	288	166	160/180	242/282	86/138
289	178	210	114	146	286	218	138	335 <sub>4bp</sub>	180	288	162/166	160/180	242/282	86/138
290	178	210	114	146	286	218	138	335 <sub>4bp</sub>	180	288	166	160/180	242/282	86/138
291	174	210	114	146	282	218	138	339 <sub>4bp</sub>	180	288	162/166	160/180	242/282	86/138
292	178	210	114	146	286	218	138	339 <sub>4bp</sub>	180	288	162/166	160/180	242/282	86/138



Table 3.S3 Continued.

Loci	Alleles	1	2	3	4	5	6	7	8	9	10	11	12	13	14	15	16	17	18	19	20	21	22	23	24	25	26	27	28	29	30	31	32	33	34	35	36	Total			
AjeD346	262																																					30	30		
	266																																								12
	270	1									1		3					7					1	1	427			1	1	15											458
	274								9	1		1		10	1	7		1	1	1	3																		38		
	278		1	1	4		1	38	200	48																							1	113	43				450		
	282					5				1																														15	
	286																																							4	
<b>Total</b>		<b>1</b>	<b>1</b>	<b>1</b>	<b>4</b>	<b>5</b>	<b>1</b>	<b>38</b>	<b>210</b>	<b>49</b>	<b>1</b>	<b>1</b>	<b>3</b>	<b>10</b>	<b>1</b>	<b>7</b>	<b>7</b>	<b>1</b>	<b>1</b>	<b>1</b>	<b>3</b>	<b>1</b>	<b>1</b>	<b>428</b>	<b>1</b>	<b>1</b>	<b>1</b>	<b>16</b>	<b>30</b>	<b>6</b>	<b>5</b>	<b>1</b>	<b>1</b>	<b>115</b>	<b>46</b>	<b>1</b>	<b>7</b>	<b>1007</b>			
AmaD42	166		1	1	4	5	1	38	210																														260		
	182																							1																2	
	186	1									1			10	1	7				1	1	3	1	1	427														581		
	218									49																														133	
	222												1	3																											31
<b>Total</b>		<b>1</b>	<b>1</b>	<b>1</b>	<b>4</b>	<b>5</b>	<b>1</b>	<b>38</b>	<b>210</b>	<b>49</b>	<b>1</b>	<b>1</b>	<b>3</b>	<b>10</b>	<b>1</b>	<b>7</b>	<b>7</b>	<b>1</b>	<b>1</b>	<b>1</b>	<b>3</b>	<b>1</b>	<b>1</b>	<b>428</b>	<b>1</b>	<b>1</b>	<b>1</b>	<b>16</b>	<b>30</b>	<b>6</b>	<b>5</b>	<b>1</b>	<b>1</b>	<b>115</b>	<b>46</b>	<b>1</b>	<b>7</b>	<b>1007</b>			
AmaD367	138																																							8	
	142																																								5
	146									49																															170
	150																																								2
	162																																								46
	166								2																1																3
	170		1	1	4	5	1		207			1	3	10	1	7	7	1	1	1	1	3	1	1	426				16	29									727		
	174							38	1																1																41
186	1									1																														5	
<b>Total</b>		<b>1</b>	<b>1</b>	<b>1</b>	<b>4</b>	<b>5</b>	<b>1</b>	<b>38</b>	<b>210</b>	<b>49</b>	<b>1</b>	<b>1</b>	<b>3</b>	<b>10</b>	<b>1</b>	<b>7</b>	<b>7</b>	<b>1</b>	<b>1</b>	<b>1</b>	<b>3</b>	<b>1</b>	<b>1</b>	<b>428</b>	<b>1</b>	<b>1</b>	<b>1</b>	<b>16</b>	<b>30</b>	<b>6</b>	<b>5</b>	<b>1</b>	<b>1</b>	<b>115</b>	<b>46</b>	<b>1</b>	<b>7</b>	<b>1007</b>			
AmmH123.L	114								1																															1	
	118		1	1	4	5	1	38	207																															259	
	122	1							2		1				1	7	6	1	1	1																					135
	126																																								3
	130																																								4
	134																																								31
	138												1	3	10																										513
	142																																								12
150									48																																48
<b>Total</b>		<b>1</b>	<b>1</b>	<b>1</b>	<b>4</b>	<b>5</b>	<b>1</b>	<b>38</b>	<b>210</b>	<b>48</b>	<b>1</b>	<b>1</b>	<b>3</b>	<b>10</b>	<b>1</b>	<b>7</b>	<b>7</b>	<b>1</b>	<b>1</b>	<b>1</b>	<b>3</b>	<b>1</b>	<b>1</b>	<b>428</b>	<b>1</b>	<b>1</b>	<b>1</b>	<b>16</b>	<b>30</b>	<b>6</b>	<b>5</b>	<b>1</b>	<b>1</b>	<b>115</b>	<b>46</b>	<b>1</b>	<b>7</b>	<b>1006</b>			

Table 3.S3 Continued.

Loci	Alleles	1	2	3	4	5	6	7	8	9	10	11	12	13	14	15	16	17	18	19	20	21	22	23	24	25	26	27	28	29	30	31	32	33	34	35	36	Total
Amm HI23.T	86	1							49	1	1	3	10	1	7	7	1	1	1	3	1	1	428	1	1	1	16	30	6	5	1	1	115	46	1	7	747	
	94		1	1	4	5	1	38	210																												260	
	<b>Total</b>	<b>1</b>	<b>1</b>	<b>1</b>	<b>4</b>	<b>5</b>	<b>1</b>	<b>38</b>	<b>210</b>	<b>49</b>	<b>1</b>	<b>1</b>	<b>3</b>	<b>10</b>	<b>1</b>	<b>7</b>	<b>7</b>	<b>1</b>	<b>1</b>	<b>1</b>	<b>3</b>	<b>1</b>	<b>1</b>	<b>428</b>	<b>1</b>	<b>1</b>	<b>1</b>	<b>16</b>	<b>30</b>	<b>6</b>	<b>5</b>	<b>1</b>	<b>1</b>	<b>115</b>	<b>46</b>	<b>1</b>	<b>7</b>	<b>1007</b>
Atex74.bp2	221							1	1		1			9					1	1																	15	
	223		1	1	4	5	1	38	209	48				1	1	7	7	1				1	1	428	1			30	6	5		1	115				912	
	233													3							3						1	16								1		
	235																																				23	
	241										1																										1	
	<b>Total</b>	<b>1</b>	<b>1</b>	<b>4</b>	<b>5</b>	<b>1</b>	<b>38</b>	<b>210</b>	<b>49</b>	<b>1</b>	<b>1</b>	<b>3</b>	<b>10</b>	<b>1</b>	<b>7</b>	<b>7</b>	<b>1</b>	<b>1</b>	<b>1</b>	<b>3</b>	<b>1</b>	<b>1</b>	<b>428</b>	<b>1</b>	<b>1</b>	<b>1</b>	<b>16</b>	<b>30</b>	<b>6</b>	<b>5</b>	<b>1</b>	<b>1</b>	<b>115</b>			<b>952</b>		
Atex74.bp4	275	1																																		1		
	335																																			5		
	339																																	1	2	3		
	491																																		4	4		
	495																																		4	4		
	499																																		2	2		
	503																																	36	36			
	<b>Total</b>	<b>1</b>																																<b>46</b>	<b>1</b>	<b>7</b>	<b>55</b>	
Atex102	128										1					7																				3		
	132																																			13		
	148																											1								1		
	152																																			5		
	164																					1														1		
	168									8																										8		
	172			1						41																										42		
	176	1												10					1	1	1														5			
	180			4																																38		
	184					1																2		1	348		1									5		
	188											1	3		1	6						1			37	1												
	196							5	42																													
	200		1		5		33	157																												3		
	204																																				42	
208																																				1		
	<b>Total</b>	<b>1</b>	<b>1</b>	<b>1</b>	<b>4</b>	<b>5</b>	<b>1</b>	<b>38</b>	<b>210</b>	<b>49</b>	<b>1</b>	<b>1</b>	<b>3</b>	<b>10</b>	<b>1</b>	<b>7</b>	<b>7</b>	<b>1</b>	<b>1</b>	<b>1</b>	<b>3</b>	<b>1</b>	<b>1</b>	<b>428</b>	<b>1</b>	<b>1</b>	<b>1</b>	<b>16</b>	<b>30</b>	<b>6</b>	<b>5</b>	<b>1</b>	<b>1</b>	<b>115</b>	<b>46</b>	<b>1</b>	<b>7</b>	<b>1007</b>

Table 3.S3 Continued.

Loci	Alleles	1	2	3	4	5	6	7	8	9	10	11	12	13	14	15	16	17	18	19	20	21	22	23	24	25	26	27	28	29	30	31	32	33	34	35	36	Total
Atex14I	220				5																																5	
	224										1													1														2
	228	1	1	1	4		1	38	209								7	1	1	1	3	1	1	427	1	1			30	6				46			781	
	232							1																													1	
	272											1	3		1	7												16						1		29		
	276								1																	1								5	1	8		
	280								48																							1	1	108		158		
	284														9																5			1		15		
	288														1																					7	8	
<b>Total</b>	<b>1</b>	<b>1</b>	<b>1</b>	<b>4</b>	<b>5</b>	<b>1</b>	<b>38</b>	<b>210</b>	<b>49</b>	<b>1</b>	<b>1</b>	<b>3</b>	<b>10</b>	<b>1</b>	<b>7</b>	<b>7</b>	<b>1</b>	<b>1</b>	<b>1</b>	<b>1</b>	<b>3</b>	<b>1</b>	<b>1</b>	<b>428</b>	<b>1</b>	<b>1</b>	<b>1</b>	<b>16</b>	<b>30</b>	<b>6</b>	<b>5</b>	<b>1</b>	<b>1</b>	<b>115</b>	<b>46</b>	<b>1</b>	<b>7</b>	<b>1007</b>
AmaD321.A	130																																			1	1	
	138																																			1	1	
	142								49																											114	170	
	154							1																9								5	1	1			10	
	158	1									1	1	3	10	1	7	7	1				1	1	1	411	1	1	1	16	29	6				43		543	
	162		1	1	4	5	1	38	208																4									2	1	5	271	
	166								1																2												2	5
	170																1	1							2												4	
178																							2													2		
<b>Total</b>	<b>1</b>	<b>1</b>	<b>1</b>	<b>4</b>	<b>5</b>	<b>1</b>	<b>38</b>	<b>210</b>	<b>49</b>	<b>1</b>	<b>1</b>	<b>3</b>	<b>10</b>	<b>1</b>	<b>7</b>	<b>7</b>	<b>1</b>	<b>1</b>	<b>1</b>	<b>1</b>	<b>3</b>	<b>1</b>	<b>1</b>	<b>428</b>	<b>1</b>	<b>1</b>	<b>1</b>	<b>16</b>	<b>30</b>	<b>6</b>	<b>5</b>	<b>1</b>	<b>1</b>	<b>115</b>	<b>46</b>	<b>1</b>	<b>7</b>	<b>1007</b>
AmaD321.B	142																																			1	1	
	146																																				1	1
	150																																				1	1
	154																																			1	1	1
	162																							1												1	2	
	166								7															4											1	1	5	18
	170	1	1	1	3	5	1	38	194		1	1	3	10	1	6	7	1				1	1	1	415	1	1	1	16	30	6			1	40		788	
	174								1																2										1	2		6
178																																			1	1		
<b>Total</b>	<b>1</b>	<b>1</b>	<b>1</b>	<b>3</b>	<b>5</b>	<b>1</b>	<b>38</b>	<b>202</b>		<b>1</b>	<b>1</b>	<b>3</b>	<b>10</b>	<b>1</b>	<b>6</b>	<b>7</b>	<b>1</b>				<b>1</b>	<b>1</b>	<b>1</b>	<b>422</b>	<b>1</b>	<b>1</b>	<b>1</b>	<b>16</b>	<b>30</b>	<b>6</b>	<b>1</b>		<b>6</b>	<b>44</b>	<b>1</b>	<b>5</b>	<b>819</b>	

Table 3.S3 Continued.

Loci	Alleles	1	2	3	4	5	6	7	8	9	10	11	12	13	14	15	16	17	18	19	20	21	22	23	24	25	26	27	28	29	30	31	32	33	34	35	36	Total	
AjeD283.A	132								1			1	3	10	1	6		1	1	1	2				1	1							2				2		
	140								3	2														1										1	46			76	
	144								2	1														1										1			7		
	148								2	1														1													4		
	152	1						1	2		1						1	7				1		1	416		1	16	30								478		
	156																								6												6		
	160																																1	1		1	7	10	
	164									2														2								5	4	1			14		
	168								1	1																												2	
	172		1	1	4	5	1	35	199	46															1								1	109			403		
176								1														1												2			4		
180																								1													1		
<b>Total</b>		<b>1</b>	<b>1</b>	<b>1</b>	<b>4</b>	<b>5</b>	<b>1</b>	<b>38</b>	<b>210</b>	<b>49</b>	<b>1</b>	<b>1</b>	<b>3</b>	<b>10</b>	<b>1</b>	<b>7</b>	<b>7</b>	<b>1</b>	<b>1</b>	<b>1</b>	<b>3</b>	<b>1</b>	<b>1</b>	<b>428</b>	<b>1</b>	<b>1</b>	<b>1</b>	<b>16</b>	<b>30</b>	<b>6</b>	<b>5</b>	<b>1</b>	<b>1</b>	<b>115</b>	<b>46</b>	<b>1</b>	<b>7</b>	<b>1007</b>	
AjeD283.B	160																																				1	1	
	164																																						2
	172							1	11	3														2			1												25
	176							5	1				3	10	1	7	7	1	1	1	1	3		1	420	1	1			1						4			493
	180	1					1																	1														54	
184																								1													1	2	
<b>Total</b>		<b>1</b>				<b>1</b>	<b>1</b>	<b>16</b>	<b>4</b>			<b>3</b>	<b>10</b>	<b>1</b>	<b>7</b>	<b>7</b>	<b>1</b>	<b>1</b>	<b>1</b>	<b>1</b>	<b>3</b>	<b>1</b>	<b>424</b>	<b>1</b>	<b>1</b>	<b>1</b>	<b>1</b>	<b>30</b>	<b>1</b>	<b>1</b>	<b>1</b>	<b>5</b>	<b>46</b>	<b>1</b>	<b>7</b>	<b>577</b>			
AjeD422.A	230																									1		1									46	48	
	234		1	1	4	5	1	38	209																														260
	238	1							1	49			1	3	10	1	7			1	1	1	3	1	1	428		1		16	29					1	556		
	242											1						7																				1	142
	246																																					1	1
<b>Total</b>		<b>1</b>	<b>1</b>	<b>1</b>	<b>4</b>	<b>5</b>	<b>1</b>	<b>38</b>	<b>210</b>	<b>49</b>	<b>1</b>	<b>1</b>	<b>3</b>	<b>10</b>	<b>1</b>	<b>7</b>	<b>7</b>	<b>1</b>	<b>1</b>	<b>1</b>	<b>3</b>	<b>1</b>	<b>1</b>	<b>428</b>	<b>1</b>	<b>1</b>	<b>1</b>	<b>16</b>	<b>30</b>	<b>6</b>	<b>5</b>	<b>1</b>	<b>1</b>	<b>115</b>	<b>46</b>	<b>1</b>	<b>7</b>	<b>1007</b>	
AjeD422.B	254		1									1				7										1	1											28	
	262									49																													49
	266																																						7
	270				4				13				1										1		210														229
	274	1		1				38	145		1		2	10	1		7	1			1	3		1	200		1		26						1			440	
	278					5	1		47																													124	
	282								5																														111
	286																																		1	15			16
	290																																					1	1
<b>Total</b>		<b>1</b>	<b>1</b>	<b>1</b>	<b>4</b>	<b>5</b>	<b>1</b>	<b>38</b>	<b>210</b>	<b>49</b>	<b>1</b>	<b>1</b>	<b>3</b>	<b>10</b>	<b>1</b>	<b>7</b>	<b>7</b>	<b>1</b>	<b>1</b>	<b>1</b>	<b>3</b>	<b>1</b>	<b>1</b>	<b>426</b>	<b>1</b>	<b>1</b>	<b>1</b>	<b>16</b>	<b>30</b>	<b>6</b>	<b>5</b>	<b>1</b>	<b>1</b>	<b>115</b>	<b>46</b>	<b>1</b>	<b>7</b>	<b>1005</b>	

**Table 3.S4.** Overall allelic richness for each locus. AmmH123 and Atex74 are separated into two columns to distinguish species-specific alleles and motifs for Amm123 and Atex74, respectively.

	<i>A. laterale</i>							
	AcroD315	AjeD23	AjeD75	AjeD94	AjeD346	AmaD42	AmaD367	AmmH123.L
Total Richness	10	7	7	2	7	5	9	9
Alleles	170	210	106	146	262	166	138	114
	174	214	110	150	266	182	142	118
	178	222	114		270	186	146	122
	182	226	118		274	218	150	126
	186	230	122		278	222	162	130
	202	234	126		282		166	134
	262	238	130		286		170	138
	266						174	142
	270						186	150
	274							

**Table 3.S4 Continued.** Overall allelic richness for each locus. AmmH123 and Atex74 are separated into two columns to distinguish species-specific alleles and motifs for Amm123 and Atex74, respectively. \*Alleles larger than 500-bp for the 4-basepair motif alleles of Atex74 are all categorized as 503 as they go beyond the ladder size and 503 is the next largest allele size after the 499-bp allele (e.g. alleles of size 507 or 531 would be classified as 503).

	<i>A. texanum</i>						Indeterminant	
	AmmH123.T	Atex74.bp2	Atex74.bp4	Atex102	Atex141	AmaD321	AjeD283	AjeD422
Total Richness	2	5	7	15	9	11	13	14
Alleles	86	221	275	128	220	130	132	230
	94	223	335	132	224	138	140	234
		233	339	148	228	142	144	238
		235	491	152	232	146	148	242
		241	495	164	272	150	152	246
			499	168	276	154	156	254
			*503	172	280	158	160	262
				176	284	162	164	266
				180	288	166	168	270
				184		170	172	274
				188		174	176	278
				196		178	180	282
				200			184	286
				204				290
				208				

**Table 3.S5.** All diversity measures calculated including MLL:N ratios for all samples, private MLL, and shared MLL. Confidence intervals based on 1000 bootstraps of 30 samples per site (excluding B3) are provided under observed diversity metrics.

		<u>Multilocus Lineages</u>				<u>Sample Size</u>			<u>MLL : N</u>		
		<u>Total</u>	<u>Private</u>	<u>Shared</u>	<u>Chao1</u>	<u>Total</u>	<u>Private MLL</u>	<u>Shared MLL</u>	<u>Total</u>	<u>Private</u>	<u>Shared</u>
<b>NW</b>	<b><i>B3*</i></b>	4	0	4	5 -	22	0	22	5.50	-	5.5
<b>NE</b>	<b><i>D1.1</i></b>	8	0	8	9 (6, 13)	54	0	54	6.75	-	6.75
	<b><i>D1.2</i></b>	6	1	5	7 (4, 11)	43	1	42	7.17	1	8.4
<b>E</b>	<b><i>C3</i></b>	6	0	6	6 (6, 6)	37	0	37	6.17	-	6.17
	<b><i>D3.1</i></b>	10	1	9	12 (4, 18)	169	1	168	16.90	1	18.67
	<b><i>D3.2</i></b>	8	1	7	16 (3, 15)	103	1	102	12.88	1	14.57
<b>S</b>	<b><i>B6</i></b>	20	16	4	75 (5, 35)	236	34	202	11.80	2.125	50.5
	<b><i>B8</i></b>	13	5	8	21 (4, 25)	225	15	210	17.31	3	26.25
	<b><i>D6.1</i></b>	4	0	4	4 (3, 4)	32	0	32	8.00	-	8
	<b><i>D7</i></b>	8	1	7	16 (3, 15)	78	1	77	9.75	1	11

**Table 3.S5 Continued.** Simpson diversity (lambda), evenness (V), Beta Pareto, and the Lineage Diversity Index (LDI) measures as suggested by Arnaud-Haond et al.<sup>108</sup>. Confidence intervals based on 1000 bootstraps of 30 samples per site (excluding B3) are provided under observed diversity metrics. Relative abundance values are provided for hosts and unisexual genotypes (from <sup>157</sup>) which required for the diploidization cycle proposed by Bogart and Bi <sup>137</sup>. \*Historic relative abundances of hosts and genotypes from Bogart and Licht <sup>156</sup> provided underneath contemporary genotype and host relative abundance values.

		Diversity Metrics				*Host Presence		*Genotype			
		lambda	V	Pareto	LDI	<i>A. laterale</i> (LL)	<i>A. texanum</i> (TT)	LLT	LTT	LLTT	
<b>NW</b>	<b>B3*</b>	0.38 -	0.26 -	0.48 -	0.14 -	1.8% 16.3%	0% 0%	32.7% 67.3%	7.3% 0.4%	1.8% 2.6%	
	<b>NE</b>	<b>D1.1</b>	0.82 (0.77, 0.84)	0.89 (0.77, 0.90)	0.66 (0.53, 1.39)	0.13 (0.17, 0.24)	0% -	3.3% -	5.5% -	14.3% -	0% -
		<b>D1.2</b>	0.51 (0.39, 0.60)	0.47 (0.27, 0.59)	0.55 (0.45, 0.64)	0.12 (0.10, 0.17)	0% -	6.7% -	1.0% -	26.0% -	0% -
<b>E</b>	<b>C3</b>	0.78 (0.74, 0.81)	0.87 (0.78, 0.91)	1.40 (0.71, 1.96)	0.14 (0.17, 0.17)	0% -	15.0% -	0% -	19.6% -	0% -	
	<b>D3.1</b>	0.59 (0.40, 0.73)	0.61 (0.20, 0.72)	0.53 (0.47, 0.82)	0.05 (0.10, 0.24)	0.2% -	11.9% -	1.0% -	28.5% -	0.3% -	
	<b>D3.2</b>	0.38 (0.18, 0.52)	0.33 (0.10, 0.51)	0.44 (0.33, 0.60)	0.07 (0.07, 0.21)	0% -	1.8% -	0.6% -	17.9% -	0% -	
<b>S</b>	<b>B6</b>	0.48 (0.24, 0.65)	0.40 (0.02, 0.49)	0.60 (0.42, 0.76)	0.08 (0.10, 0.31)	0% 0.3%	0.4% 1.4%	3.1% 31.1%	18.1% 30.8%	1.1% 4.0%	
	<b>B8</b>	0.64 (0.48, 0.74)	0.65 (0.39, 0.75)	0.51 (0.44, 0.80)	0.05 (0.10, 0.28)	0% 0%	6.6% 28.1%	1.3% 8.4%	13.4% 28.8%	0.5% 0%	
	<b>D6.1</b>	0.62 (0.59, 0.63)	0.74 (0.69, 0.82)	0.44 (0.44, 0.74)	0.10 (0.07, 0.10)	0% 1.0%	10.2% 58.3%	0% 4.2%	28.8% 15.6%	0% 0%	
	<b>D7</b>	0.66 (0.56, 0.71)	0.68 (0.57, 0.85)	0.46 (0.31, 0.72)	0.09 (0.07, 0.21)	0% -	9.1% -	0.6% -	28.6% -	0.6% -	

**Table 3.S6.** Results from model selection exercise comparing linear models which seek to predict Bray-Curtis dissimilarity of diploid unisexual lineage composition among sites on Pelee Island, Ontario. The Upland model uses a binary variable indicating whether or not two sites were located within the same patch of historic upland habitat, Geo uses a continuous variable reflecting geographic distance between sties, and Resist uses a continuous variable reflecting landscape resistance between pairs of sites based on a resistance map derived from Smith <sup>218</sup>. Null reflects an intercept-only model. Two sets of models are presented, depending on if site B6 is included or not. This is done because lineage composition at site B6 conforms least to our hypothesis but may be the result of alternative explanations that we were unable to test. Site C3 was removed from modeling due to concerns of founder effects. Additionally, model selection criteria, residual values, and F-statistics are all included in this table for complete model representation.

	Variables				Model Selection Criteria							
	Intercept	Geographical Distance	Shared Upland	Resistance	K	AICc	Δ AICc	Model Likelihood	AICc Weight	Cumulative Weight	Log-Likelihood	
<b>Complete</b>												
<b>* UPLAND 0.039</b>	0.6985 *** 1.62E-19	-	-0.1695 * 0.039	-	3	-10.133	0	1	0.591	0.591	8.441	
<b>NULL</b>	0.6608 *** 3.83E-20	-	-	-	2	-7.944	2.189	0.335	0.198	0.789	6.154	
<b>GEO 0.199</b>	0.5664 *** 3.32E-08	0.0178 0.199	-	-	3	-7.333	2.8	0.247	0.146	0.934	7.041	
<b>RESIST 0.677</b>	0.6174 *** 2.41E-06	-	-	0.0094 0.677	3	-5.744	4.389	0.111	0.066	1	6.247	
<b>Without B6</b>												
<b>*** UPLAND 0.000</b>	0.7158 *** 6.94E-19	-	-0.3273 *** 0.000	-	3	-22.537	0	1	0.996	0.996	14.768	
<b>. GEO 0.073</b>	0.5250 *** 4.83E-07	0.0248 0.073	-	-	3	-10.059	12.478	0.002	0.002	0.998	8.53	
<b>NULL</b>	0.6573 *** 1.49E-16	-	-	-	2	-9.06	13.477	0.001	0.001	1	6.77	
<b>RESIST 0.62</b>	0.6021 *** 2.03E-05	-	-	0.0118 0.62	3	-6.81	15.727	0	0	1	6.905	
Variable significance: . P < 0.1, * P < 0.05, ** P < 0.01, *** P < 0.001).												

Table 3.S6 *Continued.*

	Residual Values				Model F-Statistic		
	Standard Error	Degrees of Freedom	R <sup>2</sup>	Adjusted R <sup>2</sup>	F-Value	Numerator df	Denominator df
<b>Complete</b>							
* UPLAND 0.039	0.197	34	0.119	0.093	4.607	1	34
NULL -	0.207	35	0	0	-	-	-
GEO 0.199	0.205	34	0.048	0.02	1.718	1	34
RESIST 0.677	0.209	34	0.005	-0.024	0.176	1	34
<b>Without B6</b>							
*** UPLAND 0.000	0.148	26	0.435	0.413	20.036	1	26
. GEO 0.073	0.185	26	0.118	0.084	3.482	1	26
NULL -	0.193	27	0	0	-	-	-
RESIST 0.62	0.196	26	0.01	-0.028	0.252	1	26
Variable significance: . P < 0.1, * P < 0.05, ** P < 0.01, *** P < 0.001).							

## Chapter 4: Discussion

### Axes of Diversity

In this thesis, I build on the notion of “dimensions of diversity” arguing that there are different “axes” that can be used to further understand patterns of biodiversity. In Chapter 2: I argue that sexual hosts of an obligative reproductive parasite can be thought of as keystone species given that the structure and diversity of unisexual *Ambystoma* assemblages are underpinned by the identity and relative abundance of their available host(s). This empirically supported result follows directly from predictions drawn from our contemporary understanding of unisexual *Ambystoma* reproduction but could only have been tested using the genomotype axis of genetic diversity. Notably, even assemblages in close proximity and connected by habitat apparently conducive to emigration exhibited significant differences in genomotype structure, further reinforcing the primary role that the underlying reproductive biology of this system plays in driving assemblage structure. In Chapter 3: I demonstrate that unisexual *Ambystoma* lineage structure across the landscape has been shaped by legacy effects brought about from historic landscape structure and past interactions with multiple sexual hosts. Fortunately, knowledge of Pelee Island’s landscape history and assemblage structure allowed me to build and test these hypotheses, demonstrating the value of long-term datasets. Critically, these patterns of diversity could not have been meaningfully investigated using the genomotype axis due to the ecological factors at play at the time scales involved. Therefore, each of these explored axes of diversity provide fundamentally different interpretations on what ecological factors have shaped diversity patterns across different time scales.

In this discussion I will review the findings of this thesis in the context of two specific axes of genetic diversity: genomotype (biotype) diversity and lineage diversity. However, other axes do exist. For instance, the wide diversity of marker types and loci come with their own distinctive features and implications. Likewise, chromosomal structure can also vary in unisexual *Ambystoma* due to intergenomic recombination events<sup>264,266</sup>. Therefore the “allelic” and “chromosomal” axes may be considered as separate forms of genetic diversity as well and are explored in the Appendix.

### Genomotype Diversity

Unisexual *Ambystoma* genomotypes can be considered as a particular form of biotype<sup>130</sup>, one that is explicitly based on the ploidy and the proportional genetic contribution from each parental species. Genomotypes vary in two key aspects: genome dosage and ploidy level. While these components are certainly linked, each comes with distinct implications in terms of how it affects key traits including vital rates<sup>219,267</sup>, morphology<sup>268,269</sup>, and habitat selection<sup>146</sup>. Much like different biotypes in other systems<sup>120,270,271</sup>, unisexual *Ambystoma* genomotypes have differing niche requirements and limitations<sup>81,146</sup> likely influenced by their genetic make-up<sup>149</sup>. However, it is unclear the degree to which these factors influence distribution patterns.

Genome dosage effects are well-known to occur in the system, and growing evidence has shown that the number of chromosome compliments from specific sexual hosts have detectable impacts at the molecular<sup>149</sup>, ecological<sup>146</sup>, and physiological<sup>272</sup> levels in unisexual *Ambystoma*. Transcription rates appear to be equal across genomes in trihybrid individuals<sup>149</sup> suggesting dosage effects likely play a significant role in niche differences between triploid genomotypes<sup>146</sup>, though it is unclear how such dosage

effects might vary across ploidy level. Work in hybrid polyploid *Cobitis* fish has likewise found evidence of dosage effects, but which differ between germline and somatic cells suggesting hybrid phenotypes may be biased by dominance of individual genes rather than simple additivity<sup>273</sup>. Dosage effects in unisexual *Ambystoma* have also been suggested to affect key reproductive interactions with their sexual hosts<sup>153</sup>, such that host males are more likely to court unisexual females which have greater genomic bias. In the *Pelophylax esculentus* complex, dosage effects have been implicated in mating success variation<sup>274,275</sup>, though it seems to be contextually dependent on host-genotype density patterns<sup>276</sup>. Additionally, a greater genome dosage may help limit some genetic consequences of clonality, namely that of Muller's ratchet<sup>277</sup>, as the consequences of deleterious mutations can be more readily controlled with greater genetic dosage<sup>278,279</sup>. Similarly, genome replacement, as seen in the hybridogenetic *P. esculenta*, can also alleviate such pressures<sup>280</sup>. Moreover, the dramatic size of salamander genomes<sup>281</sup> and the number of paralogs present in their genomes<sup>282,283</sup> likewise may play a similarly protective role<sup>284</sup>, though more research is necessary.

Polyploidy likewise can have costs and benefits. For instance, in polyploid unisexual *Ambystoma*, cell sizes are generally larger, but cell count appears to decline, mitigating large changes in body size across ploidy levels<sup>268,269</sup>. One obvious consequence appears in pentaploid animals which have a far higher rate of spinal deformation<sup>220</sup> (E. Bare *personal observation*,

**Figure B.3**). Others have noted lower survivorship in higher ploidy animals across life stages<sup>219,267</sup>, independent of stress associated with metamorphosis<sup>285</sup>. The exact cause of this is unclear and may be due to several intrinsic factors, genetically influenced

behavioral factors, or ecological factors<sup>219</sup>. For instance, cellular complications are well-known in polyploid systems<sup>286,287</sup> and can likewise influence behavior. In polyploid newts, reduced reaction time and learning capacities are likely a result of interaction limitations among enlarged neurons<sup>288,289</sup>. Phenological differences among genotypes also exist in unisexual *Ambystoma* which are believed to stem from ploidy level variation<sup>130,290</sup>, and could lead to reduced access to sperm. Lastly, hydroperiods can play an important role in larval development rates<sup>291</sup>. While salamander larvae are highly plastic in their response to hydroperiod<sup>292</sup>, higher ploidy unisexuals also tend to lay eggs later in the season<sup>130</sup>. However, higher ploidy animals maintain larger body sizes throughout larval development and metamorphosis compared to their lower ploidy conspecifics<sup>269</sup> making them more competitive.

The intrinsic complexities surrounding unisexual genotypes make it challenging to derive robust ecological predictions for this allopolyploid system. This is further complicated by poorly understood interactions with extrinsic factors, including the abiotic environment and species interactions. For instance, host switching is not uncommon among allopolyploid systems and often leads to expansive ranges<sup>80,83,261</sup>. This can serve as a form of ecological fitting and promote genotype diversity at a local scale<sup>69,70</sup>. Unisexual *Ambystoma* can switch among an assortment of hosts<sup>127,128</sup>. In one such documented case, LJJ unisexual *Ambystoma* were able to utilize *A. barbouri* as a sexual host despite the lack of an *A. barbouri* haplome<sup>126</sup>. On Pelee Island, while all unisexual *Ambystoma* appear to have contributions from both potential hosts on the island (*A. laterale* and *A. texanum*), genotypes that have a genetic bias favoring a site's missing host are not uncommon (Chapter 2:). In many cases it is unclear whether this is

due to the historic presence of the missing host (i.e. a legacy effect), an unidentified host population, or immigration. In this situation, analysis comparing predictions associated with each axis of genetic diversity is necessary to disentangle the relative influence of these different explanations. However, for recently established assemblages where salamanders were previously not found, immigration seems most likely. Immigration likewise lends itself towards enhancing lineage diversity (Chapter 3:) at a regional scale by having sites with two different hosts effectively sharing triploid genotypes. While one site in isolation may not develop the symmetrical tetraploids needed for diploidization, two connected sites with alternative hosts could develop them in tandem<sup>293</sup>. To more effectively assess this potential, more fine-scaled research would be necessary to genetically link genotypes across and within lineages, thereby examining the genetic dimension across two axes of diversity simultaneously.

In Chapter 2:, I show how genotype distribution over a relatively small spatial scale is closely linked to the distribution of their sexual host(s) despite close proximity to sites with alternative hosts. However, this is likely an incomplete explanation for the variation seen given the implications of genome dosage effects and polyploidy. Furthermore, unlike across much of their range, unisexual *Ambystoma* on Pelee Island are predominantly diploid<sup>142,143</sup>. While I argue that novel diploid lineage formation is likely occurring on the island (Chapter 3:), it is unlikely that this process is the primary driver for diploid dominance as the relative abundance of diploids varied by site cluster. Diploids, in theory, should not suffer the limitations imposed on higher ploidy level individuals as their genome dosage is unbiased and they maintain smaller cell sizes within the normal range for diploid sexual species from this genus. Furthermore,

survivorship has been found to be negatively impacted by ploidy level across life stages suggesting a survival advantage for diploids <sup>219</sup>. Why is it then that diploids appear so infrequently across most of the unisexual *Ambystoma* range? In the *P. esculenta* complex, the selective advantage hypothesis was tested as an explanation for assemblage variation but could not be confirmed in either adults or their offspring <sup>294</sup>. Rather, population stabilizing mating strategies varied based on which species the hybrid crossed with, suggesting a role for reproductive plasticity contextualized by host availability <sup>295</sup>. Further research in the *P. esculenta* complex identified that survival rates of particular tadpole genotypes depends on the genotypes of the parents, suggestive of some form of postzygotic barrier <sup>296</sup>. On Pelee Island, the unique context of having two available hosts may resolve this dilemma as differential reproductive strategies or unrecognized postzygotic barriers could result in a distinct genotype distribution compared to regions with only one host, assuming the complex on Pelee Island is stable. A similar contextualization could explain the prevalence of LJ populations in southern Ontario where *A. laterale* and *A. jeffersonianum* are sympatric or parapatric <sup>297</sup>. Further research is needed to assess these hypotheses in each region. With its abundance of diploid unisexuals, and diversity of other naturally occurring genotypes, Pelee Island shows great promise to serve as a natural laboratory to explore the causes and consequences of ecological diversity across unisexual assemblages and compare those results to mainland systems and other species complexes.

### Lineage Diversity

In sexually reproducing systems, examination of mitochondrial <sup>298,299</sup> and chloroplast <sup>249</sup> lineages, or haplotypes, serves as a form of genetic diversity even though

these genetic structures are clonal. Indeed, use of lineage diversity and distribution patterns of such structures to examine historic<sup>300</sup> and contemporary<sup>117</sup> events is not uncommon and can effectively be used in conjunction with nuclear genetic data in sexual species as a method to examine temporal changes in gene flow (reviewed in<sup>41</sup>). In clonally reproducing systems, similar strategies can be employed for the same purposes even though such systems are traditionally thought of as having low genetic diversity<sup>277,301</sup>. However, it is not uncommon for these systems to develop novel lineages through multiple hybrid origins (*Cobitis* sp.<sup>262</sup>; *Phoxinus* sp.<sup>250</sup>; *Darevskia [Lacerta]* sp.<sup>302</sup>) or regular introgression/genome replacement by allochthonous parental genomes (*Pelophylax* sp.<sup>303</sup>; *Squalius* sp.<sup>304</sup>). In fact, investigations into lineage diversity can be used to age various migration events or connectivity timelines<sup>250</sup>. More intriguingly, tracking of individual haplome lineages can even reveal divergent patterns of genetic diversity<sup>82,150</sup>. So, while less commonly investigated than species diversity, studies of lineage diversity are also highly informative, particularly when considering the statistical limitations imposed by clonal reproduction such as limited allelic diversity and the breaks from conventional assumptions of genetic analyses.

Aside from examining genetic diversity, lineage-level analysis also seems to provide information about diversification trends at different time scales compared to other axes of genetic diversity. In Chapter 2:, I demonstrated a key role for the host species in determining community diversity. That work identified a likely factor, namely local host identity, in determining contemporary assemblage demographics aligning itself most closely to the temporal scale of landscape genetics<sup>305,306</sup>. In Chapter 3:, I highlight the importance of appreciating lineage diversity to examine historic community

connectivity. From this work, I found that lineage composition on Pelee Island appears to be primarily influenced by the historic structure of the island, but unique interspecific interactions may play a role at local spatial scales. Given the timescales involved, lineage-level analyses appear to examine deeper timescales than traditional landscape genetics and yet are shallower than the temporal scale of phylogeography<sup>307</sup>. Indeed, lineage-level analyses of clonal systems may provide a way to examine an intermediary temporal scale bridging landscape genetics and phylogeography in asexual groups with potential implications for our understanding of historic distributional dynamics in congeneric sexual species as well<sup>251,308</sup>.

This capacity of the lineage axis of diversity to provide novel insight about ecological and evolutionary processes may, at least in part, result from dynamics that act evenly among lineages and thus appear “neutral”. For instance, clonal populations readily display persistent founder effects<sup>101,102</sup> or high-density blocking<sup>100</sup>, each of which can effectively maintain assemblage structure<sup>34,309</sup>. Assuming temporal habitat stability, these two traits work in concert to both emphasize historic structure while muting noise in genetic data due to contemporary immigration rates, resulting in a contemporary genetic “patchiness” despite dispersal potential<sup>257,309</sup>. However, population decline following significant habitat disturbance opens the possibility for migrants of a novel lineage to colonize along contemporary migration routes<sup>310,311</sup>. As clones, migrants from novel lineages would maintain their lineage identity and be distinct from historically present lineages. While some time lag concerns may persist, such an extinction debt due to disturbance<sup>228,230</sup> or an age class gap in the colonizing lineage slowing population growth<sup>312</sup>, it is only until carrying capacity is once again reached, at which point demographic

shifts would almost exclusively be due to neutral dynamics<sup>103,313</sup>. However, it is unclear if selective pressures do act evenly among lineages and further study would be needed to determine whether this is the case.

In other clonal systems with distinct lineages, selective pressures have been found to favor some lineages over others<sup>101,314</sup>. For instance, lineages that share a particularly flexible base genotype may experience greater ecological fitting capacity<sup>293</sup>. Should a lineage have a particularly broad tolerance, it may even outperform its sexual progenitors<sup>315</sup>. Following the “Frozen Niche Hypothesis”<sup>120</sup>, individual lineages may display narrow niches within which they are more competitive against their hosts. While one or a few lineages may be able to persist alongside their host, having multiple lineages, each with their own distinct niche, may result in a highly diversified niche space for the host(s), potentially destabilizing coexistence<sup>53</sup>. This hypothesis may partially explain the proposed Clanton effect<sup>63,316</sup> as extreme unisexual-to-host ratios, or even lack of hosts, often appear in range overlaps between *A. laterale* and other potential hosts<sup>148,317</sup>. Indeed, similar destabilizing dynamics have been documented in traditional parasite-host systems<sup>68</sup>. While niche variability is known among unisexual *Ambystoma* genotypes<sup>146</sup>, no work has been done to assess if such variation exists among distinct unisexual *Ambystoma* lineages or if there are interactions between lineage-based and genotype-based niche trends. However, the relationship between ecosystem stability and diversity is highly complex and further research is necessary to establish if lineage niche diversity impacts host population dynamics<sup>318,319</sup>.

The presence of many lineages across Pelee may also be a consequence of a deeper legacy. The origins of these lineages are uncertain, though the wide distribution of

some lineages suggests they may have been present prior to the flooding of the Erie Basin. Prior to the Nipissing event that isolated Pelee Island, a land bridge existed connecting what are today Point Pelee and mainland Ohio <sup>165</sup>. During this time, some lineages may have been more widely distributed, suggesting some lineages found on Pelee Island today may also be present on other islands in Lake Erie. Unpublished results, using samples collected by James Bogart, support this hypothesis revealing that two diploid lineages known from Pelee Island are also present on Kelley's Island and at least one other found on Middle Bass Island (Bare, *unpublished*). Future work on unisexual *Ambystoma* should account for the genetic, and potentially ecological, diversity that lineage-level analyses can ascertain, while recognizing the ways that historic landscapes or interactions can influence such dynamics.

When investigating clonal systems, assessment of lineage diversity can prevent misinterpretation of allelic diversity. While clonal systems from monophyletic origins may experience divergence through mutation (*Poecilia formosa* <sup>320</sup>; *P. monacha-occidentalis* <sup>321</sup>), it is also quite common for multiple hybridization events to produce multiple clonal lineages <sup>250,322</sup>. In the former case, a single lineage may diversify in allelic representation as demonstrated with the diploid lineages found on Pelee Island. Over time, and after periods of diversification and isolation, a single monophyletic lineage may appear to be multiple lineages as they get more genetically distant. Such within-lineage variation can be used to track colonization dynamics <sup>117,263,323</sup> or estimate lineage age <sup>250,321,324</sup>. In some cases, even lineages with seemingly low genetic diversity can be investigated with karyotypic/chromosomal structure diversity <sup>325</sup>. Similar work has been done in unisexual *Ambystoma*, showing hybrid chromosomal structures can be tracked

across populations allowing for the inference of colonization pathways<sup>264,326</sup>. Indeed, this karyotype diversity serves to reinforce the importance of viewing assessing the genetic dimension of diversity along various axes. Conceivably, the “karyotype axis” could connect different lineages to one another as the unique structure of a chromosome may persist across lineages connected through recent ancestry.

## **Conclusion**

From parasite ecology to landscape genetics, or community diversity to legacy effects, unisexual *Ambystoma* provide a model system that be interrogated to explore a wide breadth of ecological and evolutionary theory. While certainly a unique system due to their distinct reproductive mode of kleptogenesis, unisexual *Ambystoma* are still subject to the same ecological processes that drive broader biodiversity patterns. My work further demonstrates that unconventional reproductive systems are an untapped resource of ecological knowledge and warrant further exploration<sup>49</sup>. Indeed, this system led me to expand on the concept of “dimensions of diversity” described by others<sup>7,36</sup>, providing the conceptual distinction of different “axes of diversity” as a framework that subdivides dimensions based on the methods used to measure diversity and the distinct interpretations of each method.

Arguably, this is analogous to work conducted in conventional sexual systems, where analyses of mitochondrial DNA and nuclear DNA are often associated with different spatiotemporal scales and classified as either “phylogenetics” or “landscape genetics”<sup>307,327</sup>. In this thesis I have also argued that the different genetic diversity axes, tested and described herein, can likewise be used to test various hypotheses at differing spatiotemporal scales. These axes of diversity can be aligned along a continuous sliding

scale of spatiotemporal resolutions, each providing their own distinct insight into the history and processes driving biodiversity. Consequentially, systems with unconventional reproductive modes provide significant opportunities for studying ecological theory as they provide a wide range of distinct axes of genetic diversity that can be explored. Continued examination and comparison of these unique systems with more refined strategies such as the use of fluorescent *in situ* hybridization <sup>266,328</sup>, use of more loci that are chromosomally unlinked (see Appendix A: Mapping of microsatellite loci to the axolotl (*A. mexicanum*) genome), or examination of intra-lineage genetic diversity, will help ecologists develop novel insights into fundamental ecological processes that are difficult or impossible to investigate in contemporary diploid sexual systems.

## Appendix A: Mapping of microsatellite loci to the axolotl (*A. mexicanum*) genome

### Introduction

Within the *Ambystoma* genus of salamanders there is a highly complex lineage of unisexual individuals that exhibit a unique reproductive mode known as ‘kleptogenesis’<sup>124</sup>. This group consists of an all-female, nuclear hybrid, mixed ploidy, obligative sexually parasitic, monophyletic lineage (based on mtDNA) that is only able to reproduce by ‘stealing’ sperm from viable male hosts<sup>128</sup>. To date there are five known sexual species (*A. laterale*, *A. texanum*, *A. barbouri*, *A. jeffersonianum*, and *A. tigrinum*) that can play host to this unisexual complex<sup>126</sup>. Through their unique mode of sexual reproduction these unisexual animals can have up to four reproductive outcomes: 1) clonal offspring, wherein the offspring are full genetic clones of the mother<sup>124</sup>, 2) ploidy elevation<sup>124,134</sup>, wherein the egg incorporates the allochthonous haplome from collected sperm, 3) genome replacement<sup>134,136</sup>, where one full set of chromosomes are discarded and replaced by the haplome of the sperm, or 4) a hypothesized track where symmetrical tetraploids, individuals possessing two *A. laterale* haplomes and two chromosome sets from one other host, produce diploids that maintain one *A. laterale* haplome and one haplome of the other donating species<sup>137</sup>. Due to this complexity, individuals are assigned ‘genomotypes’, monikers that indicate the species and number of haplome copies from each species<sup>129</sup>. For example, ‘LT’ indicates a diploid animal with one haplome derived from *A. laterale* (L) and one from *A. texanum* (T), while ‘LJJ’, indicates a triploid animal with one derived haplome from *A. laterale* and two from *A.*

*jeffersonianum* (J). To date, animals have been found up to pentaploid ploidy level, and as tetrahybrids (maintaining haplome sets from four unique sperm donors) <sup>128</sup>.

Today, Ambystomatids are genotyped most frequently using co-dominant microsatellite loci, though can also be identified using a single nucleotide polymorphism (SNP) assay <sup>329</sup>. Compared to SNPs, microsatellite markers provide the benefit of having high allelic diversity with alleles based on length rather than sequence <sup>330</sup>. Additionally, microsatellites have a high rate of mutation caused by slippage in the central region of repeat motifs during DNA replication, making them suitable for analysis at short time intervals <sup>330</sup>. The diversity associated with these regions is capable of discerning minute genetic differences between individuals even within the same sub-lineage of animals, with some having species-specific allele size ranges or amplification success in select species due to mutations in primer binding regions <sup>208</sup>. Use of microsatellites has proven valuable for work with unisexual *Ambystoma* and the sexual hosts on which they rely because this method allows for the identification of ploidy and identity of the genome(s) of origin from the chromosomes an individual possesses <sup>141</sup>. This strategy has high efficacy when compared to flow cytometry and has a better accuracy when compared to allozyme assessment that had been used originally <sup>141</sup>. Subsequent work documenting intergenomic exchange within unisexual *Ambystoma* raises concern for this strategy <sup>264,266</sup>. During such events, homeologous chromosomes crossover producing chimeric chromosomes that are comprised of genetic material originating from two different species <sup>266,326</sup>. In such cases, it is possible that genotyping based on microsatellite markers may produce faulty results due to two loci on the same chromatid indicating two different species of origin (Figure A.1).

To assess the potential for this possibility, this work aligns all published microsatellite primer sets derived from *Ambystoma* species to the fully sequenced *Ambystoma mexicanum* genome (strain DD151, project accession PGSH02000000)<sup>331</sup>. While not known to be a potential sperm donor to the unisexual complex, *A. mexicanum* is the only fully sequenced *Ambystoma* genome to date (32 Gb) and is within the *tigrinum* complex of *Ambystoma* which does have at least one confirmed viable sperm donor species (*A. tigrinum*). Additionally, this work exists as an exercise to test coalescent theory, from which we might predict that primer sets derived from close relatives to *A. mexicanum* will have greater sequence matching compared to primer sets derived from more distantly related species<sup>332,333</sup>.

## **Methods**

### Data Collection

Primer sequences were collected from available literature sources including theses, dissertations, and published agency reports (Table A.1). The full genome sequence for *A. mexicanum* was downloaded from NCBI GenBank (chromosomes only, accession #'s CM010927-CM010938, CM030316-CM030331) but is also freely available from axolotl-nomics.org (includes chromosomes and supercontig sequences). Microsatellite sequences were also downloaded from NCBI GenBank.

### Genome Mapping

Microsatellite sequences were aligned to the *A. mexicanum* genome using a the NCBI nucleotide BLAST software (Figure A.7). The minimum word limit was reduced to 15 to accommodate high variability of repeat region size and high potential for mutations within these neutral loci. Resulting subject sequences were filtered for total

query coverage ( $\geq 70\%$ ) for each chromosome, percentage of microsatellite sequence aligned per subject sequence ( $\geq 30\%$ ), and score ( $\geq 140$ ). Values were reduced as subject sequences often did not fully align along the repeat region, causing query sequences to be sectioned (

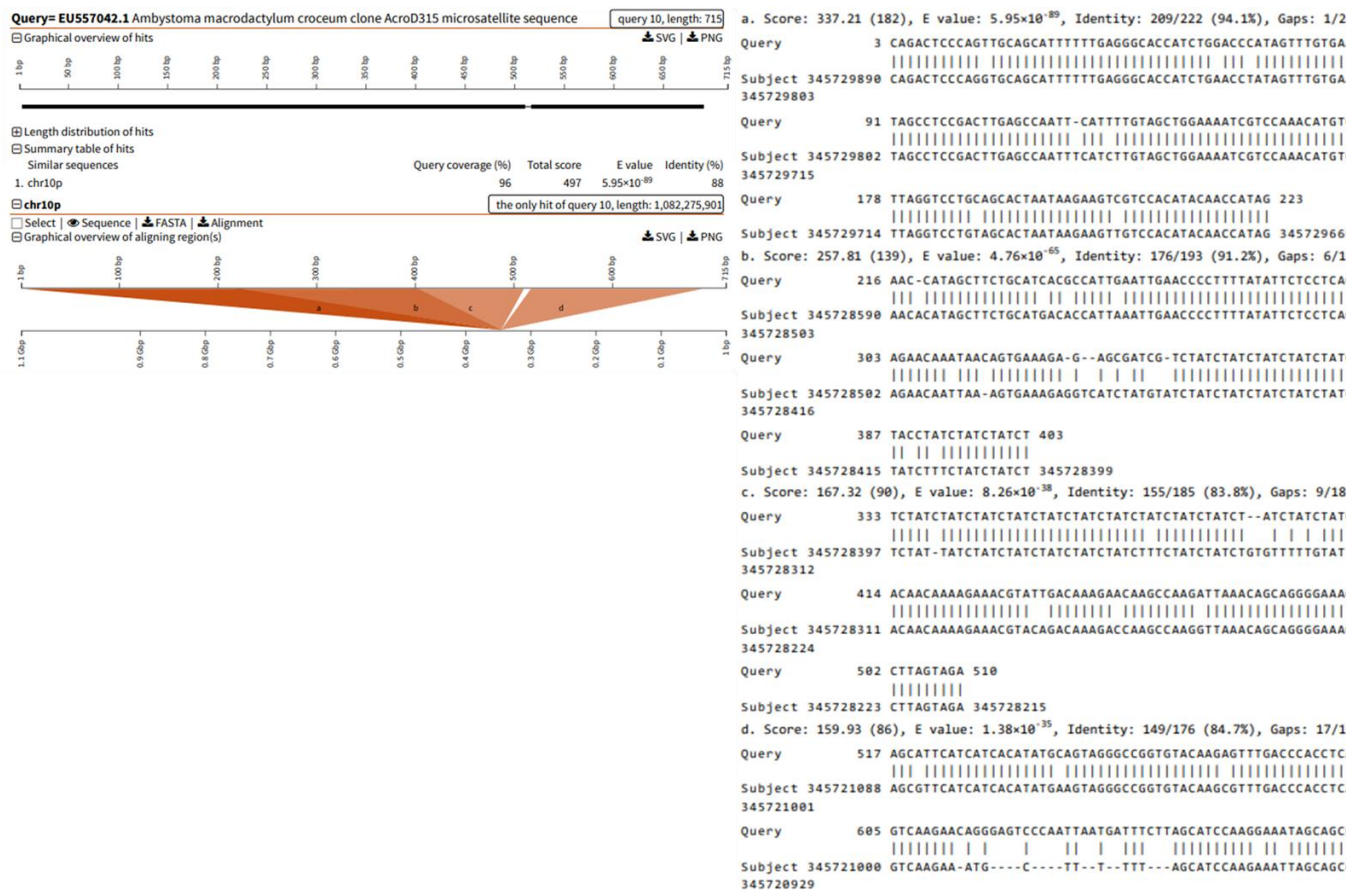


Figure A.5 and Figure A.7B). Final aligned sequences were chosen from the remaining filtered set based on lowest e-value, highest score, and longest aligned sequence length for each locus. Loci were then mapped to their respective chromosome based on their start position in R<sup>212</sup>.

### Primer Alignment Potential

Reference genome sequences aligned to microsatellite sequences were extracted and filtered by total query coverage ( $\geq 70$ ). These sequences were then developed into a searchable database and aligned to published primer sequences (Figure A.7). Matches were extracted such that only alignments where primers matched to their associated microsatellite sequence aligned reference sequences were kept. Alignments were filtered such that only the top alignment by % identity match and query coverage length were

kept. Instances where primer sequences could align to multiple points on the subject were removed, along with any instances where only a single primer from a set could be aligned. This filtering left only those primer sets that had sufficient alignment quality.

(Full flow chart of procedure provided in Figure A.6)

## Results

From the initial set of 389 microsatellite loci found in the literature and on GenBank, 206 were able to be mapped to the axolotl reference genome (Figure A.2, and Table A.1 and Table A.2). Furthermore, 11 of 14 microsatellite loci currently used for this thesis were also able to be successfully mapped (Figure A.3). With these 11 loci, 3 chromosomes (chr 3, 5, and 6) can be identified with multiple loci and therefore are of concern for causing misidentification of genotype via intergenomic crossover in unisexual *Ambystoma* being studied.

Of those loci that were mapped to the axolotl reference genome, 39 primer pair binding sites could be successfully identified. For some loci, there is no published microsatellite sequence, and therefore I could not align them at all (Table A.1). Others lacked any alignment of high confidence, primarily due to low query coverage. Lastly, a small set of loci could not be reliably placed due to multiple alignments having equal alignment scoring (e.g., Amb08\_R), suggesting the potential for multiple points for primer alignment that could produce amplified results during PCR. From mapped primer pairs, quality of sequence alignment tended to be lower in more distantly related species (based on <sup>334</sup>). Percent identity and count of mismatched base pairs showed the strongest trend (Figure A.4,

Table A.3).

## Discussion

The purpose of this study was two-fold: 1) identify likely locations of published *Ambystoma* microsatellite loci within a reference *Ambystoma* genome, and 2) determine if primer set alignment fidelity follows phylogenetic distance. I was able to map most published microsatellite sequences onto the axolotl genome, with most that are not mapped having unpublished sequences to be matched with. Furthermore, primer sets with high degree of sequence alignment also followed general expectations of coalescence theory, namely that primer sets derived from more closely related species will tend to have greater alignment capacity<sup>332,333</sup>. For research purposes, especially for unisexual *Ambystoma*, this information should prove to be of significant use to account for potential of intergenomic crossover events.

During the data collection process there were a significant number of loci that did not have published sequences in the NCBI GenBank. Without official sequences to work with, this mapping procedure cannot be effectively done. In the future, such primer sets may want to be avoided for use in unisexual *Ambystoma* studies for concern that their use limits the potential for accounting for intergenomic crossover events which may lead to misidentification of animals. While unisexual *Ambystoma* are primarily clonal<sup>128</sup>, avoiding meiosis II when crossover would occur, the cloning of these chimeric chromatids can make their signature persist within populations<sup>326</sup>. As such, the tracking of these chimeric chromosomes can prove to be quite useful for landscape genetic studies or connectivity studies. By recognizing where specific microsatellite markers are located within the genome, investigators may be able to control for misidentification of

genotypes while simultaneously increasing robustness of analysis by including chimera tracking in the analysis.

For bisexual *Ambystoma* species, these results provide similar benefits for analyses. Namely, by identifying location of loci within the reference genome, investigators can better account for allele linkage in population genetics studies<sup>335</sup>. Due to the higher rates of mutation in microsatellites, it can be hard to determine if alleles are identical-by-state or identical-by-descent. Recognizing allele linkages can provide for more refined assessments and greater precision in results as linked microsatellite markers can help tease out instances of identical-by-state vs identical-by-descent. In unisexual *Ambystoma* for instance, thanks to their clonal nature, all loci are considered highly linked. Consequently, independent genetic lineages can be tracked across a landscape to assess connectivity and intralocus genetic diversity<sup>136,250</sup>. In other cases, hybridization events can likewise be tracked and aged<sup>250,336,337</sup>.

Furthermore, linkage to microsatellites has long been used as an indirect method for tracking genetic diseases or other genetic markers<sup>338,339</sup>. While the axolotl genome has been published, the process of identifying effective primers for genotyping can still be laborious as it typically requires either bacterial cloning or next-generation sequencing of the species in question as an initial step with both procedures requiring significant time and funding. Use of primer sets already designed can expedite the initial phase of research. If tracking specific genes, use of pre-designed primers for closely linked loci may skip the need to designing such primers in the first place. By using the genome map designed here, in conjunction with the published and annotated axolotl

genome, Ambystomatid researchers can target their desired gene of interest by identifying its nearest microsatellite neighbors instead.

As genetic technology and sequencing capabilities advance, microsatellites have generally been falling out of favor as neutral genetic markers. However, their high rates of diversity lend them to being used for studies investigating population diversification over short time periods. Moreover, in highly clonal groups, microsatellites continue to prove to be useful for identifying population structure and connectivity. Microsatellite mapping can prove useful in these endeavors for both clonal and non-clonal populations. However, great care should still be taken when deciding which loci to use as primer binding sequences may significantly differ between species, particularly when primers were designed for more distantly related species from the target. In sexually reproducing species, one should aim to target loci for which primers were designed from either the same species of interest or closely related species. However, in hybrid complexes, the strategy becomes different depending on the research interest. Generally, having primers that bind to either species of origin will have greater chances for amplification, but it is no guarantee that allele size ranges won't be ambiguous leading to potential confusion during analysis. On the other hand, having primers that only amplify in one genome limits the precision of analyses. Therefore, it is advised that a suite of primers is used such that some pairs can target all genomes present, while others only target one. In this way, the ambiguity of one can compensate for the lack of detail provided by the other and vice versa. Until full-genome sequencing becomes cheap and widely available, microsatellite loci will continue to have use in research. It therefore remains essential that users understand, recognize and acknowledge both their strengths and their limitations.

## Tables and Figures

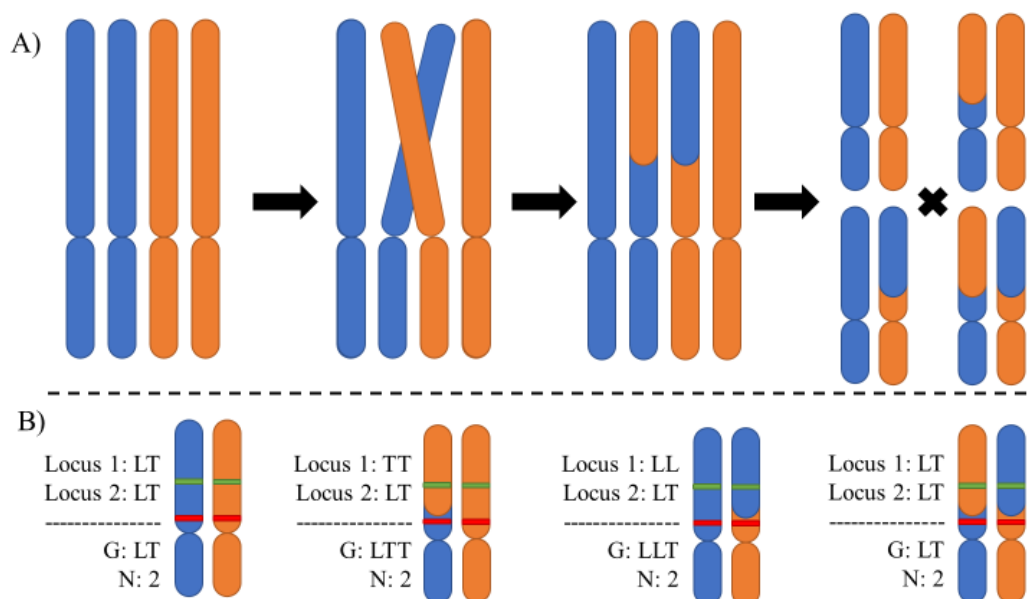


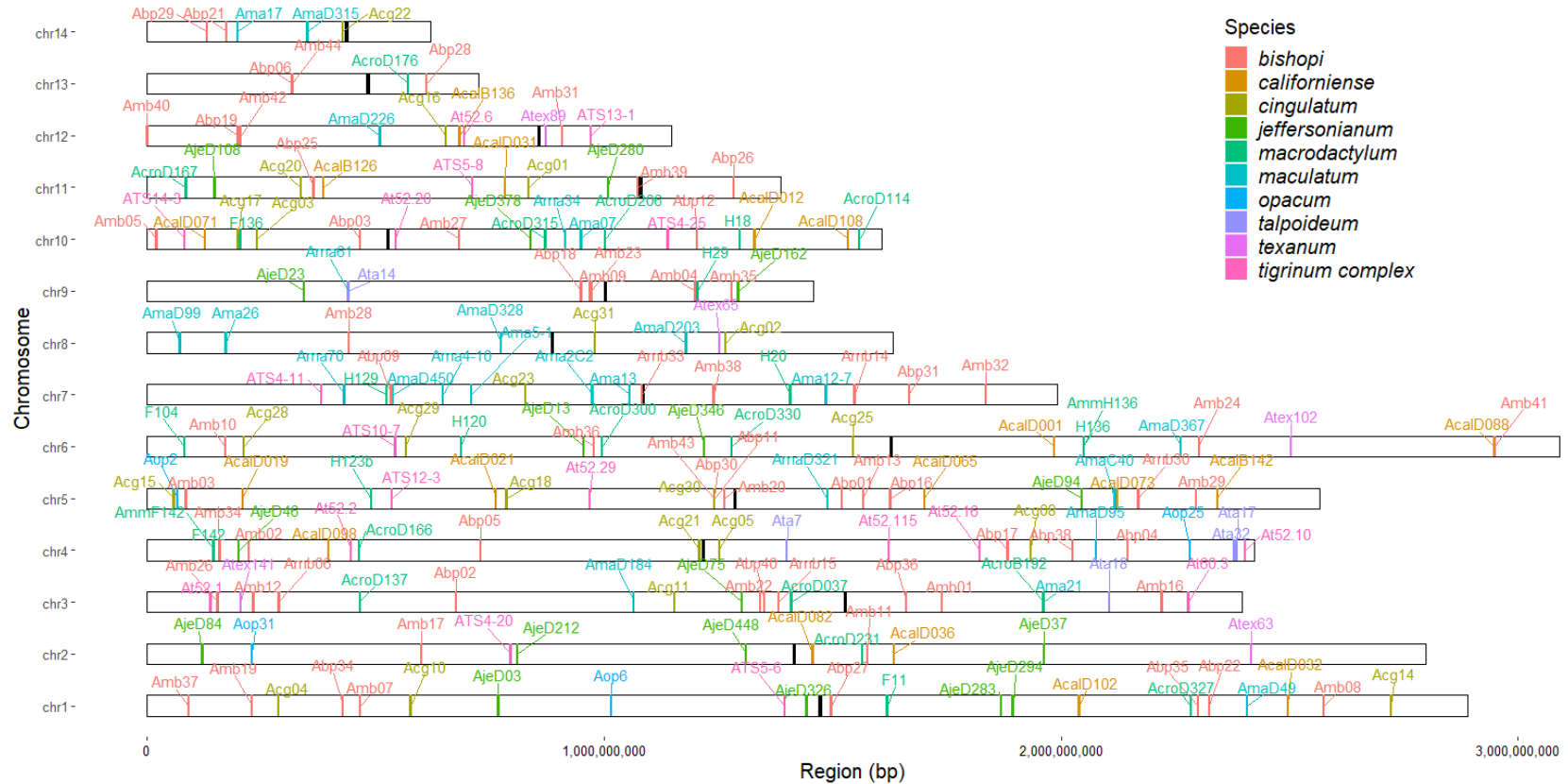
**Figure A.1.** A) Diagram of intergenomic crossover process. Within a symmetrical tetraploid (blue = *A. laterale*, orange = *A. texanum*), the hypothesized diploidization process could result in four outcomes dependent on if intergenomic crossover occurs between homeologous chromatids. In three outcomes, at least one chromatid is chimeric, possessing regions originating from two different species. B) Assuming two targeted loci map to the same chromosome (Locus 1 – green band, Locus 2 – red band), each of the four offspring have distinct genomic outcomes. Two outcomes (middle) represent a misidentification of genotype (G) due to one locus signaling two copies from one species and the second locus signaling one copy from each species. One outcome represents a correct genotype (right) but two chimeric chromatids. The last offspring (left) is a ‘true’ LT with intact chromatids.

**Table A.1.** List of citations and associated accession numbers for recognized *Ambystoma* microsatellite loci primer sets.

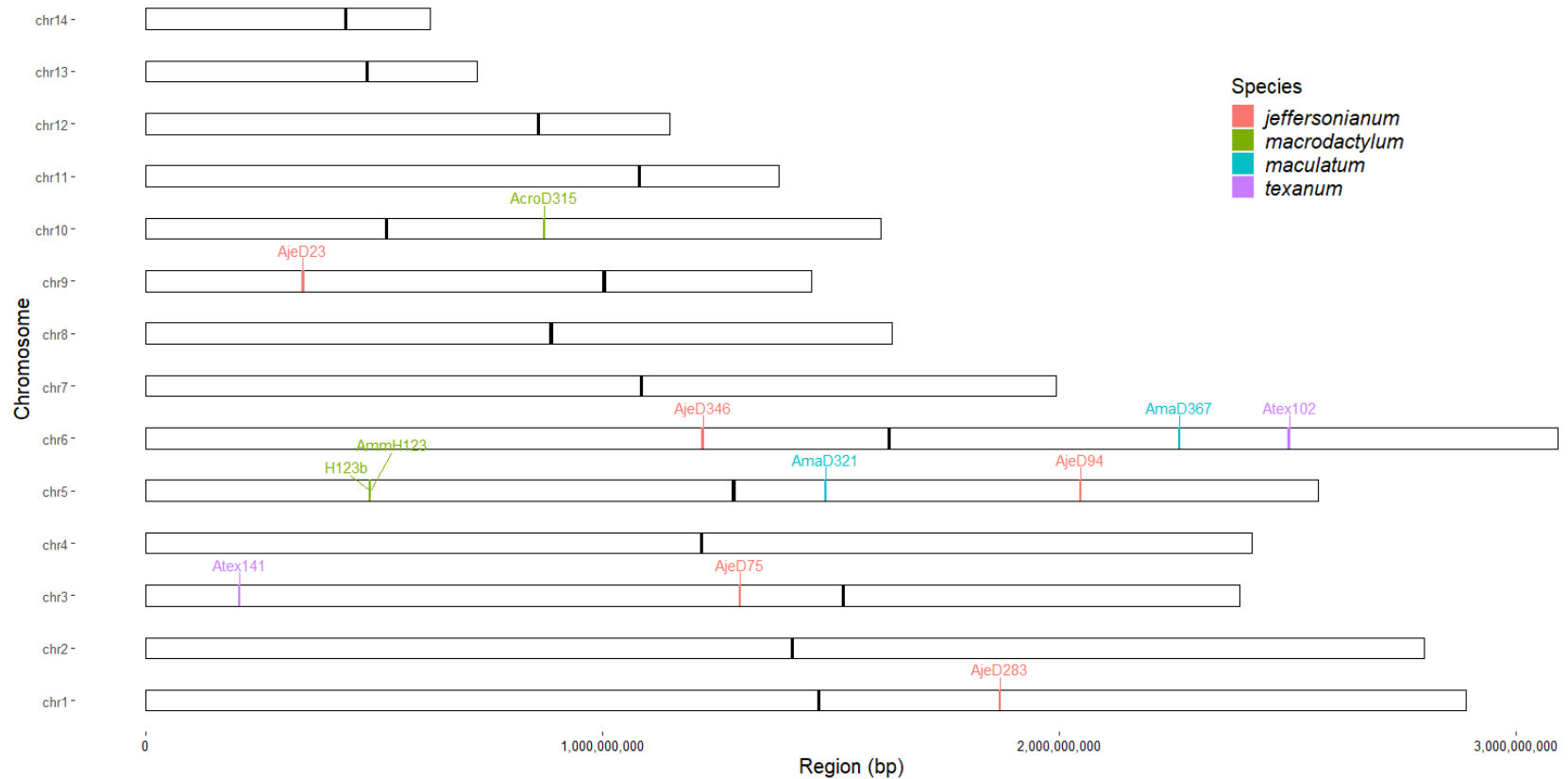
	Count	Accession #
<b><i>Ambystoma (Non-specific)</i></b>		
Savage, 2008	1	-
Williams et al., 2009	1	-
<b><i>annulatum</i></b>		
Peterman et al., 2013a	22	-
Peterman et al., 2015	2	-
<b><i>bishopi</i></b>		
Wendt, 2017	84	KP289040-123
<b><i>californiense</i></b>		
Savage, 2008	21	EU442375-95
<b><i>cingulatum</i></b>		
Wendt, 2017	32	KP289124-55
<b><i>jeffersonianum</i></b>		
Denton et al., 2015	15	-
Julian et al., 2003b	20	AY091793-812
<b><i>laterale</i></b>		
Denton et al., 2015	15	-
Denton et al., 2016	1	-
Denton et al., 2019	1	-
<b><i>macroductylum</i></b>		
Shields and Liss, 2003	12	AY234810-21
Savage, 2009	14	EU557031-44
Savage, 2009*	3	AY234812, AY234817, AY234819

Table A.1 *Continued.*

	Count	Accession #
<b><i>maculatum</i></b>		
Peterman et al., 2013b	18	-
Peterman et al., 2015	1	-
Armstrong, 2012	3	-
Julian et al., 2003a	15	AF520747-61
Wieczorek et al., 2002	16	AF108913-20; AF452178-84; AY122051
<b><i>opacum</i></b>		
Croshaw et al., 2005	8	AY667611-7; AY733034
Nunziata et al., 2011	12	-
<b><i>talpoideum</i></b>		
Croshaw et al., 2005	10	AY667618-23; AY733035-38
Love et al., 2013	31	-
<b><i>texanum</i></b>		
Williams and DeWoody, 2004	10	AY362347-56
<b><i>tigrinum complex</i></b>		
Mech et al., 2003	10	AY157747-56
Parra-Olea et al., 2007	11	EF062516-25



**Figure A.2.** Karyotype of the axolotl (*A. mexicanum*) genome. Microsatellite loci are mapped with color depicting species from which loci were originally identified from. Not all loci could be effectively placed due to either low confidence in mapping or multiple placements of equal support. Centromeres are marked as black bars. Chromosome arms are arranged q-arm on the left of the centromere and p-arm to the right.



**Figure A.3.** Loci locations for 11 of 14 loci used in this PhD thesis. Loci AmmH123 and H123b are the same locus but different primer sets derived from the same published microsatellite sequence. Three loci were unsuccessfully mapped: Atex74 (more than one region with 100% query coverage), AjeD422 (no significant alignment), and AmaD42 (no significant alignment). Chromosomes 5 and 6 each have three loci mapped to them, chromosome 3 has two loci, with chromosomes 10, 9, and 1 each having one locus each.

**Table A.2.** Locus count per chromosome arm and species where associated accession sequence could be reliably aligned to the axolotl genome.

	Species										G. Total
	<i>tig.</i>	<i>calif.</i>	<i>bish.</i>	<i>cing.</i>	<i>jeff.</i>	<i>tex.</i>	<i>macro.</i>	<i>op.</i>	<i>macul.</i>	<i>talp.</i>	
<b>chr1</b>	<b>1</b>	<b>2</b>	<b>8</b>	<b>3</b>	<b>4</b>		<b>2</b>	<b>1</b>	<b>1</b>		<b>22</b>
p		2	4	1	2		2		1		12
q	1		4	2	2			1			10
<b>chr2</b>	<b>1</b>	<b>2</b>	<b>2</b>		<b>4</b>	<b>1</b>	<b>1</b>	<b>1</b>			<b>12</b>
p		2	1		1	1	1				6
q	1		1		3			1			6
<b>chr3</b>	<b>2</b>		<b>10</b>	<b>1</b>	<b>1</b>	<b>1</b>	<b>3</b>		<b>2</b>	<b>1</b>	<b>21</b>
p	1		3				1		1	1	7
q	1		7	1	1	1	2		1		14
<b>chr4</b>	<b>4</b>	<b>1</b>	<b>6</b>	<b>3</b>	<b>1</b>		<b>2</b>	<b>1</b>	<b>1</b>	<b>3</b>	<b>22</b>
p	3		3	2				1	1	3	13
q	1	1	3	1	1		2				9
<b>chr5</b>	<b>2</b>	<b>5</b>	<b>10</b>	<b>3</b>	<b>1</b>		<b>1</b>	<b>1</b>	<b>2</b>		<b>25</b>
p		3	5		1				2		11
q	2	2	5	3			1	1			14
<b>chr6</b>	<b>1</b>	<b>2</b>	<b>4</b>	<b>3</b>	<b>2</b>	<b>1</b>	<b>5</b>		<b>1</b>		<b>19</b>
p		2	2			1	1		1		7
q	1		2	3	2		4				12
<b>chr7</b>	<b>1</b>		<b>6</b>	<b>1</b>			<b>2</b>		<b>7</b>		<b>17</b>
p			4				1		1		6
q	1		2	1			1		6		11
<b>chr8</b>			<b>1</b>	<b>2</b>		<b>1</b>			<b>4</b>		<b>8</b>
p				2		1			1		4
q			1						3		4
<b>chr9</b>			<b>5</b>		<b>2</b>		<b>1</b>		<b>1</b>	<b>1</b>	<b>10</b>
p			2		1		1				4
q			3		1				1	1	6
<b>chr10</b>	<b>3</b>	<b>3</b>	<b>4</b>	<b>2</b>	<b>1</b>		<b>5</b>		<b>2</b>		<b>20</b>
p	2	2	2		1		4		2		13
q	1	1	2	2			1				7
<b>chr11</b>	<b>1</b>	<b>2</b>	<b>3</b>	<b>2</b>	<b>2</b>		<b>1</b>				<b>11</b>
p			1								1
q	1	2	2	2	2		1				10
<b>chr12</b>	<b>2</b>	<b>1</b>	<b>4</b>	<b>1</b>		<b>1</b>			<b>1</b>		<b>10</b>
p	1		1			1					3
q	1	1	3	1					1		7
<b>chr13</b>			<b>3</b>				<b>1</b>				<b>4</b>
p			1				1				2
q			2								2
<b>chr14</b>			<b>2</b>	<b>1</b>					<b>2</b>		<b>5</b>
q			2	1					2		5
<b>Total</b>	<b>18</b>	<b>18</b>	<b>68</b>	<b>22</b>	<b>18</b>	<b>5</b>	<b>24</b>	<b>4</b>	<b>24</b>	<b>5</b>	<b>206</b>

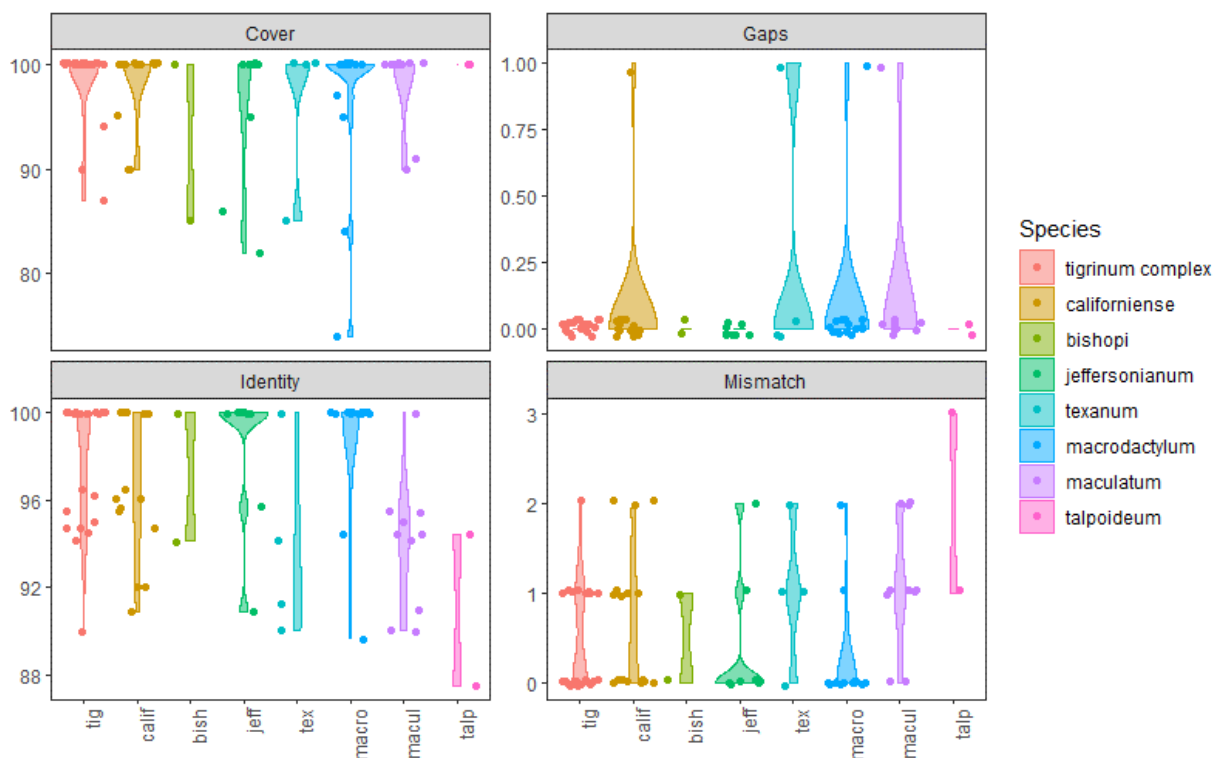


**Figure A.4.** Sequence alignment quality measures of matched primer sequences for loci where primer pairs were successfully matched. Species order from left to right goes from closest relative to most distant relative of *A. mexicanum*<sup>334</sup>. More distant relatives had comparably fewer primer pair alignments, with primer pairs derived from the most distant relatives (*A. talpoideum* and *A. maculatum*) generally having lower identity match and higher numbers of mismatched base pairs.

**Table A.3.** Total number of primer sets and average alignment metrics for each species.

Species	Primer Sets	Identity (%)	Mismatch	Gaps	Coverage (%)
<i>tigrinum</i>	11	97.78	0.45	0.00	98.68
<i>californiense</i>	8	96.82	0.69	0.06	98.44
<i>bishopi</i>	1	97.06	0.50	0.00	92.50
<i>jeffersonianum</i>	4	98.32	0.38	0.00	95.38
<i>texanum</i>	2	93.86	1.00	0.25	96.25
<i>macrodactylum</i>	7	98.86	0.21	0.07	96.43
<i>maculatum</i>	5	93.98	1.10	0.10	98.10
<i>talpoideum</i>	1	90.97	2.00	0.00	100.00

**Table A.4.** Successfully aligned loci listed by species of origin. Chromosome arm and alignment statistics provided for each primer. Species ordered by phylogenetic distance<sup>334</sup>. Loci used in this thesis are identified (\*).

Species	Locus	Arm	Direct.	Identity (%)	Mismatch	Gaps	% Coverage
<i>tigrinum</i>							
	<u>At52.2</u>	4q	F	95.00	1	0	87
			R	96.15	1	0	100
	<u>At52.10</u>	4p	F	96.43	1	0	100
			R	100.00	0	0	100
	<u>At52.20</u>	10p	F	100.00	0	0	100
			R	100.00	0	0	100
	<u>At52.6</u>	12q	F	100.00	0	0	100
			R	95.45	1	0	100
	<u>ATS4-11</u>	7q	F	100.00	0	0	100
			R	94.44	1	0	100
	<u>ATS4-25</u>	10p	F	100.00	0	0	100
			R	100.00	0	0	100
	<u>ATS5-6</u>	1q	F	90.00	2	0	100
			R	100.00	0	0	100
	<u>ATS10-7</u>	6q	F	100.00	0	0	100
			R	100.00	0	0	100
	<u>ATS12-3</u>	5q	F	100.00	0	0	100
			R	94.74	1	0	100
	<u>ATS13-1</u>	12p	F	94.74	1	0	100
			R	94.12	1	0	100
	<u>ATS14-3</u>	10q	F	100.00	0	0	90
			R	100.00	0	0	94
<i>californiense</i>							
	<u>AcalB142</u>	5p	F	96.00	1	0	100
			R	95.65	1	0	100
	<u>AcalD001</u>	6p	F	100.00	0	0	100
			R	100.00	0	0	90
	<u>AcalD012</u>	10p	F	100.00	0	0	100
			R	100.00	0	0	100
	<u>AcalD019</u>	5q	F	96.43	0	1	100
			R	90.91	2	0	100
	<u>AcalD021</u>	5q	F	95.45	1	0	100
			R	100.00	0	0	90
	<u>AcalD031</u>	11q	F	96.00	1	0	100
			R	100.00	0	0	100
	<u>AcalD071</u>	10q	F	92.00	2	0	100
			R	92.00	2	0	100
	<u>AcalD108</u>	10p	F	100.00	0	0	100
			R	94.74	1	0	95

Table A.4 *Continued.*

Species	Locus	Arm	Direct.	Identity (%)	Mismatch	Gaps	% Coverage
<i>bishopi</i>							
	<u>Amb05</u>	10q	F	94.12	1	0	85
			R	100.00	0	0	100
<i>jeffersonianum</i>							
	<u>AjeD23*</u>	9q	F	100.00	0	0	95
			R	95.65	1	0	100
	<u>AjeD108</u>	11q	F	100.00	0	0	86
			R	100.00	0	0	82
	<u>AjeD162</u>	9p	F	100.00	0	0	100
			R	90.91	2	0	100
	<u>AjeD448</u>	2q	F	100.00	0	0	100
			R	100.00	0	0	100
<i>texanum</i>							
	<u>Atex63</u>	2p	F	91.30	1	1	100
			R	100.00	0	0	100
	<u>Atex102*</u>	6p	F	94.12	1	0	85
			R	90.00	2	0	100
<i>macroductylum</i>							
	<u>AcroD231</u>	2p	F	100.00	0	0	74
			R	100.00	0	0	100
	<u>AcroD327</u>	1p	F	100.00	0	0	100
			R	89.66	2	1	97
	<u>F104</u>	6q	F	100.00	0	0	100
			R	100.00	0	0	100
	<u>H20</u>	7p	F	94.44	1	0	100
			R	100.00	0	0	100
	<u>H29</u>	9p	F	100.00	0	0	100
			R	100.00	0	0	95
	<u>H120</u>	6q	F	100.00	0	0	100
			R	100.00	0	0	84
	<u>H123b*</u>	5q	F	100.00	0	0	100
			R	100.00	0	0	100
<i>maculatum</i>							
	<u>Ama2C2</u>	7q	F	95.45	0	1	100
			R	94.44	1	0	100
	<u>Ama4-10</u>	7q	F	94.12	1	0	100
			R	100.00	0	0	100
	<u>Ama61</u>	9q	F	94.44	1	0	90
			R	90.00	2	0	100
	<u>AmaC40</u>	5p	F	95.00	1	0	91
			R	90.91	2	0	100
	<u>AmaD184</u>	3q	F	90.00	2	0	100
			R	95.45	1	0	100

**Table A.4 Continued.**

Species	Locus	Arm	Direct.	Identity (%)	Mismatch	Gaps	% Coverage
<i>talpoideum</i>							
	<u>Ata17</u>	4p	F	94.44	1	0	100
			R	87.50	3	0	100



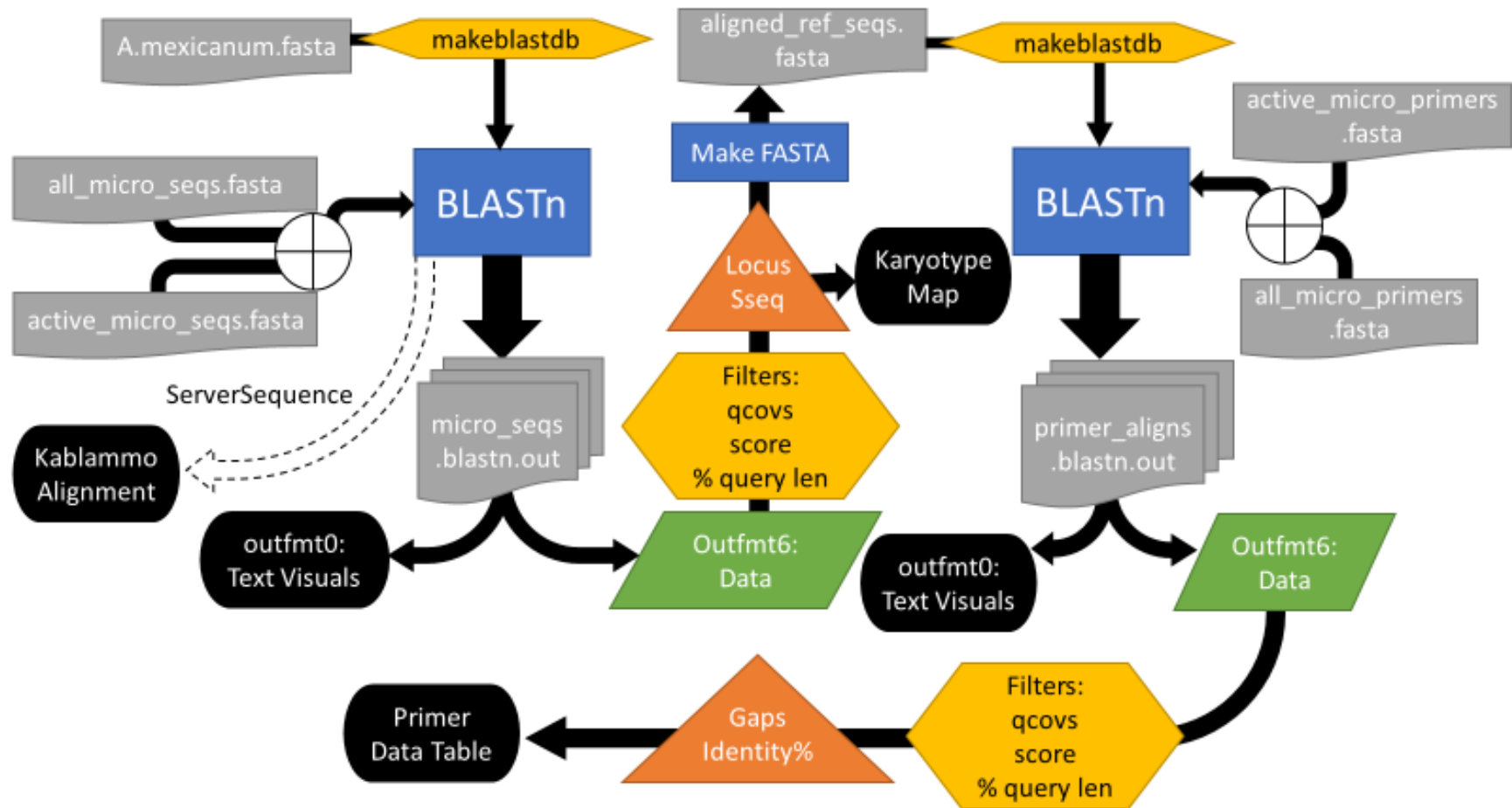


**Figure A.6.** Project flow chart detailing file inputs (grey), outputs (black), intermediary data files (green), data processing steps (orange), data management steps (yellow), and functions (blue).

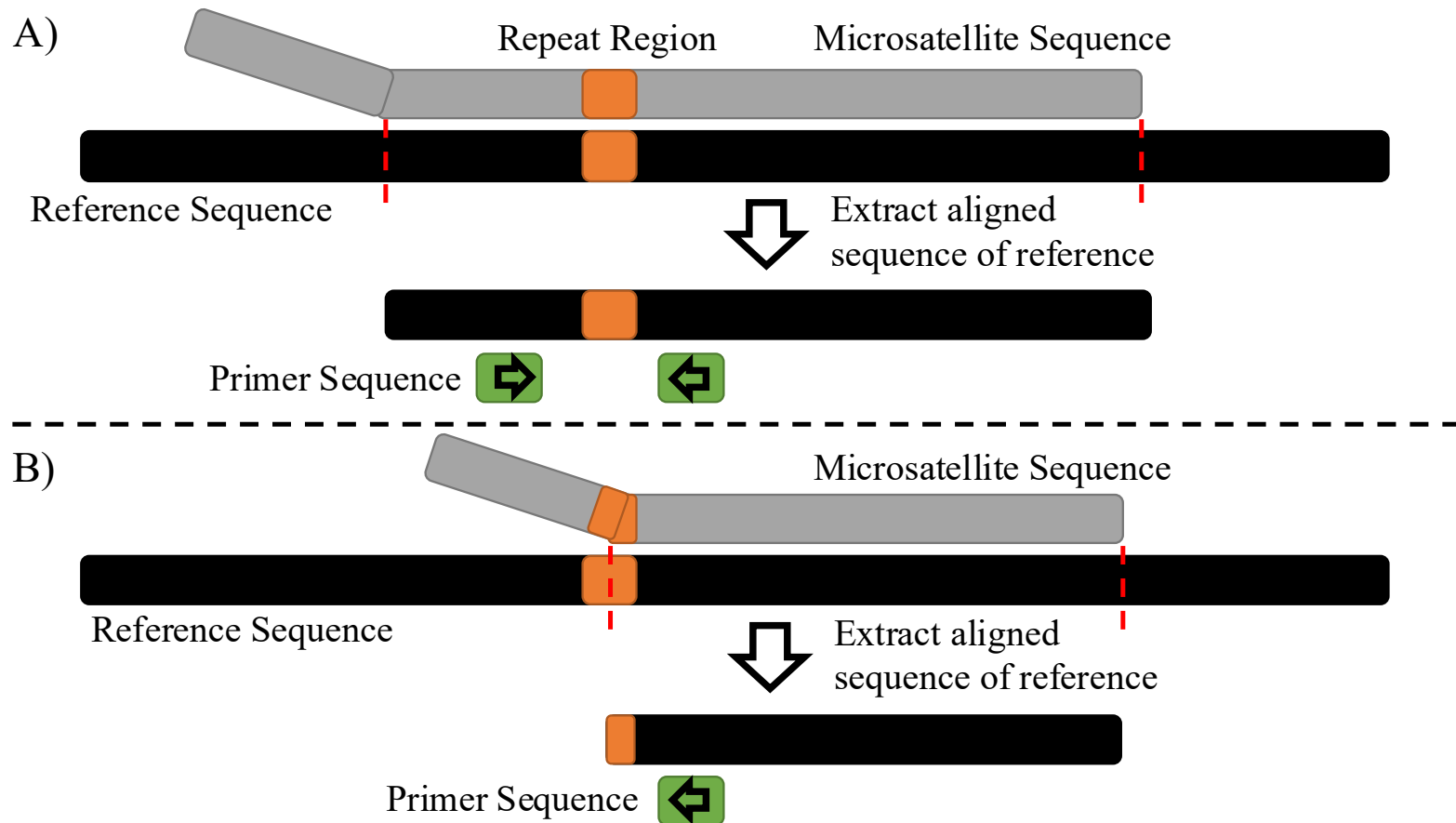


**Figure A.7.** Depiction of the general process for this project. A) Microsatellite sequence (gray) from GenBank accession is aligned to the reference genome (black), with the sequence to which the microsatellite is aligned is then pulled out and used as a reference for the alignment of the primer set (green) for that locus. B) Quite commonly, the microsatellite sequence would break alignment along the repeat region (orange) that the primer set is trying to target. Consequently, only a single primer from the pair could properly align. In these situations, the primer set would be removed from consideration in the final analysis because the complementary primer alignment could not be evaluated.

## References

1. Menge BA, Sutherland JP. Species diversity gradients: synthesis of the roles of predation, competition, and temporal heterogeneity. *Am Nat.* 1976;110(973):351-369. doi:10.1086/283073
2. Chesson P. Mechanisms of maintenance of species diversity. *Annu Rev Ecol Syst.* 2000;31(1):343-366. doi:10.1146/annurev.ecolsys.31.1.343
3. Díaz S, Cabido M. Vive la différence: plant functional diversity matters to ecosystem processes. *Trends Ecol Evol.* 2001;16(11):646-655. doi:10.1016/S0169-5347(01)02283-2
4. Hu G, Jin Y, Liu J, Yu M. Functional diversity versus species diversity: relationships with habitat heterogeneity at multiple scales in a subtropical evergreen broad-leaved forest. *Ecol Res.* 2014;29(5):897-903. doi:10.1007/s11284-014-1178-6
5. Dănescu A, Albrecht AT, Bauhus J. Structural diversity promotes productivity of mixed, uneven-aged forests in southwestern Germany. *Oecologia.* 2016;182(2):319-333. doi:10.1007/s00442-016-3623-4
6. LaRue EA, Hardiman BS, Elliott JM, Fei S. Structural diversity as a predictor of ecosystem function. *Environ Res Lett.* 2019;14(11):114011. doi:10.1088/1748-9326/ab49bb
7. Vega-Álvarez J, García-Rodríguez JA, Cayuela L. Facilitation beyond species richness. Swenson N, ed. *J Ecol.* 2019;107(2):722-734. doi:10.1111/1365-2745.13072
8. Magurran AE, Dornelas M, Moyes F, Henderson PA. Temporal  $\beta$  diversity—a macroecological perspective. Storch D, ed. *Glob Ecol Biogeogr.* 2019;28(12):1949-1960. doi:10.1111/geb.13026
9. Legendre P. A temporal beta-diversity index to identify sites that have changed in exceptional ways in space–time surveys. *Ecol Evol.* 2019;9(6):3500-3514. doi:10.1002/ece3.4984
10. Guzman LM, Thompson PL, Viana DS, et al. Accounting for temporal change in multiple biodiversity patterns improves the inference of metacommunity processes. *Ecology.* 2022;103(6):e3683. doi:10.1002/ecy.3683
11. Peet RK. The measurement of species diversity. *Annu Rev Ecol Syst.* 1974;5(1):285-307. doi:10.1146/annurev.es.05.110174.001441
12. Magurran AE, McGill BJ, eds. *Biological Diversity: Frontiers in Measurement and Assessment.* Oxford University Press; 2011.

13. Whittaker RH. Vegetation of the Siskiyou Mountains, Oregon and California. *Ecol Monogr.* 1960;30(3):279-338. doi:10.2307/1943563
14. Whittaker RH. Evolution and measurement of species diversity. *Taxon.* 1972;21(2-3):213-251. doi:10.2307/1218190
15. Swenson NG. The role of evolutionary processes in producing biodiversity patterns, and the interrelationships between taxonomic, functional and phylogenetic biodiversity. *Am J Bot.* 2011;98(3):472-480. doi:10.3732/ajb.1000289
16. Stroud JT, Bush MR, Ladd MC, Nowicki RJ, Shantz AA, Sweatman J. Is a community still a community? Reviewing definitions of key terms in community ecology. *Ecol Evol.* 2015;5(21):4757-4765. doi:10.1002/ece3.1651
17. Hill MO. Diversity and evenness: a unifying notation and its consequences. *Ecology.* 1973;54(2):427-432. doi:10.2307/1934352
18. Hurlbert SH. The nonconcept of species diversity: a critique and alternative parameters. *Ecology.* 1971;52(4):577-586. doi:10.2307/1934145
19. Chao A, Colwell RK, Chiu C, Townsend D. Seen once or more than once: applying Good–Turing theory to estimate species richness using only unique observations and a species list. Murrell D, ed. *Methods Ecol Evol.* 2017;8(10):1221-1232. doi:10.1111/2041-210X.12768
20. Grünwald NJ, Everhart SE, Knaus BJ, Kamvar ZN. Best practices for population genetic analyses. *Phytopathology*®. 2017;107(9):1000-1010. doi:10.1094/PHYTO-12-16-0425-RVW
21. Alatalo RV. Problems in the measurement of evenness in ecology. *Oikos.* 1981;37(2):199. doi:10.2307/3544465
22. Tuomisto H. An updated consumer’s guide to evenness and related indices. *Oikos.* 2012;121(8):1203-1218. doi:10.1111/j.1600-0706.2011.19897.x
23. Kvålseth TO. Evenness indices once again: critical analysis of properties. *SpringerPlus.* 2015;4(1):232. doi:10.1186/s40064-015-0944-4
24. Pielou EC. The measurement of diversity in different types of biological collections. *J Theor Biol.* 1966;13:131-144. doi:10.1016/0022-5193(66)90013-0
25. Macarthur RH. Patterns of species diversity. *Biol Rev.* 1965;40(4):510-533. doi:10.1111/j.1469-185X.1965.tb00815.x
26. Simpson EH. Measurement of diversity. *Nature.* 1949;163(4148):688-688. doi:10.1038/163688a0

27. Jost L. Entropy and diversity. *Oikos*. 2006;113(2):363-375. doi:10.1111/j.2006.0030-1299.14714.x
28. Bray JR, Curtis JT. An ordination of the upland forest communities of southern Wisconsin. *Ecol Monogr*. 1957;27(4):325-349. doi:10.2307/1942268
29. Leibold MA, Holyoak M, Mouquet N, et al. The metacommunity concept: a framework for multi-scale community ecology. *Ecol Lett*. 2004;7(7):601-613. doi:10.1111/j.1461-0248.2004.00608.x
30. Leibold MA, Chase JM. *Metacommunity Ecology*. Princeton University Press; 2018.
31. Urban MC, Skelly DK. Evolving metacommunities: toward an evolutionary perspective on metacommunities. *Ecology*. 2006;87(7):1616-1626. doi:10.1890/0012-9658(2006)87%5B1616:EMTAEP%5D2.0.CO;2
32. Urban MC, De Meester L. Community monopolization: local adaptation enhances priority effects in an evolving metacommunity. *Proc R Soc B Biol Sci*. 2009;276(1676):4129-4138. doi:10.1098/rspb.2009.1382
33. Alexander HM, Foster BL, Ballantyne F, Collins CD, Antonovics J, Holt RD. Metapopulations and metacommunities: combining spatial and temporal perspectives in plant ecology. *J Ecol*. 2012;100(1):88-103. doi:10.1111/j.1365-2745.2011.01917.x
34. De Meester L, Vanoverbeke J, Kilsdonk LJ, Urban MC. Evolving perspectives on monopolization and priority effects. *Trends Ecol Evol*. 2016;31(2):136-146. doi:10.1016/j.tree.2015.12.009
35. Cuddington K. Legacy effects: the persistent impact of ecological interactions. *Biol Theory*. 2011;6(3):203-210. doi:10.1007/s13752-012-0027-5
36. Busch MH, Allen DC, Marske KA, Kuczynski L. The only lasting truth is change: multiple dimensions of biodiversity show historical legacy effects in community assembly processes of freshwater fish. *Oikos*. 2023;2023(6):e09713. doi:10.1111/oik.09713
37. Bertassello LE, Jawitz JW, Bertuzzo E, et al. Persistence of amphibian metapopulation occupancy in dynamic wetlandscapes. *Landsc Ecol*. 2022;37(3):695-711. doi:10.1007/s10980-022-01400-4
38. Baguette M, Blanchet S, Legrand D, Stevens VM, Turlure C. Individual dispersal, landscape connectivity and ecological networks. *Biol Rev*. 2013;88(2):310-326. doi:10.1111/brv.12000
39. Thompson PL, Rayfield B, Gonzalez A. Loss of habitat and connectivity erodes species diversity, ecosystem functioning, and stability in metacommunity networks. *Ecography*. 2017;40(1):98-108. doi:10.1111/ecog.02558

40. Cosentino BJ, Brubaker KM. Effects of land use legacies and habitat fragmentation on salamander abundance. *Landsc Ecol.* 2018;33(9):1573-1584. doi:10.1007/s10980-018-0686-0
41. Epps CW, Keyghobadi N. Landscape genetics in a changing world: disentangling historical and contemporary influences and inferring change. *Mol Ecol.* 2015;24(24):6021-6040. doi:10.1111/mec.13454
42. Jacquet C, Munoz F, Bonada N, Datry T, Heino J, Jabot F. Disturbance-driven alteration of patch connectivity determines local biodiversity recovery within metacommunities. *Ecography.* 2022;2022(12):e06199. doi:10.1111/ecog.06199
43. Calcagno V, Mouquet N, Jarne P, David P. Coexistence in a metacommunity: the competition–colonization trade-off is not dead. *Ecol Lett.* 2006;9(8):897-907. doi:10.1111/j.1461-0248.2006.00930.x
44. Shoemaker LG, Melbourne BA. Linking metacommunity paradigms to spatial coexistence mechanisms. *Ecology.* 2016;97(9):2436-2446. doi:10.1002/ecy.1454
45. Neiman M, Meirmans S, Meirmans PG. What can asexual lineage age tell us about the maintenance of sex? *Ann N Y Acad Sci.* 2009;1168(1):185-200. doi:10.1111/j.1749-6632.2009.04572.x
46. Neaves WB, Baumann P. Unisexual reproduction among vertebrates. *Trends Genet.* 2011;27(3):81-88. doi:10.1016/j.tig.2010.12.002
47. Choleva L, Janko K. Rise and persistence of animal polyploidy: evolutionary constraints and potential. *Cytogenet Genome Res.* 2013;140(2-4):151-170. doi:10.1159/000353464
48. Lehtonen J, Schmidt DJ, Heubel K, Kokko H. Evolutionary and ecological implications of sexual parasitism. *Trends Ecol Evol.* 2013;28(5):297-306. doi:10.1016/j.tree.2012.12.006
49. Laskowski KL, Doran C, Bierbach D, Krause J, Wolf M. Naturally clonal vertebrates are an untapped resource in ecology and evolution research. *Nat Ecol Evol.* 2019;3(2):161-169. doi:10.1038/s41559-018-0775-0
50. Dalziel AC, Tirbhowan S, Drapeau HF, et al. Using asexual vertebrates to study genome evolution and animal physiology: Banded (*Fundulus diaphanus*) x Common Killifish (*F. heteroclitus*) hybrid lineages as a model system. *Evol Appl.* 2020;13(6):1214-1239. doi:10.1111/eva.12975
51. Janko K, Eisner J. Sperm-dependent parthenogens delay the spatial expansion of their sexual hosts. *J Theor Biol.* 2009;261(3):431-440. doi:10.1016/j.jtbi.2009.08.012

52. Janko K, Eisner J, Mikulíček P. Sperm-dependent asexual hybrids determine competition among sexual species. *Sci Rep*. 2019;9(1):722. doi:10.1038/s41598-018-35167-z
53. Case TJ, Taper ML. On the coexistence and coevolution of asexual and sexual competitors. *Evolution*. 1986;40(2):366. doi:10.2307/2408816
54. Mikulíček P, Kautman M, Demovič B, Janko K. When a clonal genome finds its way back to a sexual species: evidence from ongoing but rare introgression in the hybridogenetic water frog complex. *J Evol Biol*. 2014;27(3):628-642. doi:10.1111/jeb.12332
55. Stenberg P, Saura A. Meiosis and its deviations in polyploid animals. *Cytogenet Genome Res*. 2013;140(2-4):185-203. doi:10.1159/000351731
56. Yin M, Wolinska J, Gießler S. Clonal diversity, clonal persistence and rapid taxon replacement in natural populations of species and hybrids of the *Daphnia longispina* complex. *Mol Ecol*. 2010;19(19):4168-4178. doi:10.1111/j.1365-294X.2010.04807.x
57. Crews D, Young LJ. Pseudocopulation in nature in a unisexual whiptail lizard. *Anim Behav*. 1991;42(3):512-514. doi:10.1016/S0003-3472(05)80056-9
58. Vrijenhoek RC, Angus RA, Schultz RJ. Variation and clonal structure in a unisexual fish. *Am Nat*. 1978;112(983):41-55. doi:10.1086/283251
59. Semlitsch RD. Adaptive genetic variation in growth and development of tadpoles of the hybridogenetic *Rana esculenta* complex. *Evolution*. 1993;47(6):1805-1818. doi:10.1111/j.1558-5646.1993.tb01271.x
60. Janko K, Mikulíček P, Hobza R, Schlupp I. Sperm-dependent asexual species and their role in ecology and evolution. *Ecol Evol*. 2023;13(10):e10522. doi:10.1002/ece3.10522
61. Dries LA. Peering through the looking glass at a sexual parasite: are Amazon mollies red queens? *Evolution*. 2003;57(6):1387-1396. doi:10.1111/j.0014-3820.2003.tb00346.x
62. Meirmans S. The evolution of the problem of sex. In: Schön I, Martens K, Dijk P, eds. *Lost Sex: The Evolutionary Biology of Parthenogenesis*. Springer Netherlands; 2009. doi:10.1007/978-90-481-2770-2
63. Clanton W. An unusual situation in the salamander *Ambystoma jeffersonianum* (Green). *Occas Pap Mus Zool Univ Mich*. 1934;290:1-14.
64. Leung C, Angers B. Imitating the cost of males: a hypothesis for coexistence of all-female sperm-dependent species and their sexual host. *Ecol Evol*. 2018;8(1):266-272. doi:10.1002/ece3.3681

65. Jaenike J, Perlman SJ. Ecology and evolution of host-parasite associations: mycophagous *Drosophila* and their parasitic nematodes. *Am Nat.* 2002;160(S4):S23-S39. doi:10.1086/342137
66. Mideo N. Parasite adaptations to within-host competition. *Trends Parasitol.* 2009;25(6):261-268. doi:10.1016/j.pt.2009.03.001
67. Hatcher MJ, Dunn AM. *Parasites in Ecological Communities: From Interactions to Ecosystems*. Cambridge University Press; 2011.
68. Hatcher MJ, Dick JTA, Dunn AM. Parasites that change predator or prey behaviour can have keystone effects on community composition. *Biol Lett.* 2014;10(1):20130879. doi:10.1098/rsbl.2013.0879
69. Janzen DH. On ecological fitting. *Oikos.* 1985;45(3):308. doi:10.2307/3565565
70. Agosta SJ. On ecological fitting, plant-insect associations, herbivore host shifts, and host plant selection. *Oikos.* 2006;114(3):556-565. doi:10.1111/j.2006.0030-1299.15025.x
71. Araujo SBL, Braga MP, Brooks DR, et al. Understanding host-switching by ecological fitting. Munderloh UG, ed. *PLOS ONE.* 2015;10(10):e0139225. doi:10.1371/journal.pone.0139225
72. Bordes F, Morand S. Parasite diversity: an overlooked metric of parasite pressures? *Oikos.* 2009;118(6):801-806. doi:10.1111/j.1600-0706.2008.17169.x
73. Sures B, Nachev M, Pahl M, Grabner D, Selbach C. Parasites as drivers of key processes in aquatic ecosystems: Facts and future directions. *Exp Parasitol.* 2017;180:141-147. doi:10.1016/j.exppara.2017.03.011
74. Lafferty KD. Biodiversity loss decreases parasite diversity: theory and patterns. *Philos Trans R Soc B Biol Sci.* 2012;367(1604):2814-2827. doi:10.1098/rstb.2012.0110
75. Brian JI, Aldridge DC. Factors at multiple scales drive parasite community structure. *J Anim Ecol.* 2023;92(2):377-390. doi:10.1111/1365-2656.13853
76. Gill DE. The metapopulation ecology of the red-spotted newt, *Notophthalmus viridescens* (Rafinesque). *Ecol Monogr.* 1978;48(2):145-166. doi:10.2307/2937297
77. Start D, Gilbert B. Host-parasitoid evolution in a metacommunity. *Proc R Soc B Biol Sci.* 2016;283(1831):20160477. doi:10.1098/rspb.2016.0477
78. Papkou A, Gokhale CS, Traulsen A, Schulenburg H. Host-parasite coevolution: why changing population size matters. *Zoology.* 2016;119(4):330-338. doi:10.1016/j.zool.2016.02.001

79. Dallas T, Holian LA, Foster G. What determines parasite species richness across host species? Gill J, ed. *J Anim Ecol.* 2020;89(8):1750-1753. doi:10.1111/1365-2656.13276
80. Choleva L, Apostolou A, Ráb P, Janko K. Making it on their own: sperm-dependent hybrid fishes (*Cobitis*) switch the sexual hosts and expand beyond the ranges of their original sperm donors. *Philos Trans R Soc B Biol Sci.* 2008;363(1505):2911-2919. doi:10.1098/rstb.2008.0059
81. Mills PB, Hossie TJ, Murray DL. Niche determinants in a salamander complex: does hybridism or reproductive parasitism explain patterns of distribution? *Ecosphere.* 2020;11(10):e03265. doi:10.1002/ecs2.3265
82. Arioli M, Jakob C, Reyer HU. Genetic diversity in water frog hybrids (*Pelophylax esculentus*) varies with population structure and geographic location. *Mol Ecol.* 2010;19(9):1814-1828. doi:10.1111/j.1365-294X.2010.04603.x
83. Hoffmann A, Plötner J, Pruvost NBM, et al. Genetic diversity and distribution patterns of diploid and polyploid hybrid water frog populations (*Pelophylax esculentus* complex) across Europe. *Mol Ecol.* 2015;24(17):4371-4391. doi:10.1111/mec.13325
84. Waits LP, Storfer A. Basics of population genetics: quantifying neutral and adaptive genetic variation for landscape genetic studies. In: Balkenhol N, Cushman S, Storfer A, Waits L, eds. *Landscape Genetics: Concepts, Methods, Applications*. First ed. John Wiley & Sons Ltd; 2016:35-57.
85. Lande R, Shannon S. The role of genetic variation in adaptation and population persistence in a changing environment. *Evolution.* 1996;50(1):434-437. doi:10.2307/2410812
86. Caballero A, García-Dorado A. Allelic diversity and its implications for the rate of adaptation. *Genetics.* 2013;195(4):1373-1384. doi:10.1534/genetics.113.158410
87. Nunziata SO, Lance SL, Scott DE, Lemmon EM, Weisrock DW. Genomic data detect corresponding signatures of population size change on an ecological time scale in two salamander species. *Mol Ecol.* 2017;26(4):1060-1074. doi:10.1111/mec.13988
88. Antonovics J. The interplay of numerical and gene-frequency dynamics in host-pathogen systems. In: Real L, ed. *Ecological Genetics*. Princeton University Press; 1994:129-145.
89. Johnson PTJ, Hartson RB, Larson DJ, Sutherland DR. Diversity and disease: community structure drives parasite transmission and host fitness. *Ecol Lett.* 2008;11(10):1017-1026. doi:10.1111/j.1461-0248.2008.01212.x

90. Dixo M, Metzger JP, Morgante JS, Zamudio KR. Habitat fragmentation reduces genetic diversity and connectivity among toad populations in the Brazilian Atlantic Coastal Forest. *Biol Conserv.* 2009;142(8):1560-1569. doi:10.1016/j.biocon.2008.11.016
91. Crawford KM, Whitney KD. Population genetic diversity influences colonization success. *Mol Ecol.* 2010;19(6):1253-1263. doi:10.1111/j.1365-294X.2010.04550.x
92. Hughes AR, Inouye BD, Johnson MTJ, Underwood N, Vellend M. Ecological consequences of genetic diversity: ecological effects of genetic diversity. *Ecol Lett.* 2008;11(6):609-623. doi:10.1111/j.1461-0248.2008.01179.x
93. Jost L.  $G_{ST}$  and its relatives do not measure differentiation. *Mol Ecol.* 2008;17(18):4015-4026. doi:10.1111/j.1365-294X.2008.03887.x
94. Real L, ed. *Ecological Genetics*. Princeton University Press; 1994.
95. McLennan EA, Wright BR, Belov K, Hogg CJ, Grueber CE. Too much of a good thing? Finding the most informative genetic data set to answer conservation questions. *Mol Ecol Resour.* 2019;19(3):659-671. doi:10.1111/1755-0998.12997
96. Manel S, Schwartz MK, Luikart G, Taberlet P. Landscape genetics: combining landscape ecology and population genetics. *Trends Ecol Evol.* 2003;18(4):189-197. doi:10.1016/S0169-5347(03)00008-9
97. Balkenhol N, Cushman S, Storfer A, Waits L, eds. *Landscape Genetics: Concepts, Methods, Applications*. First ed. John Wiley & Sons Ltd; 2016.
98. Landguth EL, Cushman SA, Murphy MA, Luikart G. Relationships between migration rates and landscape resistance assessed using individual-based simulations. *Mol Ecol Resour.* 2010;10(5):854-862. doi:10.1111/j.1755-0998.2010.02867.x
99. Richardson JL, Brady SP, Wang IJ, Spear SF. Navigating the pitfalls and promise of landscape genetics. *Mol Ecol.* 2016;25(4):849-863. doi:10.1111/mec.13527
100. Waters JM, Fraser CI, Hewitt GM. Founder takes all: density-dependent processes structure biodiversity. *Trends Ecol Evol.* 2013;28(2):78-85. doi:10.1016/j.tree.2012.08.024
101. Thielsch A, Glass N, Streit B, Meester LD, Ortells R, Schwenk K. Fitness differences and persistent founder effects determine the clonal composition during population build-up in *Daphnia*. *Oikos.* 2015;124(5):620-628. doi:10.1111/oik.01575
102. Badosa A, Frisch D, Green AJ, Rico C, Gómez A. Isolation mediates persistent founder effects on zooplankton colonisation in new temporary ponds. *Sci Rep.* 2017;7(1):43983. doi:10.1038/srep43983

103. Barclay H, Van Den Driessche P. Time lags in ecological systems. *J Theor Biol.* 1975;51(2):347-356. doi:10.1016/0022-5193(75)90065-X
104. Landguth EL, Cushman SA, Schwartz MK, McKelvey KS, Murphy M, Luikart G. Quantifying the lag time to detect barriers in landscape genetics. *Mol Ecol.* 2010;19(19):4179-4191. doi:10.1111/j.1365-294X.2010.04808.x
105. Rastetter EB, Ohman MD, Elliott KJ, et al. Time lags: insights from the U.S. Long Term Ecological Research Network. *Ecosphere.* 2021;12(5):e03431. doi:10.1002/ecs2.3431
106. de Greef E, Müller C, Thorstensen MJ, et al. Unraveling the genetic legacy of commercial whaling and population dynamics in Arctic bowhead whales and narwhals. *Glob Change Biol.* 2024;30(10):e17528. doi:10.1111/gcb.17528
107. Tappeiner U, Leitinger G, Zariņa A, Bürgi M. How to consider history in landscape ecology: patterns, processes, and pathways. *Landsc Ecol.* 2021;36(8):2317-2328. doi:10.1007/s10980-020-01163-w
108. Arnaud-Haond S, Duarte CM, Alberto F, Serrão EA. Standardizing methods to address clonality in population studies. *Mol Ecol.* 2007;16(24):5115-5139. doi:10.1111/j.1365-294X.2007.03535.x
109. Arnaud-Haond S, Alberto F, Teixeira S, Procaccini G, Serrão EA, Duarte CM. Assessing genetic diversity in clonal organisms: low diversity or low resolution? Combining power and cost efficiency in selecting markers. *J Hered.* 2005;96(4):434-440. doi:10.1093/jhered/esi043
110. Halkett F, Simon J, Balloux F. Tackling the population genetics of clonal and partially clonal organisms. *Trends Ecol Evol.* 2005;20(4):194-201. doi:10.1016/j.tree.2005.01.001
111. Arnaud-Haond S, Migliaccio M, Diaz-Almela E, et al. Vicariance patterns in the Mediterranean Sea: east-west cleavage and low dispersal in the endemic seagrass *Posidonia oceanica*. *J Biogeogr.* 2007;34(6):963-976. doi:10.1111/j.1365-2699.2006.01671.x
112. Ellstrand NC, Roose ML. Patterns of genotypic diversity in clonal plant species. *Am J Bot.* 1987;74(1):123-131.
113. Devlin-Durante MK, Miller MW, Caribbean Acropora Research Group, et al. How old are you? Genet age estimates in a clonal animal. *Mol Ecol.* 2016;25(22):5628-5646. doi:10.1111/mec.13865
114. Bona A, Kulesza U, Jadwyszczak KA. Clonal diversity, gene flow and seed production in endangered populations of *Betula humilis* Schrk. *Tree Genet Genomes.* 2019;15(4):50. doi:10.1007/s11295-019-1357-2

115. Gañán-Betancur L, Peever TL, Evans K, Amiri A. High genetic diversity in predominantly clonal populations of the powdery mildew fungus *Podosphaera leucotricha* from U.S. apple orchards. *Appl Environ Microbiol.* 2021;87(15):e00469-21. doi:10.1128/AEM.00469-21
116. Dobrowolski MP, Tommerup IC, Shearer BL, O'Brien PA. Three clonal lineages of *Phytophthora cinnamomi* in Australia revealed by microsatellites. *Phytopathology*®. 2003;93(6):695-704. doi:10.1094/PHYTO.2003.93.6.695
117. Städler T, Frye M, Neiman M, Lively CM. Mitochondrial haplotypes and the New Zealand origin of clonal European *Potamopyrgus*, an invasive aquatic snail. *Mol Ecol.* 2005;14(8):2465-2473. doi:10.1111/j.1365-294X.2005.02603.x
118. Bierbach D, Laskowski KL, Wolf M. Behavioural individuality in clonal fish arises despite near-identical rearing conditions. *Nat Commun.* 2017;8(1):15361. doi:10.1038/ncomms15361
119. da Barbiano LA, Waller J, Gabor CR. Differences in competitive efficiency between a sexual parasite and its host provide insight into the maintenance of a sperm-dependent vertebrate species. *J Freshw Ecol.* 2010;25(4):523-530. doi:10.1080/02705060.2010.9664401
120. Vrijenhoek RC. Ecological differentiation among clones: the frozen niche variation model. In: Wöhrmann K, Loeschke V, eds. *Population Biology and Evolution. Proceedings in Life Sciences.* Springer Berlin Heidelberg; 1984:217-231. doi:10.1007/978-3-642-69646-6\_18
121. Hudson PJ, Dobson AP, Lafferty KD. Is a healthy ecosystem one that is rich in parasites? *Trends Ecol Evol.* 2006;21(7):381-385. doi:10.1016/j.tree.2006.04.007
122. Sessions SK. Cytogenetics of diploid and triploid salamanders of the *Ambystoma jeffersonianum* complex. *Chromosoma.* 1982;84(5):599-621. doi:10.1007/BF00286329
123. Bogart JP. Genetics and systematics of hybrid species. In: Sever DM, ed. *Reproductive Biology and Phylogeny of Urodela.* Vol 1. 1st Ed. Reproductive Biology and Phylogeny. CRC Press; 2003:109-134.
124. Bogart JP, Bi K, Fu J, Noble DWA, Niedzwiecki J. Unisexual salamanders (genus *Ambystoma*) present a new reproductive mode for eukaryotes. Bonen L, ed. *Genome.* 2007;50(2):119-136. doi:10.1139/G06-152
125. Bi K, Bogart JP. Time and time again: unisexual salamanders (genus *Ambystoma*) are the oldest unisexual vertebrates. *BMC Evol Biol.* 2010;10(1):238. doi:10.1186/1471-2148-10-238

126. Bogart JP, Bartoszek J, Noble DWA, Bi K. Sex in unisexual salamanders: discovery of a new sperm donor with ancient affinities. *Heredity*. 2009;103(6):483-493. doi:10.1038/hdy.2009.83
127. Robertson AV, Ramsden C, Niedzwiecki J, Fu J, Bogart JP. An unexpected recent ancestor of unisexual *Ambystoma*. *Mol Ecol*. 2006;15(11):3339-3351. doi:10.1111/j.1365-294X.2006.03005.x
128. Bogart JP. Unisexual salamanders in the genus *Ambystoma*. *Herpetologica*. 2019;75(4):259. doi:10.1655/Herpetologica-D-19-00043.1
129. Lowcock LA, Licht LE, Bogart JP. Nomenclature in hybrid complexes of *Ambystoma* (Urodela: Ambystomatidae): no case for the erection of hybrid “species.” *Syst Zool*. 1987;36(3):328. doi:10.2307/2413070
130. Lowcock LA. Biotype, genomotype, and genotype: variable effects of polyploidy and hybridity on ecological partitioning in a bisexual–unisexual community of salamanders. *Can J Zool*. 1994;72(1):104-117. doi:10.1139/z94-014
131. Bogart JP, Licht LE. Evidence for the requirement of sperm in unisexual salamander hybrids (genus *Ambystoma*). *Can Field-Nat*. 1987;101(1):434-436.
132. Wilbur HM. The ecological relationship of the salamander *Ambystoma laterale* to its all-female, gynogenetic associate. *Evolution*. 1971;25(1):168. doi:10.2307/2406509
133. Bogart JP, Lowcock LA, Zeyl CW, Mable BK. Genome constitution and reproductive biology of hybrid salamanders, genus *Ambystoma*, on Kelleys Island in Lake Erie. *Can J Zool*. 1987;65(9):2188-2201. doi:10.1139/z87-333
134. Bogart JP. A family study to examine clonal diversity in unisexual salamanders (genus *Ambystoma*). Bock DG, ed. *Genome*. 2019;62(8):549-561. doi:10.1139/gen-2019-0034
135. Bi K, Bogart JP, Fu J. The prevalence of genome replacement in unisexual salamanders of the genus *Ambystoma* (Amphibia, Caudata) revealed by nuclear gene genealogy. *BMC Evol Biol*. 2008;8(1):158. doi:10.1186/1471-2148-8-158
136. Beauregard F, Angers B. Influence of genome and bio-ecology on the prevalence of genome exchange in unisexuals of the *Ambystoma* complex. *BMC Evol Biol*. 2018;18(1):82. doi:10.1186/s12862-018-1200-7
137. Bogart JP, Bi K. Genetic and genomic interactions of animals with different ploidy levels. *Cytogenet Genome Res*. 2013;140(2-4):117-136. doi:10.1159/000351593
138. Spolsky C, Phillips CA, Uzzell T. Gynogenetic reproduction in hybrid mole salamanders (genus *Ambystoma*). *Evolution*. 1992;46(6):1935-1944. doi:10.1111/j.1558-5646.1992.tb01179.x

139. Charney ND. Relating hybrid advantage and genome replacement in unisexual salamanders. *Evolution*. 2012;66(5):1387-1397. doi:10.1111/j.1558-5646.2011.01523.x
140. Casto CM. *Survivorship of Ploidy-Variable Unisexual Ambystoma Salamanders across Developmental Stages*. MS thesis. Eastern Michigan University; 2013.
141. Ramsden C, Beriault K, Bogart JP. A nonlethal method of identification of *Ambystoma laterale*, *A. jeffersonianum* and sympatric unisexuals. *Mol Ecol Notes*. 2006;6(1):261-264. doi:10.1111/j.1471-8286.2005.01164.x
142. Bogart JP, Klemens MW. Hybrids and genetic interactions of mole salamanders (*Ambystoma jeffersonianum* and *A. laterale*) (Amphibia: Caudata) in New York and New England. *Am Mus Novit*. 1997;(3218):78.
143. Bogart JP, Klemens MW. Additional distributional records of *Ambystoma laterale*, *A. jeffersonianum* (Amphibia: Caudata) and their unisexual kleptogens in Northeastern North America. *Am Mus Novit*. 2008;3627(1):1. doi:10.1206/604.1
144. Noël S, Labonté P, Lapointe FJ. Genomotype frequencies and genetic diversity in urban and protected populations of blue-spotted salamanders (*Ambystoma laterale*) and related unisexuals. *J Herpetol*. 2011;45(3):294-299. doi:10.1670/09-151.1
145. Charney ND, Ireland AT, Bettencourt BR. Mapping genotype distributions in the unisexual *Ambystoma* complex. *J Herpetol*. 2014;48(2):210-219. doi:10.1670/12-212
146. Greenwald KR, Denton RD, Gibbs HL. Niche partitioning among sexual and unisexual *Ambystoma* salamanders. *Ecosphere*. 2016;7(11):e01579. doi:10.1002/ecs2.1579
147. Ramsden C. Population genetics of *Ambystoma jeffersonianum* and sympatric unisexuals reveal signatures of both gynogenetic and sexual reproduction. *Copeia*. 2008;2008(3):586-594. doi:10.1643/CE-06-280
148. Bogart JP, Linton JE, Sandilands A. A population in limbo: unisexual salamanders (genus *Ambystoma*) decline without sperm-donating species. *Herpetol Conserv Biol*. 2017;12(1):41-55.
149. McElroy KE, Denton RD, Sharbrough J, Bankers L, Neiman M, Gibbs HL. Genome expression balance in a triploid trihybrid vertebrate. *Genome Biol Evol*. 2017;9(4):968-980. doi:10.1093/gbe/evx059
150. Denton RD, Morales AE, Gibbs HL. Genome-specific histories of divergence and introgression between an allopolyploid unisexual salamander lineage and two ancestral sexual species. *Evolution*. 2018;72(8):1689-1700. doi:10.1111/evo.13528

151. Muller HJ. Why polyploidy is rarer in animals than in plants. *Am Nat.* 1925;59(663):346-353. doi:10.1086/280047
152. Muller HJ. The relation of recombination to mutational advance. *Mutat Res Mol Mech Mutagen.* 1964;1(1):2-9. doi:10.1016/0027-5107(64)90047-8
153. Licht LE, Bogart JP. Courtship behavior of *Ambystoma texanum* on Pelee Island, Ontario. *J Herpetol.* 1990;24(4):450. doi:10.2307/1565075
154. Downs FL. Unisexual *Ambystoma* from the Bass Islands of Lake Erie. *Occas Pap Mus Zool Univ Mich.* 1978;Num 685:1-36.
155. Morris MA, Brandon RA. Gynogenesis and hybridization between *Ambystoma platineum* and *Ambystoma texanum* in Illinois. *Copeia.* 1984;1984(2):324. doi:10.2307/1445188
156. Bogart JP, Licht LE. *Update COSEWIC Status Report on the Small-Mouthed Salamander Ambystoma Texanum in Canada in COSEWIC Assessment and Update Status Report on the Small-Mouthed Salamander Ambystoma Texanum in Canada. Committee on the Status of Endangered Wildlife in Canada. Ottawa. 1-20 Pp.* Committee on the Status of Endangered Wildlife in Canada; 2004:1-20 pp.
157. Bare EA, Bogart JP, Wilson C, Murray DL, Hossie TJ. Diversity and composition of mixed-ploidy unisexual salamander assemblages reflect the key influence of host species. *Oecologia.* 2023;202(4):807-818. doi:10.1007/s00442-023-05440-8
158. Bogart JP, Licht LE, Oldham MJ, Darbyshire SJ. Electrophoretic identification of *Ambystoma laterale* and *Ambystoma texanum* as well as their diploid and triploid interspecific hybrids (Amphibia: Caudata) on Pelee Island, Ontario. *Can J Zool.* 1985;63(2):340-347. doi:10.1139/z85-052
159. Petranka JW. *Salamanders of the United States and Canada.* Smithsonian Institution Press; 1998.
160. COSEWIC. *COSEWIC Assessment and Update Status Report on the Small-Mouthed Salamander Ambystoma Texanum in Canada.*; 2004. [www.sararegistry.gc.ca/status/status\\_e.cfm](http://www.sararegistry.gc.ca/status/status_e.cfm)
161. COSEWIC. *COSEWIC Status Appraisal Summary of the Small-Mouthed Salamander Ambystoma Texanum in Canada.* Committee on the Status of Endangered Wildlife in Canada; 2014:x pp. [www.registrelp-sararegistry.gc.ca/default\\_e.cfm](http://www.registrelp-sararegistry.gc.ca/default_e.cfm)
162. COSEWIC. *COSEWIC Assessment and Status Report on the Unisexual Ambystoma, Ambystoma Laterale, Small-Mouthed Salamander-Dependent Population (Ambystoma Laterale - Texanum), Jefferson Salamander-Dependent Population (Ambystoma Laterale - (2) Jeffersonianum), Blue-Spotted Salamander-Dependent Population (Ambystoma (2) Laterale - Jeffersonianum) in Canada.*

- Committee on the Status of Endangered Wildlife in Canada; 2016:xxii + 61 pp.  
[https://publications.gc.ca/collections/collection\\_2017/eccc/CW69-14-730-2016-eng.pdf](https://publications.gc.ca/collections/collection_2017/eccc/CW69-14-730-2016-eng.pdf)
163. Hossie TJ. *Recovery Strategy for Small-Mouthed Salamander (Ambystoma Texanum) and Unisexual Ambystoma Small-Mouthed Salamander Dependent Population (Ambystoma Laterale - Texanum) in Ontario*. Ontario Ministry of Natural Resources and Forestry; 2018:vii + 45 pp.
164. Holcombe TL, Taylor LA, Reid DF, Warren JS, Vincent PA, Herdendorf CE. Revised Lake Erie postglacial lake level history based on new detailed bathymetry. *J Gt Lakes Res.* 2003;29(4):681-704. doi:10.1016/S0380-1330(03)70470-5
165. Herdendorf CE. Research overview: Holocene development of Lake Erie. *Ohio J Sci.* 2013;112(2):24-36.
166. Lewis CFM, Todd BJ. *Offshore Sediments in the Lake Erie Basin, Ontario, Canada, and Michigan, Ohio, Pennsylvania, and New York, U.S.A.*; 2021:8818. doi:10.4095/328829
167. Campbell A. Plan of Point aux Pelée Island. Published online February 26, 1867. Accessed July 27, 2023. <https://recherche-collection-search.bac-lac.gc.ca/eng/Home/Record?app=fonandcol&IdNumber=3670902&q=RG10M%2078903/78%20Pelee%20ISland&ecopy=e008316399-v8>
168. P. D. Salter. Plan of Point Pelee Island. Published online 1847. Accessed July 3, 2025. [https://recherche-collection-search.bac-lac.gc.ca/eng/home/record?app=fonandcol&IdNumber=5235182&q=Pelee+Island+Salter+PD&fbclid=IwAR0mPHWrAoEw\\_0nlT4xwcAgXokV4w9rh8AAupPUE1tHfIHatIokY1TSRCYw&ecopy=e011847648](https://recherche-collection-search.bac-lac.gc.ca/eng/home/record?app=fonandcol&IdNumber=5235182&q=Pelee+Island+Salter+PD&fbclid=IwAR0mPHWrAoEw_0nlT4xwcAgXokV4w9rh8AAupPUE1tHfIHatIokY1TSRCYw&ecopy=e011847648)
169. Smith T. *Point Au Pelee Island - An Historical Sketch of and an Account of the McCormick Family, Who Were the First White Owners of the Island*. The Echo Printing Company; 1899.
170. Tiessen R, ed. *Pelee Island: Guide to a Unique Island Community*. Pelee Island Heritage Centre; 2003.
171. Krutsch DM. Renewing Pelee Island's pumped drainage schemes - a case study. PowerPoint presented at: 42nd Annual Drainage Engineers Conference; 2010.
172. Crosthwaite J. Out with the bad, in with the good: invasive species control and restoration on Pelee Island. PowerPoint presented at: Nature Conservancy Canada; 2019.
173. Nature Conservancy Canada. From marsh to farm and back again: a wetland restoration story. Where We Work: Stories From the Field. June 24, 2023. Accessed April 24, 2024. <https://www.natureconservancy.ca/en/where-we->

work/ontario/stories/pelee-wetland-restoration.html#:~:text=Home%20to%20many%20species%20of,Ontario%27s%20wetlands%20have%20been%20lost.

174. Duncan T, Box PO, Valley C, Brohl L. Flora of the Erie Islands: a review of floristic, ecological and historical research and conservation activities, 1976 – 2010. *Ohio J Sci.* 2011;110(2):3-12.
175. Township of Pelee. *Township of Pelee Official Plan*. Zelinka Priamo LTD.; 2011.
176. Herdendorf CE. *The Ecology of the Coastal Marshes of Western Lake Erie: A Community Profile*. US Department of the Interior, Fish and Wildlife Service; 1987:xi + 171.
177. Hammill E, Hawkins CP, Greig HS, Kratina P, Shurin JB, Atwood TB. Landscape heterogeneity strengthens the relationship between  $\beta$ -diversity and ecosystem function. *Ecology*. 2018;99(11):2467-2475. doi:10.1002/ecy.2492
178. Michalet R, Brooker RW, Cavieres LA, et al. Do biotic interactions shape both sides of the humped-back model of species richness in plant communities? *Ecol Lett.* 2006;9(7):767-773. doi:10.1111/j.1461-0248.2006.00935.x
179. MacArthur RH, MacArthur JW. On bird species diversity. *Ecology*. 1961;42(3):594-598. doi:10.2307/1932254
180. Paine RT. Food web complexity and species diversity. *Am Nat.* 1966;100(910):65-75. doi:10.1086/282400
181. Stachowicz JJ. Mutualism, facilitation, and the structure of ecological communities. *BioScience*. 2001;51(3):235. doi:10.1641/0006-3568(2001)051%5B0235:MFATSO%5D2.0.CO;2
182. Callaway RM, Walker LR. Competition and facilitation: a synthetic approach to interactions in plant communities. *Ecology*. 1997;78(7):1958-1965. doi:10.1890/0012-9658(1997)078%5B1958:CAFASA%5D2.0.CO;2
183. Kamiya T, O'Dwyer K, Nakagawa S, Poulin R. Host diversity drives parasite diversity: meta-analytical insights into patterns and causal mechanisms. *Ecography*. 2014;37(7):689-697. doi:10.1111/j.1600-0587.2013.00571.x
184. Baumeister D, Callaway RM. Facilitation by *Pinus flexilis* during succession: a hierarchy of mechanisms benefits other plant species. *Ecology*. 2006;87(7):1816-1830. doi:10.1890/0012-9658(2006)87%5B1816:FBPFDS%5D2.0.CO;2
185. Cottee-Jones HEW, Whittaker RJ. The keystone species concept: a critical appraisal. *Front Biogeogr.* 2012;4(3):117-127. doi:10.21425/F5FBG12533

186. Krebs CJ. *Ecology: The Experimental Analysis of Distribution and Abundance*. 6. ed. Cummings; 2009.
187. Lindtner P, Šoltis M, Kubovčík V. Translocation of keystone species may not mean translocation of keystone effect. *Eur J Wildl Res*. 2019;65(2):24. doi:10.1007/s10344-019-1261-y
188. Warren RJ, McMillan A, King JR, Chick L, Bradford MA. Forest invader replaces predation but not dispersal services by a keystone species. *Biol Invasions*. 2015;17(11):3153-3162. doi:10.1007/s10530-015-0942-z
189. Davidson AD, Lightfoot DC. Keystone rodent interactions: prairie dogs and kangaroo rats structure the biotic composition of a desertified grassland. *Ecography*. 2006;29(5):755-765. doi:10.1111/j.2006.0906-7590.04699.x
190. Davidson AD, Lightfoot DC. Interactive effects of keystone rodents on the structure of desert grassland arthropod communities. *Ecography*. 2007;30(4):515-525. doi:10.1111/j.2007.0906-7590.05032.x
191. Fahnestock JT, Detling JK. Bison-prairie dog-plant interactions in a North American mixed-grass prairie. *Oecologia*. 2002;132(1):86-95. doi:10.1007/s00442-002-0930-8
192. Helfield JM, Naiman RJ. Keystone interactions: salmon and bear in riparian forests of Alaska. *Ecosystems*. 2006;9(2):167-180. doi:10.1007/s10021-004-0063-5
193. Delibes-Mateos M, Redpath SM, Angulo E, Ferreras P, Villafuerte R. Rabbits as a keystone species in southern Europe. *Biol Conserv*. 2007;137(1):149-156. doi:10.1016/j.biocon.2007.01.024
194. Mackay KD, Gross CL, Rossetto M. Small populations of fig trees offer a keystone food resource and conservation benefits for declining insectivorous birds. *Glob Ecol Conserv*. 2018;14:e00403. doi:10.1016/j.gecco.2018.e00403
195. Bogart JP, Licht LE. Reproduction and the origin of polyploids in hybrid salamanders of the genus *Ambystoma*. *Can J Genet Cytol*. 1986;28(4):605-617. doi:10.1139/g86-089
196. De Queiroz K. Species concepts and species delimitation. *Syst Biol*. 2007;56(6):879-886. doi:10.1080/10635150701701083
197. Owen P, Juterbock J. Unisexual *Ambystoma* salamanders. In: Pfungsten R, Davis J, Matson T, Lipps Jr. G, Wynn D, Armitage, eds. *Amphibians of Ohio*. Vol 17. Ohio Biological Survey Bulletin New Series. Ohio Biological Survey; 2013:175-186.
198. Roche B, Eric Benbow M, Merritt R, et al. Identifying the Achilles heel of multi-host pathogens: the concept of keystone 'host' species illustrated by *Mycobacterium*

- ulcerans* transmission. *Environ Res Lett.* 2013;8(4):045009. doi:10.1088/1748-9326/8/4/045009
199. Kraus F. Unisexual salamander lineages in Northwestern Ohio and Southeastern Michigan: a study of the consequences of hybridization. *Copeia.* 1985;1985(2):309. doi:10.2307/1444840
  200. Ward M, Hossie TJ. Do existing constructed ponds on Pelee Island, Ontario match the habitat requirements of endangered *Ambystoma* larvae? *Wetlands.* 2020;40(6):2097-2108. doi:10.1007/s13157-020-01364-8
  201. Williams PK. *Seasonal Movements and Population Dynamics of Four Sympatric Mole Salamanders, Genus Ambystoma.* PhD Dissertation. Indiana University; 1973.
  202. Ryan KJ, Calhoun AJK. Postbreeding habitat use of the rare, pure-diploid blue-spotted salamander (*Ambystoma laterale*). *J Herpetol.* 2014;48(4):556-566. doi:10.1670/13-204
  203. Semlitsch RD, Bodie JR. Biological criteria for buffer zones around wetlands and riparian habitats for amphibians and reptiles. *Conserv Biol.* 2003;17(5):1219-1228. doi:10.1046/j.1523-1739.2003.02177.x
  204. Van Drunen SG, Linton JE, Bogart JP, et al. Estimating critical habitat based on year-round movements of the endangered Jefferson salamander (*Ambystoma jeffersonianum*) and their unisexual dependents. *Can J Zool.* 2020;98(2):117-126. doi:10.1139/cjz-2019-0228
  205. Denton RD, Greenwald KR, Gibbs HL. Locomotor endurance predicts differences in realized dispersal between sympatric sexual and unisexual salamanders. Higham T, ed. *Funct Ecol.* 2017;31(4):915-926. doi:10.1111/1365-2435.12813
  206. Canadian Herpetofauna Health Working Group. Decontamination protocol for field work with amphibians and reptiles in Canada. Published online 2017. <http://www.cwhc-rccsf.ca/docs/HHWG%20Decontamination%20Protocol%202017-05-30.pdf>
  207. Julian SE, King TL, Savage WK. Novel Jefferson salamander, *Ambystoma jeffersonianum*, microsatellite DNA markers detect population structure and hybrid complexes. *Mol Ecol Notes.* 2003;3(1):95-97. doi:10.1046/j.1471-8286.2003.00362.x
  208. Peterman WE, Connette GM, Spatola BN, Eggert LS, Semlitsch RD. Identification of polymorphic loci in *Ambystoma annulatum* and review of cross-species microsatellite use in the genus *Ambystoma*. *Copeia.* 2012;2012(3):570-577. doi:10.1643/CH-11-001.short
  209. Williams RN, DeWoody JA. Fluorescent dUTP helps characterize 10 novel tetranucleotide microsatellites from an enriched salamander (*Ambystoma texanum*)

- genomic library. *Mol Ecol Notes*. 2003;4(1):17-19. doi:10.1046/j.1471-8286.2003.00559.x
210. Julian SE, King TL, Savage WK. Isolation and characterization of novel tetranucleotide microsatellite DNA markers for the spotted salamander, *Ambystoma maculatum*. *Mol Ecol Notes*. 2002;3(1):7-9. doi:10.1046/j.1471-8286.2003.00333.x
211. Savage WK. Microsatellite loci for the critically endangered Santa Cruz long-toed salamander (*Ambystoma macrodactylum croceum*) and other *Ambystoma* taxa. *Conserv Genet*. 2009;10(3):619-622. doi:10.1007/s10592-008-9591-4
212. R Core Team. R: A language and environment for statistical computing. Published online 2023. <https://www.R-project.org/>
213. Kamvar ZN, Tabima JF, Grünwald NJ. POPPR: an R package for genetic analysis of populations with clonal, partially clonal, and/or sexual reproduction. *PeerJ*. 2014;2:e281. doi:10.7717/peerj.281
214. Kamvar ZN, Brooks JC, Grünwald NJ. Novel R tools for analysis of genome-wide population genetic data with emphasis on clonality. *Front Genet*. 2015;6. doi:10.3389/fgene.2015.00208
215. Oksanen A, Blanchet F, Friendly M, et al. VEGAN: community ecology package. Published online 2020.
216. Dray S, Dufour AB. The ADE4 package: implementing the duality diagram for ecologists. *J Stat Softw*. 2007;22(4). doi:10.18637/jss.v022.i04
217. Bogart JP, Elinson RP, Licht LE. Temperature and sperm incorporation in polyploid salamanders. *Science*. 1989;246(4933):1032-1034. doi:10.1126/science.2587986
218. Smith G. *Assessing Habitat Suitability and Connectivity for an Endangered Salamander Complex*. MS thesis. Trent University; 2022.
219. Teltser C, Greenwald KR. Survivorship of ploidy-variable unisexual *Ambystoma* salamanders across developmental stages. *Herpetologica*. 2015;71(2):81-87. doi:10.1655/HERPETOLOGICA-D-14-00007
220. Lowcock LA, Murphy RW. Pentaploidy in hybrid salamanders demonstrates enhanced tolerance of multiple chromosome sets. *Experientia*. 1991;47(5):490-493. doi:10.1007/BF01959952
221. Turner MG. Landscape ecology: the effect of pattern on process. *Annu Rev Ecol Syst*. 1989;20:171-197. doi:10.1146/annurev.es.20.110189.001131
222. Albertson LK, Sklar LS, Tumolo BB, Cross WF, Collins SF, Woods HA. The ghosts of ecosystem engineers: legacy effects of biogenic modifications. *Funct Ecol*. 2024;38(1):52-72. doi:10.1111/1365-2435.14222

223. Fenderson LE, Kovach AI, Llamas B. Spatiotemporal landscape genetics: investigating ecology and evolution through space and time. *Mol Ecol*. 2020;29(2):218-246. doi:10.1111/mec.15315
224. Barel JM, Kuyper TW, de Boer W, Douma JC, De Deyn GB. Legacy effects of diversity in space and time driven by winter cover crop biomass and nitrogen concentration. *J Appl Ecol*. 2018;55(1):299-310. doi:10.1111/1365-2664.12929
225. Shumi G, Schultner J, Dorresteijn I, et al. Land use legacy effects on woody vegetation in agricultural landscapes of south-western Ethiopia. *Divers Distrib*. 2018;24(8):1136-1148. doi:10.1111/ddi.12754
226. Hewitt G. The genetic legacy of the Quaternary ice ages. *Nature*. 2000;405(6789):907-913. doi:10.1038/35016000
227. Cavender-Bares J, Ackerly DD, Hobbie SE, Townsend PA. Evolutionary legacy effects on ecosystems: biogeographic origins, plant traits, and implications for management in the era of global change. *Annu Rev Ecol Evol Syst*. 2016;47(1):433-462. doi:10.1146/annurev-ecolsys-121415-032229
228. Mouquet N, Matthiessen B, Miller T, Gonzalez A. Extinction debt in source-sink metacommunities. *PLoS ONE*. 2011;6(3):e17567. doi:10.1371/journal.pone.0017567
229. Haddou Y, Mancy R, Matthiopoulos J, Spatharis S, Dominoni DM. Widespread extinction debts and colonization credits in United States breeding bird communities. *Nat Ecol Evol*. 2022;6(3):324-331. doi:10.1038/s41559-021-01653-3
230. Gargiulo R, Budde KB, Heuertz M. Mind the lag: understanding genetic extinction debt for conservation. *Trends Ecol Evol*. 2025;40(3):228-237. doi:10.1016/j.tree.2024.10.008
231. Janssen P, Bec S, Fuhr M, Taberlet P, Brun J, Bouget C. Present conditions may mediate the legacy effect of past land-use changes on species richness and composition of above- and below-ground assemblages. *J Ecol*. 2018;106(1):306-318. doi:10.1111/1365-2745.12808
232. Essl F, Dullinger S, Rabitsch W, et al. Historical legacies accumulate to shape future biodiversity in an era of rapid global change. *Divers Distrib*. 2015;21(5):534-547. doi:10.1111/ddi.12312
233. Reinula I, Träger S, Järvinen HT, Kuningas VM, Kaldra M, Aavik T. Beware of the impact of land use legacy on genetic connectivity: a case study of the long-lived perennial *Primula veris*. *Biol Conserv*. 2024;292:110518. doi:10.1016/j.biocon.2024.110518

234. Miller AD, Inamine H, Buckling A, Roxburgh SH, Shea K. How disturbance history alters invasion success: biotic legacies and regime change. *Ecol Lett.* 2021;24(4):687-697. doi:10.1111/ele.13685
235. Lenz L. Seed dispersal in *Yucca brevifolia* (Agavaceae) - present and past, with consideration of the future of the species. *Aliso.* 2001;20(2):61-74. doi:10.5642/aliso.20012002.03
236. Hedges SB, Bogart JP, Maxson LR. Ancestry of unisexual salamanders. *Nature.* 1992;356(6371):708-710. doi:10.1038/356708a0
237. Clark LV, Jasieniuk M. POLYSAT: an R package for polyploid microsatellite analysis. *Mol Ecol Resour.* 2011;11(3):562-566. doi:10.1111/j.1755-0998.2011.02985.x
238. Tal Galili. DENDEXTEND: an R package for visualizing, adjusting, and comparing trees of hierarchical clustering. *Bioinformatics.* 2015;31(22):3718-3720. doi:10.1093/bioinformatics/btv428
239. Chao A, Gotelli NJ, Hsieh TC, et al. Rarefaction and extrapolation with Hill numbers: a framework for sampling and estimation in species diversity studies. *Ecol Monogr.* 2014;84(1):45-67. doi:10.1890/13-0133.1
240. Hsieh TC, Ma KH, Chao A. iNEXT: an R package for rarefaction and extrapolation of species diversity (Hill numbers). *Methods Ecol Evol.* 2016;7(12):1451-1456. doi:10.1111/2041-210X.12613
241. Dorken ME, Eckert CG. Severely reduced sexual reproduction in northern populations of a clonal plant, *Decodon verticillatus* (Lythraceae). *J Ecol.* 2001;89:339-350. doi:10.1046/j.1365-2745.2001.00558.x
242. Pebesma E. Simple features for R: standardized support for spatial vector data. *R J.* 2018;10(1):439. doi:10.32614/RJ-2018-009
243. Anderson DR, Burnham KP. Avoiding pitfalls when using information - theoretic methods. *J Wildl Manag.* 2002;66(3):912-918. doi:10.2307/3803155
244. Burnham KP, Anderson DR, eds. *Model Selection and Multimodel Inference.* Springer New York; 2004. doi:10.1007/b97636
245. Kassambara A, Mundt F. FACTOEXTRA: extract and visualize the results of multivariate data analyses. Published online 2020. <https://CRAN.R-project.org/package=factoextra>
246. Paradis E, Schliep K. APE 5.0: an environment for modern phylogenetics and evolutionary analyses in R. *Bioinformatics.* 2019;35(3):526-528. doi:10.1093/bioinformatics/bty633

247. Sundqvist L, Keenan K, Zackrisson M, Prodöhl P, Kleinhans D. Directional genetic differentiation and relative migration. *Ecol Evol.* 2016;6(11):3461-3475. doi:10.1002/ece3.2096
248. Keenan K, McGinnity P, Cross TF, Crozier WW, Prodöhl PA. DIVERSITY: An R package for the estimation and exploration of population genetics parameters and their associated errors. *Methods Ecol Evol.* 2013;4(8):782-788. doi:10.1111/2041-210X.12067
249. Kling MM, Ackerly DD. Global wind patterns shape genetic differentiation, asymmetric gene flow, and genetic diversity in trees. *Proc Natl Acad Sci.* 2021;118(17):e2017317118. doi:10.1073/pnas.2017317118
250. Angers B, Schlosser IJ. The origin of *Phoxinus eos-neogaeus* unisexual hybrids. *Mol Ecol.* 2007;16(21):4562-4571. doi:10.1111/j.1365-294X.2007.03511.x
251. Janko K, Culling MA, Ráb P, Kotlík P. Ice age cloning – comparison of the Quaternary evolutionary histories of sexual and clonal forms of spiny loaches (*Cobitis*; Teleostei) using the analysis of mitochondrial DNA variation. *Mol Ecol.* 2005;14(10):2991-3004. doi:10.1111/j.1365-294X.2005.02583.x
252. Pigneur L, Etoundi E, Aldridge DC, Marescaux J, Yasuda N, Van Doninck K. Genetic uniformity and long-distance clonal dispersal in the invasive androgenetic *Corbicula* clams. *Mol Ecol.* 2014;23(20):5102-5116. doi:10.1111/mec.12912
253. Haag CR, Riek M, Hottinger JW, Pajunen VI, Ebert D. Founder events as determinants of within-island and among-island genetic structure of *Daphnia* metapopulations. *Heredity.* 2006;96(2):150-158. doi:10.1038/sj.hdy.6800774
254. Flanagan BA, Krueger-Hadfield SA, Murren CJ, Nice CC, Strand AE, Sotka EE. Founder effects shape linkage disequilibrium and genomic diversity of a partially clonal invader. *Mol Ecol.* 2021;30(9):1962-1978. doi:10.1111/mec.15854
255. Riley SPD, Bradley Shaffer H, Randal Voss S, Fitzpatrick BM. Hybridization between a rare, native tiger salamander (*Ambystoma californiense*) and its introduced congener. *Ecol Appl.* 2003;13(5):1263-1275. doi:10.1890/02-5023
256. Fitzpatrick BM, Shaffer HB. Hybrid vigor between native and introduced salamanders raises new challenges for conservation. *Proc Natl Acad Sci.* 2007;104(40):15793-15798. doi:10.1073/pnas.0704791104
257. Ventura M, Petrusek A, Miró A, et al. Local and regional founder effects in lake zooplankton persist after thousands of years despite high dispersal potential. *Mol Ecol.* 2014;23(5):1014-1027. doi:10.1111/mec.12656
258. Van Der Merwe M, Spain CS, Rossetto M. Enhancing the survival and expansion potential of a founder population through clonality. *New Phytol.* 2010;188(3):868-878. doi:10.1111/j.1469-8137.2010.03396.x

259. Canestrelli D, Sacco F, Nascetti G. On glacial refugia, genetic diversity, and microevolutionary processes: deep phylogeographical structure in the endemic newt *Lissotriton italicus*. *Biol J Linn Soc.* 2012;105(1):42-55. doi:10.1111/j.1095-8312.2011.01767.x
260. Shafer ABA, Cullingham CI, Côté SD, Coltman DW. Of glaciers and refugia: a decade of study sheds new light on the phylogeography of northwestern North America. *Mol Ecol.* 2010;19(21):4589-4621. doi:10.1111/j.1365-294X.2010.04828.x
261. Cunha C, Doadrio I, Abrantes J, Coelho MM. The evolutionary history of the allopolyploid *Squalius alburnoides* (Cyprinidae) complex in the northern Iberian Peninsula. *Heredity.* 2011;106(1):100-112. doi:10.1038/hdy.2010.70
262. Janko K, Kotusz J, De Gelas K, et al. Dynamic formation of asexual diploid and polyploid lineages: multilocus analysis of *Cobitis* reveals the mechanisms maintaining the diversity of clones. *PLoS ONE.* 2012;7(9):e45384. doi:10.1371/journal.pone.0045384
263. Pereyra RT, Rafajlović M, De Wit P, et al. Clones on the run: the genomics of a recently expanded partially clonal species. *Mol Ecol.* 2023;32(15):4209-4223. doi:10.1111/mec.16996
264. Bi K, Bogart JP, Fu J. Genealogical relationships of southern Ontario polyploid unisexual salamanders (genus *Ambystoma*) inferred from intergenomic exchanges and major rDNA cytotypes. *Chromosome Res.* 2008;16(2):275-289. doi:10.1007/s10577-007-1192-4
265. Taylor AS. Reconstitution of diploid *Ambystoma jeffersonianum* (Amphibia: Caudata) in a hybrid, triploid egg mass with lethal consequences. *J Hered.* 1992;83(5):361-366. doi:10.1093/oxfordjournals.jhered.a111232
266. Bi K, Bogart JP. Identification of intergenomic recombinations in unisexual salamanders of the genus *Ambystoma* by genomic in situ hybridization (GISH). *Cytogenet Genome Res.* 2006;112(3-4):307-312. doi:10.1159/000089885
267. Charney ND, Kubel JE, Woodard CT, et al. Survival of polyploid hybrid salamander embryos. *BMC Dev Biol.* 2019;19(1):21. doi:10.1186/s12861-019-0202-z
268. Licht LE, Bogart JP. Comparative size of epidermal cell nuclei from shed skin of diploid, triploid and tetraploid salamanders (genus *Ambystoma*). *Copeia.* 1987;1987(2):284. doi:10.2307/1445763
269. Licht LE, Bogart JP. Growth and sexual maturation in diploid and polyploid salamanders (genus *Ambystoma*). *Can J Zool.* 1989;67(4):812-818. doi:10.1139/z89-119

270. Pekár S, Šmerda J, Hrušková M, et al. Prey-race drives differentiation of biotypes in ant-eating spiders. *J Anim Ecol.* 2012;81(4):838-848. doi:10.1111/j.1365-2656.2012.01957.x
271. Chu D, Tao Y, Zhang Y, Wan F, Brown JK. Effects of host, temperature and relative humidity on competitive displacement of two invasive *Bemisia tabaci* biotypes [Q and B]. *Insect Sci.* 2012;19(5):595-603. doi:10.1111/j.1744-7917.2011.01500.x
272. Burger IJ, Itgen M, Tan L, et al. Genome composition predicts physiological responses to temperature in polyploid salamanders. *Am Nat.* Published online May 19, 2025:736728. doi:10.1086/736728
273. Bartoš O, Röslein J, Kotusz J, et al. The legacy of sexual ancestors in phenotypic variability, gene expression, and homoeolog regulation of asexual hybrids and polyploids. *Mol Biol Evol.* 2019;36(9):1902-1920. doi:10.1093/molbev/msz114
274. Som C, Anholt BR, Reyer HU. The effect of assortative mating on the coexistence of a hybridogenetic waterfrog and its sexual host. *Am Nat.* 2000;156(1):34-46. doi:10.1086/303372
275. Som C, Reyer HU. Demography and evolution of pure hybridogenetic frog (*Rana esculenta*) populations. *Evol Ecol Res.* 2006;8:1235-1248.
276. Hoffmann A, Abt Tietje G, Reyer HU. Spatial behavior in relation to mating systems: movement patterns, nearest-neighbor distances, and mating success in diploid and polyploid frog hybrids (*Pelophylax esculentus*). *Behav Ecol Sociobiol.* 2015;69(3):501-517. doi:10.1007/s00265-014-1862-0
277. Muller HJ. Some genetic aspects of sex. *Am Nat.* 1932;66(703):118-138. doi:10.1086/280418
278. Otto SP. The evolutionary consequences of polyploidy. *Cell.* 2007;131(3):452-462. doi:10.1016/j.cell.2007.10.022
279. Soltis DE, Visger CJ, Marchant DB, Soltis PS. Polyploidy: pitfalls and paths to a paradigm. *Am J Bot.* 2016;103(7):1146-1166. doi:10.3732/ajb.1500501
280. Som C, Reyer HU. Hemiclonal reproduction slows down the speed of Muller's ratchet in the hybridogenetic frog *Rana esculenta*. *J Evol Biol.* 2007;20(2):650-660. doi:10.1111/j.1420-9101.2006.01243.x
281. Sclavi B, Herrick J. Genome size variation and species diversity in salamanders. *J Evol Biol.* 2019;32(3):278-286. doi:10.1111/jeb.13412
282. Weisrock DW, Hime PM, Nunziata SO, et al. Surmounting the large-genome "problem" for genomic data generation in salamanders. In: Hohenlohe PA, Rajora OP, eds. *Population Genomics: Wildlife*. Population Genomics. Springer International Publishing; 2018:115-142. doi:10.1007/13836\_2018\_36

283. France J, Babik W, Dudek K, Marszałek M, Wielstra B. Linkage mapping vs association: a comparison of two RADseq-based approaches to identify markers for homomorphic sex chromosomes in large genomes. Preprint posted online July 19, 2024. doi:10.22541/au.172137196.69932431/v1
284. Amaya E, Offield MF, Grainger RM. Frog genetics: *Xenopus tropicalis* jumps into the future. *Trends Genet.* 1998;14(7):253-255. doi:10.1016/S0168-9525(98)01506-6
285. Benbassat J. The transition from tadpole to frog haemoglobin during natural amphibian metamorphosis: i. protein synthesis by peripheral blood cells *in vitro*. *J Cell Sci.* 1974;15(2):347-357. doi:10.1242/jcs.15.2.347
286. Fankhauser G. Cell size, organ and body size in triploid newts (*Triturus viridescens*). *J Morphol.* 1941;68(1):161-177. doi:10.1002/jmor.1050680109
287. Fankhauser G. Nucleo-cytoplasmic relations in amphibian development. In: *International Review of Cytology*. Vol 1. Academic Press; 1952:165-193. doi:10.1016/S0074-7696(08)60010-8
288. Fankhauser G. The effects of changes in chromosome number on amphibian development. *Q Rev Biol.* 1945;20(1):20-78. doi:10.1086/394703
289. Fankhauser G, Vernon JA, Frank WH, Slack WV. Effect of size and number of brain cells on learning in larvae of the salamander, *Triturus viridescens*. *Science.* 1955;122(3172):692-693. doi:10.1126/science.122.3172.692
290. Licht LE, Bogart JP. Ploidy and developmental rate in a salamander hybrid complex (genus *Ambystoma*). *Evolution.* 1987;41(4):918. doi:10.2307/2408901
291. Rowe CL, Dunson WA. Impacts of hydroperiod on growth and survival of larval amphibians in temporary ponds of Central Pennsylvania, USA. *Oecologia.* 1995;102(4):397-403. doi:10.1007/BF00341351
292. Ryan TJ. Hydroperiod and metamorphosis in small-mouthed salamanders (*Ambystoma texanum*). *Northeast Nat.* 2007;14(4):619-628. doi:10.1656/1092-6194(2007)14%5B619:HAMISS%5D2.0.CO;2
293. Agosta SJ, Klemens JA. Ecological fitting by phenotypically flexible genotypes: implications for species associations, community assembly and evolution. *Ecol Lett.* 2008;11(11):1123-1134. doi:10.1111/j.1461-0248.2008.01237.x
294. Christiansen DG, Jakob C, Arioli M, Roethlisberger S, Reyer HU. Coexistence of diploid and triploid hybrid water frogs: population differences persist in the apparent absence of differential survival. *BMC Ecol.* 2010;10(1):14. doi:10.1186/1472-6785-10-14

295. Pruvost NBM, Mikulíček P, Choleva L, Reyer H -U. Contrasting reproductive strategies of triploid hybrid males in vertebrate mating systems. *J Evol Biol.* 2015;28(1):189-204. doi:10.1111/jeb.12556
296. Dedukh D, Riumin S, Kolenda K, et al. Maintenance of pure hybridogenetic water frog populations: genotypic variability in progeny of diploid and triploid parents. Sharakhov IV, ed. *PLOS ONE.* 2022;17(7):e0268574. doi:10.1371/journal.pone.0268574
297. ORAA. *Ontario Reptile and Amphibian Atlas Publication.* Ontario Nature; 2023.
298. Morales HE, Pavlova A, Joseph L, Sunnucks P. Positive and purifying selection in mitochondrial genomes of a bird with mitonuclear discordance. *Mol Ecol.* 2015;24(11):2820-2837. doi:10.1111/mec.13203
299. Greenwald K, Stedman A, Mifsud D, et al. Phylogeographic analysis of mudpuppies (*Necturus maculosus*). *J Herpetol.* 2020;54(1):78. doi:10.1670/19-070
300. Zamudio KR, Savage WK. Historical isolation, range expansion, and secondary contact of two highly divergent mitochondrial lineages in spotted salamanders (*Ambystoma maculatum*). *Evolution.* 2003;57(7):1631-1652. doi:10.1111/j.0014-3820.2003.tb00370.x
301. White MJD. *Modes of Speciation.* Freeman; 1978.
302. Uzzell T, Darevsky IS. Biochemical evidence for the hybrid origin of the parthenogenetic species of the *Lacerta saxicola* complex (Sauria: Lacertidae), with a discussion of some ecological and evolutionary implications. *Copeia.* 1975;1975(2):204. doi:10.2307/1442879
303. Arioli M. *Reproductive Patterns and Population Genetics in Pure Hybridogenetic Water Frog Populations of Rana Esculenta.* PhD Dissertation. University of Zurich; 2007. doi:10.5167/UZH-163641
304. Alves MJ, Coelho MM, Collares-Pereira MJ. Evolution in action through hybridisation and polyploidy in an Iberian freshwater fish: a genetic review. *Genetica.* 2001;111:375-385.
305. Storfer A, Murphy MA, Evans JS, et al. Putting the 'landscape' in landscape genetics. *Heredity.* 2007;98(3):128-142. doi:10.1038/sj.hdy.6800917
306. Manel S, Holderegger R. Ten years of landscape genetics. *Trends Ecol Evol.* 2013;28(10):614-621. doi:10.1016/j.tree.2013.05.012
307. Wang IJ. Recognizing the temporal distinctions between landscape genetics and phylogeography. *Mol Ecol.* 2010;19(13):2605-2608. doi:10.1111/j.1365-294X.2010.04715.x

308. Collares-Pereira MJ, Coelho MM. Reconfirming the hybrid origin and generic status of the Iberian cyprinid complex *Squalius alburnoides*. *J Fish Biol.* 2010;76(3):707-715. doi:10.1111/j.1095-8649.2009.02460.x
309. Becheler R, Diekmann O, Hily C, Moalic Y, Arnaud-Haond S. The concept of population in clonal organisms: mosaics of temporally colonized patches are forming highly diverse meadows of *Zostera marina* in Brittany. *Mol Ecol.* 2010;19:2394-2407. doi:10.1111/j.1365-294X.2010.04649.x
310. Vandvik V, Goldberg DE. Sources of diversity in a grassland metacommunity: quantifying the contribution of dispersal to species richness. *Am Nat.* 2006;168(2):157-167. doi:10.1086/505759
311. McMahon KM, Evans RD, Van Dijk K Jent, et al. Disturbance is an important driver of clonal richness in tropical seagrasses. *Front Plant Sci.* 2017;8:2026. doi:10.3389/fpls.2017.02026
312. Snyder RE. How demographic stochasticity can slow biological invasions. *Ecology.* 2003;84(5):1333-1339. doi:10.1890/0012-9658(2003)084%5B1333:HDSCSB%5D2.0.CO;2
313. Boileau MG, Hebert PDN, Schwartz SS. Non-equilibrium gene frequency divergence: persistent founder effects in natural populations. *J Evol Biol.* 1992;5(1):25-39. doi:10.1046/j.1420-9101.1992.5010025.x
314. Vrijenhoek RC. Genetic and ecological consequences on the origins and establishment of unisexual vertebrates. In: Dawley RM, Bogart JP, eds. *Evolution and Ecology of Unisexual Vertebrates*. 1989:24-31.
315. Elder JF, Schlosser IJ. Extreme clonal uniformity of *Phoxinus eos/neogaeus* gynogens (Pisces: Cyprinidae) among variable habitats in northern Minnesota beaver ponds. *Proc Natl Acad Sci.* 1995;92(11):5001-5005. doi:10.1073/pnas.92.11.5001
316. Minton SAJr. Salamanders of the *Ambystoma jeffersonianum* complex in Indiana. *Herpetologica.* 1954;10(3):173-179.
317. Bishop SC. *The Salamanders of New York*. University of the State of New York; 1941.
318. Ives AR, Carpenter SR. Stability and diversity of ecosystems. *Science.* 2007;317(5834):58-62. doi:10.1126/science.1133258
319. Donohue I, Hillebrand H, Montoya JM, et al. Navigating the complexity of ecological stability. *Ecol Lett.* 2016;19(9):1172-1185. doi:10.1111/ele.12648

320. Stöck M, Lampert KP, Möller D, Schlupp I, Scharl M. Monophyletic origin of multiple clonal lineages in an asexual fish (*Poecilia formosa*). *Mol Ecol*. 2010;19(23):5204-5215. doi:10.1111/j.1365-294X.2010.04869.x
321. Quattro JM, Avise JC, Vrijenhoek RC. An ancient clonal lineage in the fish genus *Poeciliopsis* (Atheriniformes: Poeciliidae). *Proc Natl Acad Sci*. 1992;89(1):348-352. doi:10.1073/pnas.89.1.348
322. Avise JC. *Clonality: The Genetics, Ecology, and Evolution of Sexual Abstinence in Vertebrate Animals*. Oxford University Press; 2008.
323. Chapman HM, Parh D, Oraguzie N. Genetic structure and colonizing success of a clonal, weedy species, *Pilosella officinarum* (Asteraceae). *Heredity*. 2000;84:401-409.
324. Quattro JM, Avise JC, Vrijenhoek RC. Molecular evidence for multiple origins of hybridogenetic fish clones (Poeciliidae: *Poeciliopsis*). *Genetics*. 1991;127(2):391-398. doi:10.1093/genetics/127.2.391
325. Wilson ACC, Sunnucks P, Hales DF. Microevolution, low clonal diversity and genetic affinities of parthenogenetic *Sitobion* aphids in New Zealand. *Mol Ecol*. 1999;8(10):1655-1666. doi:10.1046/j.1365-294x.1999.00751.x
326. Bi K, Bogart JP, Fu J. An examination of intergenomic exchanges in *A. laterale*-dependent unisexual salamanders in the genus *Ambystoma*. *Cytogenet Genome Res*. 2009;124(1):44-50. doi:10.1159/000200087
327. Rissler LJ. Union of phylogeography and landscape genetics. *Proc Natl Acad Sci*. 2016;113(29):8079-8086. doi:10.1073/pnas.1601073113
328. Bi K, Bogart JP, Fu J. Two rare aneutriploids in the unisexual *Ambystoma* (Amphibia, Caudata) identified by GISH indicating two different types of meiotic errors. *Cytogenet Genome Res*. 2007;119(1-2):127-130. doi:10.1159/000109628
329. Greenwald KR, Lisle Gibbs H. A single nucleotide polymorphism assay for the identification of unisexual *Ambystoma* salamanders. *Mol Ecol Resour*. 2012;12(2):354-362. doi:10.1111/j.1755-0998.2011.03087.x
330. Wenne R. Microsatellites as molecular markers with applications in exploitation and conservation of aquatic animal populations. *Genes*. 2023;14(4):808. doi:10.3390/genes14040808
331. Smith JJ, Timoshevskaya N, Timoshevskiy VA, Keinath MC, Hardy D, Voss SR. A chromosome-scale assembly of the axolotl genome. *Genome Res*. 2019;29(2):317-324. doi:10.1101/gr.241901.118
332. Fu YX, Li WH. Coalescing into the 21st Century: an overview and prospects of coalescent theory. *Theor Popul Biol*. 1999;56(1):1-10. doi:10.1006/tpbi.1999.1421

333. Rosenberg NA, Nordborg M. Genealogical trees, coalescent theory and the analysis of genetic polymorphisms. *Nat Rev Genet.* 2002;3(5):380-390. doi:10.1038/nrg795
334. Williams JS, Niedzwiecki JH, Weisrock DW. Species tree reconstruction of a poorly resolved clade of salamanders (Ambystomatidae) using multiple nuclear loci. *Mol Phylogenet Evol.* 2013;68(3):671-682. doi:10.1016/j.ympev.2013.04.013
335. Mollinari M, Garcia AAF. Linkage analysis and haplotype phasing in experimental autopolyploid populations with high ploidy level using hidden Markov models. *G3 GenesGenomesGenetics.* 2019;9(10):3297-3314. doi:10/gsn7hc
336. Kirungu J, Deng Y, Cai X, et al. Simple sequence repeat (SSR) genetic linkage map of D genome diploid cotton derived from an interspecific cross between *Gossypium davidsonii* and *Gossypium klotzschianum*. *Int J Mol Sci.* 2018;19(1):204. doi:10/gc5jx3
337. Lampert KP, Schartl M. The origin and evolution of a unisexual hybrid: *Poecilia formosa*. *Philos Trans R Soc B Biol Sci.* 2008;363(1505):2901-2909. doi:10.1098/rstb.2008.0040
338. Vieira MLC, Santini L, Diniz AL, Munhoz C de F. Microsatellite markers: what they mean and why they are so useful. *Genet Mol Biol.* 2016;39(3):312-328. doi:10.1590/1678-4685-GMB-2016-0027
339. Bagshaw ATM, Horwood LJ, Fergusson DM, Gemmell NJ, Kennedy MA. Microsatellite polymorphisms associated with human behavioural and psychological phenotypes including a gene-environment interaction. *BMC Med Genet.* 2017;18(1):12. doi:10.1186/s12881-017-0374-y
340. Priyam A, Woodcroft BJ, Rai V, et al. Sequenceserver: a modern graphical user interface for custom BLAST databases. *Mol Biol Evol.* 2019;36(12):2922-2924. doi:10.1093/molbev/msz185
341. Wintersinger JA, Wasmuth JD. Kablammo: an interactive, web-based BLAST results visualizer. *Bioinformatics.* 2015;31(8):1305-1306. doi:10.1093/bioinformatics/btu808

## Appendix B: Field observations



**Figure B.1.** Collection of spermatophores presumptively left by an *A. texanum* male at site D3.1, found on March 23, 2019. These “sperm gardens” can be found in ponds during breeding season.



**Figure B.2.** Additional image of a “sperm garden” left by an *Ambystoma texanum* male on March 23, 2019, situated in a shallow pit left behind by a treefall.



**Figure B.3.** Image of a salamander with presumed skeletal deformity found on May 10, 2019 on Pelee Island, Ontario. This individual never straightened out and maintained distorted spinal arrangement when mobile.

## Appendix C: Historic maps of Pelee Island, Ontario

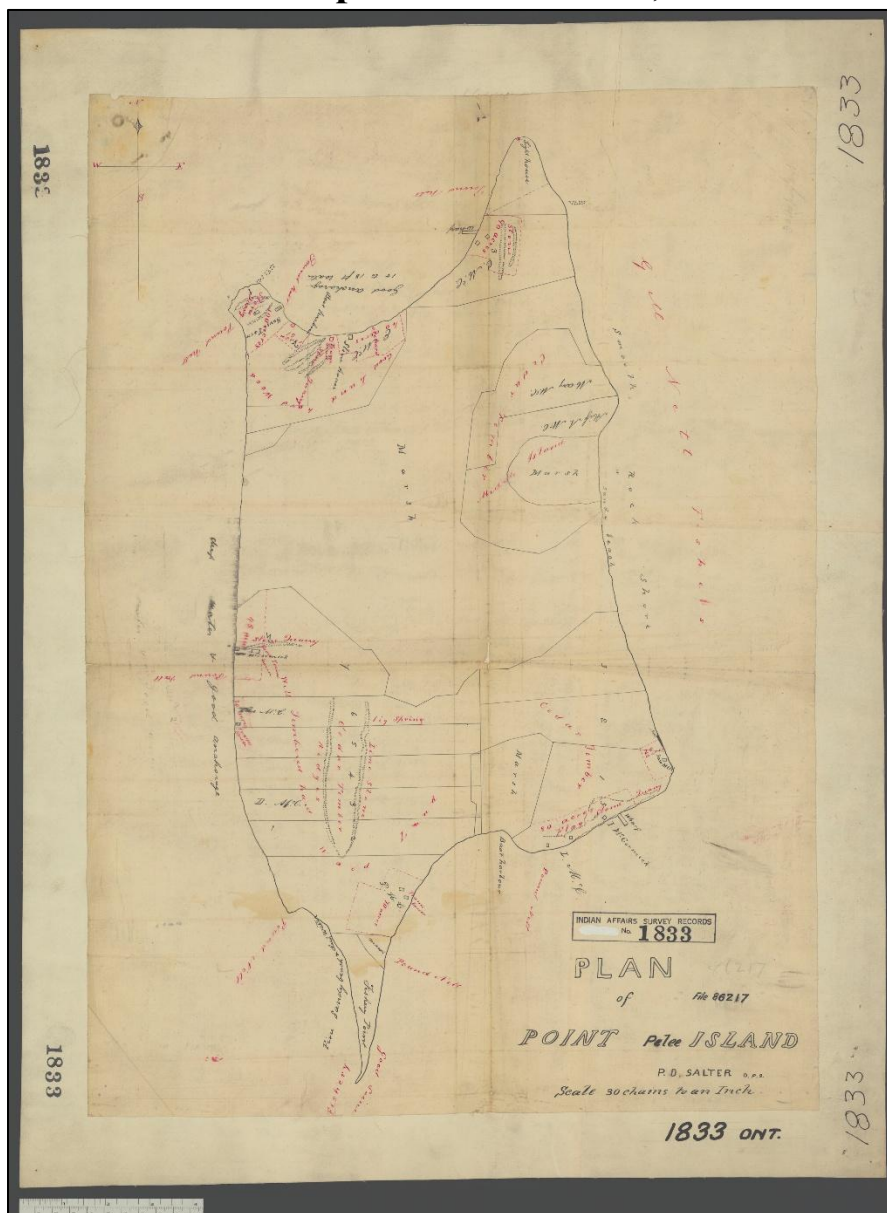


**Figure C.1.** Survey map of Pelee Island, Ontario by P. D. Salter in 1847<sup>168</sup>. The first known survey map of Pelee Island identifying historic uplands and inland marshes. A ‘Big Spring’ is identified in approximately the same location as site B6 used in this thesis.

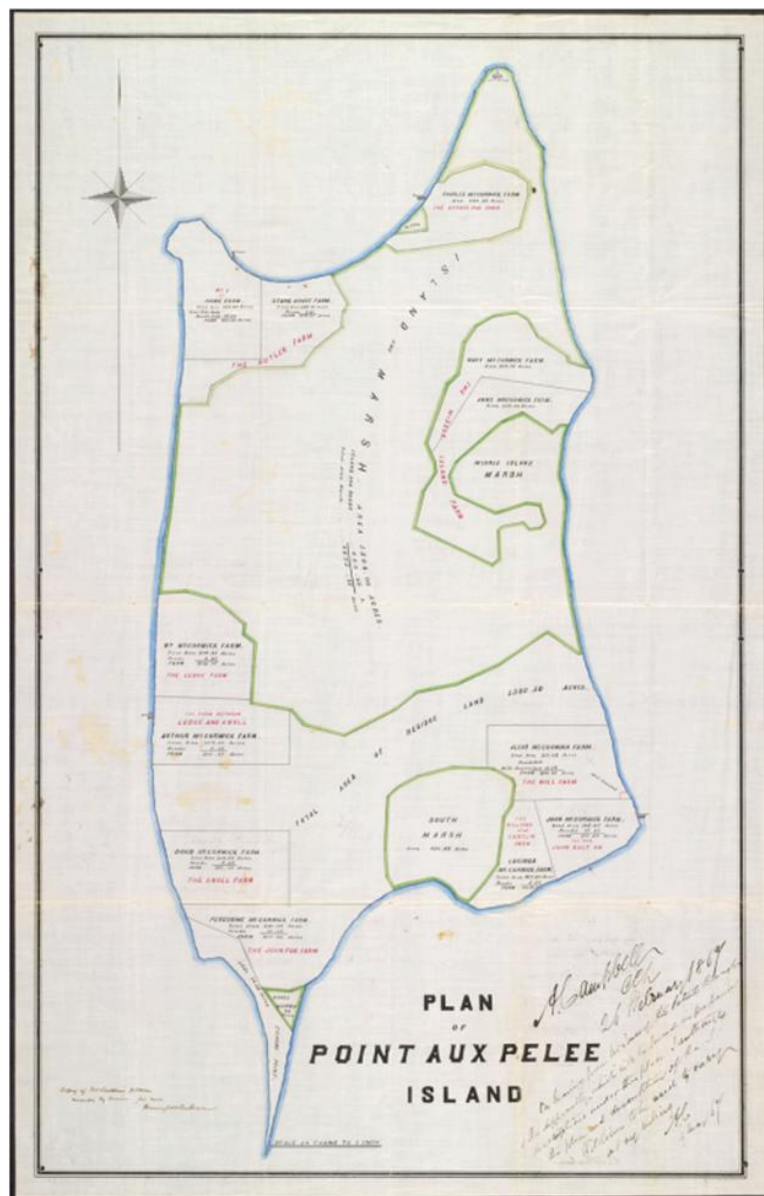


**Figure C.2.** Survey map of Pelee Island, Ontario by Campbell in 1867<sup>167</sup>. Historic upland demarcations of this reference map, outlined in green, were used in Chapter 3 to identify which sites were associated with each upland.